The Dose and Time Dependent Effects of HGF on Myf-5, MyoD and miR-31 Expression in Quiescent Primary Human Myoblasts

By

Niccolò Passerin d'Entrèves

Thesis presented in partial fulfillment of the requirements for the degree of

MASTERS IN PHYSIOLOGICAL SCIENCES

In the Department of Physiological Sciences

Faculty of Natural Science

Stellenbosch University

Supervisor: Prof. Kathryn Myburgh

Co-supervisor: Dr Marí van de Vyver

March 2017

DECLARATION

By submitting this thesis, I declare that the entirety of the work contained therein is my own, original work, that I am the sole author thereof (save to the extent explicitly otherwise stated), that reproduction and publication thereof by Stellenbosch University will not infringe any third party rights and that I have not previously in its entirety or in part submitted it for obtaining any qualification.

March 2017

Signed:_____

ABSTRACT

Satellite cells are progenitor cells that persist in adult muscle in a quiescent state. Upon injury, growth or hypertrophy, satellite cells become activated, proliferate and differentiate into myoblasts. Hepatocyte growth factor (HGF) induces activation of quiescent satellite cells *in vivo*. Also, HGF binding to its receptor, c-Met, leads eventually to transcription of key myogenic genes namely Myf-5 and MyoD. Satellite cells' responses to HGF are varied and time and concentration dependent effects on satellite cell fate have been reported, although published results are inconsistent. Previous studies have not standardised initial conditions prior to interventions, thus complicating comparison and conclusions. Finally, recent evidence implicates microRNAs (miRs) as active players maintaining quiescence in various cells, but HGF effects on miRNA expression are unknown in quiescent or activated satellite cells.

The overarching aim was to determine the time and concentration dependent effects of HGF on quiescent satellite cells by analysing key myogenic gene and miRNA expression after first standardising myoblast characteristics. Primary human myoblasts (PHM) explanted from human muscle biopsies were cultured in a serum free media, supplemented with synthetic growth factor free serum (KOSR), for 10 days to induce quiescence. Multicolour flow cytometry and cell cycle analyses were performed to characterise the PHMs maintained in serum free culture with regard to undifferentiated and quiescent status. Intervention with rh-HGF included 4 conditions: 2 different concentrations and 2 different durations. The myogenic regulatory factors, Myf-5 and MyoD were analysed using Western blotting, while their mRNA expression, along with miR-31 expression, were analysed using qPCR.

Effects of 10 d culture in quiescence media: PHMs maintained viability and undifferentiated morphology. Flow cytometry analyses of satellite cell markers indicated that 98% of PHMs remained positive for CD34 confirming their undifferentiated state. Activation and proliferation markers CD56 and Ki-67, decreased from 26% to 2% and from 85% to 46% respectively. While Myf-5 expression remained constant (~98%) for this period, MyoD expression dropped from 20% to 9%. Cell cycle progression was reduced: The percentage of G_1-phase cells increased from 58% to 87%, while S-phase cells dropped from 42% to 10%.

Effects of treating quiescent PHMs with rh-HGF: Treatment lead to significant ($p<0.0001$) time (24 h and 48 h) and concentration (2 ng/mL and 10 ng/mL) dependent increases in endogenous HGF protein. c-Met receptor content increased significantly ($p<0.01$) only with exposure to high dose HGF (10 ng/mL) within 24 h. Although MyoD mRNA expression decreased (~2 to 3-fold) with all HGF conditions, MyoD protein decreased only after 48 h in low HGF (2 ng/mL) compared to other treatment groups and untreated control. Myf-5 mRNA expression decreased moderately (up to ~0.5-fold) in all HGF conditions, but Myf-5 protein decreased only with high dose HGF (slightly). Finally, miR-31 expression decreased upon HGF treatment, although not consistently for all HGF conditions. This thesis confirmed time and concentration dependent effects of HGF on myoblasts. More specifically, diverse effects on MyoD and Myf-5 were not abolished here when satellite cells were first rendered quiescent. HGF affected miR-31, thus elucidating a new mechanism for influencing myoblasts.

OPSOMMING

Satellietselle is voorvader stamselle wat in 'n onaktiewe toestand in volwasse spiere gevind word. Met besering, groei of hipertrofie, word satellietselle geaktiveer, waarna hulle vermenigvuldig en differensiëer na mioblaste. Hepatosiet groeifaktor (HGF) ontlok aktivering van onaktiewe satellietselle *in vivo*. Ook sal HGF binding aan sy reseptor, c-Met, transkripsie van belangrike miogeniese gene, naamlik Myf-5 en MyoD, bemiddel. Satellietselle toon egter verskillende reaksies teenoor HGF, wat tyd- en konsentrasie-afhanklik is, maar resultate in verskeie gepubliseerde studies toon dat satellietsel noodlot nie noodwendig konsekwent is nie. Aangesien eksperimentale kondisies egter nie gestandardiseer was voor supplementering nie, is inter-studie vergelykings gekompliseerd. MikroRNSe (miRs) speel ook 'n aktiewe rol in handhawing van verskeie selsoorte as onaktief, maar dit is nog onbekend of HGF miR uitdrukking onaktiewe of onlangs geaktiveerde satellietselle beïnvloed.

Die hoofdoel was om die tyd- en konsentrasie-afhanklike gevolge van HGF op gevestigde onaktiewe satellietselle te bestudeer deur die ontleding van die belangrikste miogeniese gene en moontlike gepaardgaande miR- uitdrukking. Primêre menslike mioblaste (PHM) afkomstig ban spierbiopsies is vir 10 dae gekweek in serum-vrye medium, aangevul met sintetiese groeifaktor-vrye serum (KOSR), om onaktiwiteit teweeg te bring. Multikleurvloeisitometrie en selsiklusanalise is uitgevoer om karakteristieke van PHM te ontleed m.b.t. ongedifferensiëerdheid en die toestand van onaktiwiteit. Supplementering van PHM met rh-HGF het onder 4 kondisies plaasgevind: twee verskillende konsentrasies en twee verskillende tydsperiodes. Die miogeniese regulerende faktore Myf-5 en MyoD is daarna ontleed met behulp van die immunoklad-tegniek, terwyl hul mRNS en miR-31 uitdrukking, met kwantitatiewe PKR ontleed is.

Effek van 10 dae in serum-vrye kultuur: lewensvatbaarheid en 'n ongedifferensiëerde morfologie is gehandhaaf in PHM, selsiklus progressie is terselfdertyd onderdruk. Vloeisitometriese analise het bewys dat 98% van PHM deurgaans positief was vir CD34 wat ongedifferensiëerdheid kwantitatief bevestig. Merkers van aktivering en vermeerdering, CD56 en Ki-67, het gedaal van 26% tot 2%, en van 85% tot 45% respektiewelik. Alhoewel Myf-5 uitdrukking konstant gebly het oor die tydperk (~98%), het MyoD uitdrukking gedaal van 20% tot 9%. Selsiklus: die persentasie G_1-fase selle het toegeneem van 58% na 87%, terwyl die persentasie S-fase selle gedaal het van 42% tot 10%.

Effek van rh-HGF toediening: HGF het gelei tot beduidende ($p<0.0001$) stygings in endogene HGF proteine wat beide tyd (24 uur en 48 uur) en konsentrasie (2 ng/mL of 10 ng/mL) afhanklik was. Reseptorvlakke van c-Met het aansienlik toegeneem ($p<0.01$) na 24 uur behandeling met hoë dosis HGF. Alhoewel MyoD mRNS twee-tot drievoudig verminder het onder alle HGF kondisies, het MyoD protein slegs ná 48 uur behandeling met die lae HGF dosis gedaal. Dalings in Myf-5 mRNS was matig (tot ~0.5-voudig) met lae en hoë HGF, maar Myf-5 protein het slegs met hoë dosis HGF toediening gedaal. Laastens het miR-31 uitdrukking afgeneem met HGF toediening, ofskoon hierdie bevinding in party HGF kondiesies egter onbeslis was. Hierdie tesis beam tyd- en konsentrasie-afhanklike uitwerkings van HGF op mioblaste. Meer spesifiek, diwerse uitwerkings op MyoD en Myf-5 is nie deur eersgaande sinkronisasie van die onaktiewe staat verwyder nie. HGF beinvloed miR-31, dus is ‘n nuwe meganisme vir effekte op mioblaste onthul.

ACKNOWLEDGEMENTS

To my mother and father, words can't describe how thankful and grateful I am for all the opportunities you have provided me with. Thank you for always supporting me in all my choices which have enabled me to further my studies. I know that you will always be there in times of need. I don't say this enough, but from the bottom of my heart, thank you for everything. This MSc thesis is dedicated to the both of you. Vi amo tantissimo, Niccolò.

To my brother Alessando, you are quickly becoming an adult and I am incredibly proud of you. Know that you mean everything to me and that I will always be there for you. TV1KDB…. Coglione.

To my supervisor, Prof. Kathyrn Myburgh, thank you for your guidance and wisdom throughout the past two years. Coming to Stellenbosch University was a big move for me, but i'm glad I did it as it expanded my horizons and helped me grow. I am incredibly proud of the project that we built together and hope to see it flourish in the years to come.

To my co-supervisor, Dr. Mari Van de Vyver, thank you for coming on board the project with such a short notice and helping me with the editing of my thesis. I wouldn't be writing these acknowledgements if it wasn't for you.

To Zaakiyah, thank you for all the help in TC and the insightful and interesting chats we had about Islam and the Quran.

To Dr. Tanja Davis, thank you, well for everything. You were always there for me when I needed help, whether it be in TC, Western blotting or data analyses. For that I'm incredibly grateful, thank you. I don't know how many chocolates I owe you, but i'm guessing it's a lot.

To Tope, Tracey and Tayla, thanks so much for your friendship and the good times in the labs. I will miss you guys.

To Rozanne Adams and Lize Engelbrecht, thanks for all the help with flow cytometry, confocal microscopy and data analysis.

To Scott, Matthew and Francisco, thanks for your friendship and great times. I truly consider each and everyone of you not only my best friends but brothers. No matter where life takes us, I know that you will always be part of my life.

Thank you to the NRF for financial support.

LIST OF ABBREVIATIONS

ANOVA	Analysis of Variance
APS	Ammonium Persulfate
bHLH	Basic Helix loop Helix
BSA	Bovine Serum Albumin
cDNA	Complementary Dexoyribonucleic Acid
c-Met	Hepatocyte Growth Factor Receptor
CD34	Cluster of Differentiation 34
CD56	Cluster of Differentiation 56/Nerual cell adhesion molecule (NCAM)
DMEM	Dulbecco's modified Eagles Medium
DMSO	Dimethyl sulfoxide
ECL	Entactin-Collagen IV-Laminin Cell Attachment Matrix
ECM	Extracellular Matrix
ERK	Extracellular signal-Regulated Kinases
FBS	Foetal Bovine Serum
FGF	Fibroblast Growth Factor
HAM F-10	HAM F-10 Nutrient Mixture Medium
HGF	Hepatocyte Growth Factor
HS	Horse Serum
Ki-67	Antigen Ki-67
KO-DMEM	KnockOut™ Dulbecco's modified Eagles Medium
KOSR	KnockOut™ Serum Replacememt
L-Glu	L-glutamine
MAPK	Mitogen-Activated Protein Kinase
miRNA	MicroRNA
MMP	Matrix metalloproteinase
MRF	Myogenic Regulatory Factor
mRNA	Messenger Ribonucleic Acid
Myf-5	Myogenic Factor 5
MyoD	Myogenic Differentiation factor 1
P/S	Penicillin/Streptomycin
Pax3	Pair homeodomain box 3
Pax7	Pair homeodomain box 7
PBS	Phosphate Buffered Saline
PHM	Primary Human Myoblast
PHM-DM	Primary Human Myoblast Differentiation Medium
PHM-PM	Primary Human Myoblast Proliferation Medium
PI3K	Phosphatidylinositol 3-kinase
qPCR	Quantitative real-time Polymerase Chain Reaction
rh-FGF	Recombinant Human Fibroblast Growth Factor, Basic
rh-HGF	Recombinant Human Hepatocyte Growth Factor
rRNA	Ribosomal Ribonucleic Aicd
SDS-PAGE	Sodium Dodecyl Sulfate-Polyacrylamide Gel Electrophoresis
TEMED	Tetramethylethylenediamine

TABLE OF CONTENTS

LIST OF FIGURES

LIST OF TABLES

CHAPTER 1

INTRODUCTION

Skeletal muscle satellite cells are uni-potent stem cells present in adult skeletal muscle and play a key role in muscle growth and regeneration. These cells are the precursors to myocytes, which fuse together to form multinucleated myofibres surrounded by the sarcolemma that is in turn surrounded by a basement membrane. Even though satellite cells were first discovered more than 50 years ago, the underlying molecular mechanisms that regulate their activation, self-renewal and entry into the myogenic programme is still not fully understood. Elucidating these key molecular mechanisms regulating satellite cell function can provide novel insights into skeletal muscle regeneration in adults.

This chapter will focus on the physiological importance of satellite cells and discuss their regulation. The key molecular role players that govern the transition of satellite cells from a quiescent into an activated state, as well as the signaling mechanisms that regulate satellite cell activation and proliferation, will be discussed. Although numerous growth factors are known to affect satellite cell activity, the specific focus of the research project in this thesis was on Hepatocyte growth factor (HGF) and its role in stimulating quiescent satellite cells to become active, to re-enter the cell cycle and to proliferate. This chapter will therefore also discuss the binding of HGF to its cell surface receptor, c-Met, and the subsequent signaling that occurs through the MAPK/ERK pathway resulting in satellite cell activation. Furthermore, the literature highlighting potential time and concentration dependent effects of HGF signaling thought to govern differential satellite cell behaviours will be discussed. Finally, the role of microRNAs (miRNAs) in maintaining satellite cell quiescence is considered and how they may 'prime' satellite cells to re-enter the cell cycle more efficiently.

1.1 THE MUSCLE SATELLITE CELL

1.1.1 THE DISCOVERY OF SATELLITE CELLS: A BRIEF HISTORY

Research on skeletal muscle growth and repair dates back to the early and mid-19th century. As described by Scharner and Zammit (2011), embryonic myogenesis, muscle degeneration and muscle regeneration were first described during this time (Scharner & Zammit 2011). It would take another century for the key player in muscle regeneration, the muscle stem cell, to be discovered and for its role to be elucidated. Skeletal muscle stem cells were discovered by two independent groups in 1961 (Katz 1961; Mauro 1961) and were called 'satellite cells' by Mauro, based on their peripheral position on the muscle fibre. Satellite cells were described to be located on the muscle fibre itself, nestled in between the plasma membrane (sarcolemma) and the basement membrane (basal lamina) (Mauro 1961). These newly discovered cells had a unique morphology: large nuclear-to-cytoplasm ratio, few organelles (see Figure 1.1) and visibly condensed chromatin during interphase, which are characteristic of mitotically quiescent (G_0 phase) cells (Schultz et al. 1978). Due to their position, Mauro (1961) immediately hypothesized that satellite cells played a role in skeletal muscle regeneration and post-natal skeletal myogenesis. This hypothesis was confirmed shortly after the discovery of satellite cells in several landmark experiments.

Until the 1960s, only myoblasts were known to have mitotic potential, as they had been shown to incorporate tritiated thymidine during *in vivo* muscle regeneration (Bintliff & Walker 1960) and also to fuse and form myotubes *in vitro* (Capers 1960). In 1965, however, a paper by Shafiq & Gorycki (1965) showed that following muscle damage, satellite cells were often seen in the peripheral regions of the damaged area indicating a wide-spread influence (Shafiq & Gorycki 1965). In the following year, Church *et al.* (1966) showed that the satellite cell pool is replenished after a crush injury. This was evident in the reappearance of satellite cells on newly synthesized myotubes (Church et al. 1966), implying that satellite cells represented a pool of 'reserve cells'. In 1968, evidence that quiescent satellite cells could undergo mitosis was provided by Shafiq *et al.* (1968). The authors showed that satellite cells of 3 week old rats undergo mitosis after intraperitoneal injection of the cytotoxic agent, colchicine (Shafiq et al. 1968). These observations were confirmed by Reznik M. (1969) who showed that satellite cells incorporated tritiated [^{3}H] thymidine upon cold injury of the gastrocnemius muscle in normal, adult, white mice (NIH, GP) (Reznik 1969). The

observations produced in these studies proved without doubt that satellite cells undergo mitosis upon muscle injury. In further support of this notion, muscle biopsies from patients suffering from *Duchenne muscular dystrophy* (congenital and pathological condition associated with muscular degeneration) were shown to have more satellite cells in proximity of the damaged and regenerating muscle fibres. Also these satellite cells had a cytoplasmic morphology traditionally associated with proliferating cells (Laguens 1963; Shafiq et al. 1967). Taken together, it became clear that the behaviours exhibited by satellite cells in muscles that have been exposed to pathological injuries is similar to that of physically injured muscles, suggesting an inherent pattern of behaviour. The fact that the morphology exhibited by these satellite cells was akin to that of foetal myoblasts gave rise to the hypothesis that satellite cells may be the precursor cells that give rise to myoblasts in adult muscle. Proof that satellite cells are indeed precursors to myoblasts was provided in 1975 when two separate *in vitro* studies using isolated single muscle fibres harvested from adult rats and juvenile japanese quail, respectively, were published. Bischoff R. (Bischoff 1975) and Konigsberg *et al.* (Konigsberg et al. 1975) both showed that satellite cells on these single fibres started to migrate off the necrotic myofibre and then proliferated. These newly proliferating cells then fused to form multinucleated myotubes. These landmark studies (Bischoff 1975; Konigsberg et al. 1975) confirmed that satellite cells are indeed the key role players in regeneration. The question still remained whether or not satellite cells could be classified as true stem cells. By definition, a stem cell, whether it be embryonic or adult, must possess the ability to both replicate itself (self-renew) and to differentiate (Lodish & Berk 2003). By the 1980's, the notion that satellite cells were responsible for muscle regeneration and growth was fundamentally established and accepted. However, the key aspect that was still not fully addressed was their potential for self-renewal.

In 1970 and 1971, Moss and Leblond were the first to provide evidence in support of the self-renewal hypothesis. The authors showed that tritiated thymidine was being incorporated into the satellite cells of growing rats and that myonuclei at similar time points began to exhibit this label, implicating satellite cells as the main source of new myonuclei. The gain of myonuclei through the fusion of satellite cells to myofibres is key to maintain the nuclear domain during growth and hypertrophy (Moss & Leblond 1970; Moss & Leblond 1971). Also, and more importantly, it was estimated that after each division, not all of the satellite cell progeny gave rise to myonuclei. Moss and Leblond's (1970, 1971) observations were thus two-fold: firstly they demonstrated that certain divisions gave rise to a myonucleus and a daughter satellite cell (Moss & Leblond 1971), secondly their finding introduced the concept of asymmetric cell division. Conclusive evidence to the issue of

self-renewal in satellite cells was however only provided several years later, in 2005. Collins *et al.* (2005) performed a single myofibre transplantation assay, in which various single skeletal muscle myofibres were transplanted into irradiated muscle of *mdx/nude* mice incapable of regeneration due to prior experimental depletion of endogenous satellite cells (Collins et al. 2005). The authors observed that, upon transplantation, the few satellite cells present on the implanted myofibre generated a population of hundreds of satellite cells and thousands of myonuclei. Quantification of cell numbers indicated that 7-22 satellite cells proliferated and, upon fusion, were able to provide ~25,000-30,000 myonuclei, while at the same time replenishing the satellite cell population (10-fold increase) (Collins et al. 2005). Furthermore, the newly expanded satellite cell populations were proven to be fully functional, as they were capable of supporting several rounds of muscle regeneration (Collins et al. 2005). Further evidence supporting the finding of Collins *et al.* (2005) was provided when single satellite cells were transplanted into the muscles of *scid/mdx* irradiated mice. The progeny generated from these single cells not only differentiated and fused into myofibres, but also remained in the host muscle (Sacco et al. 2008). Taken together, these studies irrefutably proved the capability of satellite cells to self-renew and generate new muscle fibres. However, the factors controlling satellite cells had not been elucidated and in the first 5 yars of the decade starting in the year 2000, a wave of research led by developmental biologists, began this arduous task and laid down a substantial platform of knowledge.

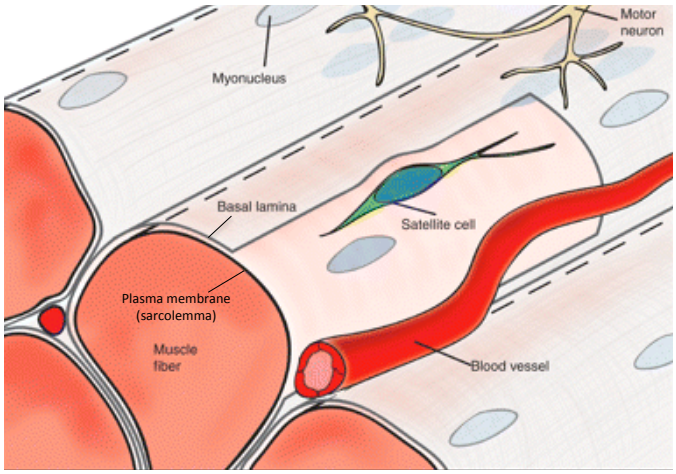

Figure 1.1: Graphical representation of a skeletal muscle fibre and its peripheral environment.

In an *in vivo* environment the quiescent satellite cell resides on the muscle fibre, between the basal lamina and the plasma membrane (sarcolemma) of the muscle fibre. Image modified and reproduced without permission from (Bentzinger et al. 2012).

1.1.2 THE EMBRYONIC ORIGINS OF ADULT SATELLITE CELLS

Adult muscle satellite cells are derived from mesodermal precursor cells, which originate from the dermomyotome, an epithelial structure that develops on the dorsal side of the presomitic paraxial mesoderm (Gros et al. 2005; Scaal & Christ 2004; Schienda et al. 2006). The dermomyotome, which can be distinguished between the epaxial and hypaxial region, gives rise to several multipotent mesodermal progenitor cells (Buckingham 2006). The different fates of the cells present in the dermomyotome are highly dependent on where they are located within it. This is due to the fact that these mesodermal progenitor cells are differentially exposed to potentiating and inhibiting signals from the surrounding tissues, specifically the notocord, neural tube, dorsal ectoderm and myotome. There they are influenced to generate different cell types and tissues (such as dermal fibroblasts, brown adipose tissue, endothelial cells, vascular smooth muscle and skeletal muscle) (Buckingham 2006).

Embryonic muscle development occurs in two distinct phases: i) the formation of the primary myotome (situated beneath the demomyotome) by post-mitotic mononucleated myocytes (Gros et al. 2004; Kalcheim & Ben-Yair 2005) which is then followed by ii) the formation and expansion of the myotome. Importantly, the formation and expansion of the myotome (2^{nd} stage) also results in the creation of myogenic progenitor cells that contribute to initial myogenesis, but are not all incorporated into fibres. During this stage the central portion of the dermomyotome undergoes an epithelial-to-mesenchymal transition and multipotent mesodermal progenitor cells present in the demomyotome begin to express Paired box 3 (Pax3) and Paired box 7 (Pax7) transcription factors (Kassar-Duchossoy et al. 2005). These Pax3/Pax7 expressing progenitor cells begin to migrate from the central region of the dermomyotome to the previously formed primary myotome and then proliferate enlarging the myotome (Gros et al. 2005; Kassar-Duchossoy et al. 2005; Relaix et al. 2004; Relaix et al. 2005). In the myotome Pax3/Pax7-expressing myogenic progenitor cells form a pool of proliferating cells with the capacity to differentiate into myoblasts and ultimately fuse together to form myofibres. This is achieved through the expression of basic helix-loop-helix (bHLH) factors associated with the myogenic regulatory factor family (MRF) (Seale & Rudnicki 2000; Otto et al. 2009). Examples of such MRFs with bHLH motifs are MyoD and Myf-5. Of the proliferating Pax3/Pax7-expressing myogenic progenitor cell pool, many will induce MyoD and Myf-5 expression, associated with exit from the cell cycle. MyoD and Myf-5 in turn regulate the transcription of

myogenin and myogenic regulatory factor-4 (MRF4), causing these cells to differentiate and fuse into myofibres (Sabourin & Rudnicki 2000). However, not all Pax3/Pax7-expressing cells present in the myotome exit the cell cycle and undergo fusion.

Some of the proliferating Pax3/Pax7-expressing myogenic progenitor cells endure into the late stages of etal development and become the source of postnatal adult muscle stem cells (Gros et al. 2005; Relaix et al. 2005). As mentioned before, the postnatal adult muscle stem cells reside in a specific location between the sarcolemma and basal lamina of muscle fibres (Mauro 1961). Ohlstein *et al*. (2004) defines such a specific location in a tissue where stem cells can reside for an indefinite period of time as the 'stem cell niche' (Ohlstein et al. 2004). A growing body of evidence indicates that the muscle satellite cell niche is incredibly complex and highly specific to ensure the survival and maintenance of the satellite cell pool (Pinto et al. 2003; Zhang et al. 2003; Calvi et al. 2003; Shen et al. 2004; Tumbar et al. 2004). The satellite cell niche is characterized by an extensive extracellular matrix (ECM) with vascular and neural networks that facilitate cell-cell interactions and allow for autocrine and paracrine molecular communication (Dumont et al. 2015). The complex interactions governing the muscle satellite cell niche ensures tight regulation of satellite cell quiescence, activation, proliferation and self-renewal. The role that the niche plays in maintaining a balance between satellite cell self-renewal and differentiation becomes crucial in the context of injury and muscle regeneration, since the proliferation and differentiation of all the satellite cells would ultimately deplete the satellite cell pool. However, if too few satellites become activated and differentiate, the outcome would be insufficient muscle regeneration. It has been shown that activated satellite cells have the ability to return to a quiescent state thus helping to maintain or even regenerate the satellite cell pool (Zammit et al. 2004). This behaviour in adult satellite cells is thought to be promoted by Pax7, again emphasizing the importance of the embryonic signals.

1.1.3 SATELLITE CELL MAINTENANCE: QUIESCENCE, ACTIVATION AND SELF-RENEWAL

In adult uninjured, fully grown and rested skeletal muscle, satellite cell quiescence would be an energetically inexpensive state. Nonetheless, the maintenance of satellite cells in a quiescent state (G_0) is a tightly controlled process.

1.1.3.1 Maintenance of quiescence

Gene expression profiling studies utilizing microarray analysis techniques have revealed that satellite cells express a vast array of genes associated with the regulation of quiescence (Fukada 2011; Liu et al. 2013). In particular, the cell cycle inhibitors: cyclin-dependent kinase inhibitors $p27^{kip1}$ and $p57^{kip2}$, the retinoblastoma protein (Rb) and Sprouty-1 were highly expressed in satellite cells. These negative regulators of the cell cycle, together with other factors such as environmental cues (mechanical interaction with ECM) and microRNAs (miR-489, and miR-31), all function in concert to maintain satellite cells in a quiescent state (G_0). The expression of these effectors is stimulated by upstream signaling pathways.

The mechanisms that promote satellite cell activation or that disrupt/override quiescence signaling remain unclear, but it is known that quiescent satellite cells respond to a plethora of niche signals *in vivo* such as changes in the composition and/or structure of the ECM (Boldrin et al. 2010) and the secretion of growth factors (Anderson 2006). The nature of their response is influenced by the type of stimulus or injury (e.g. chemical, ischemic, and traumatic) (Baj et al. 2005).

1.1.3.2 Activation and proliferation

The ECM of the basal lamina is primarily composed of type IV collagen, fibronectin, entactin, laminin, glycoproteins and proteoglycans (Sanes 2003). This ECM is fundamental to the survival and regulation of satellite cells as it provides both structural support and harbours key growth factors that influence satellite cells (Baj et al. 2005; Anderson 2006; Boldrin et al. 2010) (refer to Section 1.2 for detailed information on the role of specific growth factors in regulating satellite cell activity).

The physical interaction between the ECM and satellite cells ensures that any mechanical stimulus originating from the extracellular compartment is transduced into an intracellular signal in satellite cells resulting in activation (Boppart et al. 2006). This tethering is achieved by α7/β1-integrins present on the satellite cell surface that anchor it to the basal lamina (Song et al. 1992; Boppart et al. 2006). Also, present in the ECM are numerous growth factors of critical importance to regulating satellite cells. These molecules are generally inactive precursors and are bound to cell surface proteoglycans present on satellite cells. As soon as mechanical disruption of the ECM is incurred, proteolytic enzymes like serine proteases and matrix metalloproteinases (MMP) can be triggered to

release these inactive growth factors, which in turn become free to bind to their target receptors on satellite cells. One such growth factor *in vivo* is HGF.

The predominant growth factor known to induce dormant satellite cells to exit quiescence and enter the cell cycle is HGF. The biological effects elicited by HGF are brought about *via* signaling through its tyrosine kinase receptor, c-Met, which is able to activate several downstream effector pathways that have pleiotropic effects influencing key processes of proliferation, differentiation, migration and cell survival (Miyazawa et al. 1994; Boros & Miller 1995; Zarnegar & Michalopoulos 1995; Matsumoto & Nakamura 1997).

HGF/c-Met signaling, activates several downstream effector pathways intrinsic to receptor tyrosine kinase (RTK) signaling. In the context of activation and subsequent proliferation of satellite cells, HGF induces the activation of the mitogen-activated protein kinase/extracellular signal-regulated kinases (MAPK/ERK) pathway. A study using cultured chicken skeletal muscle satellite cells showed that MAPK/ERK activation was mediated by Grb2's association with the phosphorylated multifunctional docking site on c-Met's carboxy terminal domain (Leshem et al. 2002). Furthemore, in the same study, activation of the MAPK/ERK pathway was also shown to inhibit satellite cell differentiation (Leshem et al. 2002). This is achieved in a dual manner: Firstly, MAPK/ERK inhibits the activity of MRF/E-protein complexes required for myogenic differentiation, while at the same time inducing the expression of Twist, an inhibitor of MyoD (Gal-Levi et al. 1998; Leshem et al. 2000; Leshem et al. 2002). Secondly, it inhibits the cell cycle inhibitor $p27^{Kip1}$ resulting in the accumulation of hyper-phosphorylated retinoblastoma protein, which stimulates increased proliferation and entry into the S-phase of the cell cycle (Leshem et al. 2000; Leshem & Halevy 2002). Thus HGF/c-Met signaling through the MAPK/ERK pathway, elicits a dual effect on satellite cells by promoting their proliferation and in parallel inhibiting their differentiation.

In support of an effect of HGF on MRFs, exogenous HGF was shown to simultaneously induce the gene transcription of Myf-5 (role in proliferation) and inhibit MyoD expression (role in differentiation) *in vitro* (Yamane et al. 2004). The effects attributed to HGF injected into uninjured hindlimb muscle *in vivo* were confirmed by *in vitro* studies using satellite cells isolated from 12-month-old male Sprague-Dawley rats. Here inhibition of HGF abrogated all of the biological effects elicited by HGF *in vivo* (Tatsumi et al. 1998). In summary, because HGF activates quiescent satellite

cells and increases their proliferation, it functions mainly in the initial stages of muscle regeneration (Tatsumi et al. 1998; Miller, Thaloor, Matteson & Grace K Pavlath 2000).

Following activation satellite cells re-enter the cell cycle and begin proliferating, essentially becoming myoblasts. However, this activation isn't restricted to the satellite cells in the immediate vicinity of the damaged area; distant satellite cells also become activated and migrate to the affected area (Schultz et al. 1985). Satellite cells display remarkable mobility/migration abilities; they not only have the capacity to migrate across a particular muscle fibre, but can also migrate across the basal lamina and connective tissue to adjacent fibres (Watt et al. 1987; Hughes & Blau 1990; Jockusch & Voigt 2003) in response to chemotactic factors such as HGF, Transforming growth factor-beta (TGF-β), Fibroblast growth factor-6 (FGF-6) and Platelet-derived growth factor (PDGF) (Husmann et al. 1996; Bischoff 1997; Karalaki et al. 2009).

The activation and migration of satellite cells seems to be accompanied by decreased expression of CD34, a cell surface glycoprotein that functions as a cell-cell adhesion factor (Alfaro et al. 2011). This may facilitate not only the migration but also proliferation of satellite cells (Alfaro et al. 2011). It follows that proteins used to characterize satellite cells are themselves not stablely present. Nonetheless, proliferating myogenic precursor cells are characterized by the expression of MRFs.

The first MRFs to be upregulated are Myf-5 and MyoD. Studies using myofibres isolated from adult mice showed that satellite cells expressed either Myf-5 or MyoD after 24 h in culture, after explant and co-express them by 48 h (Cornelison & Wold 1997; Zammit et al. 2002). This *in vitro* data was supported by *in vivo* studies using mice (CD1 outbred) injected intramuscularly with cardiotoxin (10^{-5} M) (Cooper et al. 1999) This selective expression of these two MRFs suggests they may play different roles in guiding myogenic progenitor cell fates. Studies illustrating the crucial role of MyoD and Myf-5 expression in myogenic differentiation and muscle regeneration have been extensively documented (Megeney et al. 1996; Sabourin et al. 1999; Asakura et al. 2007; Gayraud-Morel et al. 2007). *MyoD*$^{-/-}$ mutant mice display significantly reduced muscle mass and muscle regeneration is impaired with evidence that myoblasts in the injured area fail to differentiate and fuse to form functional myotubes (Megeney et al. 1996). In contrast it appears that there may also be a distinct subpopulation of 'committed' satellite cells in normal uninjured muscle (Rantanen et al. 1995). These committed cells were shown to already express MyoD, desmin and myogenin as early as 12 h

after contusion injury to the *gastrocnemius* or toxic injury to the *soleus* (compared to 24 h post injury, which is more usually observed), indicating these cells may be selected to differentiate without first proliferating (Rantanen et al. 1995). Furthermore satellite cell proliferation was only seen 24 h after injury (Rantanen et al. 1995).

MyoD is thus critical for myogenic precursor cells to commit to differentiation (Sabourin et al. 1999). Furthermore, when cultured in myogenic differentiation media, *MyoD*$^{-/-}$ myoblasts exhibit sustained proliferation (Megeney et al. 1996). Conversely, *Myf5*$^{-/-}$ myoblasts have a compromised proliferative ability (Gayraud-Morel et al. 2007). Therefore predominant MyoD expression induces differentiation, as can be seen in *Myf5*$^{-/-}$ myoblasts (Montarras et al. 2000), while Myf-5 predominance in *MyoD*$^{-/-}$ myoblasts is associated with enhanced proliferation and delayed differentiation (Sabourin et al. 1999). Research therefore unequivocably points towards there being distinct roles for to MyoD and Myf-5.

These distinct roles of MyoD and Myf-5 individually serve to establish different satellite cell fates but cell fate might be dependent on the expression of these transcription factors in relation to one another within satellite cells (Rudnicki et al. 2008). Satellite cells *in vivo* express both MyoD and Myf-5 and thus show intermediate behaviours when compared to the extremes generated in KO mouse models. In addition, satellite cell-derived C2C12 myoblasts from normal mice express both MyoD and Myf-5 *in* vitro. It has been shown that they are expressed at different times during the cell cycle: MyoD expression is at its highest in mid G_1, while Myf-5 expression peaks at G_0 and G_2 (Kitzmann et al. 1998). However, in an *in vivo* environment a multitude of extrinsic factors can disrupt this balance between MyoD and Myf-5 expression and as a consequence affect the cell cycle dynamics of satellite cells. As a result, it is essential to consider extrinsic mechanisms that play a role in satellite cell activation, proliferation and differentiation, as these ultimately ensure balanced and functional muscle regeneration and growth. These considerations are important both when researching the molecular responses of satellite cells *in vitro* and when considering satellite cell-based therapy as a potential avenue for muscle regeneration.

1.1.3.3 Return to quiescence and self-renewal

Activated primary satellite cells, isolated from both rat and mice muscle, rapidly upregulate MyoD expression within the first 24 h in *in vitro* culture (Yablonka-Reuveni et al. 1999; Zammit et al. 2004). After 72 h in culture media (DMEM and 10% (v/v) horse serum), proliferating $Pax7^{+}/MyoD^{+}$ myoblasts, may even start to differentiate by downregulating Pax7 whilst starting to upregulate Myogenin expression, possibly as a result of increased confluency. However, a subpopulation of these $Pax7^{+}/MyoD^{+}$ myoblasts can repress MyoD while maintaining Pax7 expression and eventually exit the cell cycle (ie: neither remaining in proliferation nor tending to differentiate) (Halevy et al. 2004; Zammit et al. 2004). Other authors have also shown that after 3-4 weeks in culture $Pax7^{+}/MyoD^{-}$ myoblasts begin to express Nestin, an intermediate fillament protein, typical of immature cells (Day et al. 2007). Thus, it seems that MyoD expressing myoblasts which are considered to be committed to differentiation are able to regress and return to a more stem-like state. This mechanism of satellite cell renewal *via* lineage regression from $Pax7^{+}/MyoD^{+}$ myoblasts is thought to be promoted by Pax7 (Zammit et al. 2004). This could be an important mechanism to ensure survival of the satellite cell pool, as it was shown that reduction in the capacity of satellite cells to regenerate the satellite cell pool correlated with decreased number of satellite cells in aged muscle (Day et al. 2010).

Table 1.1: Summary of key studies regarding the expression of MRFs and satellite cell proliferation, differentiation, quiescence and self-renewal.

Authors	Study design (Model, culture type)	Culture period/ Time points	Results
Yablonka-Ruveni *et al.* 1999	Balb/C and MyoD$^{-/-}$ mice, isolated single muscle fibre cultures and tissue-dissociated satellite cell cultures.	0 - 9 days.	MyoD$^{-/-}$ satellite cells exhibit enhanced proliferation but fail to express myogenin and differentiate compared to wildtype satellite cells from Balb/C mice.
Zammit *et al.* 2004	Adult wildtype and 3F-*nlacz*-E transgenic mice, isolated muscle fibre cultures.	0 h - 120 h.	Small populations of proliferating Pax7^{+}/MyoD^{+} myoblasts begin to loose MyoD expression at 48 h and 72 h, exit the cell cycle (96 - 120 h) and do not differentiate.
Halevy *et al.* 2004	9 day post-hatch chicken, dissociated myoblast cultures.	0 - 15 days.	Percentage of Pax7^{+}/MyoD^{-} myoblasts increased over the 15 days culture period, resembling a reserve cell phenotype. Pax7^{+}/MyoD^{-} myoblasts do not express myogenin and do not differentiate.
Day *et al.* 2007	Juvenile (1-2 months) and adult (4-9 months) NES-GFP transgenic mice (C57BL/6 background) crossed with Myf5$^{nLacZ/+}$ mice (enriched Balb/C background), single myofibre cultures.	4 weeks.	NES/GFP expression declined following satellite cell activation but reacquired after 3 weeks in myogenic cultures by non-proliferating Pax7^{+} progeny.

The ability of satellite cells to return to quiescence has also been seen *in vivo* (Shea et al. 2010). In mice injured with barium chloride (1.2%), post-injury BrdU labelling showed that most Pax7^{+} satellite cells in the TA/EDL muscles became activated and proliferated, but a small population of satellite cells that carried the BrdU label were shown to exit the cell cycle. The exit of these Pax7^{+} satellite cells was concomitant with upregulation of Sprouty-1 expression (Shea et al. 2010). Sprouty-1 is a negative regulator of receptor tyrosine kinase (RTK) signaling and has been shown to be expressed in quiescent satellite cells (Shea et al. 2010). In a second experiment inhibition of Sprouty-1 resulted in significantly reduced numbers of remaining satellite cells after their activation and proliferation. Since HGF and FGF regulate activation and proliferation by activating the ERK pathway, the inhibitory effects of Sprouty-1 on satellite cells is most likely due to its negative regulation of the ERK signaling pathway. However, it was shown that only a specific subpopulation of these satellite cells required Sprouty-1 expression to return to a quiescent state (Shea et al. 2010). Although the concept behind the self-renewal of satellite cells is relatively well accepted, the complex mechanistic regulation is still unclear.

One mechanism to ensure the survival of a satellite cell pool lies in how satellite cells replicate. There are essentially two ways in which stem cells can replicate and self-renew: symmetrical and asymmetrical cell division. In the former type a parental cell gives rise to two identical daughter cells with the same characteristics and stemness, while the latter produces two daughter cells that are functionally different: a more differentiated daughter cell that is not able to self-renew and a daughter stem cell capable of both differentiation and self-renewal. Thus, it seems as though there are several distinct methods in place for satellite cells to self-renew and replenish the satellite cell pool.

Kuang *et al.* (2007) investigated whether satellite cells undergo symmetrical or asymmetrical cell division. They employed a Cre-LoxP based technique (*Myf5^{Cre};R26R-loxP-stop-loxP-YFP*) to track the lineage of satellite cells and were the first to show that muscle satellite cells are able to perform both symmetric and asymmetric cell division within their niche (Kuang et al. 2007). It was suggested that the orientation of the mitotic spindle relative to the longitude axis of the myofibre dictates the choice between symmetric or asymmetric division (Kuang et al. 2007). Asymmetric cell division was observed in Pax7^{+}/Myf-5^{-} cells when the mitotic spindle was orientated perpendicular to the myofibre axis, generating a daughter satellite cell (Pax7^{+}/Myf-5^{-}) and a daughter myogenic cell (Pax7^{+}/Myf-5^{+}). The more stem-like Pax7^{+}/Myf-5^{-} daughter cell was generated on the basal side, in contact with the basal lamina, while the more differentiated Pax7^{+}/Myf-5^{+} cell was generated on the apical side, next to the plasma membrane (Kuang et al. 2007). This doesn't mean that Pax7^{+}/Myf-5^{+} cells and Pax7^{+}/Myf-5^{-} cells are not both capable of further symmetric cell division, but that symmetric division was limited to situations when the mitotic spindle was parallel to the myofibre axis, causing both daughter cells to be in contact with the basal lamina and the plasma membrane equally. Further experimentation revealed that only the Pax7^{+}/Myf-5^{-} were able to reconstitute the satellite cell compartment (approximately 7-fold more efficiently than Pax7^{+}/Myf-5^{+}), when transplanted into Pax7$^{-/-}$ muscles (Kuang et al. 2007).

In an *in vivo* environment satellite cells are exposed to a variety of factors that may regulate mechanisms for satellite cell self-renewal. Under normal physiological conditions satellite cells may favour asymmetric self-renewal, as this would be sufficient to maintain muscle homeostasis and the parent pool, but then switch to symmetric proliferation in response to injury to provide the necessary amount of cells needed for functional regeneration (Morrison & Kimble 2006).

In summary, a fundamental aspect of satellite cells is their ability to self-renew, and it seems as though satellite cells that don't express Myf-5 ($Pax7^+/Myf\text{-}5^-$) are far more capable at self renewing and generating undifferentiated satellite cells. Thus $Pax7^+/Myf\text{-}5^-$ represent a *bona fide* stem cell population while $Pax7^+/Myf\text{-}5^+$ represent a population of more differentiation-prone satellite cells. However, Myf-5's primary role was earlier shown to induce proliferation, as $MyoD^{-/-}$ myoblasts elicit enhanced proliferation and delayed differentiation (Sabourin et al. 1999). Therefore it seems as though satellite cells exist as a heterogeneous population of precursors. This raises the question whether all these precursors will respond similarly to external factors such as a rapid change in growth factors, or if the responses of satellite cells to such factors needs to be qualified based on pre-exposure characteristics.

1.1.4 IDENTIFICATION AND HETEROGENEITY OF SATELLITE CELLS

The understanding that the adult muscle satellite cell population is so heterogeneous has gained more and more ground in recent years. Up until 20 years ago, satellite cells were simply classified as a homogeneous population of uni-potent muscle progenitors (Bischoff & Heintz 1994). Mounting evidence suggests otherwise and it seems as though satellite cell subpopulations can differ in gene expression signatures and myogenic proliferation propensity.

1.1.4.1 Heterogeneity of gene expression signatures

Cells that express the key myogenic genes, Pax3 and Pax7 are able to transcribe genes important for myogenesis and are thus considered to be muscle precursor cells. Studies using transgenic mice carrying reporter genes for Pax7 and Pax3 showed that only a subset of $Pax7^+$ satellite cells express Pax3 (Montarras et al. 2005; Relaix et al. 2006), potentially implying that only Pax7, its close homologue, is critical for the activation of the downstream myogenic programme and is thus the most specific marker for satellite cells. This was confirmed in a study, where FACS-isolated muscle satellite cells ($CD45^-/CD11b^-/CD31^-/Sca\text{-}1^-/\alpha7\text{-}integrin^+/CD34^+$) were analysed for Pax7, Pax3, Myf-5 and MyoD expression using qPCR. The authors reported that only Pax7 was expressed in all isolated cells, while Pax3 expression was variable and only 25% of the cells expressed MyoD (Sacco et al. 2008). *In vivo*, satellite cells also display heterogeneity e.g. in Dlk-1, c-Met and Neuronal cell adhesion molecule (NCAM/CD56) (Lindström et al. 2010), while immunofluorescence staining revealed that a subpopulation of satellite cells don't express CD34, M-cadherin and Myf-5

(Beauchamp et al. 2000). Further contributing to the idea that different populations of satellite cells display heterogeneous gene expression, two studies have shown that cranial muscle exhibits distinctly different molecular signatures to that of somatic muscle (present in the thorax, abdomen and limbs) (Schmalbruch 1976; Harel et al. 2009).

1.1.4.2 Heterogeneity in myogenic proliferation propensity

A study where continuous BrdU administration was used to label proliferating satellite cells, in growing rats *soleus* and *EDL* muscles, revealed that that only 80% of the satellite cells readily entered the cell cycle while the other 20% of satellite cells entered the cell cycle at a much slower rate (Schultz 1996). Further research is however needed to ascertain whether these differing satellite cell populations were co-localized or exposed to different signaling factors within their immediate environment, since differential exposure to signaling factors may affect the mitotic rate. Nonetheless, Schultz E. (1996) hypothesized that the slow, less responsive satellite cells represented a 'reserve population' that remain in a quiescent state, and only proliferate if extensive muscle regeneration is required (Schultz 1996). In line with this hypothesis, a recent study in which fluorescent PKH26 was used to trace cell divisions showed that long-term self-renewal abilities are retained in slow-dividing satellite cells (Ono et al. 2012). Satellite cells seem to also display heterogeneity with regards to their differentiation potential. Satellite cells from transplanted *tibialis anterior* (TA) muscle grafts were shown to contribute significantly less to the number of regenerated myofibres in *mdx/nude* mice, when compared to satellite cells grafted from the *extensor digitorum longus* (EDL) or soleus muscle (Beauchamp et al. 2000). Taken together these studies highlight the possibility that different populations of satellite cells might vary in their proliferation and differentiation potential.

In a subsequent study, Kuang *et al.* (2007) utilized reporter gene mice and showed that 13% of quiescent satellite cells on the EDL muscles, isolated from *Myf5-nLacZ* mice, were $LacZ^{-}$, suggesting a less committed cell fate (Kuang et al. 2007). In addition, using the Cre-LoxP system, the authors demonstrated that 10% of satellite cells in $Myf5^{Cre}$; *ROSA26R-YFP* mice did not express YFP. The implications of this finding were two-fold: Firstly, it signified that the small subpopulation of satellite cells had never expressed Myf-5 and secondly that these $Pax7^{+}/YFP^{-}$ satellite cells might have a distinct regenerative potential. When transplanted into regenerating muscles of $Pax7^{-/-}$ mice, these

$Pax7^+/YFP^-$ cells showed a profound ability to repair the muscle and reconstituted the stem cell niche, while the $Pax7^+/YFP^+$ cells immediately differentiated.

It's thus clear that satellite cells are not a homogeneous population of muscle progenitor cells, like once thought, but rather exist as incredibly heterogeneous populations, with different gene expression patterns, differentiation potential and cell fates during postnatal muscle growth and regeneration.

1.1.4.3 Satellite cell markers

Even in adult muscle that has no pathology, has not been subjected to damage and is not undergoing hypertrophy i.e. under normal physiological conditions, satellite cells express a plethora of markers, including the transcription factors Pax7 (Seale et al. 2000) and Pax3 (Relaix et al. 2006), the cluster of differentiation protein CD34 (Beauchamp et al. 2000), the myogenic regulatory factors MyoD (Zammit et al. 2004) and Myf-5 (Beauchamp et al. 2000), the receptor tyrosine kinase c-Met (Allen et al. 1995; Cornelison & Wold 1997; Wozniak et al. 2003), cell adhesion molecule M-cadherin (Irintchev et al. 1994), neural cell adhesion molecule (NCAM) (aka CD56) (Schubert et al. 1989; Boldrin et al. 2010), cell surface attachment receptor α7/β1-integrin (Burkin & Kaufman 1999; Gnocchi et al. 2009), myocyte nuclear factor (MNF) (Garry et al. 1997), Syndecan-3 and -4 (Cornelison et al. 2001) and Sca-1 (Mitchell et al. 2005). With the exception of Pax7, none of these markers are exclusive to adult muscle satellite cells. Rather satellite cells in muscle samples are identified according to anatomical position, nuclear morphology in addition to one or more markers. However once satellite cells have been isolated from their muscle niche and are cultured *in vitro*, analysis of specific marker expression is the primary way to ascertain their identity. Furthermore analysing the expression of specific markers can also be used to assess the activation status of satellite cells and to identify the presence of specific subpopulations. Refer to Table 1.2 below for detailed information on the major satellite cell markers and when they are known to be expressed.

It's important to note that satellite cells exhibit heterogeneity with regards to marker expression as their expression in satellite cells is a dynamic process. Gain-of-function and loss-of-function studies performed by Mitchell *et al.* (2005) showed that Sca-1 had a functional role in regulating myoblast proliferation and differentiation, and that Sca-1 expression was not static but rather dynamic in their primary mouse myoblast cell cultures (Mitchell et al. 2005). Experiments using primary cells from

Sca-1/GFP transgenic mice showed that when GFP^+- and GFP^--sorted cells were mixed in culture, GFP expression was modulated both positively and negatively (Mitchell et al. 2005). Before co-culture GFP^+ cells were infected with a β-galactosidase (β-gal) expressing retrovirus, while GFP^- cells were infected with a control retrovirus. After 48 h of co-culture, GFP^-/β-gal^+ and GFP^+/β-gal^- cells were present in the culture. In contrast, no dynamic modulation of GFP expression was seen under clonal conditions (Mitchell et al. 2005). The mechanisms underlying the dynamic expression of Sca-1 are currently unknown, however it's clear that changes in Sca-1 were highly dependent on the growth conditions (Mitchell et al. 2005). Mitchell *et al*. (2005) thus provided evidence toward the concept that satellite cell heterogeneity can be modulated by the microenvironment.

In conclusion because any intervention *in vitro* could cause satellite cells to alter their properties and make them more or less similar with regards to marker expression, it is crucial to identify satellite cells as accurately as possible, prior to intervention (e.g. addition of a growth factor) in order to determine their 'baseline' characteristics.

Table 1.2: Summary of key markers of satellite cells.

Satellite cell marker	Biological function	Satellite cell state expression	Marker localization	Expression in other cell types	Refrences
MNF	TF: myogenic cell differentiation	Q, A	Nucleus	Myonuclei in regenerating fibers, myocytes,brain and kidney	(Garry et al. 1997)
NCAM (CD56)	GP: Cell-cell adhesion	A	Cell Membrane	Myoblasts, myotubes, lymphocytes, NK cells, dendritic cells, neurons, glia	(Schubert et al. 1989; Boldrin et al. 2010)
CD34	GP: Cell-cell adhesion	Q, A	Cell Membrane	Hematopoietic stem and progenitor cells	(Beauchamp et al. 2000)
c-Met	R: Signaling	Q, A	Cell Membrane	pericytes, neural crest lineage	(Allen et al. 1995; Cornelison & Wold 1997; Wozniak et al. 2003)
M-cadherin	GP: Cell-cell adhesion	Q, A	Cell Membrane	Granular cells of the cerebellum and brain	(Irintchev et al. 1994)
β1-integrin	R: Signaling	Q, A	Cell Membrane	widely expressed	(Burkin & Kaufman 1999; Boppart et al. 2006)
α7-integrin	R: Signaling	Q, A	Cell Membrane	Fibers, neurons, vasculature and nervous system	(Burkin & Kaufman 1999; Boppart et al. 2006)
Syndecan-3	Co-R: Signaling	Q, A	Cell Membrane	Macrophages, leukocytes, chondorcytes, uterine tissue, ovarian cancer	(Cornelison et al. 2001)
Syndecan-4	Co-R: Signaling	Q, A	Cell Membrane	Macrophages, leukocytes, mammary cells, breast cancer	(Cornelison et al. 2001)
Sca-1	GP: signaling (True functions still unclear)	Q, A	Cell Membrane	Hematopoietic stem cells	(Mitchell et al. 2005)

Footnote: Table 1.2 depicts the most notable satellite cell markers, their nature and known functions, when they are expressed in/on satellite cells, their localization and other cell types that are also known to express them. TF - Transcription Factor; GP - Glycoprotein; R - Receptor; Co-R - Co-receptor. Q - Quiescent state; A - Activated state. Table adapted from (Boldrin et al. 2010).

1.2 GROWTH FACTORS IN SATELLITE CELL REGULATION

As mentioned before, upon mechanical disruption of the ECM, proteolytic enzymes like serine proteases and matrix metalloproteinases (MMPs) trigger the release of inactive growth factors, which can then induce chemotaxis, proliferation and differentiation of satellite cells. Macrophages, which invade and phagocytose areas where tissue damage is present upon injury, also release growth factors such as, Fibroblast growth factor (FGF) and Insulin-like growth factor (IGF) and cytokines such as Interleukin-6 (IL-6) which elicit mitogenic effects on satellite cells (Tidball & Villalta 2010; Kharraz et al. 2013; Saclier et al. 2013). Also, even resident supporting cells such as fibroblasts and vascular endothelial cells of damaged blood vessels, can release factors that support satellite cell proliferation (Ceafalan et al. 2014).

The released/activated growth factors in turn bind to their respective receptors on the surface of satellite cells in order to regulate satellite cell activity. This section will discuss the role of some of the most prominent growth factors known to affect satellite cell activation and will highlight the superiority of HGF signaling in inducing satellite cells to exit quiescence.

1.2.1 FIBROBLAST GROWTH FACTOR (FGF)

Fibroblast growth factors (FGFs) are a large family of related growth factors that function as powerful mitogens, and signal through the MAPK/ERK pathway. FGFs are secreted in high concentrations by satellite cells, in an autocrine fashion (Hannon et al. 1996), and fibroblasts in response to *in vivo* skeletal muscle damage. FGF signaling is mediated through binding to one of four transmembrane tyrosine kinases FGF receptors (FGFR) (FGFR1-4) with differential ligand binding specificity. In satellite cells FGFR-1 and -4 are the predominant isoforms expressed and are upregulated during muscle regeneration (Floss et al. 1997). However, they have been shown to induce opposite effects: in an *in vitro* cell culture study, constitutive expression of a full-length FGF receptor-1 and transient transfection of a truncated, non-functional form showed that this receptor regulated satellite cell proliferation (Scata et al. 1999), whereas qPCR analysis of *in vitro* satellite cell cultures showed that FGFR-4 is highly expressed in differentiating satellite cells and myofibres (Kästner et al. 2000). FGF signaling and the influence that it has on satellite cell function is thus dependent on the specific ligand. FGF-1, -2, -4 and -6 are known to greatly stimulate satellite cell

proliferation *in vitro* (Sheehan & Allen 1999; Kästner et al. 2000), whilst only FGF-1 and -2 were shown to also inhibit satellite cell differentiation. *In vivo*, FGF-6, which is expressed specifically in muscle (deLapeyrière et al. 1993), plays a crucial role during regeneration. This is evident in a study done by Floss *et al.* (1997), which demonstrated that *FGF-6*$^{-/-}$ mutant mice displayed reduced proportions of MyoD− and myogenin-expressing cells 9 days after a single freeze-crush injury (Floss et al. 1997). In addition, morphological alterations and changes to the adhesion properties of satellite cells were evident in the *FGF-6*$^{-/-}$ mutant mice (Floss et al. 1997).

1.2.2 INSULIN-LIKE GROWTH FACTOR (IGF)

Insulin-like growth factor is produced primarily in the liver in adult mammals and has two isoforms that work in a paracrine fashion: IGF-I and IGF-II are released and bind to distant cells and signal through the IGF-I receptor (IGF-1R). However during growth and regeneration other cells may synthesize IGF isoforms that act in an autocrine fashion. Both these isoforms participate in satellite cell regulation through promotion of cellular proliferation and differentiation, however the time frames for their expression during muscle regeneration is different (IGF-I expression precedes that of IGF-II) (Hayashi et al. 2000). IGF-I is known to stimulate both proliferation and differentiation (Allen & Boxhorn 1989), whereas IGF-II only induces the latter and its expression is heightened just before differentiation (Florini et al. 1996). The effect that IGF-I has on satellite cell proliferation has been attributed to the direct stimulation of Cyclin-D expression (Bark et al. 1998), whereas its downstream effects on myogenin gene expression promotes differentiation (Florini et al. 1991). Both isoforms are critical to myoblast differentiation as is evident in *in vitro* siRNA knock-down experiments, indicating compromised differentiation in the absence of either IGF-I or IGF-II (Florini et al. 1996).

1.2.3 INTERLEUKIN-6 (IL-6)

Interleukin-6 (IL-6) is a multifunctional cytokine with very powerful inflammatory properties, as it plays a central role in the acute-phase response (Geiger et al. 1988; Gauglitz et al. 2008). It's been shown to be released by a range of cells including, neutrophils, macrophages, fibroblasts, myofibers and satellite cells (Kurek et al. 1996; Gallucci et al. 1998; Tidball & Villalta 2010; Kharraz et al. 2013; Saclier et al. 2013). Due to the fact that IL-6 has been observed to promote satellite cell proliferation

in response to injury (Cantini & Carraro 1995), our group (Dr. P Steyn, Unpublished) (Steyn 2015) investigated the effects of IL-6 on satellite cells and the molecular mechanisms underlying IL-6's pro-proliferative effects. These experiments showed that IL-6 is a very powerful mitogen, with the ability to markedly increase satellite cell proliferation. However, the effects elicited by IL-6 seemed to be dose dependent, with low concentrations of IL-6 (10 pg/mL) actively maintaining satellite cells in the cell cycle. In contrast, a 1000-fold increase in IL-6 concentrations (10 ng/mL) promoted satellite cell cell-cycle exit and differentiation. These dose-dependent dual effects of IL-6 on satellite cells were shown to be due to differential activation of the Janus Kinase/Signal Transducer and Activator of Transcription/Suppressor Of Cytokine Signaling (JAK/STAT/SOCS) pathway. Low IL-6 levels caused preferential activation of JAK1/STAT3, which lead to increased proliferation, as its signaling induced hyper-phosphorylation of the retinoblastoma protein (Rb), a powerful stimulator of cell cycle progression. The high dose instead favoured cell cycle exit and differentiation by preferentially signaling through the JAK2/STAT2 pathway, which in turn induced increased MyoD expression. MyoD negatively regulates retinoblastoma, by preventing its hyper-phosphorylation (Steyn 2015). These results support the pro-proliferative effects of IL-6 on satellite cells that have been reported in the literature and provide evidence into the molecular mechanisms that underpin them.

All the growth factors listed thus far only affect the proliferation and differentiation of satellite cells. None of them are known to perform the first key aspect of muscle regeneration which is the activation of dormant satellite cells. To date only one growth factor is known to have this ability: hepatocyte growth factor (HGF).

1.2.4 HEPATOCYTE GROWTH FACTOR (HGF)

HGF (aka Scatter factor or Hepatopoietin-A) is a growth factor that was first identified in 1984, when it was shown to stimulate the growth of hepatocytes in damaged rat livers (Michalopoulos et al. 1984). HGF has since been detected in several tissues and organs and is thought to be produced by cells with mesenchymal origins (Zarnegar & Michalopoulos 1995), particularly fibroblasts, in liver, lung, epithelial and brain tissue (Stoker 1989; Hamanoue et al. 1996; Matsumoto & Nakamura 1997). This growth factor elicits pleiotropic effects, ranging from cell proliferation, differentiation and migration and is critical during embryogenesis for normal organ development (Sonnenberg et al. 1993; Santos et al. 1994; Schmidt et al. 1995; Maina et al. 1996; Takayama et al. 1996; Birchmeier &

Gherardi 1998). In addition to being required for organogenesis, it is now known that the biological effects of HGF in adult tissues range from stimulating cell proliferation, cell survival, motility, angiogenesis and morphogenesis (Miyazawa et al. 1994; Zarnegar & Michalopoulos 1995). The vast array of cellular processes HGF is known to induce in different tissues and cell types, is also seen in adult skeletal muscle and more specifically with satellite cells. In skeletal muscle, HGF can stimulate satellite cell proliferation (Miller, Thaloor, Matteson & Grace K Pavlath 2000), induce differentiation (Miller, Thaloor, Matteson & Grace K Pavlath 2000), aid in their migration and is a powerful mitogen (Miller, Thaloor, Matteson & Grace K Pavlath 2000). It therefore, along with other known growth factors, plays a central role in all stages of the satellite cell life cycle. However, within the context of muscle regeneration following damage, HGF plays the most crucial role: satellite cell activation through both paracrine and autocrine signaling (Allen et al. 1995).

1.2.4.1 The structure and properties of HGF

Although several isoforms of HGF exist in humans, the main isoform is synthesized from a ~6 Kb mRNA transcript located on Chromosome 7 which generates an 83 kDa protein (Seid et al. 1991). This protein is then secreted as an inactive single chain precursor (pro-HGF) and stored in the ECM, bound to heparan sulfate proteoglycans (HSPG) (Strain 1993; Derksen et al. 2002). Proteolytic cleavage of pro-HGF, by urokinase-type plasminogen activator (uPA) or HGF activator (HGFA) (Miyazawa et al. 1994; Shimomura et al. 1995; Miyazawa 2010), generates a mature and active α/β heterodimer, with a 69 kDa alpha subunit linked to a 34 kDa beta subunit (Nakamura et al. 1989). The alpha subunit is comprised of an N-terminal hairpin loop (HL) and four kringle domains (K1-K4), while the beta subunit contains a serine protease-like (SPH) domain. HGF binds with high affinity to specific transmembrane receptors and induces intracellular signaling.

To date sequences of 6 isoforms of HGF have been deposited on UniProtKB, of which only 2 alternatively spliced transcript variants are known to generate functional proteins: NK1 and NK2 (Chan et al. 1991; Miyazawa et al. 1991; Cioce et al. 1996). These isoforms represent functionally active truncated versions of the full HGF protein, which compete with HGF for binding to its receptor c-Met (discussed in Section 1.2.4.3) (Lokker & Godowski 1993; Cioce et al. 1996; Jakubczak et al. 1998). However, they differ from HGF in both their regulation and their biological and cellular activities (Lokker et al. 1992).

1.2.4.2 Pro-HGF vs. mature HGF

Under normal physiological conditions pro-HGF is maintained sequestered in the ECM bound to HSPGs due to its high affinity for them (Naldini et al. 1991). The pro-HGF form does however have low affinity for c-Met but is unable to induce any tyrosine activity (Naldini et al. 1992). Thus, two critical steps are required to induce receptor activation: a) release of pro-HGF from HSPGs and b) the conversion of pro-HGF into the mature and active heterodimer.

Release of pro-HGF from HSPGs

Matrix metalloproteinases (MMPs) play a key role in ECM degradation during wound healing and tissue remodelling, and it is now also known that MMPs mediate HGF release from HSPGs (Yamada et al. 2006). It has been reported previously that nitric oxide (NO) mediates activation of satellite cells after crush injury (Anderson 2000), whilst mechanical stretching of quiescent satellite cells induced their activation *in vitro* (Tatsumi et al. 2001). There could thus be a link between chemical signaling and mechanical perturbation in the activation of satellite cells. Indeed, studies geared to elucidate this possible link showed that mechanical stretching of satellite cells *in vitro* induced nitric oxide synthase (NOS) activity and that both the neuronal (nNOS) and endothelial (eNOS) isoforms of NOS were present in the culture medium (Tatsumi et al. 2006). Furthermore, the HGF released from mechanical stretching was shown to be NO-dependent (Tatsumi et al. 2002). It therefore seems as though an intimate relationship between nitric oxide production and HGF release exists, supporting the notion that in an *in vivo* muscle injury scenario, satellite cell activation is mediated by chemical signals and mechanical perturbation of the ECM. Anderson (2000) proposed a model for NO-mediated HGF release following mechanical shearing of the muscle fibre (Anderson 2000). This incomplete model has been supported by growing evidence (Anderson 2000; Tatsumi et al. 2001; Tatsumi et al. 2002; Tatsumi et al. 2006). The model hypothesises that insult to the muscle fibre causes mechanical shearing of the myofibre and surrounding ECM, which stimulates activation of nNOS, present beneath the sarcolemma of the skeletal muscle fibres (Grozdanovic & Baumgarten 1999). Activation of nNOS causes a massive release of nitric oxide which in turn mediates the release of pro-HGF from HSPGs. The manner by which NO mediates this is however unknown, although recent evidence suggests that MMPs are in fact involved in the NO-mediated release of HGF (Yamada et al. 2006). MMP-2 was subsequently shown to be produced in satellite cells treated with

a NO donor (sodium nitroprusside), which resulted in HGF release into the culture medium (Yamada et al. 2008). NO-activated MMP-2 may thus well mediate release of pro-HGF from HSPGs *in vivo*.

Conversion of pro-HGF into the mature and active HGF

Newly released pro-HGF, in response to mechanical perturbation of the ECM, requires subsequent proteolytic cleavage and conversion into its mature and active form: the α/β heterodimer. This conversion takes place in the ECM where a milieu of proteases, (comprising urokinase-type plasminogen activator (uPA), tissue-type plasminogen activator (tPA), blood coagulation factor XII, factor XI, hepatocyte growth factor activator (HGFA), plasma kallikrein, matriptase and hepsin) convert HGF to its active form (Naldini et al. 1992; Shimomura et al. 1995; Lee et al. 2000; Peek et al. 2002; Kirchhofer et al. 2005). Of note, urokinase-type plasminogen activator (uPA) proteolytically cleaves specific residues on pro-HGF (Naldini et al. 1992), due to the proteolytic cleavage site present on HGF being identical to that found on plasminogen (Miyazawa et al. 1989; Miyazawa et al. 1994). Similarly to HGF, uPA is present in the ECM in an inactive form, and needs to be enzymatically cleaved to its active form, which is carried out by serum derived proteases (Naldini et al. 1992). In contrast, hepatocyte growth factor activator (HGFA) (a blood coagulation factor XII-like serine protease) (Miyazawa et al. 1993; Miyazawa et al. 1998) is present both in serum and in plasma. However, the HGFA present in serum is in an active form, while the one found in plasma is found in an inactive form, and requires proteolytic cleavage to become active (Shimomura et al. 1993). Conversion of inactive HGFA into its mature form is performed by thrombin (Shimomura et al. 1993) thereby linking the activation of HGFA exclusively to injured tissue (Miyazawa et al. 1996). It is thus clear that maturation involves an intricate series of events, each with numerous players interacting with each other, to coordinate the release of pro-HGF from HSPGs and subsequently convert it to its mature and active heterodimer, able to bind c-Met with high affinity. However, HGF does not only act in a paracrine fashion, but also in an autocrine manner, with satellite cells having been reported to actively synthesize and release HGF when cultured *in vitro* (Sheehan et al. 2000).

HGF mRNA is present in cultured satellite cells and has been shown to be translated into protein (Sheehan et al. 2000). Moreover, HGF protein has been detected in the conditioned media, signifying that satellite cells were secreting HGF. Evidence that the secreted HGF was acting on the satellite cells to promote proliferation in an autocrine fashion, was confirmed by Sheehan *et al.* (2000), who used the addition of neutralizing HGF antibodies and showed a significant reduction in

satellite cell proliferation (Sheehan et al. 2000). Taken together, these data indicate that satellite cells are able to synthesize and release the active form of HGF, which then acts as an autocrine signaling molecule to stimulate further satellite cell proliferation. The *in vitro* data suggests the source of mature HGF evident in an injured ECM environment, may not only be as a result of proteolytic cleavage of pro-HGF but could also be derived from *de novo* HGF production. Mature HGF has also been extracted from the ECM of uninjured rat muscles (Tatsumi & Allen 2004), suggesting that the active form of HGF is also present in the ECM in an uninjured *in vivo* environment. It therefore seems as though mature HGF, just like pro-HGF, is also sequestered in the ECM by HSPGs (Sheehan et al. 2000; Tatsumi & Allen 2004). The biological significance for this is still unclear, however, mature HGF displays a far greater affinity for c-Met compared to HSPGs.

1.2.4.3 The HGF receptors

On the surface of satellite cells there are two main types of receptors to which HGF is able to bind: i) c-Met, a high-affinity receptor and ii) heparan sulphate proteoglycans (HSPGs) which represent a group of low-affinity ligand biding sites.

c-Met

c-Met, is a heterodimeric transmembrane glycoprotein composed of an alpha subunit (50 kDa) and a larger beta subunit (145 kDa), which are linked together *via* a disulphide bond (Tempest et al. 1988; Giordano et al. 1989; Komada et al. 1993). The alpha subunit is entirely extracellular and together with the amino-terminal region of the beta subunit, forms the semaphorin (Sema) domain (Stamos et al. 2004). The extracellular portion of the beta subunit, however, is further composed of a plexin-semaphorin-integrin (PSI) domain (Kozlov et al. 2004) and four immunoglobulin-plexin-transcription (IPT) domains (Bork et al. 1999). The intracellular portion of the beta subunit is composed of a distinctive juxtamembrane sequence located just underneath the plasma membrane and has two domains: i) a tyrosine kinase catalytic domain and ii) a multifunctional docking site domain, on the carboxy-terminal region. The kinase domain is central to c-Met activity as once it's phosphorylated, it induces activation of the receptor while the two flanking domains modulate c-Met signaling: The juxtamembrane sequence negatively regulates c-Met signaling, while the multifunctional docking site is critical to the recruitment of signal transducers and adaptors required for c-Met signaling (Comoglio et al. 2008; Trusolino et al. 2010).

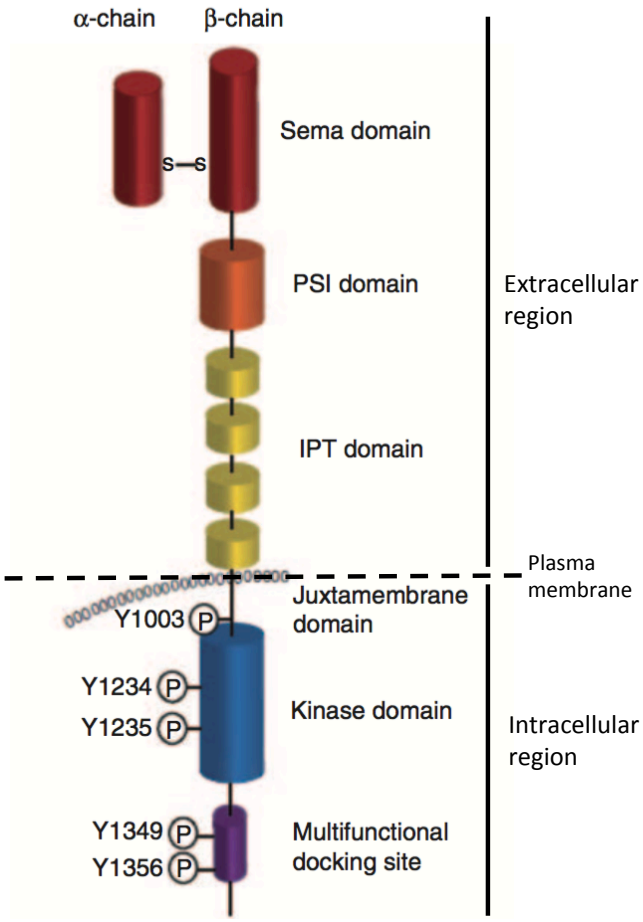

Figure 1.2: Domain structure of c-Met receptor.

c-Met is composed of two subunits: the α chain, which is entirely extracellular and the beta chain. The alpha chain together with the amino-terminal region of the β-chain, forms the semaphorin (Sema) domain. Located on the extracellular portion of the beta subunit are also the plexin-semaphorin-integrin (PSI) domain and four immunoglobulin-plexin-transcription (IPT) domains. The intracellular portion of the beta subunit is composed of: i) a distinctive juxtamembrane sequence located just underneath the plasma membrane and ii) a tyrosine kinase catalytic domain and a multifunctional docking site domain. Image modified and reproduced without permission from (Organ & Tsao 2011).

Both the alpha and beta chains of HGF play key roles in c-Met binding and activation, and their cooperation is necessary to elicit HGF's biological activities. HGF is a bivalent ligand, as it contains both high and low affinity binding sites for c-Met: The high affinity binding site for c-Met is present on the alpha chain of HGF, while the low affinity binding site is present on the beta chain, within the SPH domain (Matsumoto et al. 1998). In 2008, Basilico *et al.* showed that it's the IPT domain, specifically IPT 3 and 4, on c-Met that binds the alpha chain of HGF with high affinity (Basilico et al. 2008), and that this interaction provided the necessary binding strength to keep HGF bound to c-Met. In contrast, the beta chain of HGF complexes with the Sema domain on c-Met but this weak interaction is required for correct c-Met activation, rather than actual binding (Stamos et al. 2004;

Matsumoto et al. 1998). Indeed, pro-HGF is able to bind c-Met with high affinity, but is not able to induce signaling (Lokker et al. 1992), due to the fact that proteolytic cleavage of pro-HGF is required to expose the residues on the β-chain of HGF that bind the Sema domain (Kirchhofer et al. 2004; Kirchhofer et al. 2007). However, the interaction of the α-chain of HGF with IPT3 and 4, on a c-Met receptor lacking a Sema domain, is sufficient to activate the kinase domain (Basilico et al. 2008). It therefore seems as though the interaction between β-HGF and the Sema domain is critical for c-Met to distinguish between the inactive and active forms of HGF. In conclusion, it's clear that there is a complex interaction between HGF and c-Met: The IPT domain provides a stable anchorage site to which the α-chain of HGF is able to bind, while the interaction between the Sema domain and the β-chain of HGF confers selective sensitivity to mature HGF.

Heparan sulphate proteoglycans

HSPGs are cell surface molecules that can function as secondary receptors for a variety of growth factors (Casar et al. 2004; Dreyfuss et al. 2009). By binding to them, they enhance the formation of their receptor-signaling complexes, and play a role in their signaling (reviewed in Bernfield et al. 1999).

In the case of HGF, HSPGs are not critical for HGF/c-Met signaling, but function as low affinity co-receptors that interact with the ligand-receptor complex to enhance signaling (Zioncheck et al. 1995; Kemp et al. 2006). There are several proposed theories as to how HSPGs can increase ligand-receptor signaling. Firstly, HSPGs may bind the ligand and help present it to its high affinity receptor. However, high affinity receptors display binding constants 10- to 100-fold higher for their ligands compared to the low affinity receptors, ligands will thus always preferentially bind their high affinity receptors (Schlessinger et al. 1995). A more plausible role for HSPG, is that due to their abundance on the cell surface, they may concentrate the ligand at the cell surface, thereby increasing the chances of HGF/c-Met interactions (Schlessinger et al. 1995; Kemp et al. 2006). Furthermore, HSPGs seem to promote HGF oligomerization and stabilize the dimeric ligand, resulting in facilitated receptor dimerization and activation (Zioncheck et al. 1995). Finally, HSPG-HGF interactions may potentiate c-Met signaling as their association can mediate the formation of a ternary c-Met-HGF-HSPG complex. This complex could result in bringing intracellular effectors of the c-Met signaling pathway in closer proximity, thereby aiding their activation (Derksen et al. 2002). However, HSPGs seem critical for the activity of the naturally occurring isoforms of HGF, NK1 and NK2, since in the

absence of HSPGs *in vitro*, these isoforms are shown to be unable to bind c-Met (Schwall et al. 1996; Chirgadze et al. 1999). Interactions between HSPGs and NK1, has been demonstrated to induce conformational changes to the HGF splice variant, enabling it to bind to c-Met (Schlessinger et al. 1995).

The interaction between HSPGs and growth factors bound to their primary receptors, is mediated by the heparan sulphate chains located on HSPG, which are selectively sulphated at specific positions by Sulf1 (Robertson et al. 1992). The degree to which these heparan sulphate (HS) chains are sulphated, and at what positions, can therefore affect HPSG interactions with growth factors, ultimately impacting the receptor-ligand signaling (Bernfield et al. 1999). A direct correlation has been found between increasing amounts of sulphated HSPGs and increased c-Met receptor phosphorylation (Zioncheck et al. 1995), implicating that the amount of HSPG sulphation is important for efficient binding to HGF, and the higher degree of sulphation on HS chains, the stronger the interactions are between HGF and HSPGs.

1.2.4.4 HGF signaling

Once HGF binds to c-Met it induces receptor homodimerization and phosphorylation of two conserved tyrosine residues within the catalytic domain: Y1234 and Y1235 (Rodrigues & Park 1994). Their phosphorylation is critical for intracellular signaling as they induce phosphorylation of tyrosines 1349 and 1356 which in turn are located in the multifunctional docking site (Ponzetto et al. 1994). Phosphorylated Y1349/1356 then recruit effectors of the c-Met signaling pathways (Birchmeier et al. 2003; Trusolino et al. 2010; Organ & Tsao 2011), including e.g. the ERK pathway, the phosphoinositide 3'-kinase/Akt (PI3K/Akt) (Leshem et al. 2002; Halevy & Cantley 2004), the p38/MAPK (Wu et al. 2000) and the JAK/STAT (Jang & Baik 2013) (refer to Figure 1.3). Activation of these intracellular pathways results in the expression of key myogenic genes which guide satellite cell activation and fate.

HGF has a very powerful control over satellite cells, inducing their activation and proliferation in order to generate sufficient numbers of proliferating myogenic precursor cells required for functional muscle regeneration. However c-Met signaling is tightly controlled and modulated. c-Met signaling is regulated in the intracellular compartment *via* negative feedback loops that inhibit its signaling. This is achieved by phosphorylation of tyrosine (Y1003), present on the juxtamembrane

sequence of c-Met, which recruits a ubiquitin ligase to the receptor (Comoglio et al. 2008; Trusolino et al. 2010). Also, some of the pathways downstream of c-Met can also signal satellite cells to exit from the cell cycle and differentiate or return to quiescence. PI3K/Akt signaling was shown to enhance transcriptional activity of MyoD and MEF2, both important regulators of cellular differentiation, with MyoD critical to myoblast differentiation as it regulates myogenin expression (Xu & Wu 2000). Similarly p38/MAPK signaling is also a positive regulator of myogenesis through MyoD and MEF2 proteins, as it was shown to enhance their transcriptional activities (Wu et al. 2000). Activation of the p38/MAPK pathway is independent of the PI3K/Akt pathway, and could function parallel to PI3K/Akt signaling to induce myogenesis, however, inhibiting either pathway resulted in loss of myoblast differentiation (Wu et al. 2000). Finally, the JAK/STAT family has been implicated in promoting and repressing both myoblast proliferation and differentiation. JAK1-STAT1/3 induces proliferation while it seems as though STAT2/3 phosphorylation through JAK2 is required for differentiation.

It's clear that depending on which pathway is activated in response to HGF binding, different molecular and cellular responses are elicited that ultimately stimulates satellite cell proliferation or differentiation.

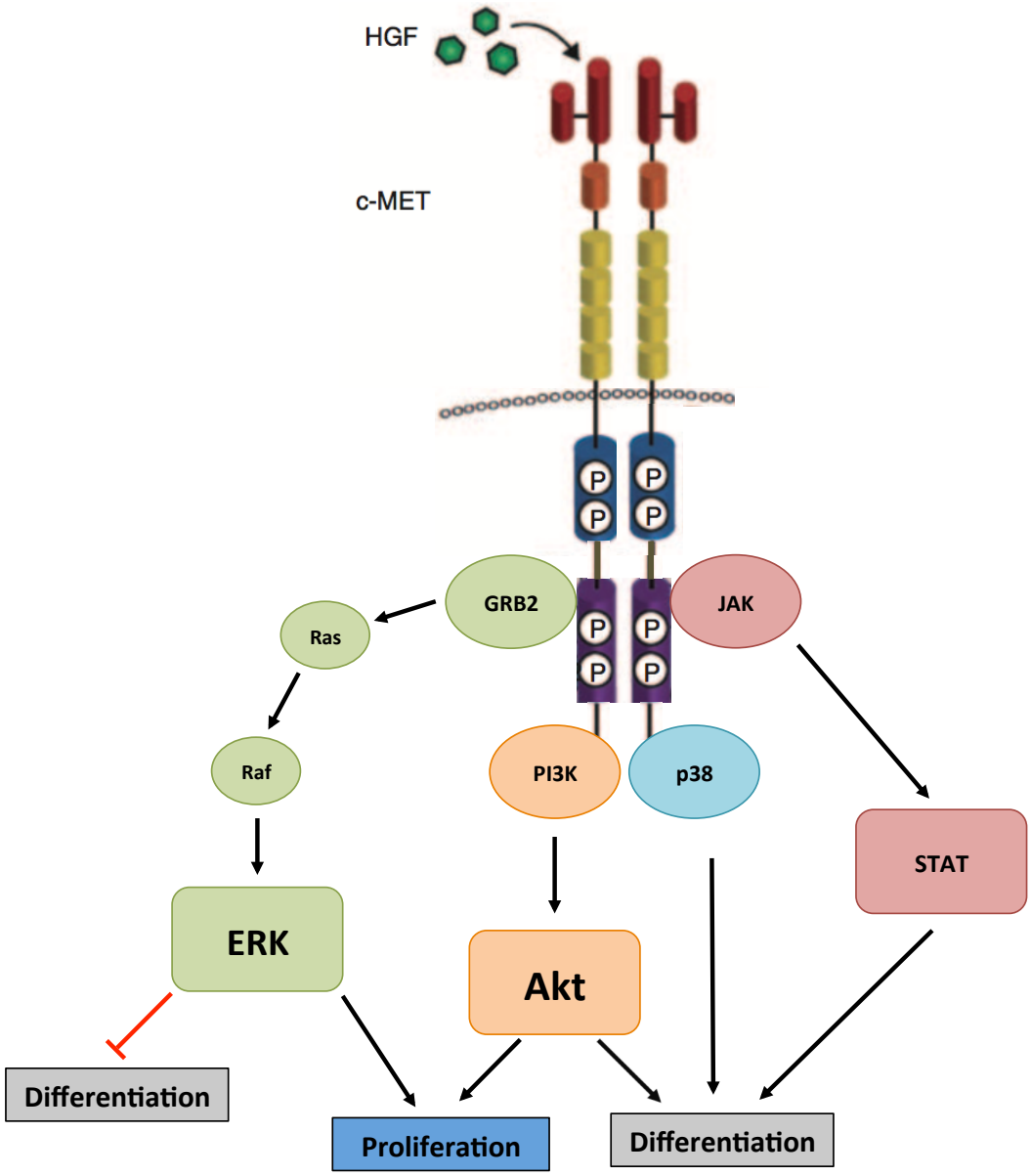

Figure 1.3: HGF signaling through c-Met

HGF binding to c-Met causes receptor homodimerization, which leads to phosphorylation of two conserved tyrosine residues within the catalytic domain (in blue): Y1234 and Y1235. Their phosphorylation induce phosphorylation of tyrosines 1349 and 1356 located in the multifunctional docking site (in purple). Phosphorylated Y1349/1356 then recruit effectors of the c-Met signaling pathway, which signal through the ERK pathway or the PI3K/Akt pathway. c-Met also signals through the p38/MAPK and JAK/STAT pathway. Image modified and reproduced without permission from (Organ & Tsao 2011).

1.3 THE INTRICATE RELATIONSHIP BETWEEN SATELLITE CELLS AND HGF

1.3.1 DOSE DEPENDENT EFFECTS OF HGF ON SATELLITE CELLS: LOW vs. HIGH CONCENTRATIONS

HGF's effect on satellite cells has recently been shown to be concentration dependent, perhaps explaining the complexity to HGF/c-Met signaling and satellite cell regulation in muscle regeneration. It was observed that satellite cells elicit different behaviours *in vitro* depending on the concentrations of HGF (Yamada et al. 2010). Varying HGF concentrations in the culture media either stimulated or repressed satellite cell proliferation. It was shown that 2.5 ng/mL of HGF maximally stimulated satellite cell proliferation, while proliferating satellite cells treated for 24 h - 76 h with concentrations of HGF ranging from 10-500 ng/mL showed decreased proliferation, in an HGF dose-dependent manner (Yamada et al. 2010). The reduced proliferation exhibited by the satellite cells cultured with high concentrations of HGF was not due to impairment of their cellular viability nor were the satellite cells differentiating, as subsequent treatment with lower HGF concentrations (2.5 ng/mL) induced re-activation and re-established increased proliferation within a 48 h time frame. Yamada *et al*. (2010), hypothesized that high levels of HGF were inducing cellular quiescence.

Evidence supporting their hypothesis was provided by analysing the satellite cell mRNA expression levels of known negative (myostatin) and positive (MyoD) regulators of myogenesis post-HGF treatment. In cells treated with high concentrations of HGF elevations in intracellular myostatin protein levels as well as the release of myostatin into the conditioned media was evident. Concentrations of HGF ranging from 10 - 50 ng/mL were enough to induce significant increases of intracellular myostatin levels (Yamada et al. 2010). Furthermore, low levels of myogenin expression were seen in cells treated with 2.5 ng/mL and 500 ng/mL HGF, while MyoD protein expression was only seen in the 2.5 ng/mL HGF cultures (Yamada et al. 2010). These findings support the idea that high concentrations of HGF induce cellular quiescence, as both myogenin and MyoD expression, which are pivotal for myoblast differentiation, were inhibited by high HGF concentrations. Similar results have been described by other groups: i) addition of 50 and 100 ng/mL of HGF in an organ culture system of embryonic mouse tongue decreased myogenin and MyoD mRNA levels significantly (Yamane et al. 2004), ii) 2 ng/mL of HGF stimulated C2C12 and human skeletal myoblasts (HSkM) proliferation *in vitro*, while 10 ng/mL resulted in significantly decreased

proliferation (Walker et al. 2015), and iii) MyoD expression along with myotube fusion was significantly decreased in differentiating C2C12 and HSkM cells treated with 2 ng/mL of HGF (Walker et al. 2015). Conversely, Walker *et al*. (2015) reported that 10 ng/mL of HGF stimulated differentiation in C2C12 and HSkM cell cultures, as they displayed increased $MyoD^+$ cells and increased myotube formation. This is not in agreement with the findings of Yamada *et al.* (2010), as they reported no MyoD expression in their study. However the concentrations of HGF used in the two studies were 50-fold different, 10 ng/mL versus 500 ng/mL, and thus cannot be compared directly. On the other hand Walker *et al.*'s (2015) findings are consistent with the *in vivo* data reported by Miller *et al.* (2000). The authors reported a 3-fold increase in $MyoD^+$ myoblasts in the *TA* muscles of mice, 1 day after simultaneous injury and injection with 50 ng of HGF (Miller, Thaloor, Matteson & Grace K Pavlath 2000). Miller *et al*. (2000) also investigated the dose effects of HGF in their studies. In an experiment, Miller *et al*. (2000) showed that injured muscles treated with a single, daily injection of 50 ng of HGF, starting on the day of injury and continuing through day 3, displayed significantly less regenerated fibres (7 days post-injury) compared to injured muscles injected daily with only 6.25 ng HGF (Miller, Thaloor, Matteson & Grace K Pavlath 2000). This *in vivo* data corroborates previous work by Gal-Levi *et al.* (1998) with chicken satellite cells and supports the notion that HGF inhibits differentiation, in a dose-dependent manner (Gal-Levi et al. 1998). Thus it seems that different concentrations of HGF affect the expression of key myogenic genes differently, supporting the notion that HGF can regulate satellite cell fate and promote either proliferation or differentiation. However, effects of 'high' concentrations may be influenced by the model being investigated.

1.3.2 TIME DEPENDENT EFFECTS OF HGF ON SATELLITE CELLS: EARLY vs. LATE

Another important consideration is the timing of HGF exposure and possible timing-dose interactions. In an 'early' time phase after muscle injury HGF present in the ECM in a low amount is released and would bind to c-Met, stimulating satellite cell activation and proliferation. In a 'late' time phase the concentrations of HGF in the ECM are much higher due to i) a large amount of HGF being released from HSPGs following extensive ECM degradation; ii) autocrine secretion; and iii) additional HGF, produced from the liver and spleen, delivered to the site of injury *via* blood flow (Suzuki et al. 2002).

In experimental models satellite cells seem to elicit different responses to HGF, depending on when in the muscle regeneration time-frame they are exposed to HGF. Miller *et al.* (2000) showed that treatment with 50 ng of HGF 2 and 3 days post-injury did not further increase myoblast numbers compared to muscles treated with HGF on the day of injury (Miller, Thaloor, Matteson & Grace K Pavlath 2000). Furthermore, multiple injections of HGF significantly inhibited muscle regeneration and this inhibition was found to be time dependent. In this experiment, injured muscles were treated with a single daily injection of 50 ng of HGF starting on different days after injury (0-2 days; 2-4 days and 4-6 days). Muscle samples treated with 50 ng of HGF on days 2-4, after injury, displayed the least regeneration (Miller, Thaloor, Matteson & Grace K Pavlath 2000). Miller *et al*. (2000) hypotheiszed the reason as to why HGF treatment inhibited fibre formation so significantly when administered 2-4 days after injury is due to the fact that, *in vivo*, myoblast fusion occures in the period between day 2 and day 3. But the effect of HGF may be influenced by the c-Met protein expression, which has been shown to be upregulated in proliferating satellite cells but downregulated in differentiating myoblasts (Gal-Levi et al. 1998; Miller, Thaloor, Matteson & Grace K Pavlath 2000; Yamada et al. 2010).

In summary the regulation of satellite cell proliferation and differentiation is thus tightly regulated by HGF/c-Met signaling and the effects of this signaling seem to be both concentration and time dependent. The data presented in Sections 1.1.3.2 and 1.2.4.4. implicate HGF's regulation of satellite cells to be mediated by different downstream signaling pathways which favour either proliferation or differentiation, while data present in Sections 1.3.1 and 1.3.2 explain a time and concentration component to HGF regulation of satellite cell fate during muscle regeneration.

Table 1.3: Summary of key studies regarding the dose- and time-dependent effects of HGF on satellite cells *in vivo* and *in vitro.*

Authors	Study design (model, intervention)	Time points/culture period	Results
Yamada *et al*. 2010	Primary culture of satellite cells isolated from 9-month-old Sprague-Dawley rats; 2.5 ng/mL - 500 ng/mL of HGF.	0 h - 76 h treatment period for HGF dose time course study (48 h post-plating) and 0 h - 48 h for HGF reactivation study.	2.5 ng/mL HGF induced maximal proliferation as seen by increased BrdU positive cells. 10 - 500 ng/mL HGF induced decreased proliferation activity in a concentration dependent manner. 10 - 50 ng/mL HGF induced myostatin expression. MyoD and myogenin levels were low or absent at 500 ng/mL HGF.
Yamane *et al*. 2004	Organ culture system of embryonic (E13) ICR mouse tongue; 0, 50 or 100 ng/mL of HGF.	8 day culture.	50 and 100 ng/mL HGF decreased MyoD, myogenin and muscle creatine kinase mRNA expression significantly. 50 and 100 ng/mL HGF increased Myf-5 mRNA expression.
Walker *et al*. 2015	C2C12 and human skeletal myoblasts (HSkM) cell culture; 0, 2 or 10 ng/mL of HGF.	Up to 7 day cell culture. Samples analysed at 1, 3, 5 and 7 days.	2ng/mL of HGF stimulated C2C12 and HSkM proliferation; 10 ng/mL resulted in significantly decreased proliferation. 2 ng/mL of HGF significantly decreased MyoD levels along with myotube fusion in differentiating C2C12s and HSkMs. 10 ng/mL of HGF stimulated differentiation in C2C12 and HSkM as seen by increased $MyoD^+$ cells and myotube formation.
Miller *et al*. 2000	4 - 6 week old C57BL/6 male mice; *in vivo* administration of 0, 6.25 and 50 ng HGF.	Muscle samples collected 7 days post-injury. HGF administered on day of injury and daily from day of injury.	50 ng HGF induced 3-fold increase in $MyoD^+$ myoblasts 1 day after simultaneous injury and injection. Injured muscles displayed significantly less regenerated fibres when treated with a single, daily injection of 50 ng of HGF compared to 6.25 ng HGF. Injured muscles displayed significantly less regenerated fibres when treated with 50 ng of HGF on days 2-4, after injury, when compared to injured muscles treated with 50 ng of HGF on days 0-2 or 4-6, after injury.
Gal-Levi *et al*. 1998	Primary chicken satellite cells (4-5 days old chickens) and C2C12s; 0 - 100 ng/mL of HGF and pCSAcHGF plasmids for transient transfection	4 days culture. Samples analysed at 2 and 4 days.	2 - 20 ng/mL HGF stimulated DNA synthesis, but higher concentrations (50 - 100 ng/mL) reduced DNA synthesis. Myosin heavy chain protein was decreased in an HGF dose-dependent manner. Ectopic expression of HGF inhibited differentiation and decreased MyoD and myogenin protein levels.

Whether the dose and time dependent effects presented affect all satellite cells or just a sub population still remains unclear, especially since distinct populations of satellite cells with different mitotic rates have been observed *in vivo* (Schultz 1996; Ono et al. 2010) and satellite cells differ in expression of typical markers and may, for this reason, differ in their responses to HGF. Furthermore, the *in vivo* agonistic and antagonistic effects elicited by other growth factors (eg: NK1, NK2, IGF-I, FGF, IL-6) could also influence HGF's dose and time dependent effects. Finally, HGF's regulation of satellite cells could be due to an influence on the expression of specific microRNAs (miRNAs), which are present in muscle cells and have been found to regulate all stages of myogenesis, during both embryogenesis and adulthood.

1.4 MICRO RNA: BIOGENESIS AND FUNCTION IN SKELETAL MUSCLE AND SATELLITE CELLS

MicroRNAs (miRNAs) are short (18-24 nucleotides) single-stranded non-coding RNA molecules, involved in post-transcriptional gene regulation. Expression of miRNAs, has been detected in muscle cells and they play specific roles in their differentiation during embryogenesis and adulthood. Mounting evidence has however shown that miRNAs interact with MRFs in all stages of myogenesis: beginning with the earliest evidence of satellite cell differentiation into myoblast precursor cells (MPCs); subsequent differentiation of MPCs into myoblasts; fusion of myoblasts into myotubes and finally myotube maturation into functional myofibres. The muscle specific miRNAs are termed 'myomiRs' and have also been implicated in actively maintaining satellite cells in a quiescent state (Crist et al. 2012; Cheung et al. 2012).

In eukaryotic cells, miRNAs can be encoded in both the intronic regions of a coding gene or from non-coding intergenic sequences (Lee et al. 2002; Mourelatos et al. 2002). RNA Polymerase II transcribes miRNA from these sequences (see Step 1, Figure 1.4) as long precursor molecules, termed primary-miRNA (pri-miRNA), which may contain several miRNAs embedded within hairpin folds (Kim 2005). The RNA binding protein DGCR8 associates with the hairpins present on the pri-miRNA and together with Drosha, an RNase III endonuclease, forms a microprocessor complex (see Step 2, Figure 1.4) (Lee et al. 2003; Denli et al. 2004; Landthaler et al. 2004). This complex then generates a ~70 nt precursor-miRNA (pre-miRNA) hairpin in the nucleus. The pre-miRNA is then exported into the cytoplasm *via* the nucleocytoplasmic shuttler Exportin-5 (see Step 3, Figure 1.4), for further processing (Yi et al. 2003; Bohnsack et al. 2004; Lund et al. 2004). In the cytoplasm the pre-miRNA hairpin is bound by the endonuclease Dicer, which cleaves the stem-loop region off the pre-miRNA, generating a short double-stranded miRNA (see Step 4, Figure 1.4) (Hammond et al. 2000; Bernstein et al. 2001). TRBP, another RNA binding protein, binds a miRNA strand and loads it into Argonaute, forming an RNA-induced silencing complex (RISC) (see Step 5, Figure 1.4) (Chendrimada et al. 2005; Haase et al. 2005).

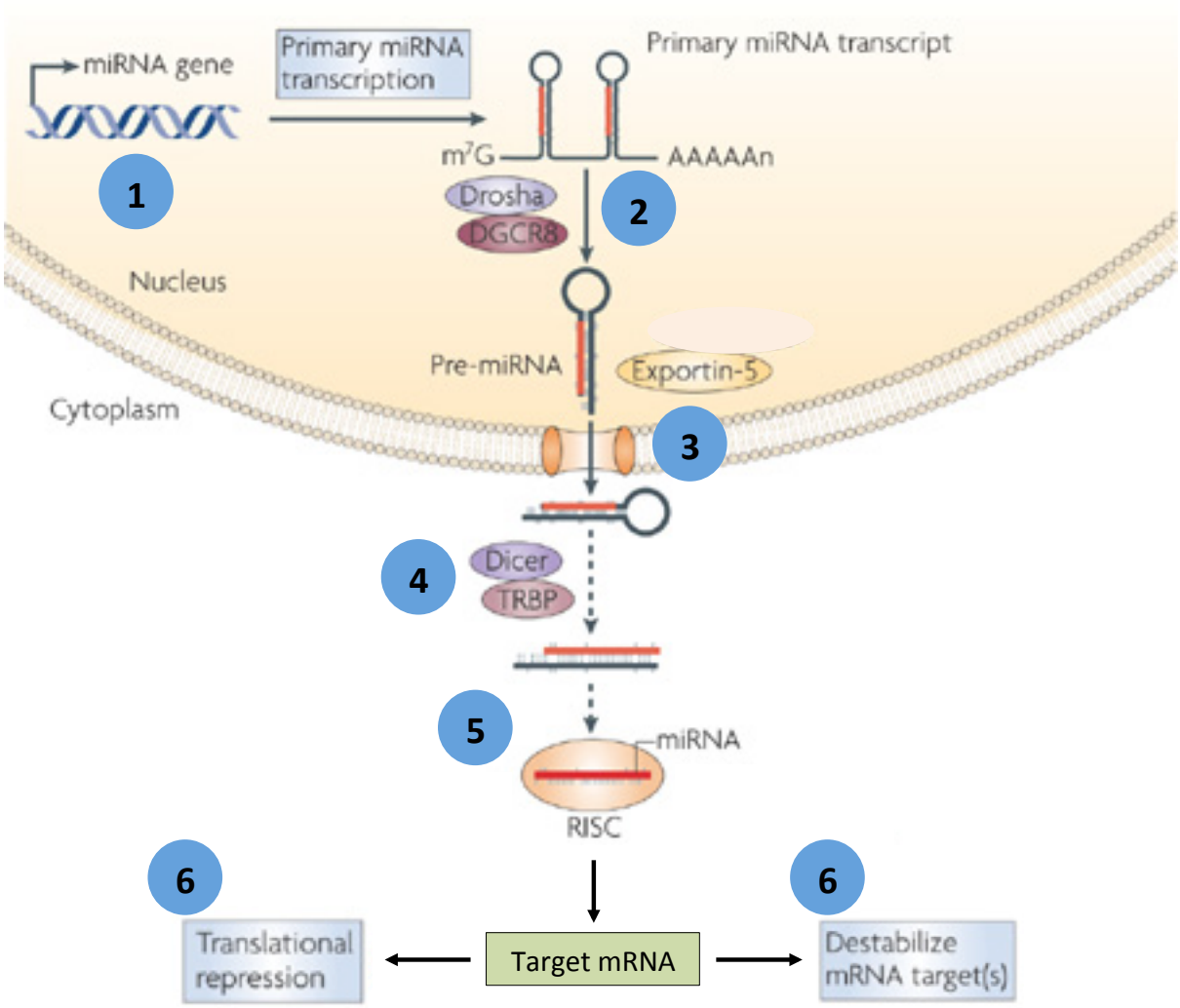

Figure 1.4: MicroRNA (miRNA) biosynthesis and functions in eukaryotic cells.

In the canonical microRNA (miRNA) bosynthesis pathway, (1) RNA Polymerase II transcribes long precursor molecules, termed primary-miRNA (pri-miRNA), from intronic or intergenic sequences. (2) The RNA binding protein DGCR8 associates with the hairpins present on the pri-miRNA and together with Drosha, an RNase III endonuclease, forms the microprocessor complex. This complex then generates a ~70 nt precursor-miRNA (pre-miRNA) hairpin in the nucleus. (3) The pre-miRNA is then exported into the cytoplasm *via* the nucleocytoplasmic shuttler Exportin-5 for further processing (see step 4-5 in text). (6) The RISC complex then binds target mRNA stands and either inhibits their translation or causes their degradation. Image modified and reproduced without permission from (Lodish et al. 2008).

The sequence similarity between the miRNA and its target mRNA allows the RISC complex to associate with the mRNA, usually within its 3'-UTR, and silence its expression (Bartel 2009). Depending on the degree of complementarity between the miRNA and the mRNA, the RISC complex can either inhibit the translation of the mRNA (partial complementarity) or degrade the mRNA (total complementarity) (see Step 6, Figure 1.4). Since RISC-mediated gene silencing doesn't require 100%

complementarity between the miRNA and the mRNA, a single miRNA can target multiple mRNAs. This mechanism could target a multi-gene network driving a specific cell fate transition.

Therefore, miRNAs represent an incredibly powerful tool for post-transcriptional gene regulation. In addition, miRNAs have tissue- and organ-specific expression, implicating them as important regulators of cellular differentiation and this is the case during embryogenesis and adulthood. Indeed differentiation of stem cells into their terminally differentiated counterparts requires the precise and coordinated activation and silencing of specific genetic programmes, which is mediated in part by miRNA-induced silencing reviewed extensively by Shenoy and Blelloch (Shenoy & Blelloch 2014).

1.4.1 MICRO RNAs IN MUSCLE

Muscle specific miRNAs, termed 'myomiRs', play a far greater role than was expected when they were first discovered (Wang et al. 2009; Crist & Buckingham 2009). Of note miR-1, miR-133 and miR-206, elicit muscle specific expression and have been shown to play a key role in myoblast differentiation (Wang et al. 2009; Crist & Buckingham 2009). miR-1 has been shown to promote myoblast differentiation by repressing histone deacetylase (HDAC-4), thereby maintaining MEF2 activity (Chen et al. 2006; Lu et al. 2000) and miR-206 targets the p180 subunit of DNA polymerase alpha, facilitating cell cycle withdrawal (Kim et al. 2006). In contrast, miR-133, promotes myoblast proliferation by repressing serum response factor (SRF) and by doing so inhibits myogenesis (Chen et al. 2006). miR-1 and miR-133 are present on the same pri-miRNA and thus get expressed together, even though they perform directly opposing roles in myogenesis (Kim et al. 2006). Moreover, non-myo miRNAs such as miR-29 and miR-181 for example are also known to play a regulatory role in myogenesis. miR-29 promotes myoblast differentiation by repressing the mRNA of transcription factor Ying Yang 1 (YY1), which functions as a gene transcription silencer (*via* chromatin modification) (Wang et al. 2008). On the other hand, miR-181 targets Hox-A11, a homeobox protein that represses MyoD transcription (Yamamoto & Kuroiwa 2003; Naguibneva et al. 2006).

Due to myogenesis being a stepwise process requiring an intricate cooperation between positive and negative regulators of gene expression, it comes as no surprise that miRNAs, both specific to muscle tissue and ubiquitously expressed, play important roles in mediating key events of myogenesis.

miRNAs can selectively repress specific genes involved in the myogenic programme, either directly by inhibiting their mRNA translation, or indirectly by repressing their activators. Recently, miRNAs have been discovered to regulate different stages of satellite cell activity - quiescence, activation, proliferation and differentiation.

1.4.2 MICRO RNAs IN SATELLITE CELLS

In 2009, Crist *et al*. discovered a novel miRNA (miR-27) present in Pax3 expressing satellite cells and showed that it regulates the initiation of the myogenic programme (Crist et al. 2009). The authors demonstrated that miR-27 expression was concomitant with the downregulation of Pax3 in activated satellite cells (Crist et al. 2009). Further analysis revealed that miR-27, negatively regulates Pax3 protein expression by binding to a single target site on the 3'-UTR of Pax 3 mRNA (Crist et al. 2009). Pax3 and Pax7 downregulation is required for differentiation to proceed (Boutet et al. 2012; Olguín et al. 2011). miRNA regulation of Pax7 has also been shown at the time of satellite cell differentiation: miR-1 and miR-206 expression is upregulated and target Pax7 that in turn leads to cell cycle exit (Chen et al. 2010). The predicted binding sites for miR-1 and miR-206 are also present on the 3'UTRs of Pax 3 variants (Blake & Ziman 2005), indicating that in satellite cells as in muscles a single miRNA can regulate different genes in a specific gene network. Furthermore, miR-146a (Kuang et al. 2009) miR-21 (Tatsuguchi et al. 2007; Thum et al. 2008) and miR-489 (Cheung et al. 2012) have been found to be expressed in satellite cells.

It is therefore clear that there are several miRNAs present in satellite cells and they may well operate in a coordinated fashion to either promote satellite cell quiescence, or activation or differentiation. Interestingly, miR-31 has been shown to play an important role in the former and it has been shown to target Myf-5 in quiescent satellite cells, thereby potentially maintaining quiescence.

1.4.3 miR-31 AND MYF-5

Maintaining satellite cells in a quiescent state, in the absence of muscle regeneration, is fundamental to ensure the survival of the satellite cell pool. As mentioned before, satellite cells are incredibly responsive to the plethora of molecules present in their niche and other endocrine factors. Mechanisms regulating the effetcs of these external stimuli are thus crucial to prevent hyper

activation and to keep satellite cells dormant within their niche. The notion that quiescent cells (G_0 phase) are actively being maintained in a dormant state is starting to gain ground as more insight into miRNA functions is obtained.

Since quiescent cells display condensed chromatin and overall less gene activation it was assumed that they are completely transcriptionally inactive (Schultz et al. 1978). It is however now known that even quiescent cells need intrinsic and extrinsic cues to maintain them in their current state. Maintaining satellite cells in a G_0 state, is thus an active process. Recently, it was observed that quiescent satellite cells were expressing Myf-5 mRNA, without activating the myogenic programme (Crist et al. 2012). Further analysis revealed that, although these satellite cells were indeed expressing Myf-5 mRNA, no Myf-5 protein was detectable (Crist et al. 2012). These observations could be explained by a prior study done by Daubas *et al*. (2009), who discovered that a target sequence for miR-31 was present in the 3'-UTR of Myf-5 (Daubas et al. 2009). In a subsequent investigation, Crist *et al*. (2012) set out to determine if miR-31 was indeed targeting Myf-5 in quiescent satellite cells, and by doing so preventing the accumulation of Myf-5 protein. Not only did the authors observe higher levels of miR-31 in the quiescent cells compared to activated cells, but they also showed that miR-31 was targeting Myf-5 mRNA and maintaining it transcriptionally inactive. The authors furthermore showed that miR-31 was sequestered with Myf-5 transcripts inside messenger ribonucleoprotein (mRNP) granules in the cytoplasm of quiescent satellite cells, whereas association of Myf-5 mRNA with the mRNP granules was not evident in activated satellite cells. Upon activation the mRNP granules were shown to dissociate and release Myf-5 transcripts which then allowed for the translation and Myf-5 protein accumulation and activation of the myogenic programme (Crist et al. 2012). Quiescent satellite cells therefore seem to be maintained in a 'halted' or intermediate state, where cells are quiescent, but 'primed' for myogenesis, since relevant mRNA has already been transcribed.

1.4.4 SATELLITE CELLS AND THEIR 'PRIMED' STATE

The concept of an alternate or intermediate state between G_0 and proliferating was first put forward by Rodgers *et al*. (2014). Using an animal model of unilateral muscle injury, the authors noticed that quiescent satellite cells in the muscle contralateral to the injured limb displayed unique cycling properties that are different from activated satellite cells or quiescent satellite cells (Rodgers et al.

2014). These contralateral satellite cells displayed a propensity to cycle and when explanted were able to re-enter the cell cycle far quicker than fully quiescent satellite cells and took less time to complete a full G_1-S-G_2-M cycle (Rodgers et al. 2014). Phenotypically, these satellite cells resembled quiescent satellite cells more than activated satellite cells, and their ability to self-renew and engraft was unaltered, thus ruling out the possibility that these satellite cells were actually already committed cells (Rodgers et al. 2014). In contrast, these satellite cells displayed enrichment in genes regulating cells cycle (Rodgers et al. 2014). These contralateral satellite cells seemed to represent an intermediate state, displaying similarities with both quiescent and activated satellite cells: they possessed all the abilities and characteristics of a true unipotent stem cell, but were more 'alert' as they displayed increased transcriptional activity and accelerated cell cycle re-entry and cycling.

The characteristics displayed by these contralateral satellite cells described by Rodgers *et al*. (2014) are very alike to cells under mTOR signaling reviewed by (Laplante & Sabatini 2012). Rodgers *et al*. (2014) showed that mTORC1 signaling was present in the 'alert' contralateral satellite cells and that HGF/c-Met signaling was regulating mTORC1 activity *via* PI3K-Akt signaling. Indeed mTORC1 signaling was shown to be responsible for the functional and transcriptional changes seen in this 'alert' state and that once mTORC1 signaling subsides this 'alert' state is lost. The authors therefore concluded that this 'alert' state is reversible (Rodgers et al. 2014). Finally, it was shown that these 'alert' satellite cells were primed into this state in response to multiple types of unrelated injuries (skin wounds, bone injuries, muscle injuries), and in response to subsequent injury, they displayed enhanced muscle regenerative capacity.

In summary the data present by Rodgers *et al*. (2014) show that quiescent stem cells have the ability to transition to a 'primed' state, which they termed G_{Alert}, whereby they are primed to re-enter the cell cycle and proliferate more profusely. It is tempting to speculate that the capacity of these G_{Alert} satellite cells to elicit enhanced muscle regeneration may not only be due to their increased ability to proliferate, but also due to their 'priming' to enter the myogenic differentiation programme (achieved by prescence of MRF mRNA's albeit translationally repressed by myo-miRs).

Careful scrutiny of the currently available literature has highlighted several gaps in the understanding of how HGF causes differential levels of MyoD and Myf-5 in recently activated satellite cells. Some data points to different concentrations of HGF leading to changes in regulation

of MyoD and Myf-5 at the mRNA level, resulting in more or less expression of one or the other. In addition, it is though that different intracellular levels of MyoD and Myf-5 protein elicit different responses in satellite cells, ultimately guiding their fate. Understanding the mechanistic regulation of satellite cells is now further complicated with the introduction of miRNAs and their role as powerful regulators of gene expression. It has been shown that intermediate satellite cells upregulate gene transcription and re-enter the cell cycle far too quickly for *de novo* gene expression, further implicating miRNAs as actively playing a role in maintaining satellite cells in a 'primed' or 'G_{Alert}' state. This new understanding opens the way to reinterpretation of earlier studies, particularly in relation to the effects of factors present in the satellite cell niche.

1.5 HYPOTHESIS, AIMS AND OBJECTIVES

We hypothesize that the known effect of HGF on the expression of MyoD and Myf-5 which differs depending on its concentration is in part due to an effect HGF may have on miR-31 expression and satellite cell exit from quiescence.

The central focus of this study is thus to understand how different concentrations of HGF affect the expression and translation of MyoD and Myf-5, along with the expression of miR-31, in primary human myoblasts.

In this study we aim to:

- Drive primary human myoblasts (PHM) into a quiescent state (G_0/G_1) *in vitro* and re-activate them by addition of low or high concentrations of exogenous rh-HGF.
- Investigate the time and concentration dependent effects of HGF on MyoD and Myf-5 mRNA and protein levels and the expression of miR-31.

We have set out the following objectives to satisfy out aims.

Firsty to:

- Expand previously isolated Primary Human Myoblast (PHM) cells.
- Drive PHMs into a quiescent state, *via* FBS removal and supplementation with a synthetic, growth factor-free serum replacement: KnockOut™ Serum Replacement (KOSR).
- Determine the state (quiescent, activated or proliferating) of the PHMs before and after 10 days in KOSR.
    - To ascertain the state in which PHMs find themselves, multi-colour flow cytometry and cell cycle analysis will be employed.

Secondly to determine the effects of different concentrations of rh-HGF (2 ng/mL and 10 ng/mL) after 24 h and 48 h on cell cycle progression in PHMs.

Thirdly to determine the effects of different concentrations of rh-HGF (2 ng/mL and 10 ng/mL) after 24 h and 48 h on the:

- Expression of MyoD and Myf-5 mRNA in PHMs.
- Synthesis of MyoD and Myf-5 protein in PHMs.
- Expression of miR-31 in PHMs.

CHAPTER 2

MATERIALS AND METHODS

All experimental procedures that formed part of this research study were performed *in vitro* on previously isolated primary human myoblasts (PHM) (Steyn 2015). This research study and the associated experimental protocols were approved by the Committee for Human Research at Stellenbosch University (Ethics reference #:N12/08/051). Experiments were conducted according to the ethical guidelines and principles of the International Declaration of Helsinki.

All chemicals used were of analytical grade.

2.1 PRIMARY HUMAN MYOBLAST CELL CULTURE

2.1.1 ISOLATION OF PRIMARY HUMAN MYOBLAST CULTURE (MICROEXPLANT TECHNIQUE)

The isolation and expansion of primary human myoblasts (PHM) from healthy male subjects (n=8) were performed by a former Ph.D. student (Dr P. Steyn) (Steyn 2015) using the micro-explant technique (Smith & Merrick 2010). Briefly, a qualified medical doctor performed the needle biopsy procedures (5 mm trephine biopsy needle with assisted suction) on the *vastus lateralis* of the subjects to harvest approximately 50-100 mg of skeletal muscle. The muscle sample was immediately transferred to a harvesting 1x phosphate buffered saline (PBS) solution containing 10% (v/v) penicillin/streptomycin (P/S) (Sigma-Aldrich, Germany, P43333) and 1% (v/v) gentamicin (C_f = 0.5 mg/mL) (GIBCO™, Paisley, Scotland, 50 mg/mL, 15750-060). Muscle samples were then removed from the harvesting PBS and washed with 1x PBS before being transferred into a 96-well tissue culture plate (Corning, USA, #3595). Prior to that the wells were coated overnight at 37 °C with an entactin-collagen IV-laminin (ECL) cell attachment matrix (Merck, USA, 08-110). Each individual piece of muscle was transferred into a well in a 96-well plate containing media ideal for the proliferation of PHM. The proliferation media consisted of Ham's F-10 Nutrient Mixture Medium (Sigma-Aldrich, Germany, N6908) that was supplemented with 20% (v/v) foetal bovine serum (FBS) (Life Technologies, USA, 10499-044), 2% (v/v) P/S (Sigma-Aldrich, Germany, P43333), 0.1% (v/v) gentamicin (C_f = 0.05 mg/mL) (GIBCO™, Paisley, Scotland, 50 mg/mL, 15750-060), 6.8% (v/v) (200

mM, 100x) L-glutamine (Sigma-Aldrich, Germany, G7513) and 10 ng/mL rh-FGF (Promega, USA, G5071). The muscle samples were maintained in a semi-conditioned media by regularly removing half of the old media in each well and replacing it with fresh proliferation media every 48 hours (h). The myoblast cells started to migrate off the muscle fibers approximately 10 days (d) post transfer. The biopsy samples were removed from the culture dish 14 d post transfer and then transferred to a new ECL-coated well so as to allow more PHMs to migrate off and generate a larger population. The adherent cells were then cryo-preserved in liquid nitrogen (LN_2) (-195 °C) for long term storage at a p0 state/stage. The freezing media consisted of Ham's F-10 Nutrient Mixture Medium (Sigma-Aldrich, Germany, N6908) that was supplemented with 20% (v/v) FBS (Life Technologies, USA, 10499-044), 2% (v/v) P/S (Sigma-Aldrich, Germany, P43333), 0.1% (v/v) gentamicin (C_f = 0.05 mg/mL) (GIBCO™, Paisley, Scotland, 50 mg/mL, 15750-060), 6.8% (v/v) (200 mM, 100x) L-glu (Sigma-Aldrich, Germany, G7513) and 5% (v/v) dimethyl sulphoxide (DMSO) (Sigma-Aldrich, Germany, D2650) Prior to storage in LN_2, the identity of the subcultured cells were confirmed using flow cytometry as previously described (Steyn 2015). Cells were analysed for Pax7/desmin expression to confirm the presence of a homogeneous population of PHMs and to determine the extent of fibroblast contamination. The flow cytometric analysis confirmed that the isolation of PHMs from all eight donors were successful and yielded a highly pure population of PHMs, with an average of 93.4±1.71% cells positive for Pax7. Refer to Table 2.1 for detailed information on the purity of the PHM populations derived from each of the individual donors.

Table 2.1: Percentage values of $PAX7^+$ and $Desmin^+$ cells isolated from the various donors.

DONOR #	PAX7+	DESMIN+	Pax7/Desmin+	Desmin Only
1	97.4	65.9	65.6	0.3
2	82.6	61	59.8	1.2
3	92.5	62.9	62.1	0.8
4	95	63.2	62.9	0.3
5	91.7	80.1	79.2	0.9
6	**95.8**	**75.6**	**74.9**	**0.7**
7	97.5	79.6	78.8	0.8
8	95	83.7	81.6	2.1
AVERAGE	**93.4±1.71**	**71.5±3.25**	**70.6±3.15**	**0.89±0.20**

Footnote: Data obtained from (Steyn 2015). Donor 6 is in bold as this subject's cells were expanded and used for all experimental procedures in this study.

2.1.2 PHM EXPANSION AND STORAGE

PHMs from subjects 1, 2, 4, 6 and 9 were selected randomly and expanded *in vitro* to generate a large working stock of PHMs. For initial expansion, a T25 cell culture flask (NEST Biotechnology, USA, 707003) was coated with ECL matrix (Millipore, USA, 08-110) and placed at 37 °C for 1 h. A cryovial containing 3 x 10^5 PHMs was then removed from LN_2 storage and placed in 37 °C waterbath to thaw for approximately 2 minutes (min). The cell suspension was transferred to a 15 mL centrifuge tube (NEST Biotechnology, USA, 601002) containing 5 mL of pre-warmed (37 °C) primary human myoblast proliferation media (PHM-PM). To make PHM-PM, Ham F-10 Nutrient Mixture Medium (Sigma-Aldrich, Germany, N6908) was supplemented with 20% (v/v) foetal bovine serum (Life Technologies, USA, 10499-044), 1% (v/v) PenStrep (Life Technologies, USA, 15140-122), 6.8% (v/v) (200 mM, 100x) L-glutamine (Life Technologies, USA, 25030-081) and 10 ng/mL rh-FGF (Promega, USA, G5071). Cells were centrifuged for 3 min at 1500 RPM at room temperature (20-25 °C). After centrifugation, the media was aspirated to remove all traces of DMSO (Sigma-Aldrich, Germany, D2650). The pelleted cells were resuspended in warm PHM-PM and triturated. The cell suspension was then transferred to the ECL-coated T25 cell culture flask, and the cells were incubated at 37 °C with a constant 5% CO_2 (ESCO, Singapore, CCL-170B-8-UV). The cells plated initially were assigned a p1 passage number and coded 'PHM' along with the donor subject number (e.g PHM 6 - p1). Refer to Appendix A for detailed information on cell culture reagents used and for media recipies.

PHMs were subcultured in T75 cell culture flasks (NEST Biotechnology, USA, 708003) to obtain a high yield of cell stocks for future experiments. A full media change (PHM-PM) was performed every 48 h until cells covered 70-80% of the cell culture flask growth surface. To perform cell passaging old media was removed and cells were rinsed twice with pre-warmed 1x sterile PBS (Sigma-Aldrich, Germany, P4417). 0.25% Trypsin-EDTA (1x) (Life Technologies, USA, 25200-072) was added to the culture flask and the cells incubated in a heated shaking incubator set at 37 °C for 5 min. This was essential to dislodge the adherend cells from the flask surface. After 5 min, an equal volume of warm PHM-PM was added to the flask and the cell suspension transferred to a 15 mL centrifuge tube (NEST Biotechnology, USA, 601002). The culture flask was rinsed with PHM-PM in order to collect remaining cells. The centrifuge tube containing the PHM cell suspension was centrifuged (Eppendorf, Germany, 5810R) at 1500 RPM for 3 min at room temperature. The media was discarded and the pelleted cells were resuspended in 1 mL warm PHM-PM and then transferred into a new tissue ECL-

coated culture flask. Cells were passaged until p4 and then cryopreserved in freezing media and stored in LN_2. Freezing media consisted of Ham F-10 Nutrient Mixture Medium (Sigma-Aldrich, Germany, N6908) was supplemented with 20% (v/v) foetal bovine serum (Life Technologies, USA, 10499-044), 1% (v/v) P/S (Life Technologies, USA, 15140-122), 6.8% (v/v) (200 mM, 100x) L-glutamine (Life Technologies, USA, 25030-081) and 5% (v/v) DMSO (Sigma-Aldrich, Germany, D2650). Refer to Appendix B for more detailed protocols on cell passaging, thawing and cryopreservation.

For the purpose of this study only PHMs expanded from subject 6, were used, as they proliferated rapidly and generated a large working stock. For all experimental procedures performed on subject 6's PHMs, only cells between passage 6 (p6) and 8 (p8) were used.

Prior to cryopreservation and subsequent experimental procedures, cells were checked for both bacterial and fungal contamination (Refer to Appendix C).

2.1.3 KNOCKOUT SERUM REPLACEMENT TREATMENT TO INDUCE CELLULAR QUIESCENCE

To stimulate PHMs to return to a quiescent state, FBS (Life Technologies, USA, 10499-044) was removed from the culture media and substituted with a synthetic, growth factor free serum replacement known as KnockOut™ Serum Replacement (KOSR) (Life Technologies, USA, 10828-010). The resulting media was termed quiescence media and contained Ham's F-10 Nutrient Mixture Medium (Sigma-Aldrich, Germany, N6908), supplemented with 20% (v/v) KnockOut™ Serum Replacement (KOSR) (Life Technologies, USA, 10828-010), 1% (v/v) P/S (Life Technologies, USA, 15140-122) and 6.8% (v/v) (200 mM, 100x) L-glutamine (Life Technologies, USA, 25030-081) (Refer to Appendix A). Cells were cultured for 10 days in this media, with daily media changes, in order to induce cellular quiescence.

2.2 FLOW CYTOMETRIC ANALYSIS OF THE PRIMARY HUMAN MYOBLASTS

2.2.1 DETERMINING THE STATE OF PHMs AFTER 10 DAYS OF CULTURE IN QUIESCENCE MEDIA

Cells were trypsinized and pelleted as described in Section 2.1.2. Cell numbers were quantified using a haemocytometer (Neubauer-improved, Marienfeld, Germany, #0640010) and resuspended at a concentration of 1 x 10^6 cells/100 µL of 1x PBS (Sodium Azide, Tris and Protein Free). To differentiate between live and dead cells a Zombie Aqua™ Fixable viability kit (BioLegend, USA, 423101) was used. 1 µL of Zombie dye was added to the cell suspension followed by 30 min of incubation at room temperature in the dark. Following incubation, cells were washed with 2 mL 1x PBS and then fixed in 500 µL of 4% paraformaldehyde for 10 min. Cells were then washed twice with 1 mL of freshly made staining buffer (1x PBS, 2% (w/v) Bovine Serum Albumin (BSA) (Roche, Germany, 10735086001)). To permeabilize cells, 3 mL of ice-cold (-20 °C) 70% Ethanol (EtOH) was added and the cell suspension placed in a freezer (-20 °C) for 1 h. After permeabilization, cells were washed three times with 1 mL staining buffer and resuspended at a concentration of 2 x 10^5 cells in staining buffer. Each antibody (Refer to Table 2.2) was added proportional to the number of cells and the final volume was brought to 100 µL. Cells were incubated at room temperature in the dark for 30 min and then washed twice with staining buffer. Prior to flow cytometric analysis (BD FACSAria™ Cell Sorter,BD Biosciences, San Jose, CA 95133, USA), cells were filtered through a 50 µm nylon mesh. A minimum of 1 x 10^5 cells were acquired and analysed. Compensation was performed with BD™ CompBead Plus (BD Biosciences, USA, 560497) and data analyses was performed on the FACSDiva™ software v6.1.3. Refer to Appendix D for detailed information on the setup and antibody optimization for titration curve analysis and FMO optimization.

Table 2.2: Multicolour Flow cytometry antibodies.

Antibody	Volume (µL/1 x 10^6 cells)	Manufacturer	Fluorophore	Host	Reactivity	Reference
Pax7	10	Novus Biological	PE	Mouse	Human	NBP2-34706
MyoD	10	Novus Biological	APC	Mouse	Human	NBP2-34772
Myf-5	5	Novus Biological	ALEX 488	Mouse	Human	IC4027G
CD56	2.5	BioLegend	PE/Dazzle	Mouse	Human	363544
CD34	2.5	BioLegend	APC/Cy7	Mouse	Human	350526
Ki-67	5	BioLegend	PE/Cy7	Mouse	Human	343514

Footnote: Antibody optimization was performed *via* titration experiments. Fluorescence-minus-one (FMO) analysis was performed to ascertain the presence of any spectral overlap of the fluorophores in different channels. Refer to Appendix D for Flow cytometry setup and antibody optimization for titration curve analysis and FMO optimization data.

2.2.2 CELL CYCLE ANALYSIS AFTER 10 DAYS IN QUIESCENCE MEDIA

Cells were trypsinized and pelleted as described in Section 2.1.2. To study the phase of the cell cycle the BD Cycletest™ Plus DNA Reagent Kit was employed (BD Biosciences, USA, 340242), that stains the DNA with Propidium Iodide, a fluorescent dye. Pelleted cells were washed twice with 1 mL of the Wash Buffer supplied in the kit. The Wash Buffer was removed and 250 µL of Solution A (Trypsin Buffer) was added and left for 10 min. 200 µL of Solution B (Trypsin inhibitor and RNase buffer) was then added and left for another 10 min. Finally, 200 µL of ice-cold Solution C (PI Stain solution) was added to the cell suspension and cells were incubated in the dark on ice for a further 10 min. Cells were filtered through a 50 µm nylon mesh and immediately analysed using a flow cytometer (BD FACSAria™ Cell Sorter, BD Biosciences, San Jose, CA 95133, USA) to determine the DNA ploidy. BD™ DNA QC Particles (BD biosciences, USA, 349523) was used to verify the instruments performance and quality control according to manufacturer's instructions. Cell cycle fractions were quantified with ModFitL 3.0 (Verity Software). A minimum of 3 x 10^4 cells were acquired and analysed for each sampling group. Refer to Figure 2.1 below for graphical illustration demonstrating the different phases of the cell cycle as determined using this technique.

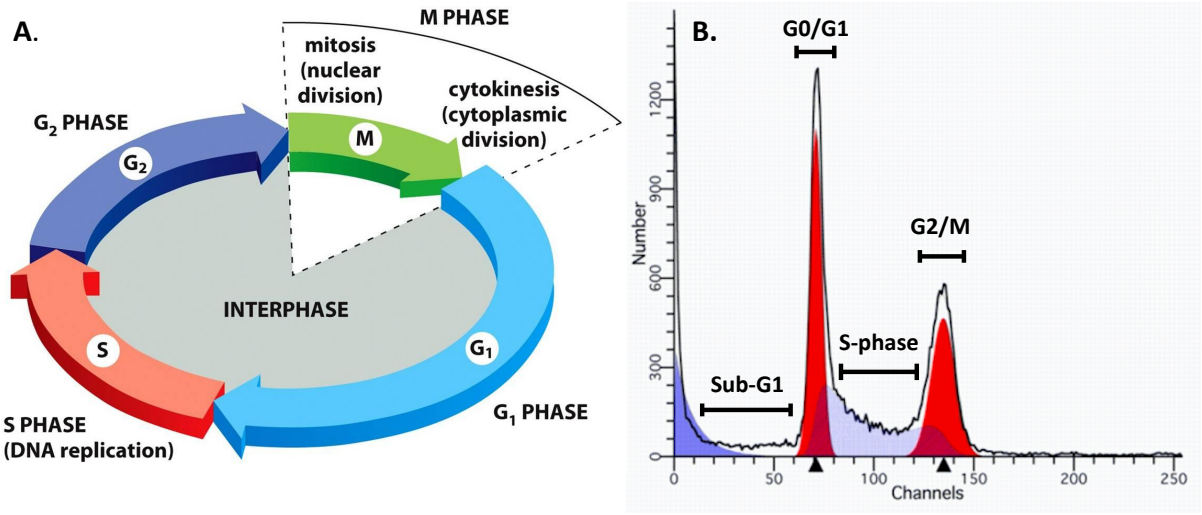

Figure 2.1: Graphical illustration of the phases of the cell cycle as assessed using flow cytometry.

Panel A: Depicts the various phases of the cell cycle composed of Interphase and Mitosis. Interphase is composed of 3 separate stages: G1, S and G2. In the G1-phase the cell has 1 copy of each chromosome (*n*). In S-phase the DNA is replicated. In the G2-phase the cell has 2 copies of each chromosome (*2n*). Mitosis is where the mother cell divides to form 2 daughter cells. **Panel B**: Depicts a typical DNA content histogram generated with ModFitL 3.0 (Verity Software). Here the different cell cycle phases are distinguished by fluorescence intensity. The G0/G1 peak represents cells with *n* amount of chromosomes. The G2/M peak represents cells with *2n* amount of chromosomes. The S-phase peak represents cells with *n* to *2n* amounts of DNA. The Sub-G1 phase represents a population of cellular debris or apoptotic cells. Image modified and reproduced without permission from (Tabll & Ismail 2011).

2.3 HEPATOCYTE GROWTH FACTOR TREATMENT

2.3.1 PREPARATION OF RH-HGF

Lyophilized recombinant human hepatocyte growth factor (rh-HGF) (5 µg) (R&D Systems, USA, 294-HG) was reconstituted at 50 µg/mL in sterile 1x PBS with 0.1% (w/v) of BSA (Roche, Germany, 10735086001). The reconstituted rh-HGF (50 µg/mL) was then diluted by a factor of 10, to yield a 5 µg/mL working stock, which was aliquoted and stored at -20 °C (Refer to Appendix A). For all subsequent experiments using either a high or low concentration of rh-HGF, the working stock was diluted as follows:

- **High concentration** of rh-HGF (10 ng/mL) - 30 µL of stock rh-HGF (5 µg/mL) added to 14.97 mL of quiescence media.
- **Low concentration** of rh-HGF (2 ng/mL) - 3 mL of High concentration (10 ng/mL) added to 12 mL of quiescence media.

2.3.2 RH-HGF TREATMENT

Before rh-HGF treatment, PHMs were cultured in 6-well cell culture plates (Corning, USA, #3516) in quiescence media for 10 days in order to induce a quiescent state (refer to Section 2.1.3). The quiescent PHMs were then treated with either low (2 ng/mL) or high (10 ng/mL) dose of rh-HGF for a period of 24 h and 48 h respectively. The 48 h-low and -high rh-HGF treatment groups were treated with freshly made media at an initial time point (Time 0) and then again exactly 24 h later. The 24 h-low and -high rh-HGF groups were also treated at the initial (Time 0) time point, but after 24 h, the rh-HGF containing media was removed. The cells were washed twice with 1x sterile PBS and cultured for a further 24 h in quiescence media. The purpose for this was to see whether brief exposure to rh-HGF was enough to stimulate and maintain gene expression. After 48 h in culture, protein and RNA from the low (24 h rh-HGF and 48 h rh-HGF) and high (24 h rh-HGF and 48 h rh-HGF) were isolated and stored at -80 °C for subsequent analysis. The rh-HGF was added freshly to all quiescence media for all treatment groups. Refer to Appendix E for detailed information on the rh-HGF treatment tissue culture plate setup.

2.4 WESTERN BLOTTING

2.4.1 PROTEIN HARVESTING FROM CULTURED CELLS

Media was removed and cells were washed twice with ice-cold 1x PBS. 100 µL of RIPA-buffer containing 50 mM Tris (hydroxymethyl) aminomethane ($NH_2C(CH_2OH)_3$, (MW = 121.14) (Sigma-Aldrich, Germany, 201-064-4), 2.5 mM TRIS-HCl pH 7.8 1 M (Sigma-Aldrich, Germany, T2913), 1% (v/v), Triton X-100 (Sigma-Aldrich, Germany, X100), 0.5% (v/v) sodium deoxycholate (MW = 414.55) (Sigma-Aldrich, Germany, DA5670), 0.25% (w/v) ethylenediaminetetraacetic acid disodium salt dihydrate (EDTA, M = 372.24) (Sigma-Aldrich, Germany, 205-358-3), 2x protease inhibitor cocktail (Roche, Germany, 04-693-116-001) and 1x phosphatase inhibitor cocktail (Roche, Germany, 04-906-837-001) was added to each culture well (Refer to Appendix F). Culture plates were kept on ice and cells were harvested from the culture surface with a cell scraper (NEST, USA, 710001) and transferred into a 1.5 mL Eppendorf tube. The collected cell suspension was sonicated for 15 seconds and centrifuged at 14,000 RPM for 10 min at 4 °C. The supernantant was transferred into a new 1.5 mL Eppendorf tube and protein concentrations were determined spectrophotometrically *via* the Direct Detect® infrared spectrophotometer (EDM Millipore, USA, DDHW00010-00). Samples were stored at -80 °C. Refer to Appendix F for detailed information on protein lysate preparation and quantification for raw protein concentration readouts.

2.4.2 POLYACRYLAMIDE GEL ELECTROPHORESIS AND WESTERN BLOTTING PROTOCOL

Protein lysates were thawed on ice and a specific volume of the sample was aliquoted in order to contain a total of 10 µg of protein. A pre-made 5x Laemmli sample buffer containing a 10% (v/v) of 2-mercaptoethanol (Bio-Rad, USA, 161-0710) was added to the proteins and the lysates placed in a heating block at 95 °C for 5 min to denature the proteins. Cell lysates containing 10 µg of protein were loaded and separated on a polyacrylamide gel by sodium dodecyl sulfate polyacylamide gel electrophoresis (SDS-PAGE). A TGX Stain-Free™ FastCast™ Acrylamide kit, 12% (BioRad, USA, 161-0185) was used to separate proteins. Refer to Appendix G - Western blot reagents, for detailed recipies.

For electrophoresis run, power was set at a constant voltage of 120V for 10-15 min to allow the protein samples to pass into the resolving gel and then increased to 200V for 1 h or until satisfactory separation was observed (Bio-Rad PowerPac 1000, Bio-Rad Laboratories, USA). Gels were placed in a ChemiDoc™ MP Imaging System (Bio-Rads Laboratories, USA) and activated for total protein visualization and quantification. After activation, proteins samples were transferred to a 0.45 µm low-autofluorescence polyvinylidene difluoride (LF PVDF) membrane using a Trans-Blot® Turbo™ RTA Transfer Kit, LF PVDF (Bio-Rad, USA, 170-4274) and a Bio-Rad Trans-Blotv® Turbo™ Transfer system. The apparatus was run according to Bio-Rad's standard protocol for 1.5 mm gels (25V and 1.3A for 10 min), to ensure maximal protein transfer onto the membrane. After proteins were successfully transferred to the LF PVDF membrane, it was washed three times in 1x TBS-Tween buffer for 5 min. The membrane was then blocked with 5% (v/v) fat free milk (Parmalat) in 1x TBS-Tween buffer for 1 h, to prevent non-specific binding. The membrane was then washed three times in 1x TBS-tween buffer for 5 min to remove traces of milk.

Primary antibody was added to 1x TBS-Tween with 2% (w/v) BSA (Roche, Germany, 10735086001) buffer at a 1:1000 dilution and incubated overnight at 4 °C with constant agitation. After primary antibody incubation was complete the membrane was washed six times in 1x TBS-Tween buffer for 5 min and then incubated with secondary HRP-linked (horse radish peroxidase) antibodies at room temperature for 1 h with constant agitation. Finally, the membrane was washed again six times in 1x TBS-Tween buffer for 5 min to remove any non-specific binding. Proteins were visualized with the aid of chemiluminescence SuperSignal® West Femto Maximum Sensitivity Substrate Kit (Thermo Scientific, USA, 34096) and imaged using the ChemiDoc™ MP Imaging system (Bio-Rad Laboratories, USA). Densitometric analysis of the protein samples was performed on the Image Lab™ Software (Bio-Rad Laboratories, USA) and normalized to total protein. Refer to Appendix H for more detailed protocols on polyacrylamide gel electophoresis and Western blotting.

Table 2.3: Primary antibodies used for Western blotting.

1° Antibody	Clonality	Host Species	Reactivity	IsoType	MW (kDa)	Dilution	Product Reference
MyoD1	Monoclonal	Rabbit	H	IgG	± 45	1:1000	D8G3
Myf-5	Polyclonal	Rabbit	H,M,R	N/A	± 29	1:2000	ABD19
c-Met	Monoclonal	Rabbit	H	IgG	± 160	1:1000	Ab51067
HGF	Monoclonal	Rabbit	H	IgG	± 83	1:1000	Ab178395

Footnote: The table demonstrates the optimal dilution of primary antibodies used for Western blotting. These concentrations are based on the manufacturer's recommendations and optimization experiments. MyoD1 was purchased from Cell Signaling Technologies. Myf-5 was purchased from Merck. C-Met and HGF were purchased from Abcam. H - Human; M - Mouse; R - Rabbit. IgG - Immunoglobulin G. MW - Molecular weight.

Table 2.4: Secondary antibodies used for Western blotting.

2° Antibody	Product Reference	MyoD1	Myf-5	c-Met	HGF
Anti-Rabbit IgG	7074	1:10000	1:15000	1:15000	1:10000

Footnote: Optimal dilution of secondary anti-rabbit IgG antibody used. These concentrations are based on the manufacturer's recommendations and optimization experiments. Secondary Anti-rabbit IgG was conjugated to horse radish peroxidase (HRP) and purchased from Cell Signaling Technologies.

2.5 RNA ANALYSIS

2.5.1 RNA EXTRACTION

Media was removed and cells were washed twice with ice-cold 1x PBS and placed on ice. 300 µL TriPure Isolation Reagent (Roche, USA, 11667157001) was added and cells were harvested from the culture surface *via* the aid of a cell scraper. Cell suspensions were placed in a 1.5 mL Eppendorf tube and placed at -80 °C. The lysates were thawed and left at room temperature for 5 min. Chloroform (0.2 mL/1 mL of TriPure reagent) was added and the tubes shaken vigorously and allowed to incubate for 15 min. The tubes were the centrifuged at 12,000 x *g* for 15 min at 2-8 °C. The upper aqueous phase was collected and mixed with an equal volume of 70% Ethanol. The entire solution was transferred to a High Pure Filter Tube, which was placed in a 2 mL Collection Tube, supplied in the kit. The High Pure Filter Tube assembly was centrifuged at 8000 x *g* for 1 min at room temperature. Each sample was then DNase treated, with 10 µL of DNase I mixed with 90 µL of DNase I Incubation Buffer and allowed to incubate for 15 min at room temperature. After the DNase treatment, 500 µL of Wash Buffer I was added to the upper reservoir of the Filter Tube assembly and centrifuged at 8,000 x *g* for 1 min. This wash step was performed twice to further decrease 280 nm contamination. Wash buffer II (500 µL) was added and the Filter Tube assembly centrifuged at 8,000 x *g* for 1 minute at room temperature. Wash Buffer II was added a second time, albeit only 200 µL, and centrifuged at 13,000 x *g* for 2 min to remove any residual Wash Buffer. RNA was then eluted by adding 30 µL of pre-warmed (45 °C) Elution Buffer and centrifuging the Filter Tube assembly for 1 min at 8,000 x *g*. RNA yield and purity was quantified by spectrophotometry using a NanoDrop Lite (Thermo Scientific, USA). An A260/A280 ratio of ~2.0 is accepted as 'pure' for RNA. Refer to Appendix I for RNA quantification, raw RNA concentration and purity readouts.

2.5.2 cDNA SYNTHESIS

Reverse transcription (RT) of the isolated RNA to obtain cDNA was performed with a High Capacity RNA-to-cDNA kit (Roche, USA, 4387406). The RNA sample was added to the RT reaction mix composed of 10 µL of 2x RT Buffer and 1 µL of 20x RT Enzyme Mix. Nuclease-free H_2O was used to bring the total reaction volume to 20 µL in each tube. The tubes were mixed, and placed in a thermal cycler (Applied Biosystems 2720 Thermal Cycler, USA). The Thermal cycler was programmed for a 3-

Step cycling condition optimized for the High Capacity RNA-to-cDNA Kit according to manufacturer's instructions. Refer to Table 2.5 for optimized cycling conditions.

Table 2.5: Optimized cycling conditions for the High Capacity RNA-to-cDNA Kit.

	STEP 1	STEP 2	STEP 3
Temperature (°C)	37	95	4
Time (min)	60	5	∞

Footnote: 3-Step cycling condition optimized for the High Capacity RNA-to-cDNA Kit according to manufacturer's instructions.

2.5.3 QUANTITATIVE POLYMERASE CHAIN REACTION

Samples were loaded in duplicate into MicroAmp® Fast optical 96-well reaction plates (Applied biosystems, USA, 4346907). Each well contained 10 µL of 2x TaqMan Gene Expression Master mix (Applied biosystems, USA, 4369016), 1 µL of 20x TaqMan gene expression assays (probe (5 µM) and primer (18 µM)) and 10-100 ng of cDNA template. Samples were run on a StepOnePlus™ realtime PCR machine (Life Technologies, USA) with the following cycling conditions optimized according to manufacturer's instructions (Refer to Table 2.6).

Table 2.6: qPCR thermal cycling conditions for TaqMan gene expression master mix and assays.

Step	UDG Incubation	AmpliTaq Gold, UP Enzyme Activation	PCR	
			CYCLE (40 Cycles)	
	HOLD	HOLD	Denature	Anneal/Extend
Time	2 min	10 min	15 sec	1 min
Temp	50 °C	95 °C	95 °C	60 °C

Footnote: The cycling conditions are optimized for use with the TaqMan gene expression master mix and TaqMan gene expression assays according to manufacturer's instructions. The 2-minute, 50 °C step is required for Uracil-DNA Glycosylase (UDG) enzyme activity. UDG prevents the reamplification of carryover-PCR products by removing any uracil incorporated into the single- or double-stranded amplicons (Longo et al. 1990). The 10-minute, 95 °C is required to activate the AmpliTaq Gold® DNA polymerase, Ultra Pure (UP). The AmpliTaq Gold® DNA polymerase, UP, is a chemically modified form of AmpliTaq Gold® DNA polymerase, that is only active at temperatures where the DNA is fully denatured.

Each sample was run in duplicate and the resultant C_T was calculated by the the software (StepOne™ Software v2.2.2, Life Technologies, USA) and a mean C_T value was calculated for each sample. The C_T value represents the cycle number, at which the amplification plot crosses a threshold, for which the fluorescent signal generated is significant with regards to the background levels. The 18 S ribosomal

sunbunit was used as endogenous reference gene (Goidin et al. 2001). This allowed for the normalization of gene expression for each target gene, to the amount of input cDNA. Briefly, calculation of $\Delta\Delta C_T$ was obtained first by subtracting the mean C_T value for each target gene, to the mean C_T value for the reference gene (C_T target gene - C_T endogenous reference gene). The obtained value, termed ΔC_T, was then used to determine the $\Delta\Delta C_T$ value. The $\Delta\Delta C_T$ describes the difference between the average ΔC_T value of the sample of interest and the average ΔC_T value of a reference sample. This sample, known as the calibrator sample, is usually obtained from unstimulated or untreated cells and is used to normalize all other (stimulated) samples. Thus, $\Delta\Delta C_T$ = average ΔC_T (sample of interest) - average ΔC_T (reference sample). Finally, relative expression levels for each target gene were calculated by the following formula (2^{-ddCT}). Refer to Appendix J - qPCR raw data, for raw C_T readouts.

Table 2.7: TaqMan Probes utilized for qPCR.

TaqMan Probe	Amplicon Length (bp)	Catalogue #	Reference
MyoD1	87	4331182	Hs02330075_g1
Myf-5	114	4331182	Hs00929416_g1
Pax7	73	4331182	Hs00242962_m1
18S	187	4331182	Hs99999901_s1

Footnote: TaqMan Probes were purchased from Applied Biosystems.

2.6 MICRORNA ANALYSIS

2.6.1 miRNA EXTRACTION

Media was removed and cells were washed twice with ice-cold 1x PBS and placed on ice. QIAzol® lysis reagent, included in the miRNeasy® mini kit (Qaigen, Germany, 217004), was added and cells were harvested from the culture surface *via* the aid of a cell scraper. Cell suspensions were placed in a 1.5 mL Eppendorf tube and placed at -80 °C. Samples were thawed and allowed to incubate at room temperature for 5 min. Chloroform (0.2 mL/1 mL of QIAzol® reagent) was added to the tubes and shaken vigorously for 15 seconds. The tubes were left to stand for 2-3 min after which they were centrifuged at 12,000 x *g* at 4 °C for 15 min. The upper aqueous phase was placed in a new collection tube and 1.5 volumes of 100% ethanol was added and mixed. The sample was transferred into an RNeasy mini spin column and inserted into a 2 mL collection tube, supplied in the kit. The RNeasy mini spin column was centrifuged at 8000 x *g* for 15 seconds at room temperature. 700 µL of Buffer RWT was added to the column and centrifuged at 8000 x *g* for 15 seconds, followed by two separate additions of 500 µL of Buffer RPE. Finally, 30 µL of RNase-Free water was added directly onto the RNeasy Mini column membrane and centrifuged for 1 min at 8,000 x *g* to elute the RNA. RNA yield and purity was quantified by spectrophotometry using a NanoDrop™ Lite (Thermo Scientific, USA, ND-LITE). An A260/A280 ratio of ~2.0 is accepted as 'pure' for RNA. Refer to Appendix I for raw RNA concentration and purity readouts.

2.6.2 cDNA SYNTHESIS

Isolated miRNA was reverse transcribed into cDNA using the miScript II RT Kit (Qiagen, Germany, 218161), which allows for the selective reverse transcription of mature miRNAs. The miRNA sample was added to the RT reaction mixed composed of 4 µL of 5x miScript HiSpec Buffer, 2 µL of 10x miScript Nucleics mix and 2 µL of miScript reverse transcriptase mix. Nuclease-free H_2O was used to bring the total reaction volume to 20 µL in each tube. The tubes were then mixed and centrifuged and then placed in a thermal cycler (Applied Biosystems 2720 Thermal Cycler, USA). The Thermal cycler was programmed for a 3-Step cycling condition, optimized according to manufacturer's instructions (see Table 2.8).

Table 2.8: Cycling condtions for the miScript II RT Kit.

	STEP 1	STEP 2	STEP 3
Temperature (°C)	37	95	4
Time (min)	60	5	∞

Footnote: 3-Step cycling condition for the miScript II RT Kit, optimized according to manufacturer's instructions.

2.6.3 QUANTITATIVE POLYMERASE CHAIN REACTION

Samples were loaded in triplicate into MicroAmp® Fast optical 96-well reaction plates (Applied biosystems, USA, 4346907). Each well contained 12.5 µL of 2x QuantiTect® SYBR Green PCR Master mix, 2.5 µL of 10x miScript Universal Primer, 2.5 µL of 10x miScript primer assay and ≤ 2.5 µL of template cDNA. RNase-Free water was used to bring the final reaction volume to 25 µL. Samples were run on a StepOnePlus™ realtime PCR machine (Life Technologies, USA) with the following setup (see Table 2.9).

Table 2.9: qPCR thermal cycling conditions for SYBR® Green master mix and primer assays.

STEP	PCR Initial activation step	3-Step Cycling (40 Cycles)			Dissociation/Melt curve analysis
		Denaturation	Annealing	Extension	
Temperature	95°C	94°C	55°C	70°C	55 - 95°C
Time	15 min	15 sec	30 sec	30 sec	NA

Footnote: The 15-minute, 95 °C step is required to activate the HotStarTaq® DNA Polymerase. Fluorescence data collection was performed at the extension stage. Melt curve analysis was performed to ascertain that only the desired PCR product was amplified.

Relative target miRNA expression levels were calculated by the 2^{-ddCT} formula as described in section 2.5.3. For normalization RNU6-2 was used as an endogenous miRNA control, while a miRTC control was used to confirm successful cDNA systhesis. Refer to Appendix J for qPCR raw data and raw C_T readouts.

Table 2.10: miScript primer assays utilized for qPCR.

miScript primer	Catalogue #	Lot #
Hs_miR-31_1	MS00003290	20160303132
Ctrl_miRTC_1	MS00000001	20160122129
Hs_RNU6-2_11	MS00033740	20160505112

Footnote: miScript primer assays were reconstituted in 550 µL TE Buffer (pH 8.0) as per manufacturer's instructions. miScript primer assays were purchased from Qaigen.

2.7 STATISTICAL ANALYSES

Statistical analyses of the obtained data were performed with Graphpad Prism 5 (GraphPad Software, Inc., La Jolla, CA, 92037, USA). One-way ANOVA (analysis of variance), with Bonferroni post hoc test, was used to infer statistical significance between each treatment groups. Values are expressed as mean ± standard error of the mean (S.E.M). Statistical significance was accepted at $p < 0.05$.

CHAPTER 3

RESULTS

3.1 OPTIMIZATION OF CULTURE CONDITIONS TO INDUCE A QUIESCENT STATE IN PRIMARY HUMAN MYOBLASTS

The first objective of this project was to drive activated and proliferating primary human myoblasts (PHMs) into a quiescent state. These PHMs had previously been cultured and expanded in Ham's F-10 nutrient medium mixture supplemented with 20% (v/v) foetal bovine serum (FBS), 10 ng/mL rh-FGF, 1% (v/v) P/S and 6.8% (v/v) (200 mM, 100x) L-glutamine. Henceforth this culture media is referred to as PHM-PM and only to describe the expansion conditions prior to day 0 of experimentation. For the series of experiments described in this thesis FBS and rh-FGF were replaced with 20% (v/v) of KnockOut™ Serum Replacement (KOSR) in the culture media.

3.1.1 COMPARISON OF KNOCKOUT DMEM vs. HAM's F-10 CULTURE

Two nutrient media mixtures were selected: Ham's F-10 nutrient medium mixture and KnockOut™ DMEM (KO-DMEM) (Life Technologies, USA, 10829-018). These were selected as the former is the standard media used for PHM culture *in vitro* (Motohashi et al. 2014; Liu et al. 2015), while the latter is specifically formulated for serum free culture supplemented with KnockOut™ Serum Replacement (KOSR).

For the first series of experiments KOSR was added to the two choice media (Ham's F-10 or KO-DMEM) to determine if this affected PHM survival and morphology over a 10 day culture period. Furthermore, to observe the effects of cell to cell proximity on morphology and alignment, each culture plate contained different amounts of cells on day 0 (50×10^3, 75×10^3, 100×10^3, 125×10^3, 150×10^3, 200×10^3). The effects of different plating densities was observed 10 days later (see Figure 3.1).

Observations

After 10 days in culture cells were in very close proximity (90%-100% confluency) and began showing morphological changes (Figure 3.1, Panels A-F), namely elongation (yellow arrow) and alignment (red arrow), similar to differentiating myoblasts. These changes became more prominent on plates seeded with higher cell numbers (Figure 3.1, Panels B-F). Figure 3.1, Panel A, indicates that even plating 50 x 10^3 cells on day 0 resulted in a high degree of confluency in the culture plates after 10 days of culture, with confluency even greater with 75 x 10^3 - 200 x 10^3 cell plating densities.

Consequently, these results suggested that plating fewer cell numbers than 50 x 10^3 on day 0 would be worth investigating to determine if the morphological changes suggestive of early differentiation would be reduced when cells are plated at a lower seeding density. This prompted the next experiments, with results presented in Figure 3.2. Plating density was decreased so that the number of cells plated on day 0 was either 20 x 10^3, 30 x 10^3 or 40 x 10^3 (Figure 3.2, Panels A, C, E). Not only plating density but also the culture media was changed. It was also decided to culture PHMs in their typical media, Ham's F-10, supplemented with 20% (v/v) KOSR, instead of KO-DMEM supplemented with 20% (v/v) KOSR.

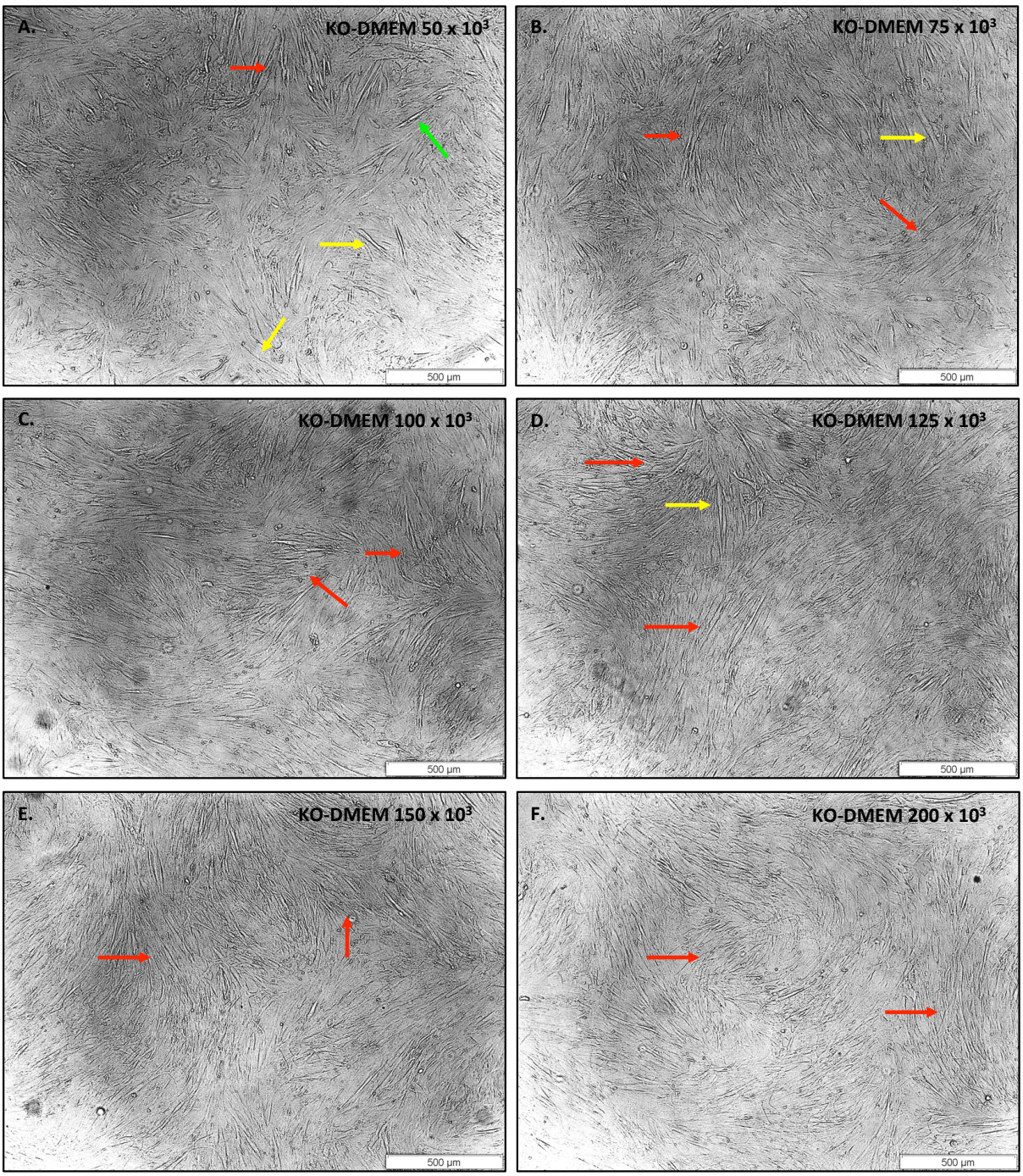

Figure 3.1: PHM morphology after a 10 day period of culture in KO-DMEM and 20% KOSR, plated at different confluencies.

Cells were plated into 6-well tissue culture plates (35 mm). Plating densities on day 0: **Panel A** - 50 x 10^3 cells. **Panel B** - 75 x 10^3 cells. **Panel C -** 100 x 10^3 cells. **Panel D** - 125 x 10^3 cells. **Panel E** - 150 x 10^3 cells. **Panel F** - 200 x 10^3 cells. The culture media was changed daily and cells were washed once with 1x PBS. **Red arrows** - aligned PHMs. **Yellow arrows** - elongated PHMs. **Green arrows** - Normal PHM morphology *in vitro*.

Observations

Both KO-DMEM and Ham's F-10, each supplemented with 20% (v/v) KOSR, maintained cellular viability over the 10 day culture period (Figure 3.2, Panels A-F) and reduced cellular proliferation (KO-DMEM from 5 days onwards and Ham's F-10 from 3 days onwards - qualitative assessment only). Specifically, after 10 days in culture, Ham's F-10 seemed to reduce cellular proliferation to a greater extent than KO-DMEM as evident from visibly less confluent culture surfaces (Figure 3.2, Panels A vs. B, C vs. D and E vs. F). It was then noted that the cell culture media choice (KO-DMEM) not only did not rapidly reduce proliferation, but favoured PHM growth (more elongated and less spindle-like morphology), whereas Ham's F-10 allowed for maintainance of typical PHM morphology *in vitro* (Figure 3.2, Panels A vs. B, C vs. D and E vs. F). Specifically, PHMs cultured in Ham's F-10, maintained a single cell spindle-shaped morphology. The fact that plating densities ranged from 20 x 10^3 - 40 x 10^3 all maintained the typical morphology, suggests the effect can be ascribed to the Ham's F-10 media (Figure 3.2, Panels B, D and F).

Based on these observations, it was decided that for all subsequent experiments, PHMs were to be cultured in Ham's F-10, supplemented with 20% (v/v) KOSR. Since the objective of expsoure to KOSR is to promote quiescence, the culture media was called quiescence media from this point forward.

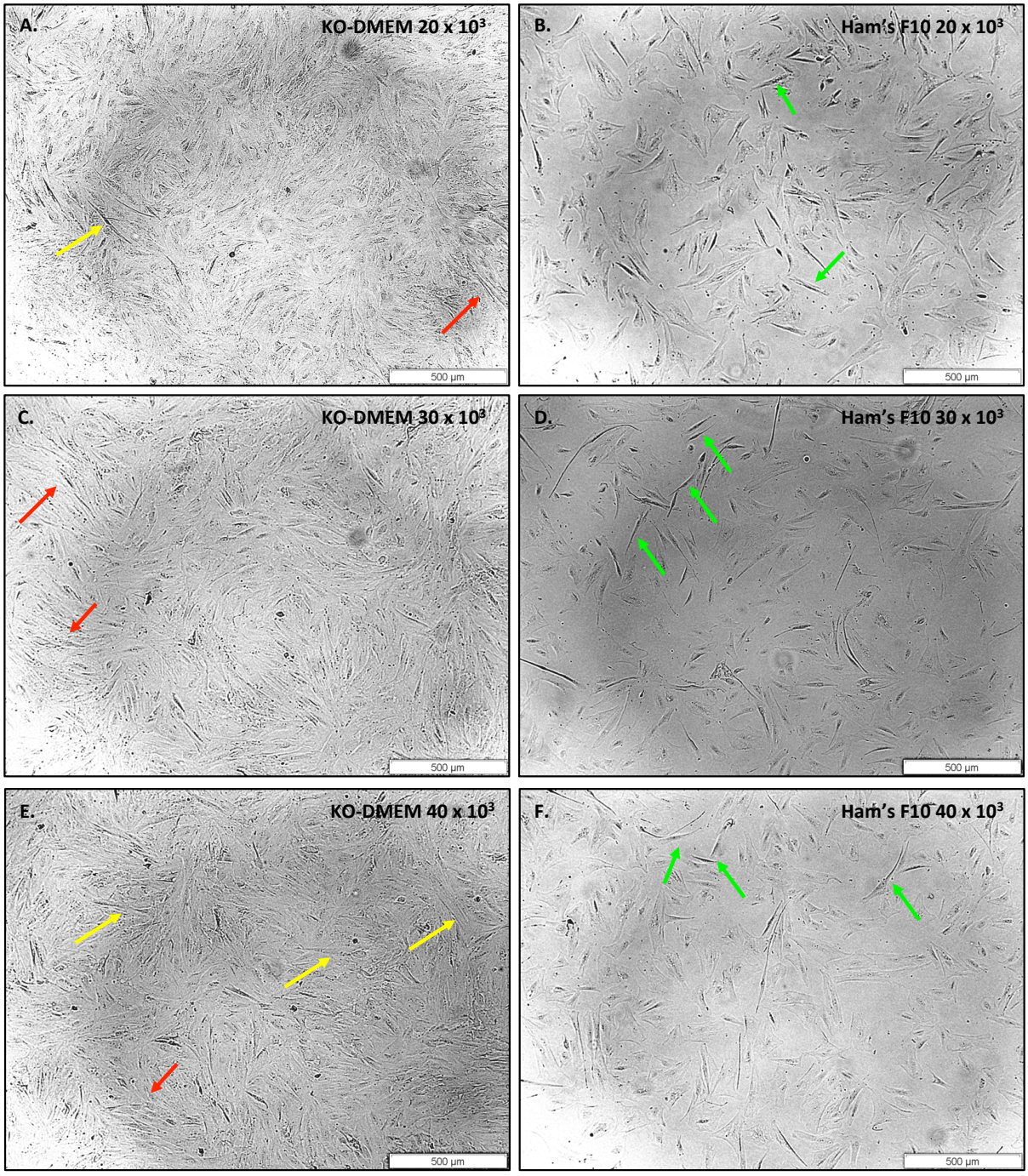

Figure 3.2: PHM morphology after a 10 day period of culture in either KO-DMEM and 20% KOSR or quiescence media (Ham's F-10 and 20% KOSR), plated at different low confluencies.

Cells were plated into 6-well tissue culture plates (35 mm). Plating densities on day 0: **Panel A** - 20 x 10^3 cells plated on day 0 in KO-DMEM and 20% KOSR. **Panel B** - 20 x 10^3 cells plated on day 0 in quiescence media. **Panel C** - 30 x 10^3 cells plated on day 0 in KO-DMEM and 20% KOSR. **Panel D** - 30 x 10^3 cells plated on day 0 in quiescence media. **Panel E** - 40 x 10^3 cells plated on day 0 in KO-DMEM and 20% KOSR. **Panel F** - 40 x 10^3 cells plated on day 0 in quiescence media. The culture media was changed daily, and cells were washed once with 1x PBS. **Red arrows** - aligned PHMs. **Yellow arrows** - elongated PHMs. **Green arrows** - Normal PHM morphology *in vitro*.

3.1.2 THE EFFECT OF QUIESCENCE MEDIA ON THE EXPRESSION OF SATELLITE CELL MARKERS

Criteria to confirm that culturing PHMs in Ham's F-10 supplemented with 20% KOSR (quiescence media) induced the cells to exit the cell cycle and return to a quiescent state, included multicolour flow cytometry and cell cycle analysis. Specifically, multicolour flow cytometry was used to assess the expression of key satellite cell markers. The markers selected are known to be differentially expressed depending on the state of the satellite cell (quiescent, activated or proliferating). Furthermore, the selected markers were used to confirm the identity of the cells used for this study and to accurately determine their state before and after culturing in quiescence media. Marker expression was analysed at day 0, 3, 5, 7 and 10.

Several multicolour flow cytomety experiments were run for this study in order to optimise the technique. Flow cytometry settings were modified for each new optimization experiment. PHMs from subjects 1, 2, 4, 6, and 9 were expanded and used during optimization experiments. Cells were not pooled, rather PHMs from a different subject were used for each optimization experiment. Optimization included for example adjustments to cytometer voltages, and compensation for fluorophore spectral overlaps as well as background fluorescence. Since several variables changed each time, data cannot be compared between the different optimization experiments. The first experiment after optimization was completed, compared PHMs from four subjects. Unfortunately between the final optimizations and the real experiment, the violet laser malfunctioned causing all optimized setting to be obsolete. The only observation that could be made was that CD34 was a consistant marker and its expression was always seen in all subjects and at all time points (day 0 - 10).

PHMs harvested from different subjects had differing expansion capabilities and only substantial cellular stocks were generated for subject 6. Therefore, a further two experiments were done using PHMs from subject 6 only. These PHMs were in passage 6-7. The first experiment was performed in exactly the same way as the final optimization in terms of culture conditions and cell harvest ie: cells were cultured in 35mm wells and trypsynized for harvest. Results presented in Table 3.1 indicate once again, the high expression of CD34. Also, Myf-5 and Ki-67 were highly expressed. A third

observation was an unexpected lack of Pax7 on day 0 in the culture. These observations did not change for the first 7 days. However, by day 10, it seemed that Pax7 expression was responding.

Table 3.1: Summary of marker expression as analysed in flow cytometry in PHMs from subject 6, cultured in 35mm wells in quiescence media for 10 days.

Marker		Days									
		0		3		5		7		10	
		Cells counted	% (+)	Cells counted	% (+)	Cells counted	% (+)	Cells counted	% (+)	Cells counted	% (+)
Cell Surface	CD34	7,346	98.6	15,582	99.0	9,588	99.6	21,998	97.7	19,749	98.7
	CD56	2,747	36.9	11,831	75.2	6,556	68.1	9,540	42.4	5,811	29.1
Nuclear	Pax7	59	0.8	286	1.8	210	2.2	522	2.3	6,874	34.4
	Myf-5	7,387	99.2	15,631	99.3	9,597	99.7	22,145	98.3	19,996	100
	MyoD	146	2.0	1,314	8.3	782	8.1	840	3.7	1,178	5.9
	Ki-67	7,297	98.0	15,399	97.8	9,569	99.4	21,489	95.4	19,115	95.8

Footnote: Satellite cell events: **Day 0** - 7,447, **Day 3** - 15,739, **Day 5** - 9,626, **Day 7** - 22,518, **Day 10** - 20,000. Only live satellite cells were analysed. PHMs from subject 6 were used at p6. PHMs were cultured in 6-well (35 mm) plates for 10 days in quiescence media. 40 x 10^3 cells were plated on day 0 in each sampling well. PHMs used for day 0 sampling time point were cultured in PHM-PM. The culture media was changed daily, and cells were washed once with 1x PBS. % (+) = Percentage of expressing cells for that marker.

As per protocol, preparation of cells for flow cytometry includes a substantial number of washing steps. It was observed that a significant proportion of cells were lost during the preparation procedure for flow cytometric analysis, which prompted a change in culture conditions. Instead of repeating the experiment using 6-well (35 mm) plates which would have allowed for direct comparison between the two flow cytometry result sets of subject 6, the decision was taken to culture cells in T75 flasks with seeding densities similar to that used for the wells. This allowed for greater cell numbers at the start of the preparation procedure for flow cytometric analysis. To further mitigate the loss of cells the speed (RPM) at which the cells were spun down in between wash steps was increased, from 1500 RPM for 3 min to 3000 RPM for 3 min. This was due to the fact that the permeabilization procedure made the cells more buoyant. Furthermore the wash buffer used for wash steps in the preparation procedure, composed of 1x PBS and 2% (w/v) BSA, has a different density than normal culture media (DMEM or Ham's F-10), causing cells to be more buoyant when placed in it. Furthermore, the staining protocol was also slightly altered. Since both CD34 and CD56 are cell surface markers and were present in a high proportion of PHMs, whereas

Pax7 and MyoD are nuclear transcription factors, a longer time period for antibody incubation was introduced for the final experiment (1 h rather than 30 min).

Table 3.2 presents the flow cytometry data for PHMs isolated from subject 6 at p7. These cells were cultured in T75 flasks and incubated with antibodies for 1 h. Refer to Appendix K for detailed data.

Similar to the first data set, the expression of the stem cell marker, CD34 was constant over the entire 10 day culture period, with the entire PHM population (> 97%) expressed CD34 on their cell surfaces (Table 3.2 and Figure 3.3, Panels B-F). However, protocol adjustments appeared to alter the Pax7 data: Before culturing in quiescence media (day 0) 61.1% of the PHM population were expressing Pax7 (Figure 3.4, Panel B). Over the 10 day culture period the percentage of PHMs expressing Pax7 steadily decreased (Figure 3.4, Panel B-F). On the last day of culture (day 10) only 32.6% of PHMs were expressing Pax7, suggesting that prolonged culturing in quiescence media may cause Pax7 expression in PHMs to decrease over time. Virtually all Pax7 positive PHMs also expressed CD34 (Figure 3.5, Panel F). Taken together, although the population of Pax7 expressing cells decreased, the fact that CD34 is expressed in the entire population, signified that the PHMs had not differentiated, as they did not lose their stem cell status.

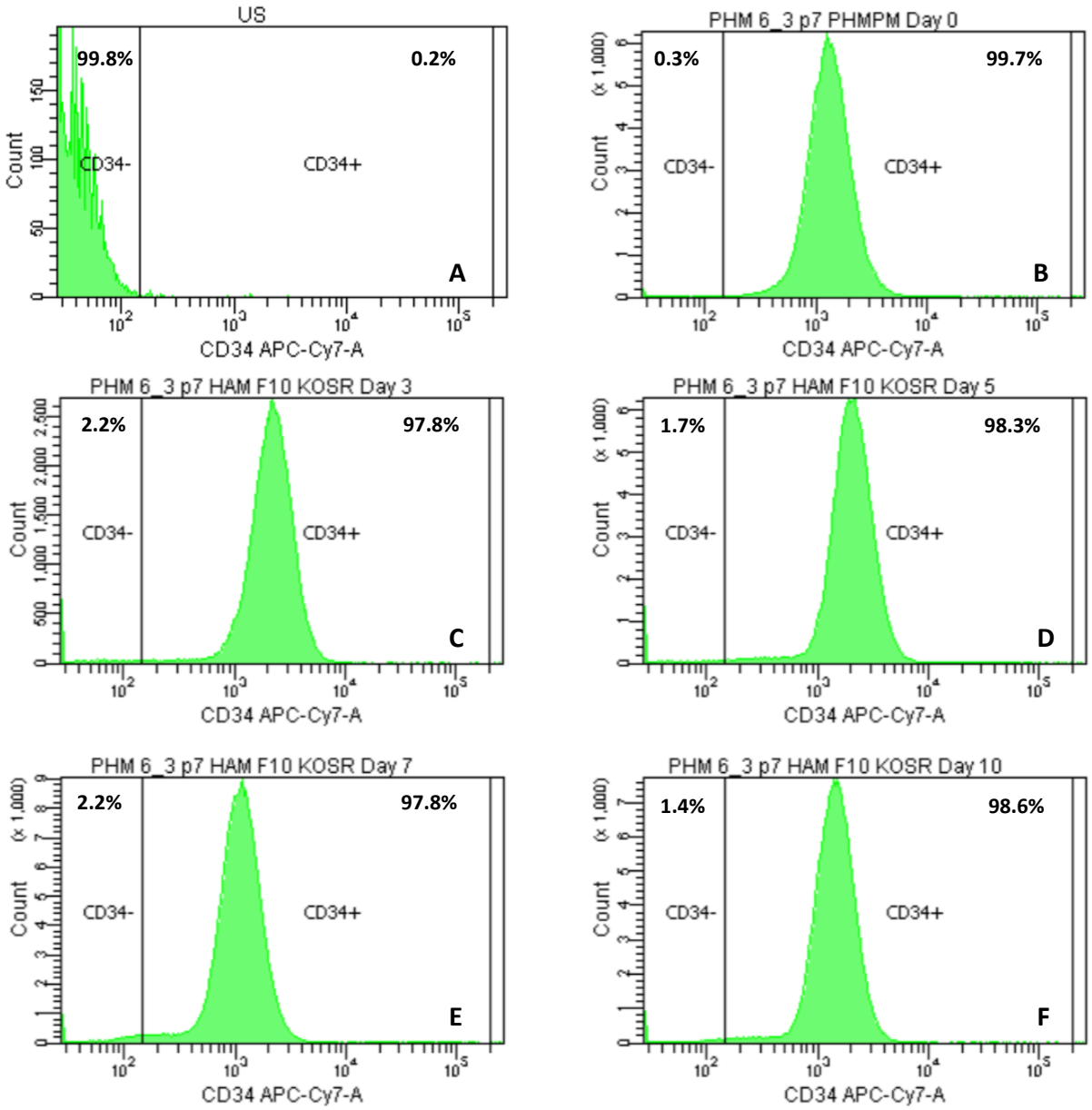

Figure 3.3: CD34 expression in PHMs over a 10 day culture period in quiescence media.

Cells were plated into a T75 tissue culture flask. **Panel A:** Unstained control (US). **Panel B:** Percentage of CD34 expressing PHMs prior to quiescence media exposure. **Panel C - F :** Percentage of CD34 expressing PHMs after 3 days (**Panel C**), after 5 days (**Panel D**), after 7 days (**Panel E**), after 10 days (**Panel F**). The culture media was changed daily, and cells were washed once with 1x PBS. A minimum of 1 x 10^5 satellite cells were analysed for each time point. Data analyses were performed on the FACSDiva™ software v6.1.3.

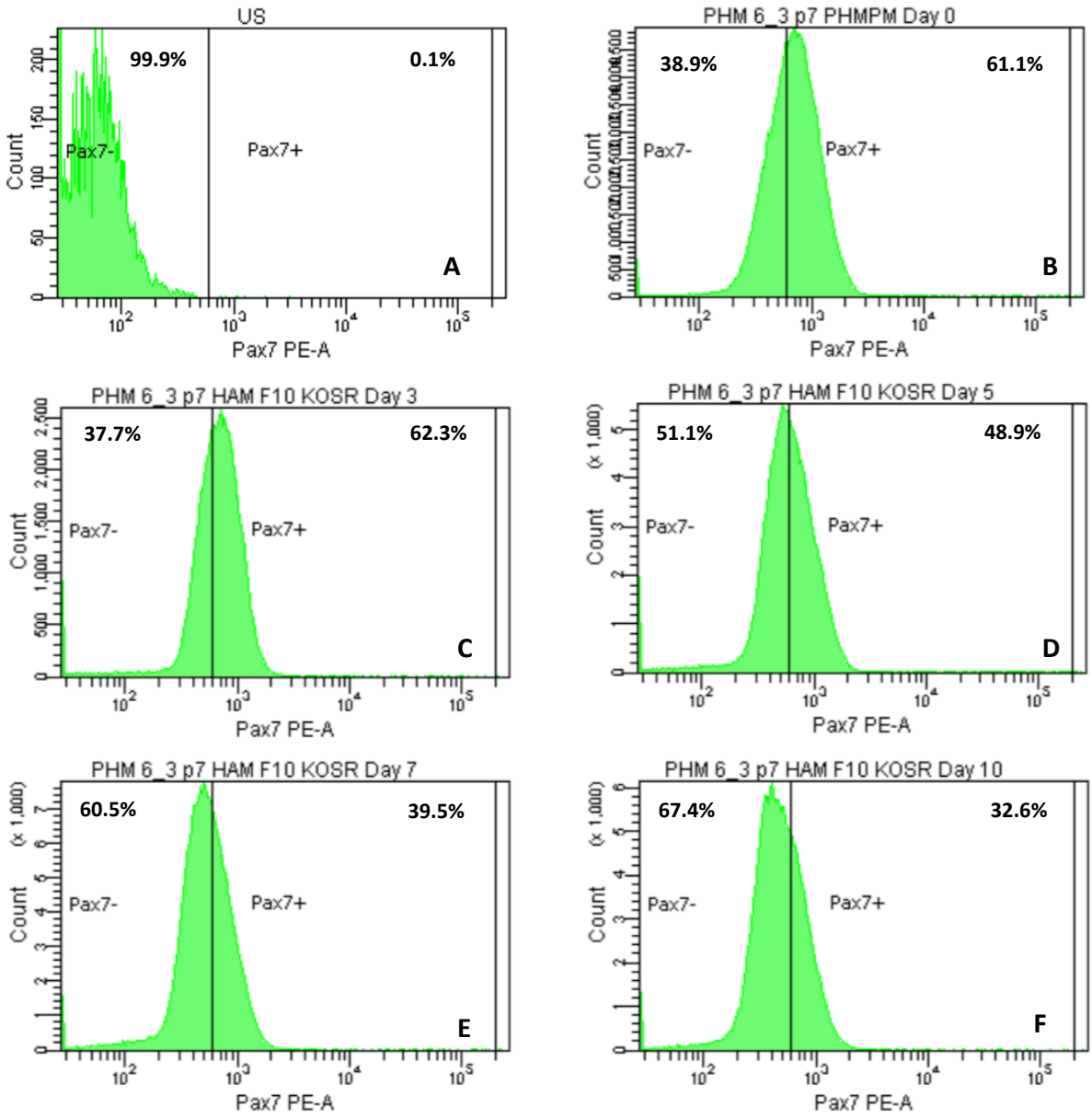

Figure 3.4: Pax7 expression in PHMs over a 10 day culture period in quiescence media.

Cells were plated into a T75 tissue culture flask. **Panel A:** Unstained control (US). **Panel B:** Percentage of CD34 expressing PHMs prior to quiescence media exposure. **Panel C - F :** Percentage of Pax7 expressing PHMs after 3 days (**Panel C**), after 5 days (**Panel D**), after 7 days (**Panel E**), after 10 days (**Panel F**). The culture media was changed daily, and cells were washed once with 1x PBS. A minimum of 1 x 10^5 satellite cells were analysed for each time point. Data analyses were performed on the FACSDiva™ software v6.1.3.

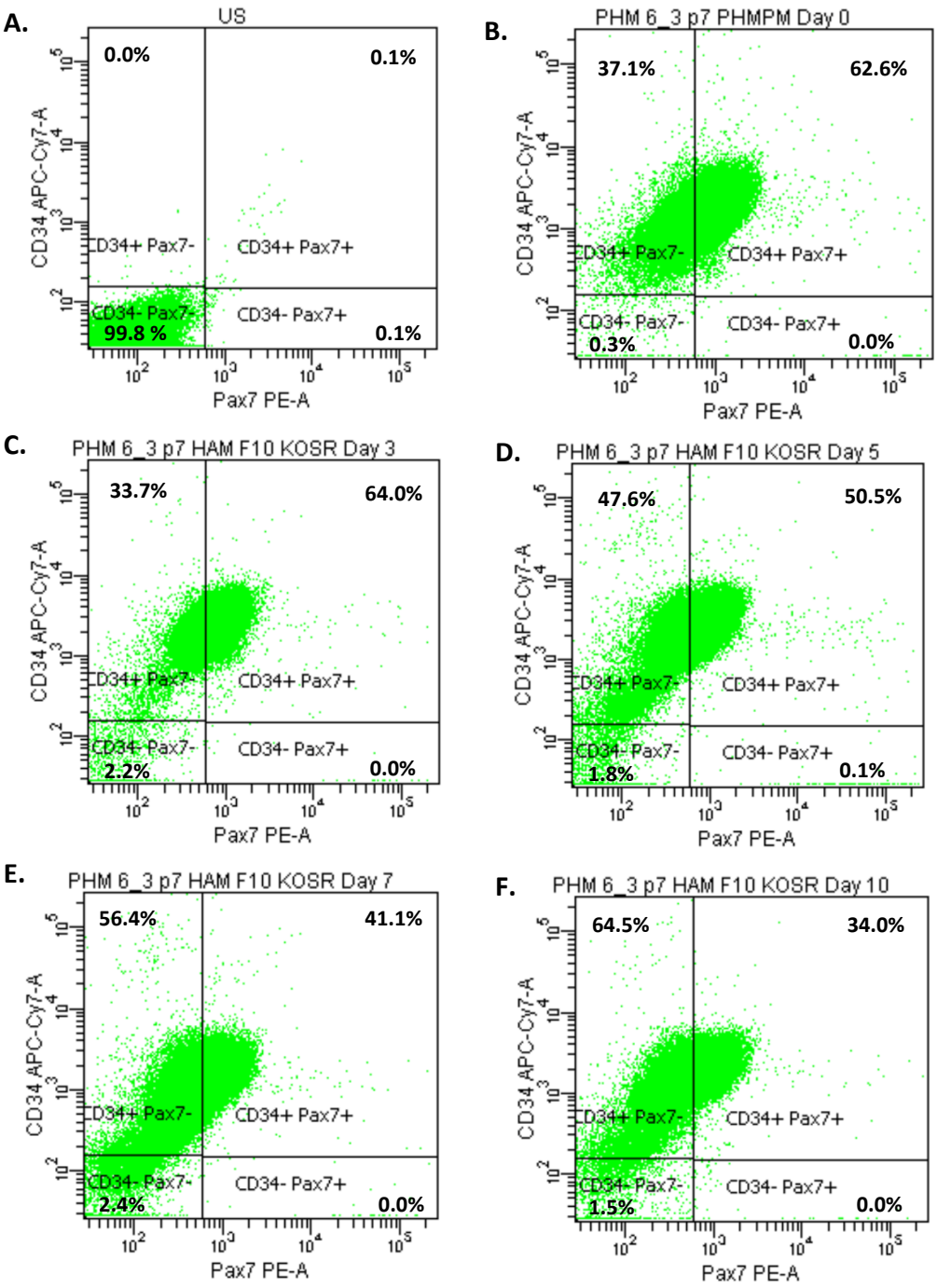

Figure 3.5: Pax7 vs. CD34 expression in PHMs over a 10 day culture period in quiescence media.

Cells were plated into a T75 tissue culture flask. **Panel A:** Unstained control (US). **Panel B:** Percentage of CD34 and Pax7 co-expressing PHMs prior to quiescence media exposure. **Panel C - F :** Percentage of CD34 and Pax7 co-expressing PHMs after 3 days (**Panel C**), after 5 days (**Panel D**), after 7 days (**Panel E**), after 10 days (**Panel F**). The culture media was changed daily, and cells were washed once with 1x PBS. A minimum of 1 x 10^5 satellite cells were analysed for each time point. Data analyses were performed on the FACSDiva™ software v6.1.3.

The expression of the cell surface marker, CD56, which is typically expressed on 'activated' satellite cells, consistently decreased over the 10 day culture period. Before culturing in quiescence media, 25.8% of the PHM population was actively expressing it (Figure 3.6, Panel B). This population dropped to only 2.1% by day 10 (Figure 3.6, Panel F). The expression of Ki-67 is normally only present in the nucleus of cells that are in the cell cycle and undergoing proliferation. PHMs cultured in PHM-PM had high expression of the nuclear antigen, with 84.5% of the entire population expressing it before KOSR exposure (Figure 3.7, Panel B). Throughout the 10 day culture period in quiescence media, however, the percentage of PHMs expressing Ki-67 dropped, until less than half of the PHM population were expressing Ki-67 on day 7 and day 10 (Figure 3.7, Panels E and F). Therefore, culturing the PHMs in the quiescence media reduced cellular proliferation, but quiescence was not achieved in all PHMs. In order to make use of subject 6's expanded PHM stocks to investigate the effects of HGF on a population of PHMs that were at least substantially quiescent, it was decided not to try a KOSR exposure of even longer than 10 days to determine if greater proportion of quiescence might have been achieved.

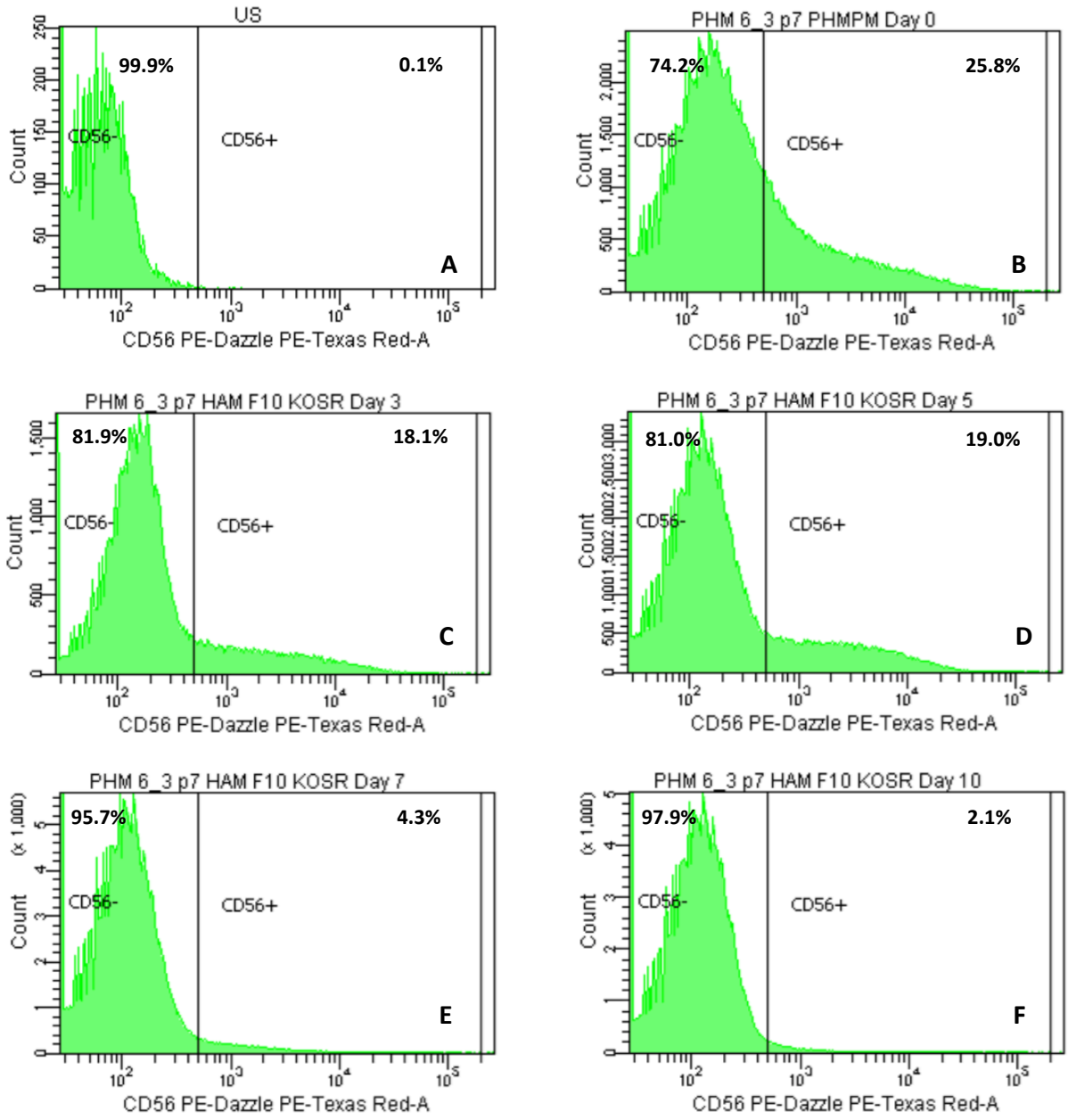

Figure 3.6: CD56 expression in PHMs over a 10 day culture period in quiescence media.

Cells were plated into a T75 tissue culture flask. **Panel A:** Unstained control (US). **Panel B:** Percentage of CD34 expressing PHMs prior to quiescence media exposure. **Panel C - F :** Percentage of CD56 expressing PHMs after 3 days (**Panel C**), after 5 days (**Panel D**), after 7 days (**Panel E**), after 10 days (**Panel F**). The culture media was changed daily, and cells were washed once with 1x PBS. A minimum of 1 x 10^5 satellite cells were analysed for each time point. Data analyses were performed on the FACSDiva™ software v6.1.3.

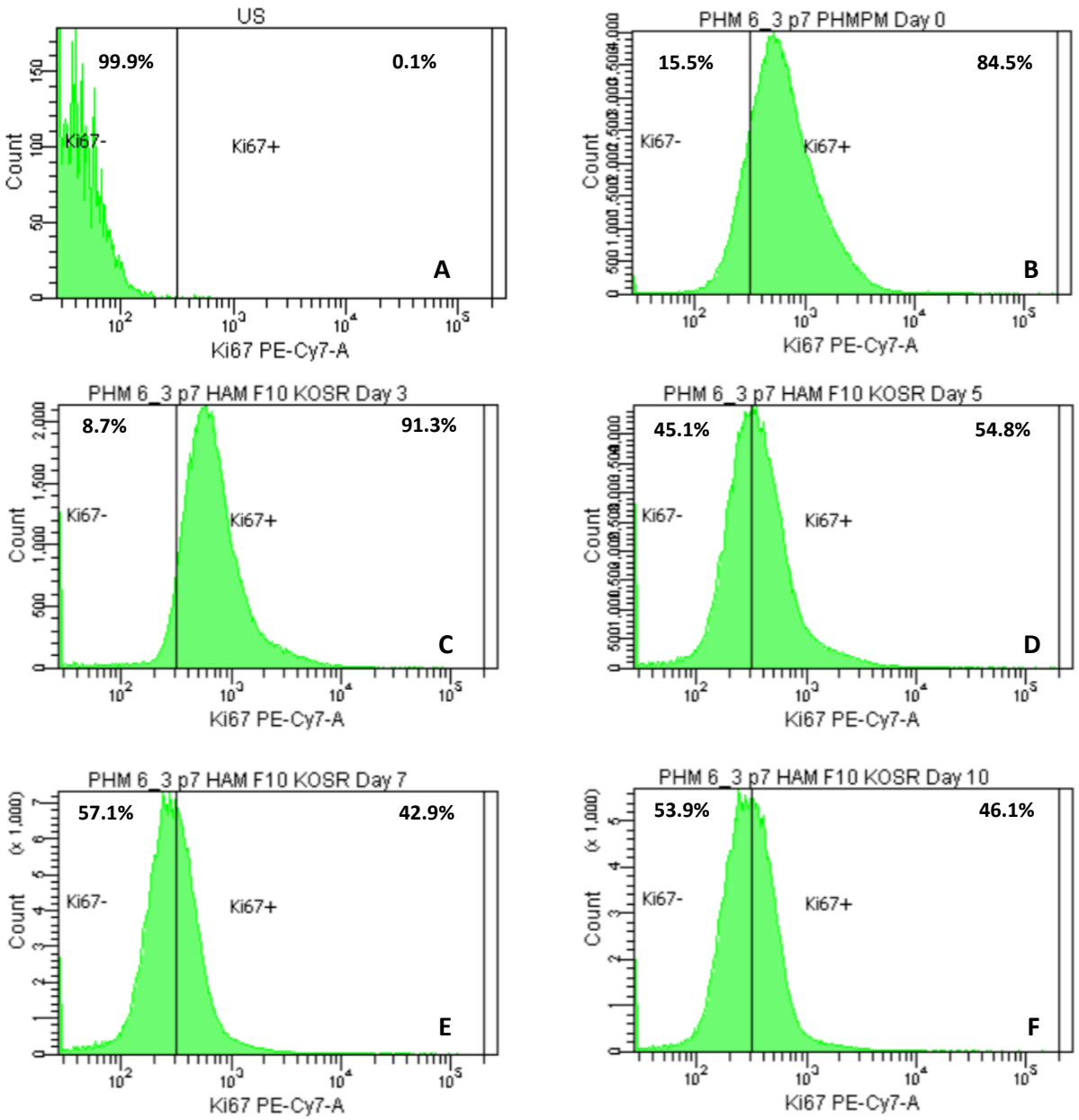

Figure 3.7: Ki-67 expression in PHMs over a 10 day culture period in quiescence media.

Cells were plated into a T75 tissue culture flask. **Panel A:** Unstained control (US). **Panel B:** Percentage of CD34 expressing PHMs prior to quiescence media exposure. **Panel C - F :** Percentage of Ki-67 expressing PHMs after 3 days (**Panel C**), after 5 days (**Panel D**), after 7 days (**Panel E**), after 10 days (**Panel F**). The culture media was changed daily, and cells were washed once with 1x PBS. A minimum of 1 x 10^5 satellite cells were analysed for each time point. Data analyses were performed on the FACSDiva™ software v6.1.3.

3.1.3 THE EFFECT OF QUIESCENCE MEDIA ON THE EXPRESSION OF MYOGENIC REGULATORY FACTORS

To ascertain whether the quiescence media could prevent PHMs from entering the myogenic programme, the expression of the myogenic regulator factors, MyoD and Myf-5, were assessed. Like Pax7, MyoD expression steadily decreased over the 10 day culture period. Only 20.1% of PHMs expressed the myogenic regulatory factor before culturing in quiescence media (Figure 3.8, Panel B) and after 7 and 10 days in culture only just over 9% of the population was positive for MyoD (Figure 3.8, Panels E and F). This confirms that the quiescence media did not induce the expression of MyoD and therefore did not stimulate myogenesis. Myf-5 expression remained constant throughout the entire 10 day culture period in quiescence media (Figure 3.9, Panels B-F) and no changes in expression were noticed between PHMs cultured in proliferation media (PHM-PM) and quiescence media (Figure 3.9, Panels B and F), suggesting that the culture conditions did not affect Myf-5 expression in the PHMs.

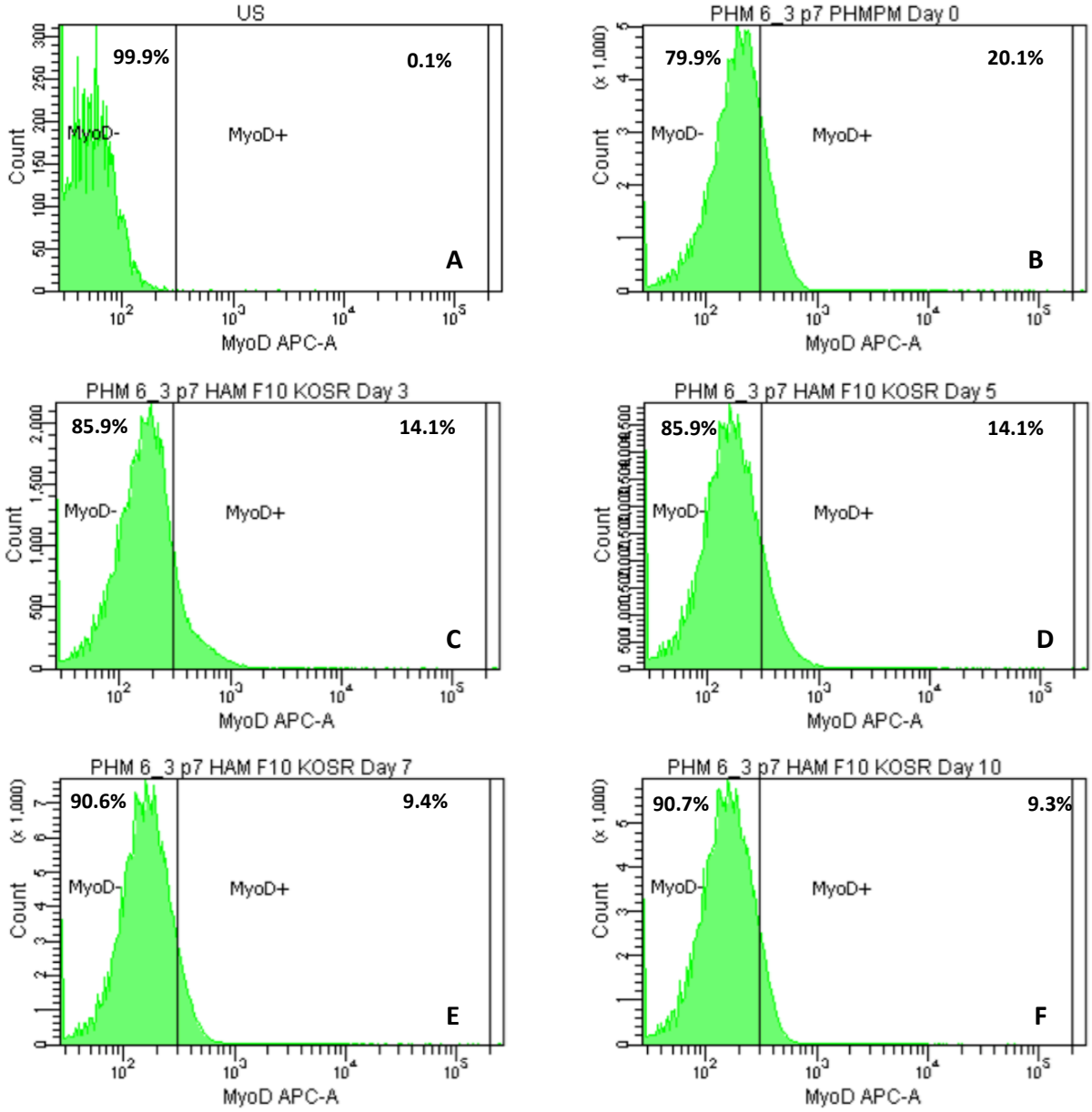

Figure 3.8: MyoD expression in PHMs over a 10 day culture period in quiescence media.

Cells were plated into a T75 tissue culture flask. **Panel A:** Unstained control (US). **Panel B:** Percentage of CD34 expressing PHMs prior to quiescence media exposure. **Panel C - F :** Percentage of MyoD expressing PHMs after 3 days (**Panel C**), after 5 days (**Panel D**), after 7 days (**Panel E**), after 10 days (**Panel F**). The culture media was changed daily, and cells were washed once with 1x PBS. A minimum of 1 x 10^5 satellite cells were analysed for each time point. Data analyses were performed on the FACSDiva™ software v6.1.3.

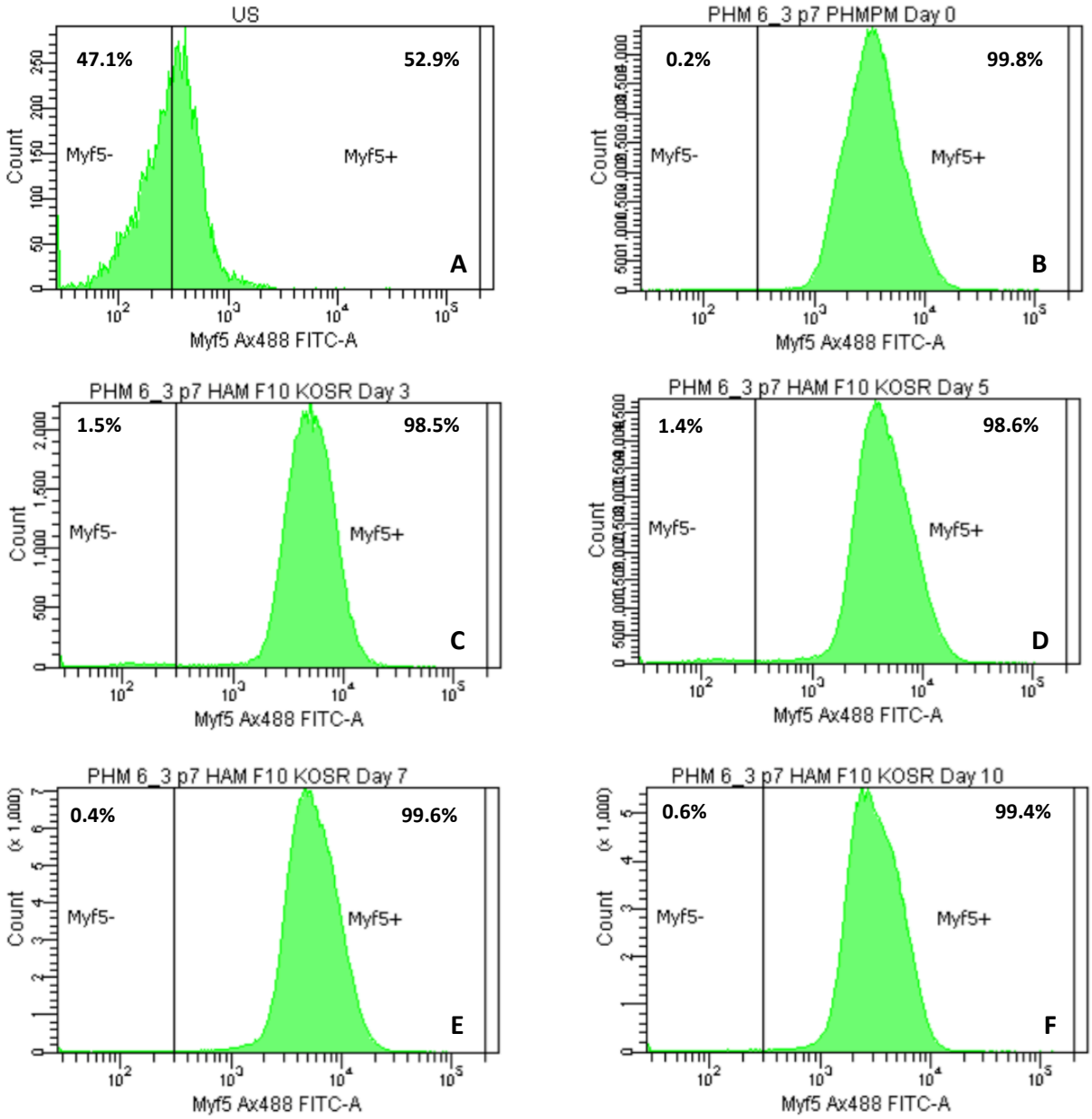

Figure 3.9: Myf-5 expression in PHMs over a 10 day culture period in quiescence media.

Cells were plated into a T75 tissue culture flask. **Panel A:** Unstained control (US). **Panel B-F:** Proportion of cells expressing Myf-5, after compensation for auot-fluorescence indicated in Panel A. **Panel B:** Percentage of Myf-5 expressing PHMs prior to quiescence media exposure. **Panel C - F :** Percentage of Myf-5 expressing PHMs after 3 days (**Panel C**), after 5 days (**Panel D**), after 7 days (**Panel E**), after 10 days (**Panel F**). The culture media was changed daily, and cells were washed once with 1x PBS. A minimum of 1 x 10^5 satellite cells were analysed for each time point. Data analyses were performed on the FACSDiva™ software v6.1.3.

Table 3.2: Summary of marker expression as analysed in flow cytometry in PHMs from subject 6, cultured in T75 flasks in quiescence media for 10 days, for the final flow cytometry experiment.

Marker		Days									
		0		3		5		7		10	
		Cells counted	% (+)	Cells counted	% (+)	Cells counted	% (+)	Cells counted	% (+)	Cells counted	% (+)
Cell Surface	CD34	171,894	99.7	73,047	97.8	175,577	98.3	244,363	97.8	204,850	98.6
	CD56	44,520	25.8	13,533	18.1	34,034	19.0	10,822	4.3	4,456	2.1
Nuclear	Pax7	105,289	61.1	46,534	62.3	87,416	48.9	98,767	39.5	67,711	32.6
	Myf-5	171,977	99.8	73,510	98.5	176,171	98.6	248,833	99.6	206,344	99.4
	MyoD	34,642	20.1	10,510	14.1	25,252	14.1	23,526	9.4	19,418	9.3
	Ki-67	145,691	84.5	68,148	91.3	97,847	54.8	107,256	42.9	95,643	46.1

Footnote: Satellite cell events: **Day 0** - 172,351, **Day 3** - 74,667, **Day 5** - 178,691, **Day 7** - 249,761, **Day 10** - 207,681. Only live satellite cells were analysed. PHMs from subject 6 were used at p7. PHMs were cultured in T75 flasks for 10 days in quiescence media. 500 K cells were plated on day 0 in each T75 flask. PHMs used for day 0 sampling time point were cultured in PHM-PM. The culture media was changed daily, and cells were washed once with 1x PBS. % (+) = Percentage of expressing cells for that marker. Staining procedure was adjusted compared to data presented in Table 3.1.

When analysing pro-myogenesis, pro-proliferation and pro-quiescence, the expression of individual markers should be supplemented by analysis of relevant co-expression. For example, MyoD is known to be a substantially pro-differentiation MRF, whereas Myf-5 positive cells are typically orientated towards self-renewal and maintenance of the parent pool without necessarily being subject to further proliferation. Co-expression of MyoD and Myf-5 is indicative of cells under control of MRFs but not solely pro-differentiation. In contrast, co-expression of CD34 and Myf-5 can be presented to indicate proportion of pro-quiescent cells.

As can be seen in Figure 3.10, the increased co-expression of Myf-5 and CD34 from day 0 (59.6%) to day 7 (89.5%) (Figure 3.10, Panels B - E) during culture in quiescence media substantiates the claims that PHMs were promoted to return to quiescence. Myf-5 vs. CD34 co-expression results pointed toward the fact that culturing PHMs from subject 6 in quiescence media promoted quiescence.

Results for co-expression of MyoD and Myf-5 dropped from 19.4% (Figure 3.11, Panel B) to only 9% (Figure 3.11, Panel F), over the 10 day culture period. This suggested that the culturing of PHMs in quiescence media actively reduces the pro-differentiation environment.

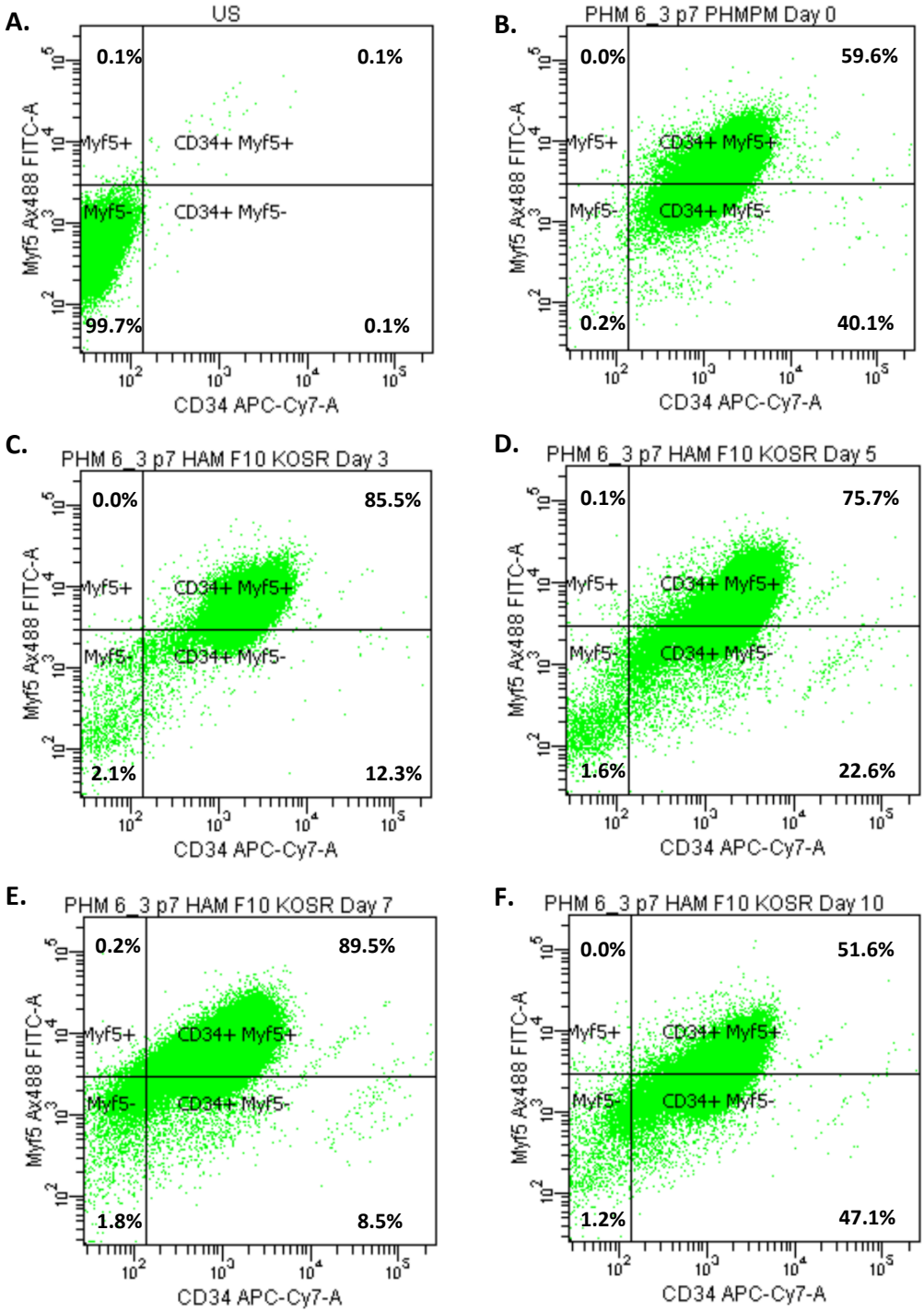

Figure 3.10: Myf-5 vs. CD34 expression in PHMs over a 10 day culture period in quiescence media.

Cells were plated into T75 tissue culture plates. **Panel A:** Unstained control (US). **Panel B:** Percentage of Myf-5 and CD34 expressing PHMs in PHM-PM. **Panel C:** Percentage of Myf-5 and CD34 expressing PHMs after 3 days. **Panel D:** Percentage of Myf-5 and CD34 expressing PHMs after 5 days. **Panel E:** Percentage of Myf-5 and CD34 expressing PHMs after 7 days. **Panel F:** Percentage of Myf-5 and CD34 expressing PHMs after 10 days. The culture media was changed daily, and cells were washed once with 1x PBS. A minimum of 1 x 10^5 satellite cells were analysed for each time point. Data analyses was performed on the FACSDiva™ software v6.1.3.

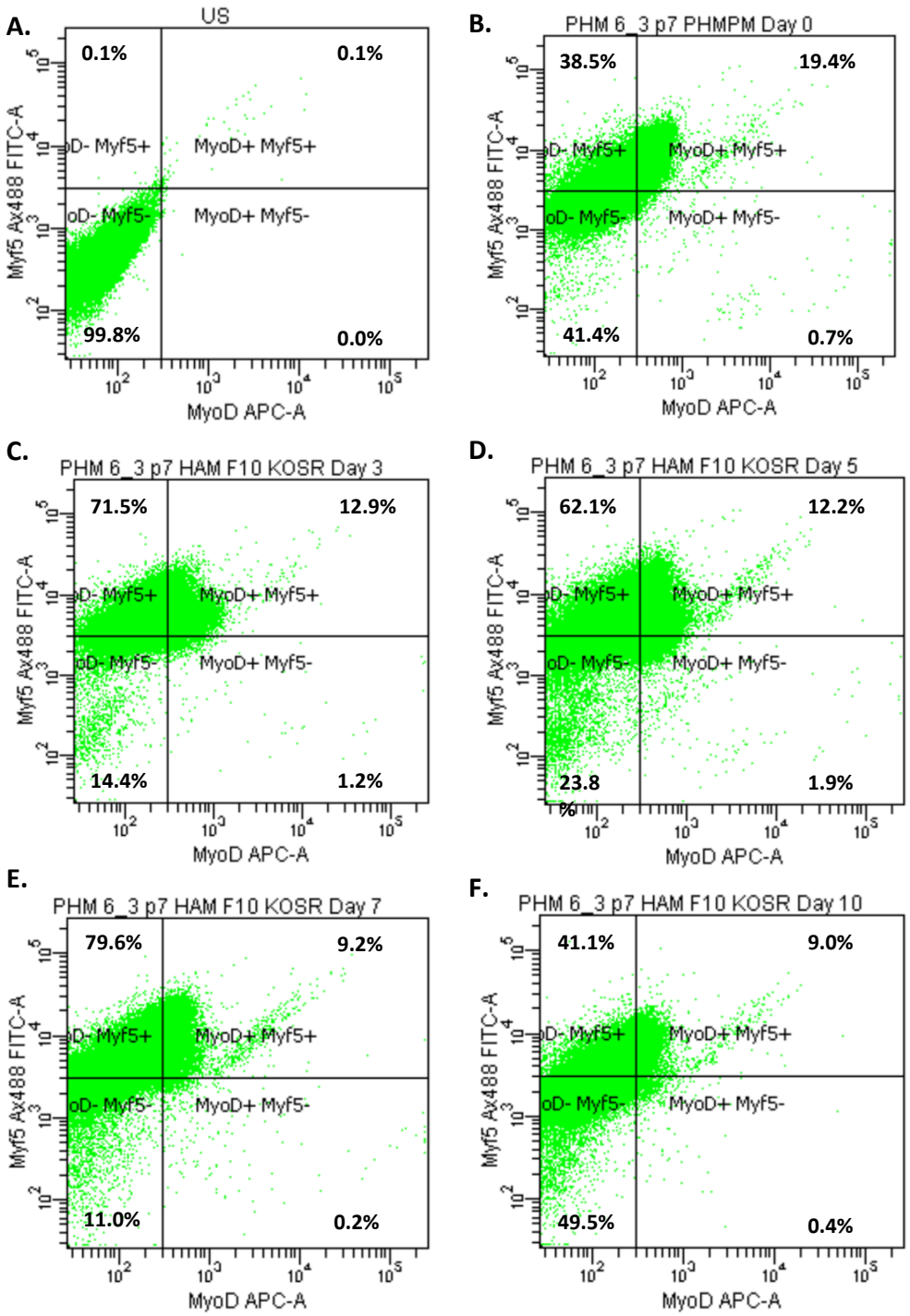

Figure 3.11: MyoD vs. Myf-5 expression in PHMs over a 10 day culture period in quiescence media.

Cells were plated into a T75 tissue culture flask. **Panel A:** Unstained control (US). **Panel B:** Percentage of Myf-5 and MyoD co-expressing PHMs prior to quiescence media exposure. **Panel C - F :** Percentage of Myf-5 and MyoD co-expressing PHMs after 3 days (**Panel C**), after 5 days (**Panel D**), after 7 days (**Panel E**), after 10 days (**Panel F**). The culture media was changed daily, and cells were washed once with 1x PBS. A minimum of 1 x 10^5 satellite cells were analysed for each time point. Data analyses were performed on the FACSDiva™ software v6.1.3

3.1.4 PHMs DO NOT LOOSE THEIR DIFFERENTIATION ABILITY AFTER 10 DAYS IN QUIESCENCE MEDIA

It was important to ascertain that 10 days of culturing PHMs in Ham's F-10 supplemented with 20% KOSR (quiescence media) didn't affect their inherent capabilities to become activated, proliferate and differentiate ie: follow the myogenic path. Since differentiation is the final step in the myogenic path, it was elected to test the effect of quiescence media on subsequent differentiation. PHMs were cultured for 10 days in quiescence media, and then cultured for a further 7 days in culture media that promoted differentiation (PHM-DM, with addition of 2% horse serum) (Refer to Appendix A). Myoblast fusion and myotube formation was first seen after 2 days. This process continued for the next 5 days, and after 7 days, almost no single cells were visible in the culture wells. These data suggested that prolonged culture of PHMs in quiescence media did not affect their subsequent ability to differentiate into myotubes, when exposed to pro-differentiation conditions. It is not clear whether or not PHMs exposed for similar time period to these pro-differentiation conditions without prior quiescence media exposure would have exhibited more myotube formation. Here some proliferative myoblasts are still observed.

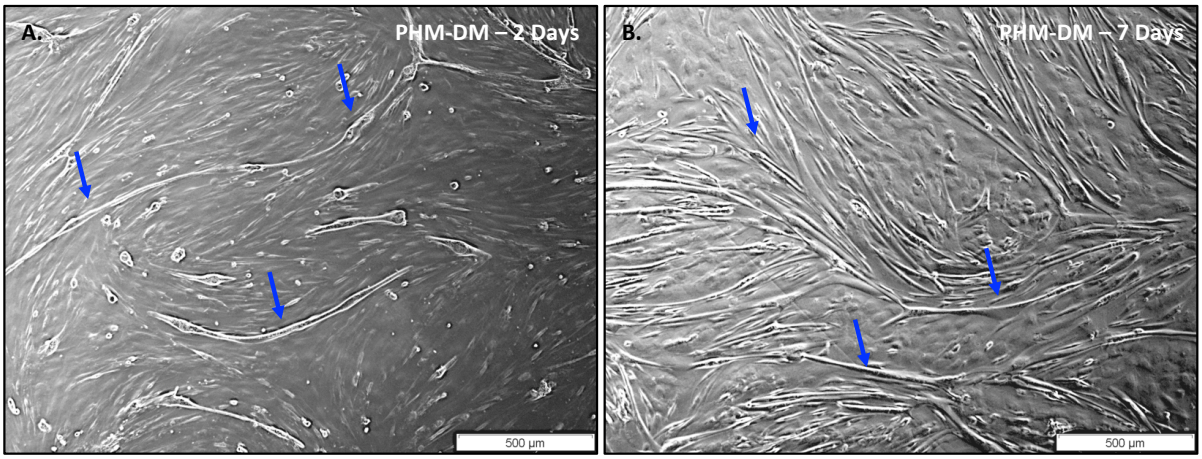

Figure 3.12: PHMs cultured in PHM-DM after 10 days in quiescence media.

Cells were plated into 6-well tissue culture plates (35 mm) and cultured for 10 days quiescence media, followed by a 7 day culture in differentiation media (PHM-DM). The culture media was changed daily, and cells were washed once with 1x PBS. **Panel A**: Image of PHM morphology after 2 days in PHM-DM. **Panel B**: Image of PHM morphology after 7 days in PHM-DM. **Blue arrows** - Myotubes.

3.1.5 THE EFFECT OF QUIESCENCE MEDIA ON THE CELL CYCLE OF PHMs

To corroborate the cell surface marker data obtained with multicolour flow cytometry and provide conclusive evidence toward achieving the first objective of the project, cell cycle analysis was used to ascertain whether culturing PHMs in quiescence media induced them to exit the cell cycle and return to a quiescent state (G_1/G_0). Propidium iodide staining of DNA was used to determine the proportion of cells in each cell cycle stage (G_1/G_0-phase, S-phase, G_2-phase).

As was the case for multicolour flow cytometry, several cell cycle optimisation experiments were performed. Firstly, the effect of KO-DMEM supplemented with 20% (v/v) KOSR on the cell cycle of PHMs was investigated. The optimisation data show that culturing PHMs in this media over a 10 day period substantially decreased the number of cells in S-phase and G_2/M-phase: The percentage of PHMs in S-phase decreased from 11.47% (in PHM-PM) to 2.97%, while the percentage of cells in G_2/M-phase decreased from 5.57% (in PHM-PM) to 1.14%. The decreased percentages of cells in S-phase and G_2/M-phase was reflected in the increased numbers of cells in G_0/G_1 - from 82.96% (in PHM-PM) to 95.62%. Refer to Appendix L for detailed information on the cell cycle histograms and population data. It thus seemed as though culturing cells in KO-DMEM supplemented with 20% KOSR, inhibited cellular proliferation, as >95% of the PHM population was arrested in G_0/G_1 after 10 days of culture. However, due to the observations made in Section 3.1.1 and Figure 3.2 and the results obtained *via* multicolour flow cytometry (for cells cultured in KO-DMEM/20% KOSR), the possibility that the increased numbers of PHMs in G_0/G_1 was due to PHMs differentiating couldn't be excluded.

Cell cycle analysis was thus performed on PHMs cultured in Ham's F-10 supplemented with 20% (v/v) KOSR (quiescence media), as previous results showed that quiescence media favoured proliferation arrest without inducing differentiation.

The effects of culturing PHM's isolated from several different subjects (subject 1, 2, 4, 6 and 9) in quiescence media were investigated (data not shown). Briefly, the optimisation data showed similar effects of quiescence media, on the cell cycle of PHMs (isolated from different subjects). This signified that culturing in quiescence media was inducing the same effects on different PHM populations. These data are not presented, however, due to the extensive optimization and differing

expansion capabilities of PHMs harvested from different subjects, which ultimately caused insufficient cell stocks to enable running the final cell cycle analysis. Due to the fact that enough cellular stocks were generated for subject 6, the final cell cycle analysis optimisation experiment was performed only on PHMs isolated from subject 6. The following qualitative data is presented from the final cell cycle analysis experiment, which was performed after the final optimization experiment using PHMs from subject 6 cultured in quiescence media for 10 days.

The majority (>50%) of PHMs were in the G_1-phase throughout the entire culture period, however the percentage of PHMs actively in the cell cycle varied between the sampling time points (Figure 3.13, Panels A-D). A high proportion of cells in the S-phase were observed in both the PHM-PM (36.11%) and day 3 group (42.87%). There was a noticeable G_2-phase decrease from the PHM-PM group (5.1%) to the day 3 group (0.17%) (Figure 3.13, Panels A and B). The percentage of cells in S-phase substantially decreased on day 7 (9.23%) and day 10 (10.09%) (Figure 3.13, Panels C and D) compared to the day 3 group (42.87%) (Figure 3.13, Panel B). The decreased proportion of cells the S-phase was reflected in the increased proportion of G_0/G_1-phase cells (Figure 3.13, Panels C and D). The percentage of cells in G_2/M-phase was relatively constant in each sampling time point.

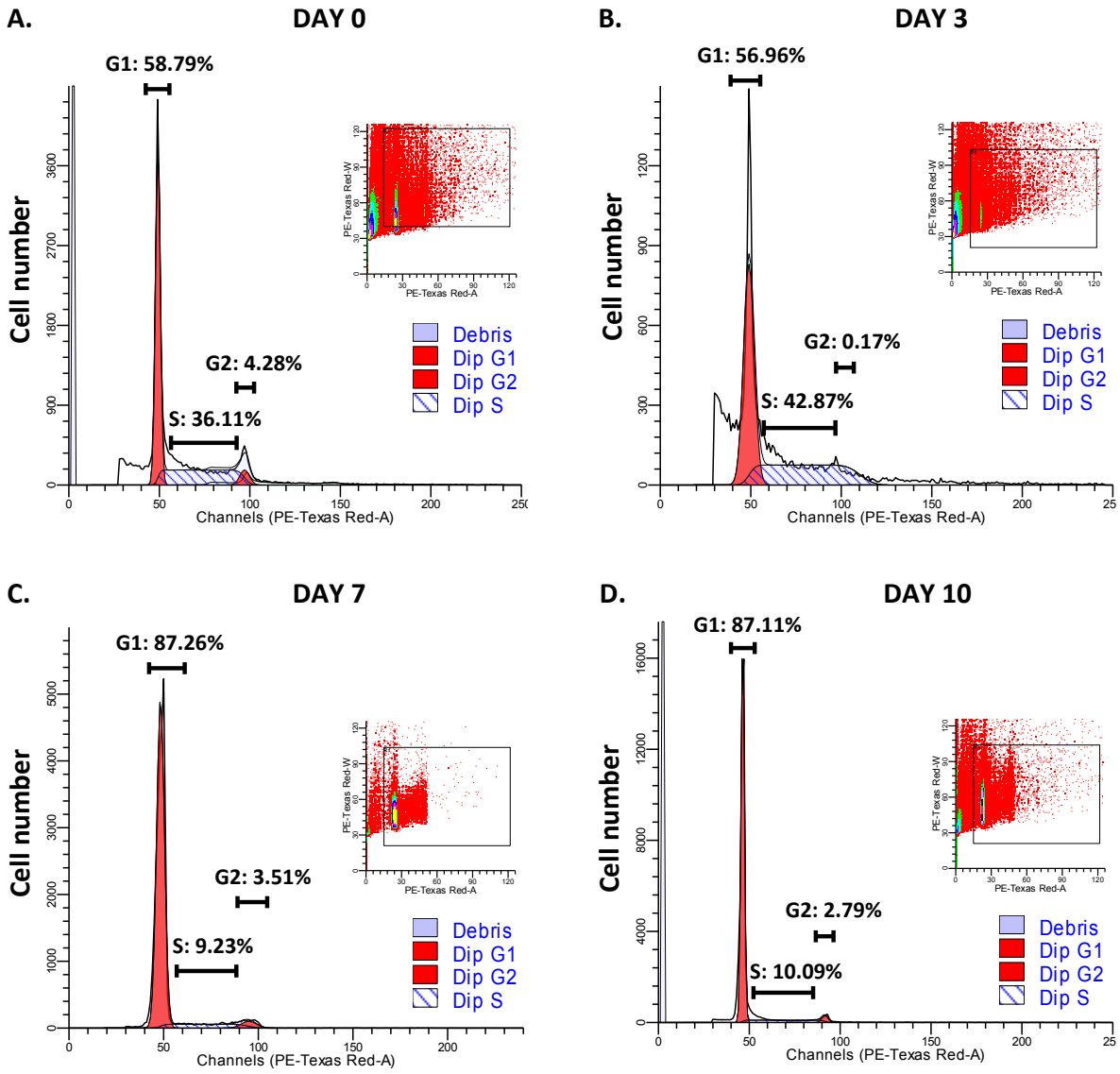

Figure 3.13: Cell cycle analysis of PHMs cultured in quiescence media for 10 days.

Single cells were selected based on the size (FSC-A) and granularity (SSC-A). The propidium Iodide (PI) stained (PE-Texas Red-A) nuclei of the PHMs were analysed for cell cycle proportions by the ModfitLT 3.0 software. The software assumes a Gaussian distribution (bell-shaped curve). The G_0/G_1 Proportion is first identified by the peak with single copies of DNA (*n*) and shows lower PI staining (around 45). The S-phase ranges from 45 to 90, as cells will contain a range of DNA from *n* to *2n*. Cells in G_2 will have a peak doule to that of G_1 as they have diploid nuclei (*2n*).

Taken together, the data obtained for both cell cycle analysis (Section 3.1.5) and multicolour flow cytometer (Sections 3.1.2 and 3.1.3) demonstrated that culturing PHMs in quiescence media induced quiescence without promoting differentiation nor affecting their intrinsic functions (differentiation abilities, Section 3.1.4, Figure 3.12, Panels A and B). The first objective of the project was thus achieved.

3.2 RH-HGF TREATMENT DOESN'T STIMULATE PHMS TO RE-ENTER THE CELL CYCLE

The second objective of the project was to treat quiescent PHMs with rh-HGF and reactivate them, thereby stimulating cell cycle re-entry.

The subsequent experiments were done to determine whether treament with low (2 ng/mL) or high (10 ng/mL) concentrations of rh-HGF had any effect on stimulating the PHMs to re-enter the cell cycle after 10 days in quiescence media. Four conditions were tested. Regardless of dose and time period, treatment with rh-HGF similarly affected the percentage of PHMs in either the S-phase or G_2-phase (Figure 3.14, Panels A - D). However, when the proportion of cells in S and G_2-phase in these rh-HGF-treated groups are compared to that of cells cultured in quiescence media for 10 days (Figure 3.13, Panel D), a small increase of G_2-phase cells is noticable in the treated groups. This increase in G_2/M-phase cells from 2.79% pre-treatment (Figure 3.13, Panel D) to >4% in the treated groups (Figure 3.14, Panels A - D), is reflected in a decreased proportion of S-phase cells (10.1% KOSR 10 days vs. ±7.5% in the rh-HGF treated groups). This could be due to the effects of rh-HGF treatment which re-activated PHMs arrested in S-phase, and stimulated them to progress to a G_2/M-phase.

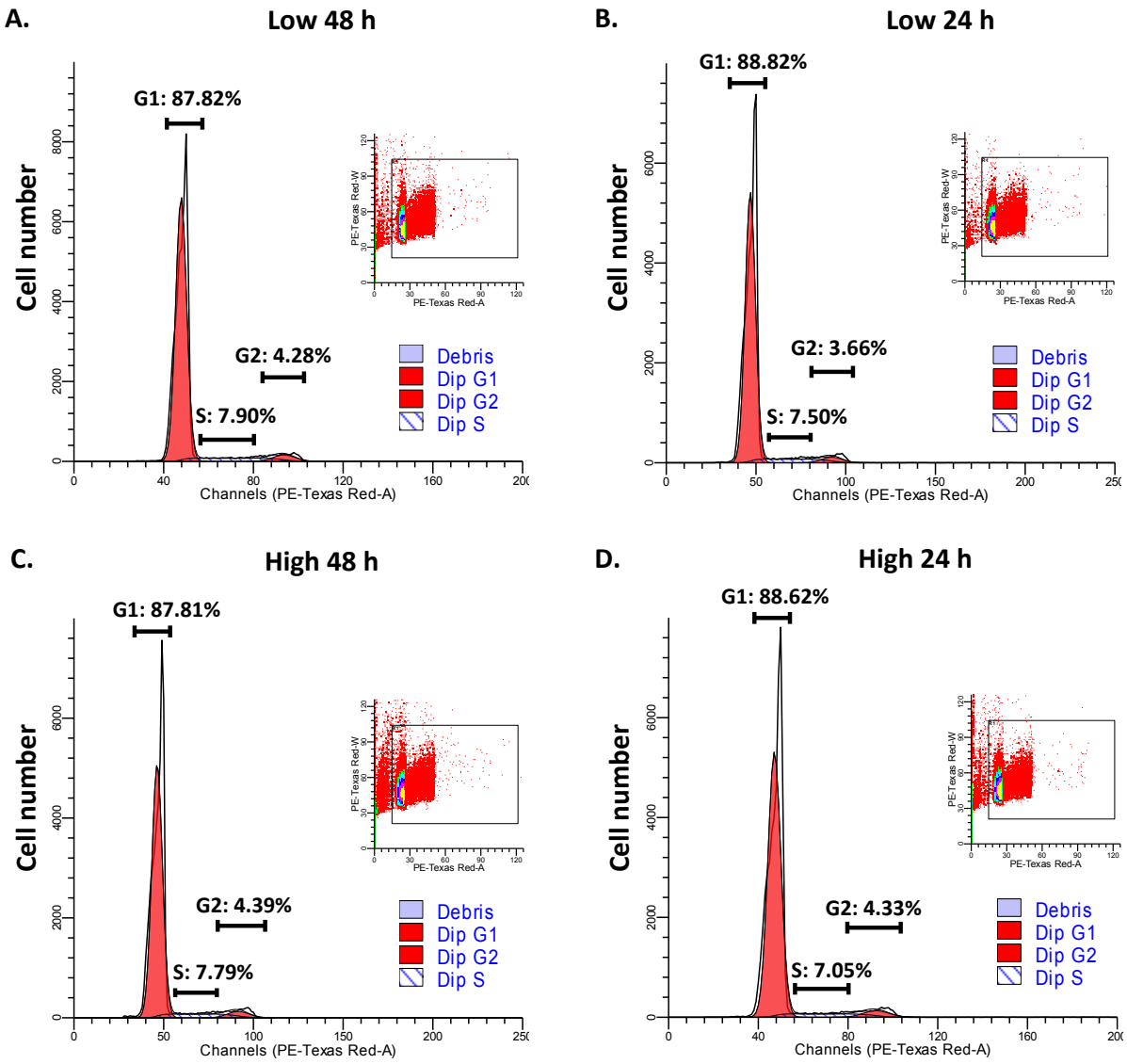

Figure 3.14: Cell cycle analysis of PHMs treated with different concentrations of rh-HGF for 24 h and 48 h.

Single cells were selected based on the size (FSC-A) and granularity (SSC-A). The propidium Iodide (PI) stained (PE-Texas Red-A) nuclei of the PHMs were analysed for cell cycle proportions by the ModfitLT 3.0 software. The software assumes a Gaussian distribution (bell-shaped curve). The G_0/G_1 Proportion is first identified by the peak with single copies of DNA (*n*) and shows lower PI staining (around 45). The S-phase ranges from 45 to 90, as cells will contain a range of DNA from *n* to *2n*. Cells in G_2 will have a peak doule to that of G_1 as they have diploid nuclei (*2n*).

3.3 THE EFFECTS OF RH-HGF TREATMENT ON THE EXPRESSION OF SELECTED GENES

The third objective of the project was to treat quiescent PHMs with rh-HGF and study its effects on expression of various genes under the four different conditions described below. Genes to investigate were selected on the basis of their importance in satellite cell biology.

PHMs were cultured for 10 days in quiescence media and then treated with either low (2 ng/mL) or high (10 ng/mL) concentrations of rh-HGF for either 24 h followed by a period of 24 h without treatment or for a period of 48 h with treatment (24 h followed immediately by a second dose for 24 h). After 48 h protein and RNA were collected from cell lysates of each treatment group. Western blotting and qPCR were used to investigate protein levels and mRNA expression, respectively, in PHMs treated with either low (2 ng/mL) or high (10 ng/mL) rh-HGF for 24 h or 48 h. These data were compared to protein levels and mRNA expression in PHMs cultured in quiescence media for 10 days (control). Refer to Appendix E for the rh-HGF treatment tissue culture plate setup and refer to Appendix J for qPCR raw data and C_T values for mRNA and miRNA expression.

3.3.1 PAX7 EXPRESSION DECREASES UPON RH-HGF TREATMENT IN PHMs

The results obtained from qPCR analysis of relative expression showed a tendency towards decreased Pax7 mRNA levels following rh-HGF treatment. Both low (24 h and 48 h) and high (24 h and 48 h) treatment groups had almost 50% less expression of Pax7 mRNA when compared to the control (KOSR 10 d). However, relative to each other, Pax7 expression did not differ between treatment groups (Figure 3.15).

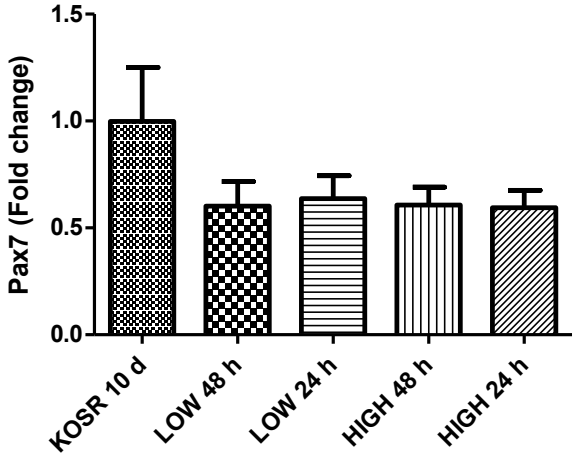

Figure 3.15: Pax7 mRNA expression levels in PHMs treated with rh-HGF at two different doses for 24 h or 48 h.

Cells were cultured in 6-well (35 mm) plates. A total of 3 (n=3) experimental repeats were used for statistical analysis for each treatment group. Within each treatment group 3 wells were pooled to gain sufficient RNA for extraction. qPCR analyses of relative expression levels of Pax7 mRNA in PHMs treated with low (2 ng/mL) or high (10 ng/mL) of rh-HGF for 24 h or 48 h. Samples were run on a StepOnePlus™ realtime PCR machine. The resultant C_T was calculated by the the StepOne™ software v2.2.2. After normalization to a housekeeping gene (18 S ribosomal subunit), each treatment group was normalized to a reference sample (PHM from subject 6 at p7 cultured in PHM-PM). Fold changes in Pax7 mRNA expression are relative to that of the reference sample. Values reported as mean ± S.E.M.

3.3.2 RH-HGF TREATMENT INDUCES ELEVATED HGF PROTEIN IN PHMs

Exposure to rh-HGF was repeated on 3 occasions (passages 6 to 8) for each of the 4 rh-HGF treatment conditions. On each occasion each treatment was done in 3 wells which were pooled to gain sufficient protein for extraction. The control group (KOSR 10 d) had minimal levels of endogenous HGF. All rh-HGF treated groups had increased HGF protein when compared to the control group (Figure 3.16). Although treatment with 2 ng/mL rh-HGF for both 24 h and 48 h significantly changed the level of HGF compared to control, an even greater increase in HGF levels was evident following 10 ng/mL rh-HGF treatment (Figure 3.16), especially after continuous treatment with a high concentration of rh-HGF for a period of 48 h. This was despite washing of cells to remove exogenously added rh-HGF.

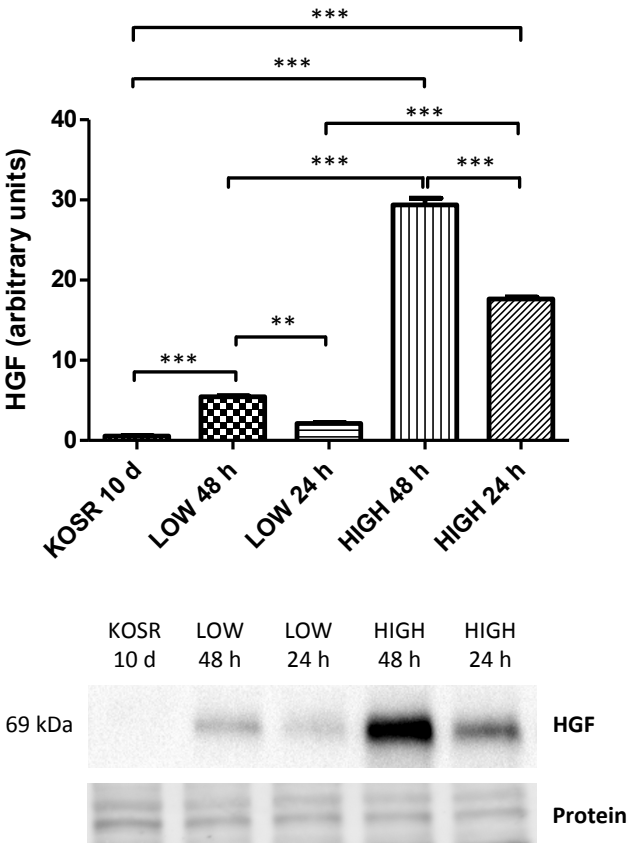

Figure 3.16: HGF levels in PHMs treated with rh-HGF at two different doses for 24 h or 48 h.

Three experimental repeats (done on PHMs from passages 6 to 8) were used for statistical analysis (n=3 for each treatment group). Cells were cultured in 6-well (35 mm) plates. Relative HGF protein was assessed by means of Western blotting. Blots were imaged using the ChemiDoc™ MP Imaging system. Densitometric analysis of the protein samples was performed on the Image Lab™ Software and normalized to total protein. After total protein normalization, each treatment group was normalized to a reference sample (PHMs from subject 6 at p7 cultured in PHM-PM). Arbitrary levels of HGF protein are relative to that of the reference sample. Values reported as mean ± S.E.M. n=3; **p<0.01; ***p<0.0001.

3.3.3 c-MET LEVELS AFTER RH-HGF TREATMENT IN PHMs

Exposure to a ligand may induce regaulation of its receptor. The receptor for HGF is c-Met. c-Met protein was relatively constant when comparing the rh-HGF treated groups, with no statistically significant variations, between treatment groups. Compared to the control, a significant increase in c-Met levels was noticed in the PHMs treated with a high dose of rh-HGF for a period of 24 h (Figure 3.17).

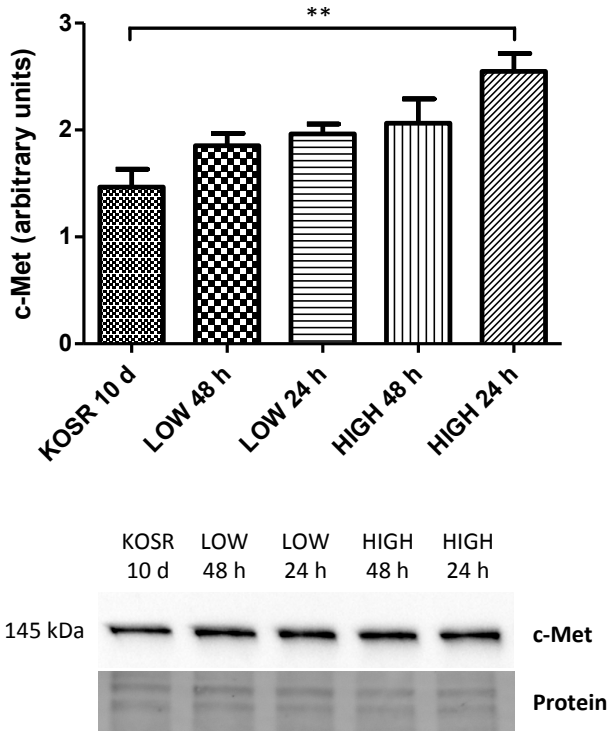

Figure 3.17: c-Met protein in PHMs treated with rh-HGF at two different doses for 24 h or 48 h.

Three experimental repeats (done on PHMs from passages 6 to 8) were used for statistical analysis (n=3 for each treatment group). Cells were cultured in 6-well (35 mm) plates. Within each treatment group 3 wells were pooled to gain sufficient protein for extraction. Relative c-Met protein was assessed by means of Western blotting. Blots were imaged using the ChemiDoc™ MP Imaging system. Densitometric analysis of the protein samples was performed on the Image Lab™ Software and normalized to total protein. After total protein normalization, each treatment group was normalized to a reference sample (PHMs from subject 6 at p7 cultured in PHM-PM). Arbitrary levels of c-Met protein are relative to that of the reference sample. Values reported as mean ± S.E.M. n=3; **p<0.01.

3.3.4 MYOD mRNA AND PROTEIN VARY IN PHMs AFTER RH-HGF TREATMENT

Since MyoD is the master MRF it was important to consider effects of rh-HGF on MyoD at mRNA and protein levels. MyoD protein levels did not differ between the control group and the treatment groups (Figure 3.18).

qPCR analyses of MyoD mRNA showed a roughly 3-fold decrease in the expression levels in the rh-HGF treated samples, compared to the non-treated control. Due to variability, significant differences in mRNA expression was however only detected between the non-treated control and the high 24 h treated sample (Figure 3.19). Within the rh-HGF treated groups, the 24 h treated samples did however seem to have lower levels of mRNA compared to the 48 h treated samples (Figure 3.19).

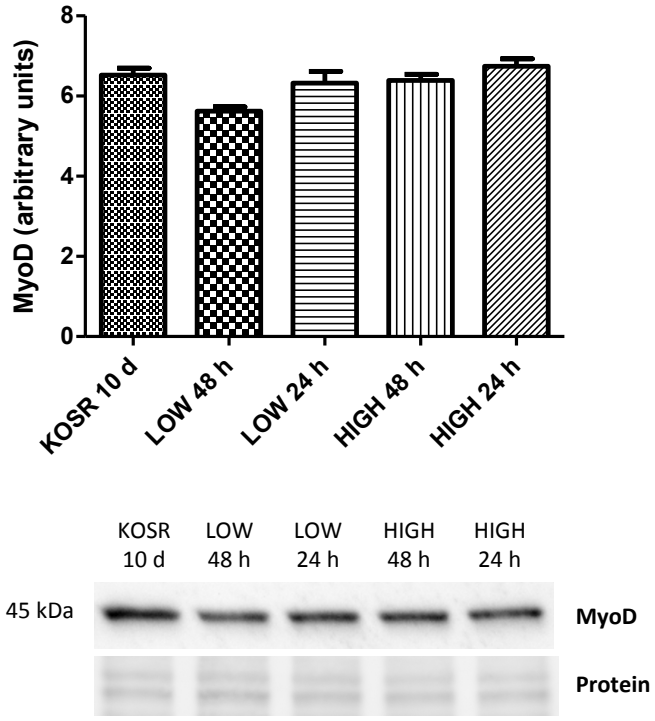

Figure 3.18: MyoD protein in PHMs treated with rh-HGF at two different doses for 24 h or 48 h.

Three experimental repeats (done on PHMs from passages 6 to 8) were used for statistical analysis (n=3 for each treatment group). Cells were cultured in 6-well (35 mm) plates. Within each treatment group 3 wells were pooled to gain sufficient protein for extraction. Relative MyoD protein was assessed by means of Western blotting. Blots were imaged using the ChemiDoc™ MP Imaging system. Densitometric analysis of the protein samples was performed on the Image Lab™ Software and normalized to total protein. After total protein normalization, each treatment group was normalized to a reference sample (PHMs from subject 6 at p7 cultured in PHM-PM). Arbitrary levels of MyoD protein are relative to that of the reference sample. Values reported as mean ± S.E.M. n=3.

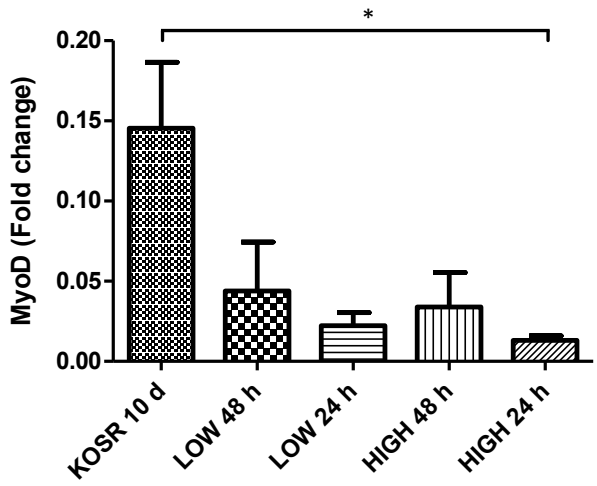

Figure 3.19: MyoD mRNA expression levels in PHMs treated with rh-HGF at two different doses for 24 h or 48 h.

Three experimental repeats (done on PHMs from passages 6 to 8) were used for statistical analysis (n=3 for each treatment group). Cells were cultured in 6-well (35 mm) plates. Within each treatment group 3 wells were pooled to gain sufficient RNA for extraction. qPCR analyses of relative expression levels of MyoD mRNA in PHMs treated with low (2 ng/mL) or high (10 ng/mL) of rh-HGF for 24 h or 48 h. Samples were run on a StepOnePlus™ realtime PCR machine. The resultant C_T was calculated by the the StepOne™ software v2.2.2. After normalization to a housekeeping gene (18 S ribosomal subuint), each treatment group was normalized to a reference sample (PHM from subject 6 at p7 cultured in PHM-PM). Fold changes in MyoD mRNA expression are relative to that of the reference sample. Values reported as mean ± S.E.M. n=3; *$p<0.05$.

3.3.5 MYF-5 mRNA AND PROTEIN IS UNCHANGED IN PHMs AFTER RH-HGF TREATMENT

Myf-5 protein levels were constant in all rh-HGF treatment groups and did not differ from the control at any time point. There was however a trend towards decreased Myf-5 protein in both groups treated with 10 ng/mL rh-HGF (Figure 3.20).

Similarly, a moderate non-significant decrease was evident in Myf-5 mRNA expression in the treated samples compared to the control. All 4 treatment groups did however have similar expression levels of Myf-5 mRNA (Figure 3.21).

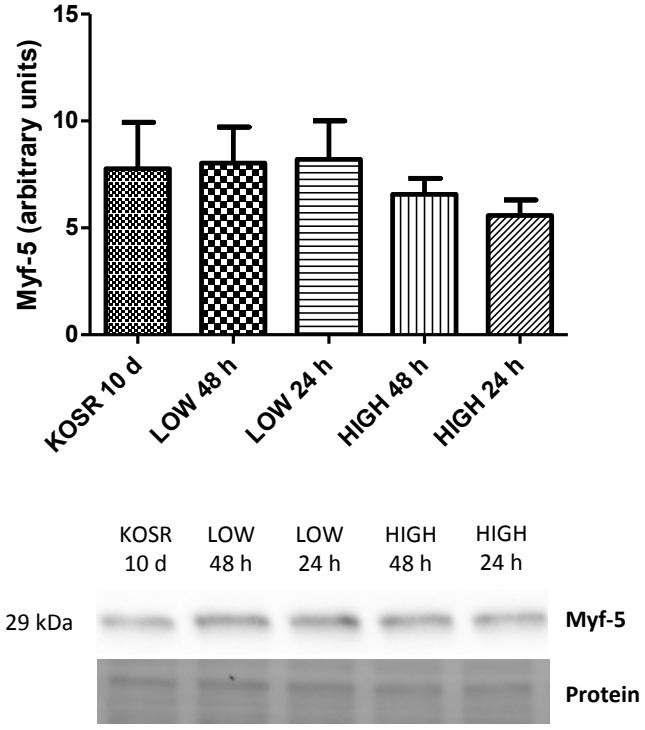

Figure 3.20: Myf-5 protein in PHMs treated with rh-HGF at two different doses for 24 h or 48 h.

Three experimental repeats (done on PHMs from passages 6 to 8) were used for statistical analysis (n=3 for each treatment group). Cells were cultured in 6-well (35 mm) plates. Within each treatment group 3 wells were pooled to gain sufficient protein for extraction. Relative Myf-5 protein was assessed by means of Western blotting. Blots were imaged using the ChemiDoc™ MP Imaging system. Densitometric analysis of the protein samples was performed on the Image Lab™ Software and normalized to total protein. After total protein normalization, each treatment group was normalized to a reference sample (PHM from subject 6 at p7 cultured in PHM-PM). Arbitrary levels of Myf-5 protein are relative to that of the reference sample. Values reported as mean ± S.E.M. n=3.

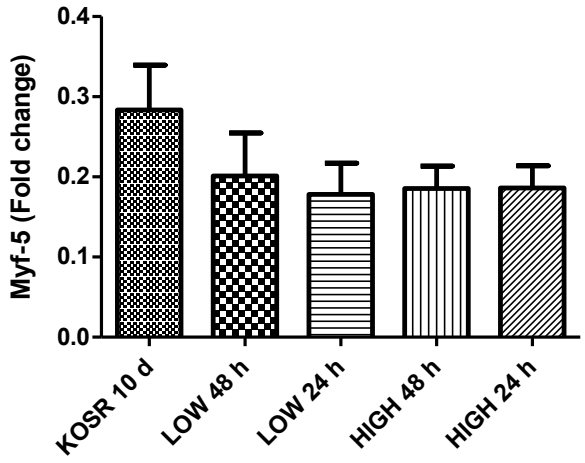

Figure 3.21: Myf-5 mRNA expression levels in PHMs treated with rh-HGF at two different doses for 24 h or 48 h.

Three experimental repeats (done on PHMs from passages 6 to 8) were used for statistical analysis (n=3 for each treatment group). Cells were cultured in 6-well (35 mm) plates. Within each treatment group 3 wells were pooled to gain sufficient RNA for extraction. qPCR analyses of relative expression levels of Myf-5 mRNA in PHMs treated with low (2 ng/mL) or high (10 ng/mL) of rh-HGF for 24 h or 48 h. Samples were run on a StepOnePlus™ realtime PCR machine. The resultant C_T was calculated by the the StepOne™ software v2.2.2. After normalization to a housekeeping gene (18 S ribosomal subuint), each treatment group was normalized to a reference sample (PHM from subject 6 at p7 cultured in PHM-PM). Fold changes in Myf-5 mRNA expression are relative to that of the reference sample. Values reported as mean ± S.E.M. n=3.

3.3.6 A COMPARISON OF MYOD AND MYF-5 AFTER RH-HGF TREATMENT

MyoD and Myf-5 potein was relatively unchanged between treatment groups and compared to the control (Figure 3.22, Panel A). This is also true for the ratio between MyoD and Myf-5 protein (Figure 3.22, Panel C). The low (48 h & 24 h) treatment groups do show more differences in protein compared to the high rh-HGF treatment groups, suggesting that rh-HGF stimulates MyoD protein at higher concentrations.

When analysing mRNA expression, Myf-5 mRNA levels are generally higher than MyoD levels in all rh-HGF treated groups and the treated control groups. However, both genes showed similar patterns in relative expression changes upon exposure to HGF. Indeed, when compared to the controls, all the treatment groups showed decreased mRNA expression for MyoD and Myf-5 (Figure 3.22, Panel B). Although there is too much variation in the samples to make accurate statistical assumptions, it is worthy to note that MyoD mRNA expression tended to be higher in both the low and high 48 h groups compared to their 24 h counterparts. The ratio of Myf-5 mRNA to MyoD mRNA expression indicate a substantial difference in expression levels in the treated groups compared to the control (KOSR 10 day) (Figure 3.22, Panel D). Taken together, the results displayed in Figure 3.22, Panels B and D, indicate that rh-HGF treatment decreases both Myf-5 and MyoD mRNA expression, however its effects are more pronounced on MyoD expression. Consequently, the ratio of Myf-5 to MyoD mRNA is increased in the treated groups (Figure 3.22, Panel D).

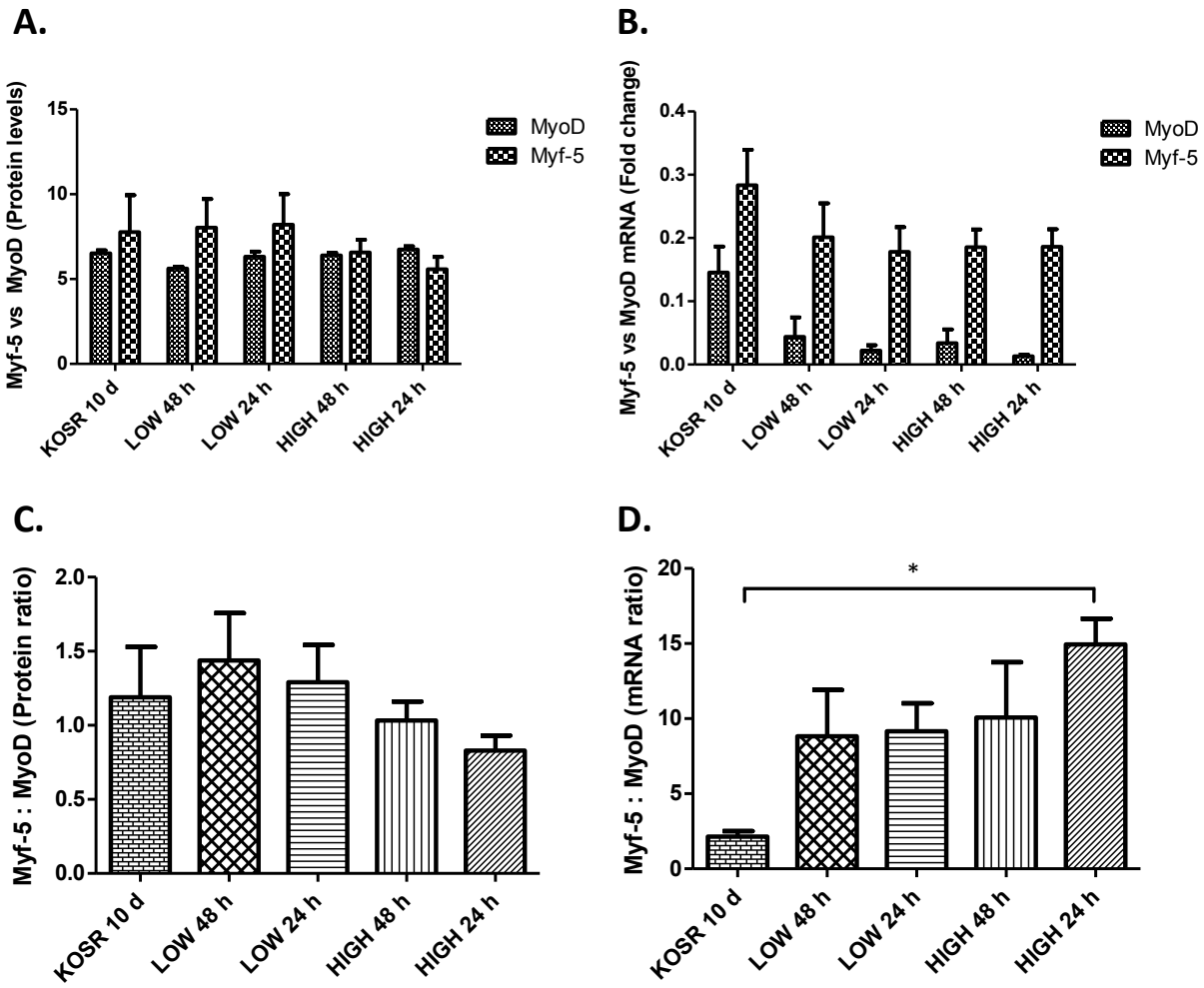

Figure 3.22: Comparison of MyoD vs. Myf5 mRNA and protein levels in PHMs treated with rh-HGF at two different doses for 24 h or 48 h.

Western blot and qPCR analyses for relative MyoD vs. Myf-5 protein and mRNA expression in PHMs treated with low (2 ng/mL) or high (10 ng/mL) of rh-HGF for 24 h or 48 h. **Panel A:** Comparison of MyoD protein to Myf-5 protein for each treatment group. **Panel B:** Comparison of MyoD mRNA expression levels to Myf-5 mRNA expressions levels for each treatment group. **Panel C:** Myf-5 to MyoD protein ratio for each treatment group. **Panel D:** Myf-5 to MyoD mRNA ratio for each treatment group. Three experimental repeats (done on PHMs from passages 6 to 8) were used for statistical analysis (n=3 for each treatment group). Cells were cultured in 6-well (35 mm) plates. Blots were imaged using the ChemiDoc™ MP Imaging system. Densitometric analysis of the protein samples was performed on the Image Lab™ Software and normalized to total protein. After total protein normalization, each treatment group was normalized to a reference samples. mRNA samples were run on a StepOnePlus™ realtime PCR machine. The resultant C_T was calculated by the the StepOne™ software v2.2.2. After normalization to a housekeeping gene (18 S ribosomal subuint), each treatment group was normalized to a reference sample (PHM from subject 6 at p7 cultured in PHM-PM). Arbitrary levels of MyoD and Myf-5 protein along with the fold changes in MyoD and Myf-5 mRNA expression are relative to that of the reference sample. Values reported as mean ± S.E.M. n=3; *p<0.05.

3.4 MICRORNA ANALYSIS

3.4.1 miR-31 EXPRESSION IS UNCHANGED AFTER EXPOSURE TO RH-HGF

qPCR analyses for miR-31 expression showed that rh-HGF treatment did not induce significant changes in relative miR-31 levels. It was however noted that the low 48 h and high (48 h and 24 h) treatment groups showed an almost 2-fold decrease in the miR-31 levels compared to the control group. Due to variability in the control group (KOSR 10 d), statistical significance was not observed.

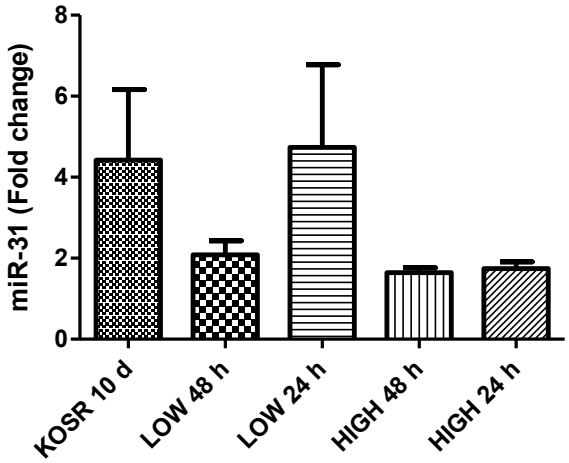

Figure 3.23: miR-31 expression levels in PHMs treated with rh-HGF at two different doses for 24 h or 48 h.

Three experimental repeats (done on PHMs from passages 6 to 8) were used for statistical analysis (n=3 for each treatment group). Cells were cultured in 6-well (35 mm) plates. Within each treatment group 3 wells were pooled to gain sufficient RNA for extraction. qPCR analyses of relative expression levels of miR-31 in PHMs treated with low (2 ng/mL) or high (10 ng/mL) of rh-HGF for 24 h or 48 h. Samples were run on a StepOnePlus™ realtime PCR machine. The resultant C_T was calculated by the the StepOne™ software v2.2.2. After normalization to an endogenous housekeeping miRNA gene (RNU6-2), each treatment group was normalized to a reference sample (PHM from subject 6 at p7 cultured in PHM-PM). Fold changes in miR-31 expression are relative to that of the reference sample. Values reported as mean ± S.E.M. n=3.

CHAPTER 4

DISCUSSION

This study aimed to improve the understanding of how different concentrations of HGF affect the expression of MyoD and Myf-5, in quiescent primary human myoblasts (PHMs). This is important as these two MRFs are upregulated after activation *in vivo*, but *in vitro* studies seldom, if ever, attempted to ensure quiescence prior to intervention. Furthermore, this study investigated the expression of miR-31, a microRNA known to target Myf-5 mRNA and maintain satellite cells in a quiescent, but primed state, known as $G_{Alert.}$ To accomplish these objectives, PHM cell numbers were expanded in culture and a quiescent state induced by FBS removal and supplementation of the culture media with a synthetic, growth factor-free serum replacement: KnockOut™ Serum Replacement (KOSR). The cell cycle analyses and multicolour flow cytometer data provided evidence that PHMs were driven into a quiescent state and light microscopy ascertained that culturing PHMs in quiescence media for 10 days did not induce any morphological changes suggestive of activation. Full functionality of PHMs, despite long exposure to KOSR, was confirmed when it was subsequently established that it did not affect the intrinsic differentiation capacity of PHMs.

Once in a quiescent state the PHMs were treated with low (2 ng/mL) or high (10 ng/mL) concentrations of rh-HGF for 24 h and 48 h to investigate the effects of concentration and time effects of gene expression. Analysis of MyoD and Myf-5 protein levels showed that rh-HGF did not affect protein synthesis significantly, regardless of concentration. Analysis of mRNA levels for the two MRFs showed that Myf-5 expression was not affected by rh-HGF treatment, while MyoD mRNA levels greatly decreased upon exposure to rh-HGF, albeit significant differences were only observed between the 24 h-high treatment group vs control. Pax7 mRNA expression, was not statisticaly significantly changed throughout all rh-HGF treatments, confirming the cultured PHMs were not differentiating. Since light microscopy images revealed some evidence of elongation and alignment (in KO-DMEM) this deserves further investigation. Due to variability, it was however inconclusive whether miR-31 played an active role in maintaining PHMs in a quiescent state.

4.1 KNOCKOUT SERUM REPLACEMENT INDUCED A QUIESCENT STATE IN PRIMARY HUMAN MYOBLASTS

It has been reported extensively that *in vitro* culture of animal cells requires the use of FBS to ensure cell survival, as it contains a vast array of growth factors essential for supporting cellular processes (Brunner et al. 2010). The optimal growth and survival media for culturing PHMs or isolated muscle satellite cells is Ham's F-10 nutrient medium (Motohashi et al. 2014; Liu et al. 2015), which is then supplemented with a variety of sera, typically 20% FBS. The media of choice routinely used in our laboratory, consists of Ham's F-10 nutrient medium supplemented with FBS (20%, v/v), L-glutamine (6.8%, v/v) and recombinant human fibroblast growth factor (rh-FGF) (10 ng/mL). The essential amino acid, glutamine, supports the proliferation of cells that have high energy demands and synthesize large amounts of proteins and nucleic acids (Newsholme et al. 2003). The addition of rh-FGF further promotes cell survival and stimulates cellular proliferation (Sheehan & Allen 1999; Kästner et al. 2000). The present study, however, required the PHMs to be in a quiescent state, to enable re-activation with rh-HGF in order for investigation of the expression of myogenic genes during the initial stages of satellite cell activation.

To induce cellular quiescence the FBS and rh-FGF were replaced with a synthetic, growth factor-free serum known as KnockOut™ Serum Replacement (KOSR). Supplementing the Ham's F-10 nutrient medium with 20% (v/v) of KOSR ensured the survival of PHMs over a 10 day culture period and promoted cells to shift into a G_0/G_1 state. Other techniques have been used with success to induce isolated primary human myoblasts into a quiescent state (Sellathurai et al. 2013). Instead of removing mitogens and growth factors from the culture media of adherent cultures, Sellathurai et al. (2013) utilized a suspension culture technique to induce cellular quiescence, which had previously been reported to efficiently arrest C2C12 myoblasts proliferation and maintain cells in a quiescent (G_0) phase (Milasincic et al. 1996). These studies employed a semi-solid suspension medium (DMEM supplemented with 10% FBS, 1% P/S and 2% methylcellulose) to maintain PHMs in suspension, thereby causing the loss of substrate attachment, which triggered the 'suspended' PHMs to become quiescent (G_0) (Sellathurai et al. 2013). However lack of attachement is not an inherent state for satellite cells, as *in vivo* they are always in contact with the basal lamina, the sarcolemma of muscle fibres and other ECM components.

In the present study cell cycle analysis showed that culturing adherent PHMs in a growth factor free environment (quiescence media) lead to a 30% increase in the proportion of PHMs cells in G_0/G_1 state and a 32% decrease in the proportion of S-phase cells, compared to PHMs cultured in PHM-PM. Cell cycle analysis results were supported by the multicolour flow cytometer data showing that both Ki-67 and CD56 expression steadily decreased over the 10 day culture period in quiescence media. This reduction in proliferation marker was not due to PHM's differentiation, as the expression of the stem cell marker, CD34, was maintained (stem cells that differentiate loose expression of this marker). Similarly, Sellathurai *et al.* (2013) showed that when PHMs were placed in suspension medium, levels of Ki-67 and BrdU (pulse labelling) expression steadily decreased over a 48 h period (12 h, 24 h, 48 h) and disappeared after 96 h in suspension media (Sellathurai et al. 2013). Thus both methodologies induce PHM quiescence effectively. Sellathurai *et al.*'s (2013) protocol allows for a more rapid induction into G_0 (96 h vs. 10 days) and induced a G_0 state in the entire cultured population of PHMs thus enabling synchronized reactivation of a homogeneous PHM population (Sellathurai et al. 2013). Having a homogeneous synchronized population is an advantage when performing MRF gene expression analysis, in satellite cell re-activation studies, as all cells 'have a common starting ground'. However, the decision to test the use of KOSR was in part motivated by the fact that the current study wished to assess the effect of a growth factor and the KOSR conditions allowed for absence of an amorphous FBS environment. With these observations, it was confirmed that using KOSR with Ham's F-10 nutrient media mixture inhibited cellular proliferation to a certain extent without inducing differentiation. The lack of complete cell cycle arrest could potentially be explained by the heterogeneity of the PHM population. For future studies the suspension culture in combination with the KOSR should be tested to investigate whether this combined methodology induces cellular quiescence more efficiently than simply suspension culture or KOSR culture alone.

4.2 HETEROGENEOUS POPULATION OF MYOBLAST PRECURSOR CELLS: PAX7^{+}/CD34^{+}/MYF-5^{+} AND PAX7^{-}/CD34^{+}/MYF-5^{+}

The concept of satellite cell heterogeneity and the existence of satellite cell subpopulations has been a topic of discussion over the past several years, and mounting evidence has been presented in support of this (Schultz 1996; Beauchamp et al. 2000; Montarras et al. 2005; Sacco et al. 2008; Lindström et al. 2010) Satellite cells differ in their gene expression patterns and myogenic differentiation predisposition (as described in Section 1.1.4). In the present study, analysis of the expression of specific satellite cell markers revealed that the PHMs used, despite their origin from a single muscle biopsy, was a heterogeneous population of satellite cells, with regards to marker expression.

Only a subset of the PHM population (61%) were positive Pax7 protein when cultured in primary human myoblast-proliferation media (PHM-PM) with even fewer of the PHMs (32%) expressing Pax7 following 10 days of culture in quiescence media. The entire population of PHMs however maintained the expression of Myf-5 (99.4%) and CD34 (98.6%) over the entire 10-day culture period in quiescence media. The presence of CD34 and Myf-5 expression in the culture model confirmed that the PHMs were undifferentiated myoblast precursor cells (MPCs). The high levels of Myf-5, but low levels of MyoD expression is furthermore indicative that the quiescence media reduced the pro-differentiation environment. However, the decreases in Pax7 expression in the PHM population used in the current investigation, suggests that the cell population in culture are no longer true satellite cells, which are defined as expressing Pax7 *in vivo* (Seale et al. 2000) but rather MPCs. There are numerous accounts in the literature of satellite cells existing as a heterogeneous population *in vivo*, with regards to gene expression patterns and myogenic differentiation predisposition (Kallestad & McLoon 2010; Rossi et al. 2010).

Kallestad and Macloon (2010) showed that *ex vivo* sorting of skeletal muscle derived cells exhibited heterogeneous (with regards to marker expression) and overlapping (with regards to the nature of the cell) populations (Kallestad & McLoon 2010). Sorted for accepted myogenic precursor cell markers (CD34, Sca-1, Pax7 and M-cadherin), FACS analysis showed that both a 'side population', thought to be progenitor enriched and a 'main population' contained both satellite cells and multipotent progenitor cells (Kallestad & McLoon 2010). Similarly, Rossi *et al*. (2010), identified the

presence of two main satelllite cell populations on isolated single muscle fibres from rat *flexor digitorum brevis* (Rossi et al. 2010). These two satellite cell populations were identified on the surface of the muscle fibres, based on the number of clones the parent satellite cell generated after 5 days in suspension culture (aka hanging drops). Clonal characterization showed that these two subpopulations differed based on their proliferative abilites, with the 'low-proliferative' clones present in major proportion (~75%) (Rossi et al. 2010). The differences in proliferation potential between the two subpopulations were shown to be caused by innate differences in their mitochondrial membrane potential, ATP synthesis efficiency and Reactive Oxygen Species (ROS) generation: the 'high-proliferative' clones had a more glycolytic phenotype. The 'low-proliferative' clones spontaneously differentiated and generated myotubes and thus had a higher myogenic potential than the 'high-proliferative' clones. However, when co-cultured together, the 'low-proliferative' clones were able to induce the 'high-proliferative' clones to express MyoD and differentiate into myoblasts (Rossi et al. 2010). How isolated PHMs used in this study may have influenced each other during their expansion is not known. But they remain heterogeneous despite 10 d exposure to the same KOSR. The majority of PHMs in the current study represent a $Pax7^{-}$ /$CD34^{+}$/$Myf\text{-}5^{+}$ MPC population, with a small population of more 'parent-like' satellite cells that expressed both Pax7 and CD34. Published data suggests that a $Pax7^{+}$/$CD34^{+}$/$Myf\text{-}5^{-}$ subpopulation of PHMs would represent a more stem-like satellite cell population with self-renewal capabilities: $Pax7^{+}$/$Myf\text{-}5^{-}$ and $Pax7^{+}$/$Myf\text{-}5^{+}$ subpopulations have been shown to exist *in vivo* and the 'less differentiated' $Pax7^{+}$/$Myf\text{-}5^{-}$ satellite cells were able to self-renew better than $Pax7^{+}$/$Myf\text{-}5^{+}$ (Kuang et al. 2007).

4.3 RH-HGF TREATMENT MODERATELY STIMULATED PHMS TO RE-ENTER THE CELL CYCLE

Cell cycle analysis of PHMs treated with low (2 ng/mL) or high (10 ng/mL) rh-HGF for 24 h or 48 h, overall showed signs of cell cycle re-entry. Although the G_1 fractions didn't vary from the control (KOSR 10 d), the percentage of S-phase cells decreased upon exposure to all rh-HGF conditions. This decrease in S-phase was mirrored by an increased percentage of G_2-phase cells. No decreases in G_1 cells were noted for either low or high rh-HGF concentrations, with either the 24 h or 48 h exposure. These results indicate that rh-HGF was unable to effectively restimulate cells to re-enter the cell cycle. The lack of observable PHM re-activation is not in agreement with literature. One major difference in the current study was the KOSR media condition to which the PHMs had been exposed and in which they remained during rh-HGF exposure. But the concentration of rh-HGF used in in different studies also differs significantly.

Yamada et al., (2010) showed that rat satellite cells cultured in extremely high doeses of HGF (500 ng/mL) to induce decreased proliferation, were reactivated and showed newly BrdU-positive cells after 48 h of culture with 2.5 ng/mL of HGF (Yamada et al. 2010). The media used to culture satellite cells in the study of Yamada *et al.* (2010) contained 10% horse serum (HS), and the potential effects of HS on satellite cell reactivation needs to be taken into account. Furthermore, the growth factors contained in their nutrient media (DMEM) may have contributed to the increases in BrdU positive cells, or at least augmented the effects elicited by the 2.5 ng/mL of HGF treatment. Walker *et al*. (2015) reported similar results to the ones seen by Yamada *et al*. (2010) regarding increased cellular proliferation upon HGF treatment. In their study, both C2C12s and human skeletal muscle myoblasts (HSkM) showed increased cellular proliferation, as determined by cell counts, after 24 h of rh-HGF treatment (2 ng/mL) (Walker et al. 2015). In the study by Walker *et al.* (2015) the rh-HGF proliferation experiments were performed in media containing 10% (v/v) and 20% (v/v) FBS, respectively.

Furthermore, in the published studies cellular quiescence was not induced prior to rh-HGF treatment. One hypothesis as to why the quiescent PHMs did not shown concrete signs of re-established proliferation, even after 48 h of rh-HGF treatment (2 ng/mL), is that cell cycle analysis is not sensitive enough. Alternatively, quiescent PHMs may require the presence of mitogenic factors

as well as HGF to truly become re-activated. Performing qPCR analysis of known cell cycle inhibitors like $p27^{kip1}$ and $p57^{kip2}$ alongside cell cycle promoters, could more accurately determine the influence of rh-HGF on cell cycle parameters. This was not done here but the possibility that lack of significant effect of rh-HGF may have been related to available receptor was investigated.

4.4 HGF AND C-MET

c-Met is the recepetor for HGF. Binding of HGF to c-Met causes receptor dimerization and intracellular signaling. This in turn activates specific gene expression, mediated by the activation of different intracellular signaling pathways. Because HGF signaling is thought to also promote further expression of c-Met on satellite cells, changes in c-Met expression should be seen with different concentrations of HGF (Organ & Tsao 2011). HGF itself is normally not present in satellite cells but it can be produced and secreted from them upon stimulation by exogenous HGF. This is part of a positive feedback mechanism that ensures that enough satellite cells get activated and begin proliferating.

Western blot analysis revealed that quiescent satellite cells (KOSR 10 d) did not express endogenous HGF, which is logical as if they did they wouldn't be in a quiescent state. *In vivo* endogenous HGF production is stimulated only after c-Met activation (Sheehan et al. 2000). Here, PHMs were treated *in vitro* with either low (2 ng/mL) or high (10 ng/mL) concentrations of rh-HGF for 24 h or 48 h. The data suggests that endogenous production of HGF was both concentration and time dependent. 24 h of low (2 ng/mL) and high (10 ng/mL) rh-HGF treatment stimulated less intracellular HGF production compared to the 48 h treated group. Furthermore, the high rh-HGF concentration stimulated more endogenous HGF production that the low concentration.

Western blot data for c-Met showed that treating PHMs with rh-HGF stimulated its expression. Furthermore, in accordance with literature, higher concentrations of rh-HGF stimulated more receptor expression. These findings are similar to those reported by Walker *et al.* (2015) in C2C12s. There, 10 ng/mL of HGF stimulated greater c-Met expression than C2C12s treated with only 2 ng/mL (Walker et al. 2015). Although the signaling pathways that HGF/c-Met signaling activates are known (Leshem et al. 2002; Halevy & Cantley 2004; Walker et al. 2015), they were not investigated here. A limitation of using PHMs is that expansion of stock is more limited than is possible when using the C2C12 line. The decision was made for the current study to focus on the c-Met receptor and the MRFs, Myf-5 and MyoD.

4.5 MYF-5 AND MYOD EXPRESSION IN QUIESCENT PHMS

The vast array of literature around the expression MyoD and Myf-5 point toward their different roles. Proliferating myoblast precursor cells are characterized by the expression of Myf-5 and MyoD. *In vivo* studies using adult mice, injured with cardiotoxin (10^{-5} M) (Cooper et al. 1999) and *in vitro* studies using myofiber cultures isolated from mice (Cornelison & Wold 1997; Zammit et al. 2002) showed that most satellite cells express either Myf-5 or MyoD after 24 h and co-express them by 48 h (Cornelison & Wold 1997; Cooper et al. 1999). The current study's data show that MyoD and Myf-5 expression were present in the quiescent PHMs both at the protein and mRNA level.

It has been shown that within the entire satellite cell population, there may also be a distinct subpopulation of more 'committed' satellite cells. These cells were shown to express MyoD, desmin and myogenin already only 12 h after injury, indicating these cells may differentiating without first proliferating (Rantanen et al. 1995). Although desmin and myogenin were not assessed in the current study, the cultured PHMs didn't show morphological signs of differentiation. However, due to the presence of MyoD and Myf-5 protein and mRNA in the quiescence cells, these cells can also be considered committed progenitor cells (aka myoblast precursor cells). It is a possibility that these committed cells have expressed either MyoD, Myf-5 or both during the course of their history: before isolation, during expansion or before the actual experiments.

The data obtained for Myf-5 mRNA expression in quiescent cells is in agreement with Crist *et al.*'s (2012) findings, however, Crist *et al.* (2012) didn't report any Myf-5 protein presence. Crist *et al.* hypothesized that the reason why Myf-5 mRNA was observed but no protein, was due to miR-31's targeted repression of Myf-5 mRNA (Crist et al. 2012). In the current study miR-31 was present in the quiescent cells. However, no co-localization studies were performed for Myf-5 mRNA and miR-31, to ascertain whether sufficient miR-31 was targeting all Myf-5 mRNA. Thus, due to the fact that Myf-5 protein was shown in the quiescent PHMs and that the expression levels of Myf-5 was relatively similar to that of MyoD, one may assume that the PHMs were not truly quiescent (in G_0-phase) or that the the PHMs expanded from subject 6 still contained signatures from that period. Myf-5 and MyoD protein levels were relatively similar in quiescent cells but their mRNA levels differed by a greater margin, with Myf-5 mRNA levels ~2- to 3-fold higher than MyoD. This may be due to the fact that changes in mRNA expression are generally seen before that of protein, as there

is always a time lag between mRNA expression and protein sysnthesis. These data are not inconsistent with the interpretation that the proteins were still present from the expansion time period or that myo-miRs, likely miR-31 was suppressing Myf-5 translation.

4.6 MYF-5 AND MYOD EXPRESSION IS VARIED WITH RH-HGF TREATMENT IN PHMS

The literature is generally in agreement with distinct roles assigned to MyoD and Myf-5. The former is critical for myoblast differentiation while the latter plays a bigger role in maintaining a capacity to proliferate. These distinct roles may serve to establish different satellite cell fates depending on the amount of either transcription factor relative to the other present in the satellite cell (Rudnicki et al. 2008). Decreases in MyoD expression are expected in cultures treated with 2-2.5 ng/mL of HGF as this concentration range has been shown to maximally stimulate proliferation (Yamada et al. 2010; Walker et al. 2015). Upon treatment with rh-HGF, MyoD and Myf-5 mRNA expression responded, but MyoD and Myf-5 intracellular protein levels in all treatment groups, remained similar to that of the control group. Using C2C12 cells Walker *et al.* (2015) showed treatment with 2 ng/mL of HGF decreased MyoD positive cells, while treatment with 10 ng/mL of HGF increased MyoD positive cells. These results were also seen with the human skeletal muscle myoblast (HSkM) cells that were used (Walker et al. 2015). The data obtained here indicated that MyoD protein did not vary significantly between any treatment groups and the control group. However, when comparing the different treatments, the PHMs group treated with 2 ng/mL of rh-HGF for 48 h did show the most decreased MyoD expression compared to all the other treatment groups, which is in agreement with current literature (Yamada et al. 2010; Walker et al. 2015).

Although neither Walker *et al.* (2013) nor Yamada *et al.* (2010) assessed Myf-5 expression after HGF treatment in their studies, one might expect Myf-5 expression to be opposite to that of MyoD: higher with 2-2.5 ng/mL of HGF and lower with HGF concentrations >10 ng/mL of HGF. The Myf-5 protein data instead showed no differences in expression at this low concentration compared to the control group. Beauchamp *et al*. (2000) showed that most quiescent cells isolated from uninjured mouse muscle express Myf-5 (Beauchamp et al. 2000), potentially providing a reason as to why Myf-5 levels may not change too much between quiescent cells and ones treated with low concentrations of rh-HGF. The high (10 ng/mL) treatment groups exhibited slightly lower Myf-5 protein levels, which would be a logical concequence as this higher concentration of HGF is thought to stimulate decreased proliferation.

Data for Myf-5 mRNA expression was consistant with the Myf-5 protein data: PHMs treated with both low and high concentrations of rh-HGF showed no significant differences between treatments. But, Myf-5 mRNA expression was decreased in all treated groups compared to the control. On the other hand, the MyoD mRNA expression levels dropped more, around 3-fold, in all treatment groups compared to control PHMs. Again, these results are in disagreement with previously published data and the overall literature reporting HGF has different effects on Myf-5 and MyoD regulation. Yamane et al. (2004) showed that exogenous HGF inhibited myoblast differentiation by inducing the expression of Myf-5 mRNA, while at the same time inhibiting MyoD mRNA expression (Yamane et al. 2004). However, these changes in MyoD and Myf-5 mRNA expression were seen at very high HGF concentrations - 50 and 100 ng/mL - in an organ culture system of embryonic (E13) mouse tongue myoblasts, cultured in BGJb medium for 8 d. These high concentrations of HGF are thought to only induce myoblast proliferation arrest and to promote differentiation. Therefore, the current study is not the only one reporting results that are contrary to what has been reported or expected. Furthermore, Yamane *et al.'s* (2004) data cannot be directly compared to the mRNA data in literature or this study, as the type of cell culture, HGF concentrations and duration of HGF treatment are different. Finally, although there was a lot of variability in expression levels within the treatment groups in this study, it was observed that MyoD mRNA expression was overall lower in the 24 h low and high HGF treatment groups compared to their 48 h counterparts. These data seem to add also a time component to HGF's effects on mRNA synthesis, but does not support the notion that HGF's effects on gene expression in satellite cells, are mainly at the earliest stages of activation (Miller, Thaloor, Matteson & G K Pavlath 2000).

In conclusion, although the trends for MyoD and Myf-5 mRNA expression that were seen have had some similarities to those reported in literature, the protein and mRNA data were generally inconclusive and cannot accurately elucidate the effects that HGF has on PHMs exposed to KOSR prior to treatment. Furthermore conclusive evidence on miR-31 and its role in satellite cells in quiescence promoting media was not achieved. Finally, it was not determined whether HGF has any effect on its expression.

CHAPTER 5

CONCLUSION AND FUTURE PERSPECTIVES

The findings presented in this thesis can be considered as preliminary since no previous studies have subjected PHMs to KOSR. Nontheless they open up several interesting avenues of research into the promotion of quiescence and the subsequent activation of quiescent satellite cells, along with their gene expression and protein contents.

After careful consideration, certain recommendations for future experiments became apparent. Firstly repeating all the experiments performed here, with PHMs from different subjects to more accurately determine the state of PHM cultures after 10 days in quiescence media. Analysis of cyclin-dependent kinase inhibitors, p21, p27 and p57, which are known to be expressed in cells in G_0 will help in ascertaining whether the PHMs are truly quiescent. Secondly, to obtain a greater understanding of how HGF affects satellite cell activation, we recommend the addition of two further rh-HGF treatment groups: i) a 'very-high' (50 ng/mL) rh-HGF and ii) an 'extremely high' (100 ng/mL) rh-HGF. This will further help to elucidate the effects high HGF concentrations have on PHM proliferation and MRF expression, when treatment is administered to quiescent cells. In addition to more rh-HGF treatment groups the addition of 12 h and 72 h sampling time points, would elucidate whether rh-HGF treatment affects MyoD and Myf-5 expression at these earlier and later time points. Furthermore, with regards to miRNA expression, performing whole miR-nome analysis, to determine which known miRNAs are upregulated in quiescent PHMs and then determining their potential targets using *in silico* databases. This would not only help elucidate the roles of miRNAs in satellite cell quiescence, but also identify which ones play a role in 'priming' satellite cells to re-enter the cell cycle, by maintaining them in the hypothesized G_{Alert} state. However, better expansion techniques prior to repeating the studies must be investigated for use in PHMs derived from muscle biopsies, especially when frozen stocks are to be re-utilized. Otherwise insufficient cell numbers will again hamper the study.

In conclusion, the preliminary data presented here adds, albeit modestly, to the growing body of literature surrounding the responses of primary human myoblasts to differing concentrations of HGF. Furthermore, it sets up future potential avenues of research into the time and concentration dependent effects HGF has on satellite cell proliferation and MRFs. Finally, it introduces novel insights into HGF's effects on miRNA expression.

REFERENCES

Alfaro, L.A.S. et al., 2011. CD34 promotes satellite cell motility and entry into proliferation to facilitate efficient skeletal muscle regeneration. *Stem Cells*, 29(12), pp.2030–41.

Allen, R.E. et al., 1995. Hepatocyte growth factor activates quiescent skeletal muscle satellite cells in vitro. *Journal of Cellular Physiology*, 165(2), pp.307–312.

Allen, R.E. & Boxhorn, L.K., 1989. Regulation of skeletal muscle satellite cell proliferation and differentiation by transforming growth factor-beta, insulin-like growth factor I, and fibroblast growth factor. *Journal of Cellular Physiology*, 138(2), pp.311–5.

Anderson, J.E., 2000. A role for nitric oxide in muscle repair: nitric oxide-mediated activation of muscle satellite cells. *Molecular Biology of the Cell*, 11(5), pp.1859–74.

Anderson, J.E., 2006. The satellite cell as a companion in skeletal muscle plasticity: currency, conveyance, clue, connector and colander. *The Journal of Experimental Biology*, 209(Pt 12), pp.2276–92.

Asakura, A. et al., 2007. Increased survival of muscle stem cells lacking the MyoD gene after transplantation into regenerating skeletal muscle. *Proceedings of the National Academy of Sciences of the United States of America*, 104(42), pp.16552–7.

Baj, A. et al., 2005. Culture of skeletal myoblasts from human donors aged over 40 years: dynamics of cell growth and expression of differentiation markers. *Journal of Translational Medicine*, 3(1), p.21.

Bark, T.H. et al., 1998. Increased protein synthesis after acute IGF-I or insulin infusion is localized to muscle in mice. *The American Journal of Physiology*, 275(1 Pt 1), pp.E118-23.

Bartel, D.P., 2009. MicroRNA Target Recognition and Regulatory Functions. *Cell*, 136(2), pp.215–233.

Basilico, C. et al., 2008. A high affinity hepatocyte growth factor-binding site in the immunoglobulin-like region of met. *Journal of Biological Chemistry*, 283(30), pp.21267–21277.

Beauchamp, J.R. et al., 2000. Expression of CD34 and Myf5 defines the majority of quiescent adult skeletal muscle satellite cells. *The Journal of Cell Biology*, 151(6), pp.1221–34.

Bentzinger, C.F., Wang, Y.X. & Rudnicki, M.A., 2012. Building muscle: molecular regulation of myogenesis. *Cold Spring Harbor Perspectives in Biology*, 4(2), pp.1–16.

Bernfield, M. et al., 1999. Functions of cell surface heparan sulfate proteoglycans. *Annual Review of Biochemistry*, 68, pp.729–77.

Bernstein, E. et al., 2001. Role for a bidentate ribonuclease in the initiation step of RNA interference. *Nature*, 409(6818), pp.363–6.

Bintliff, S. & Walker, B.E., 1960. Radioautographic study of skeletal muscle regeneration. *American*

Journal of Anatomy, 106(3), pp.233–245.

Birchmeier, C. et al., 2003. Met, metastasis, motility and more. *Nature Reviews Molecular Cell Biology*, 4(12), pp.915–25.

Birchmeier, C. & Gherardi, E., 1998. Developmental roles of HGF/SF and its receptor, the c-Met tyrosine kinase. *Trends in Cell Biology*, 8(10), pp.404–10.

Bischoff, R., 1997. Chemotaxis of skeletal muscle satellite cells. *Developmental Dynamics: An Official Publication of the American Association of Anatomists*, 208(4), pp.505–15.

Bischoff, R., 1975. Regeneration of single skeletal muscle fibers in vitro. *The Anatomical Record*, 182(2), pp.215–35.

Bischoff, R. & Heintz, C., 1994. Enhancement of skeletal muscle regeneration. *Developmental Dynamics: An Official Publication of the American Association of Anatomists*, 201(1), pp.41–54.

Blake, J.A. & Ziman, M.R., 2005. Pax3 transcripts in melanoblast development. *Development, Growth and Differentiation*, 47(9), pp.627–635.

Bohnsack, M.T., Czaplinski, K. & Gorlich, D., 2004. Exportin 5 is a RanGTP-dependent dsRNA-binding protein that mediates nuclear export of pre-miRNAs. *RNA*, 10(2), pp.185–91.

Boldrin, L., Muntoni, F. & Morgan, J.E., 2010. Are Human and Mouse Satellite Cells Really the Same. *Histochemistry*, 58(11), pp.941–955.

Boppart, M.D., Burkin, D.J. & Kaufman, S.J., 2006. Alpha7beta1-integrin regulates mechanotransduction and prevents skeletal muscle injury. *American Journal of Cell Physiology*, 290(6), pp.C1660-5.

Bork, P. et al., 1999. Domains in plexins: links to integrins and transcription factors. *Trends in Biochemical Sciences*, 24(7), pp.261–3.

Boros, P. & Miller, C.M., 1995. Hepatocyte growth factor: a multifunctional cytokine. *The Lancet*, 345(8945), pp.293–295.

Boutet, S.C. et al., 2012. Alternative Polyadenylation Mediates MicroRNA Regulation of Muscle Stem Cell Function. *Cell Stem Cell*, 10(3), pp.327–336.

Brunner, D. et al., 2010. Serum-free Cell Culture : The Serum-free Media Interactive Online Database. *Altex*, 27(December 2009), pp.53–62.

Buckingham, M., 2006. Myogenic progenitor cells and skeletal myogenesis in vertebrates. *Current Opinion in Genetics & Development*, 16(5), pp.525–32.

Burkin, D.J. & Kaufman, S.J., 1999. The alpha7beta1 integrin in muscle development and disease. *Cell and Tissue Research*, 296(1), pp.183–90.

Calvi, L.M. et al., 2003. Osteoblastic cells regulate the haematopoietic stem cell niche. *Nature*, 425(6960), pp.841–846.

Cantini, M. & Carraro, U., 1995. Macrophage-released factor stimulates selectively myogenic cells in primary muscle culture. *Journal of Neuropathology and Experimental Neurology*, 54(1), pp.121–8.

Capers, C.R., 1960. Multinucleation of skeletal muscle in vitro. *The Journal of Biophysical and Biochemical Cytology*, 7, pp.559–66.

Casar, J.C. et al., 2004. Heparan sulfate proteoglycans are increased during skeletal muscle regeneration: requirement of syndecan-3 for successful fiber formation. *Journal of Cell Science*, 117(Pt 1), pp.73–84.

Ceafalan, L.C., Popescu, B.O. & Hinescu, M.E., 2014. Cellular Players in Skeletal Muscle Regeneration. *BioMed Research International*, 2014, pp.1–21.

Chan, A.M. et al., 1991. Identification of a competitive HGF antagonist encoded by an alternative transcript. *Science*, 254(5036), pp.1382–5.

Chen, J.-F. et al., 2010. microRNA-1 and microRNA-206 regulate skeletal muscle satellite cell proliferation and differentiation by repressing Pax7. *The Journal of Cell Biology*, 190(5), pp.867–79.

Chen, J.-F. et al., 2006. The role of microRNA-1 and microRNA-133 in skeletal muscle proliferation and differentiation. *Nature Genetics*, 38(2), pp.228–33.

Chendrimada, T.P. et al., 2005. TRBP recruits the Dicer complex to Ago2 for microRNA processing and gene silencing. *Nature*, 436(7051), pp.740–4.

Cheung, T.H. et al., 2012. Maintenance of muscle stem-cell quiescence by microRNA-489. *Nature*, 482(7386), pp.524–8.

Chirgadze, D.Y. et al., 1999. Crystal structure of the NK1 fragment of HGF/SF suggests a novel mode for growth factor dimerization and receptor binding. *Nature Structural Biology*, 6(1), pp.72–9.

Church, J.C.T., Noronha, R.F.X. & Allbrook, D.B., 1966. Satellite cells and skeletal muscle regeneration. *British Journal of Surgery*, 53(7), pp.638–642.

Cioce, V. et al., 1996. Hepatocyte growth factor (HGF)/NK1 is a naturally occurring HGF/scatter factor variant with partial agonist/antagonist activity. *The Journal of Biological Chemistry*, 271(22), pp.13110–5.

Collins, C.A. et al., 2005. Stem cell function, self-renewal, and behavioral heterogeneity of cells from the adult muscle satellite cell niche. *Cell*, 122(2), pp.289–301.

Comoglio, P.M., Giordano, S. & Trusolino, L., 2008. Drug development of MET inhibitors: targeting oncogene addiction and expedience. *Nature Reviews Drug Discovery*, 7(6), pp.504–16.

Cooper, R.N. et al., 1999. In vivo satellite cell activation via Myf5 and MyoD in regenerating mouse skeletal muscle. *Journal of Cell Science*, 112 (Pt 1), pp.2895–901.

Cornelison, D.D. et al., 2001. Syndecan-3 and syndecan-4 specifically mark skeletal muscle satellite cells and are implicated in satellite cell maintenance and muscle regeneration. *Developmental*

Biology, 239(1), pp.79–94.

Cornelison, D.D. & Wold, B.J., 1997. Single-cell analysis of regulatory gene expression in quiescent and activated mouse skeletal muscle satellite cells. *Developmental Biology*, 191(2), pp.270–283.

Crist, C.G. et al., 2009. Muscle stem cell behavior is modified by microRNA-27 regulation of Pax3 expression. *Proceedings of the National Academy of Sciences of the United States of America*, 106(32), pp.13383–7.

Crist, C.G. & Buckingham, M., 2009. microRNas gain magnitude in muscle. *Cell Cycle*, 8(22), pp.3627–3628.

Crist, C.G., Montarras, D. & Buckingham, M., 2012. Muscle satellite cells are primed for myogenesis but maintain quiescence with sequestration of Myf5 mRNA targeted by microRNA-31 in mRNP granules. *Cell Stem Cell*, 11(1), pp.118–126.

Daubas, P. et al., 2009. The regulatory mechanisms that underlie inappropriate transcription of the myogenic determination gene Myf5 in the central nervous system. *Developmental Biology*, 327(1), pp.71–82.

Day, K. et al., 2007. Nestin-GFP reporter expression defines the quiescent state of skeletal muscle satellite cells. *Developmental Biology*, 304(1), pp.246–59.

Day, K. et al., 2010. The depletion of skeletal muscle satellite cells with age is concomitant with reduced capacity of single progenitors to produce reserve progeny. *Developmental Biology*, 340(2), pp.330–43.

deLapeyrière, O. et al., 1993. Expression of the Fgf6 gene is restricted to developing skeletal muscle in the mouse embryo. *Development*, 118(2), pp.601–11.

Denli, A.M. et al., 2004. Processing of primary microRNAs by the Microprocessor complex. *Nature*, 432(7014), pp.231–235.

Derksen, P.W.B. et al., 2002. Cell surface proteoglycan syndecan-1 mediates hepatocyte growth factor binding and promotes Met signaling in multiple myeloma. *Blood*, 99(4), pp.1405–1410.

Dreyfuss, J.L. et al., 2009. Heparan sulfate proteoglycans: structure, protein interactions and cell signaling. *Anais da Academia Brasileira de Ciencias*, 81(3), pp.409–29.

Dumont, N.A., Wang, Y.X. & Rudnicki, M.A., 2015. Intrinsic and extrinsic mechanisms regulating satellite cell function. *Development*, 142(9), pp.1572–1581.

Florini, J.R., Ewton, D.Z. & Coolican, S.A., 1996. Growth hormone and the insulin-like growth factor system in myogenesis. *Endocrine Reviews*, 17(5), pp.481–517.

Florini, J.R., Ewton, D.Z. & Roof, S.L., 1991. Insulin-like growth factor-I stimulates terminal myogenic differentiation by induction of myogenin gene expression. *Molecular Endocrinology*, 5(5), pp.718–24.

Floss, T., Arnold, H.H. & Braun, T., 1997. A role for FGF-6 in skeletal muscle regeneration. *Genes &*

Development, 11(16), pp.2040–51.

Fukada, S.-I., 2011. Molecular regulation of muscle stem cells by "quiescence genes". *Yakugaku Zasshi: Journal of the Pharmaceutical Society of Japan*, 131(9), pp.1329–32.

Gal-Levi, R. et al., 1998. Hepatocyte growth factor plays a dual role in regulating skeletal muscle satellite cell proliferation and differentiation. *Biochimica et Biophysica Acta*, 1402(1), pp.39–51.

Gallucci, S. et al., 1998. Myoblasts produce IL-6 in response to inflammatory stimuli. *International Immunology*, 10(3), pp.267–73.

Garry, D.J. et al., 1997. Persistent expression of MNF identifies myogenic stem cells in postnatal muscles. *Developmental Biology*, 188(2), pp.280–94.

Gauglitz, G.G. et al., 2008. Characterization of the inflammatory response during acute and post-acute phases after severe burn. *Shock*, 30(5), pp.503–7.

Gayraud-Morel, B. et al., 2007. A role for the myogenic determination gene Myf5 in adult regenerative myogenesis. *Developmental Biology*, 312(1), pp.13–28.

Geiger, T. et al., 1988. Induction of rat acute-phase proteins by interleukin 6 in vivo. *European Journal of Immunology*, 18(5), pp.717–21.

Giordano, S. et al., 1989. Tyrosine kinase receptor indistinguishable from the c-met protein. *Nature*, 339(6220), pp.155–6.

Gnocchi, V.F. et al., 2009. Further characterisation of the molecular signature of quiescent and activated mouse muscle satellite cells. *PloS ONE*, 4(4), p.e5205.

Goidin, D. et al., 2001. Ribosomal 18S RNA prevails over glyceraldehyde-3-phosphate dehydrogenase and beta-actin genes as internal standard for quantitative comparison of mRNA levels in invasive and noninvasive human melanoma cell subpopulations. *Analytical Biochemistry*, 295(1), pp.17–21.

Gros, J. et al., 2005. A common somitic origin for embryonic muscle progenitors and satellite cells. *Nature*, 435(7044), pp.954–958.

Gros, J., Scaal, M. & Marcelle, C., 2004. A two-step mechanism for myotome formation in chick. *Developmental Cell*, 6(6), pp.875–82.

Grozdanovic, Z. & Baumgarten, H.G., 1999. Nitric oxide synthase in skeletal muscle fibers: a signaling component of the dystrophin-glycoprotein complex. *Histology and Histopathology*, 14(1), pp.243–56.

Haase, A.D. et al., 2005. TRBP, a regulator of cellular PKR and HIV-1 virus expression, interacts with Dicer and functions in RNA silencing. *EMBO Reports*, 6(10), pp.961–7.

Halevy, O. et al., 2004. Pattern of Pax7 expression during myogenesis in the posthatch chicken establishes a model for satellite cell differentiation and renewal. *Developmental Dynamics: An Official Publication of the American Association of Anatomists*, 231(3), pp.489–502.

Halevy, O. & Cantley, L.C., 2004. Differential regulation of the phosphoinositide 3-kinase and MAP kinase pathways by hepatocyte growth factor vs. insulin-like growth factor-I in myogenic cells. *Experimental Cell Research*, 297(1), pp.224–34.

Hamanoue, M. et al., 1996. Neurotrophic effect of hepatocyte growth factor on central nervous system neurons in vitro. *Journal of Neuroscience Research*, 43(5), pp.554–64.

Hammond, S.M. et al., 2000. An RNA-directed nuclease mediates post-transcriptional gene silencing in Drosophila cells. *Nature*, 404(6775), pp.293–6.

Hannon, K. et al., 1996. Differentially expressed fibroblast growth factors regulate skeletal muscle development through autocrine and paracrine mechanisms. *Journal of Cell Biology*, 132(6), pp.1151–1159.

Harel, I. et al., 2009. Distinct origins and genetic programs of head muscle satellite cells. *Developmental Cell*, 16(6), pp.822–32.

Hayashi, S. et al., 2000. Sequence of IGF-I, IGF-II, and HGF expression in regenerating skeletal muscle. *Histochemistry and Cell Biology*, 122(5), pp.427–434.

Hughes, S.M. & Blau, H.M., 1990. Migration of myoblasts across basal lamina during skeletal muscle development. *Nature*, 345(6273), pp.350–3.

Husmann, I. et al., 1996. Growth factors in skeletal muscle regeneration. *Cytokine & Growth Factor Reviews*, 7(3), pp.249–258.

Irintchev, A. et al., 1994. Expression pattern of M-cadherin in normal, denervated, and regenerating mouse muscles. *Developmental Dynamics: An Official Publication of the American Association of Anatomists*, 199(4), pp.326–37.

Jakubczak, J.L., LaRochelle, W.J. & Merlino, G., 1998. NK1, a natural splice variant of hepatocyte growth factor/scatter factor, is a partial agonist in vivo. *Molecular and Cellular Biology*, 18(3), pp.1275–83.

Jang, Y.-N. & Baik, E.J., 2013. JAK-STAT pathway and myogenic differentiation. *Jak-Stat*, 2(2), p.e23282.

Jockusch, H. & Voigt, S., 2003. Migration of adult myogenic precursor cells as revealed by GFP/nLacZ labelling of mouse transplantation chimeras. *Journal of Cell Science*, 116(Pt 8), pp.1611–6.

Kalcheim, C. & Ben-Yair, R., 2005. Cell rearrangements during development of the somite and its derivatives. *Current Opinion in Genetics & Development*, 15(4), pp.371–80.

Kallestad, K.M. & McLoon, L.K., 2010. Defining the heterogeneity of skeletal muscle-derived side and main population cells isolated immediately ex vivo. *Journal of Cellular Physiology*, 222(3), pp.676–684.

Karalaki, M. et al., 2009. Muscle regeneration: cellular and molecular events. *In Vivo*, 23(5), pp.779–96.

Kassar-Duchossoy, L. et al., 2005. Pax3/Pax7 mark a novel population of primitive myogenic cells

during development. *Genes & Development*, 19(12), pp.1426–31.

Kästner, S. et al., 2000. Gene expression patterns of the fibroblast growth factors and their receptors during myogenesis of rat satellite cells. *The Journal of Histochemistry and Cytochemistry: Official Journal of the Histochemistry Society*, 48(8), pp.1079–96.

Katz, B., 1961. The Terminations of the Afferent Nerve Fibre in the Muscle Spindle of the Frog. *Philosophical Transactions of the Royal Society of London. Series B, Biological Sciences*, 243(703), pp.221–240.

Kemp, L.E., Mulloy, B. & Gherardi, E., 2006. Signalling by HGF/SF and Met: the role of heparan sulphate co-receptors. *Biochemical Society Transactions*, 34(Pt 3), pp.414–417.

Kharraz, Y. et al., 2013. Macrophage Plasticity and the Role of Inflammation in Skeletal Muscle Repair. *Mediators of Inflammation*, 2013, pp.1–9.

Kim, H.K. et al., 2006. Muscle-specific microRNA miR-206 promotes muscle differentiation. *The Journal of Cell Biology*, 174(5), pp.677–87.

Kim, V.N., 2005. MicroRNA biogenesis: coordinated cropping and dicing. *Nature Reviews Molecular Cell Biology*, 6(5), pp.376–85.

Kirchhofer, D. et al., 2005. Hepsin activates pro-hepatocyte growth factor and is inhibited by hepatocyte growth factor activator inhibitor-1B (HAI-1B) and HAI-2. *FEBS Letters*, 579(9), pp.1945–50.

Kirchhofer, D. et al., 2004. Structural and functional basis of the serine protease-like hepatocyte growth factor beta-chain in Met binding and signaling. *The Journal of Biological Chemistry*, 279(38), pp.39915–24.

Kirchhofer, D. et al., 2007. Utilizing the activation mechanism of serine proteases to engineer hepatocyte growth factor into a Met antagonist. *Proceedings of the National Academy of Sciences of the United States of America*, 104(13), pp.5306–11.

Kitzmann, M. et al., 1998. The muscle regulatory factors MyoD and myf-5 undergo distinct cell cycle-specific expression in muscle cells. *The Journal of Cell Biology*, 142(6), pp.1447–59.

Komada, M. et al., 1993. Proteolytic processing of the hepatocyte growth factor/scatter factor receptor by furin. *FEBS Letters*, 328(1–2), pp.25–9.

Konigsberg, U.R., Lipton, B.H. & Konigsberg, I.R., 1975. The regenerative response of single mature muscle fibers isolated in vitro. *Developmental Biology*, 45(2), pp.260–75.

Kozlov, G. et al., 2004. Insights into function of PSI domains from structure of the Met receptor PSI domain. *Biochemical and Biophysical Research Communications*, 321(1), pp.234–40.

Kuang, S. et al., 2007. Asymmetric self-renewal and commitment of satellite stem cells in muscle. *Cell*, 129(5), pp.999–1010.

Kuang, W. et al., 2009. Cyclic stretch induced miR-146a upregulation delays C2C12 myogenic differentiation through inhibition of Numb. *Biochemical and Biophysical Research*

Communications, 378(2), pp.259–263.

Kurek, J.B. et al., 1996. Leukemia inhibitory factor and interleukin-6 are produced by diseased and regenerating skeletal muscle. *Muscle & Nerve*, 19(10), pp.1291–301.

Laguens, R., 1963. SATELLITE CELLS OF SKELETAL MUSCLE FIBERS IN HUMAN PROGRESSIVE MUSCULAR DYSTROPHY. *Virchows Archiv fur Pathologische Anatomie und Physiologie und fur Klinische Medizin*, 336, pp.564–9.

Landthaler, M., Yalcin, A. & Tuschl, T., 2004. The Human DiGeorge Syndrome Critical Region Gene 8 and Its D. melanogaster Homolog Are Required for miRNA Biogenesis. *Current Biology*, 14(23), pp.2162–2167.

Laplante, M. & Sabatini, D.M., 2012. MTOR signaling in growth control and disease. *Cell*, 149(2), pp.274–293.

Lee, S.L., Dickson, R.B. & Lin, C.Y., 2000. Activation of hepatocyte growth factor and urokinase/plasminogen activator by matriptase, an epithelial membrane serine protease. *The Journal of Biological Chemistry*, 275(47), pp.36720–5.

Lee, Y. et al., 2002. MicroRNA maturation: stepwise processing and subcellular localization. *The EMBO journal*, 21(17), pp.4663–70.

Lee, Y. et al., 2003. The nuclear RNase III Drosha initiates microRNA processing. *Nature*, 425(6956), pp.415–419.

Leshem, Y. et al., 2000. Hepatocyte growth factor (HGF) inhibits skeletal muscle cell differentiation: a role for the bHLH protein twist and the cdk inhibitor p27. *Journal of Cellular Physiology*, 184(1), pp.101–9.

Leshem, Y. et al., 2002. Preferential binding of Grb2 or phosphatidylinositol 3-kinase to the met receptor has opposite effects on HGF-induced myoblast proliferation. *Experimental Cell Research*, 274(2), pp.288–98.

Leshem, Y. & Halevy, O., 2002. Phosphorylation of pRb is required for HGF-induced muscle cell proliferation and is p27kip1-dependent. *Journal of Cellular Physiology*, 191(2), pp.173–182.

Lindström, M., Pedrosa-Domellöf, F. & Thornell, L.-E., 2010. Satellite cell heterogeneity with respect to expression of MyoD, myogenin, Dlk1 and c-Met in human skeletal muscle: application to a cohort of power lifters and sedentary men. *Histochemistry and Cell Biology*, 134(4), pp.371–85.

Liu, L. et al., 2013. Chromatin modifications as determinants of muscle stem cell quiescence and chronological aging. *Cell Reports*, 4(1), pp.189–204.

Liu, L. et al., 2015. Isolation of skeletal muscle stem cells by fluorescence-activated cell sorting. *Nature Protocols*, 10(10), pp.1612–1624.

Lodish, H. & Berk, A., 2003. *Molecular Cell Biology* Sixth., W. H. Freeman.

Lodish, H.F. et al., 2008. Micromanagement of the immune system by microRNAs. *Nature Reviews Immunology*, 8(2), pp.120–130.

Lokker, N.A. et al., 1992. Structure-function analysis of hepatocyte growth factor: identification of variants that lack mitogenic activity yet retain high affinity receptor binding. *The EMBO Journal*, 11(7), pp.2503–10.

Lokker, N.A. & Godowski, P.J., 1993. Generation and characterization of a competitive antagonist of human hepatocyte growth factor, HGF/NK1. *The Journal of Biological Chemistry*, 268(23), pp.17145–50.

Longo, M.C., Berninger, M.S. & Hartley, J.L., 1990. Use of uracil DNA glycosylase to control carry-over contamination in polymerase chain reactions. *Gene*, 93(1), pp.125–8.

Lu, J. et al., 2000. Regulation of skeletal myogenesis by association of the MEF2 transcription factor with class II histone deacetylases. *Molecular Cell*, 6(2), pp.233–44.

Lund, E. et al., 2004. Nuclear export of microRNA precursors. *Science*, 303(5654), pp.95–8.

Maina, F. et al., 1996. Uncoupling of Grb2 from the Met receptor in vivo reveals complex roles in muscle development. *Cell*, 87(3), pp.531–42.

Matsumoto, K. et al., 1998. Cooperative interaction between alpha- and beta-chains of hepatocyte growth factor on c-Met receptor confers ligand-induced receptor tyrosine phosphorylation and multiple biological responses. *The Journal of Biological Chemistry*, 273(36), pp.22913–20.

Matsumoto, K. & Nakamura, T., 1997. Hepatocyte growth factor (HGF) as a tissue organizer for organogenesis and regeneration. *Biochemical and Biophysical Research Communications*, 239(3), pp.639–44.

Mauro, A., 1961. Satellite cell of skeletal muscle fibers. *The Journal of Biophysical and Biochemical Cytology*, 9, pp.493–495.

Megeney, L.A. et al., 1996. MyoD is required for myogenic stem cell function in adult skeletal muscle. *Genes & Development*, 10(10), pp.1173–83.

Michalopoulos, G. et al., 1984. Control of hepatocyte replication by two serum factors. *Cancer Research*, 44(10), pp.4414–9.

Milasincic, D.J., Dhawan, J. & Farmer, S.R., 1996. Anchorage-dependent control of muscle-specific gene expression in C2C12 mouse myoblasts. *In Vitro Cellular & Developmental Biology. Animal*, 32(2), pp.90–9.

Miller, K.J., Thaloor, D., Matteson, S. & Pavlath, G.K., 2000. Hepatocyte growth factor affects satellite cell activation and differentiation in regenerating skeletal muscle. *American Journal of Physiology. Cell Physiology*, 278(1), pp.C174-81.

Miller, K.J., Thaloor, D., Matteson, S. & Pavlath, G.K., 2000. Hepatocyte growth factor affects satellite cell activation and differentiation in regenerating skeletal muscle. *American Journal of Physiology. Cell Physiology*, 278(1), pp.C174-81.

Mitchell, P.O. et al., 2005. Sca-1 negatively regulates proliferation and differentiation of muscle cells. *Developmental Biology*, 283(1), pp.240–52.

Miyazawa, K. et al., 1991. An alternatively processed mRNA generated from human hepatocyte growth factor gene. *European Journal of Biochemistry*, 197(1), pp.15–22.

Miyazawa, K., 2010. Hepatocyte growth factor activator (HGFA): A serine protease that links tissue injury to activation of hepatocyte growth factor. *FEBS Journal*, 277(10), pp.2208–2214.

Miyazawa, K. et al., 1989. Molecular cloning and sequence analysis of cDNA for human hepatocyte growth factor. *Biochemical and Biophysical Research Communications*, 163(2), pp.967–73.

Miyazawa, K. et al., 1993. Molecular cloning and sequence analysis of the cDNA for a human serine protease reponsible for activation of hepatocyte growth factor. Structural similarity of the protease precursor to blood coagulation factor XII. *The Journal of Biological Chemistry*, 268(14), pp.10024–8.

Miyazawa, K. et al., 1994. Proteolytic activation of hepatocyte growth factor in response to tissue injury. *The Journal of Biological Chemistry*, 269(12), pp.8966–70.

Miyazawa, K. et al., 1998. Structural organization and chromosomal localization of the human hepatocyte growth factor activator gene--phylogenetic and functional relationship with blood coagulation factor XII, urokinase, and tissue-type plasminogen activator. *European Journal of Biochemistry*, 258(2), pp.355–61.

Miyazawa, K., Shimomura, T. & Kitamura, N., 1996. Activation of hepatocyte growth factor in the injured tissues is mediated by hepatocyte growth factor activator. *The Journal of Biological Chemistry*, 271(7), pp.3615–8.

Montarras, D. et al., 2000. Cultured myf5 null and myoD null muscle precursor cells display distinct growth defects. *Biology of the Cell*, 92(8–9), pp.565–72.

Montarras, D. et al., 2005. Direct isolation of satellite cells for skeletal muscle regeneration. *Science*, 309(5743), pp.2064–7.

Morrison, S.J. & Kimble, J., 2006. Asymmetric and symmetric stem-cell divisions in development and cancer. *Nature*, 441(7097), pp.1068–1074.

Moss, F.P. & Leblond, C.P., 1970. Nature of dividing nuclei in skeletal muscle of growing rats. *The Journal of Cell Biology*, 44(2), pp.459–62.

Moss, F.P. & Leblond, C.P., 1971. Satellite cells as the source of nuclei in muscles of growing rats. *The Anatomical Record*, 170(4), pp.421–35.

Motohashi, N., Asakura, Y. & Asakura, A., 2014. Isolation, Culture, and Transplantation of Muscle Satellite Cells. *Journal of Visualized Experiments*, (86), pp.1–7.

Mourelatos, Z. et al., 2002. miRNPs: a novel class of ribonucleoproteins containing numerous microRNAs. *Genes & Development*, 16(6), pp.720–8.

Naguibneva, I. et al., 2006. The microRNA miR-181 targets the homeobox protein Hox-A11 during mammalian myoblast differentiation. *Nature Cell Biology*, 8(3), pp.278–84.

Nakamura, T. et al., 1989. Molecular cloning and expression of human hepatocyte growth factor.

Nature, 342(6248), pp.440–3.

Naldini, L. et al., 1992. Extracellular proteolytic cleavage by urokinase is required for activation of hepatocyte growth factor/scatter factor. *The EMBO Journal*, 11(13), pp.4825–33.

Naldini, L. et al., 1991. Scatter factor and hepatocyte growth factor are indistinguishable ligands for the MET receptor. *The EMBO Journal*, 10(10), pp.2867–78.

Newsholme, P. et al., 2003. Glutamine and glutamate as vital metabolites. *Brazilian Journal of Medical and Biological Research*, 36(2), pp.153–163.

Ohlstein, B. et al., 2004. The stem cell niche: Theme and variations. *Current Opinion in Cell Biology*, 16(6), pp.693–699.

Olguín, H.C., Patzlaff, N.E. & Olwin, B.B., 2011. Pax7-FKHR transcriptional activity is enhanced by transcriptionally repressed MyoD. *Journal of Cellular Biochemistry*, 112(5), pp.1410–1417.

Ono, Y. et al., 2010. Muscle satellite cells are a functionally heterogeneous population in both somite-derived and branchiomeric muscles. *Developmental Biology*, 337(1), pp.29–41.

Ono, Y. et al., 2012. Slow-dividing satellite cells retain long-term self-renewal ability in adult muscle. *Journal of Cell Science*, 125(Pt 5), pp.1309–17.

Organ, S.L. & Tsao, M.-S., 2011. An overview of the c-MET signaling pathway. *Therapeutic Advances in Medical Oncology*, 3(1 Suppl), pp.S7–S19.

Otto, A., Collins-Hooper, H. & Patel, K., 2009. The origin, molecular regulation and therapeutic potential of myogenic stem cell populations. *Journal of Anatomy*, 215(5), pp.477–497.

Peek, M. et al., 2002. Unusual Proteolytic Activation of Pro-hepatocyte Growth Factor by Plasma Kallikrein and Coagulation Factor XIa. *Journal of Biological Chemistry*, 277(49), pp.47804–47809.

Pinto, D. et al., 2003. Canonical Wnt signals are essential for homeostasis of the intestinal epithelium. *Genes & Development*, 17(14), pp.1709–13.

Ponzetto, C. et al., 1994. A multifunctional docking site mediates signaling and transformation by the hepatocyte growth factor/scatter factor receptor family. *Cell*, 77(2), pp.261–71.

Rantanen, J. et al., 1995. Satellite cell proliferation and the expression of myogenin and desmin in regenerating skeletal muscle: evidence for two different populations of satellite cells. *Laboratory Investigation: A Journal of Technical Methods and Pathology*, 72(3), pp.341–7.

Relaix, F. et al., 2005. A Pax3/Pax7-dependent population of skeletal muscle progenitor cells. *Nature*, 435(7044), pp.948–53.

Relaix, F. et al., 2004. Divergent functions of murine Pax3 and Pax7 in limb muscle development. *Genes & Development*, 18(9), pp.1088–105.

Relaix, F. et al., 2006. Pax3 and Pax7 have distinct and overlapping functions in adult muscle progenitor cells. *The Journal of Cell Biology*, 172(1), pp.91–102.

Reznik, M., 1969. Thymidine-3H uptake by satellite cells of regenerating skeletal muscle. *The Journal of Cell Biology*, 40(2), pp.568–571.

Robertson, D.A. et al., 1992. A cDNA clone for human glucosamine-6-sulphatase reveals differences between arylsulphatases and non-arylsulphatases. *The Biochemical Journal*, 288 (Pt2), pp.539–44.

Rodgers, J.T. et al., 2014. mTORC1 controls the adaptive transition of quiescent stem cells from G0 to G(Alert). *Nature*, 509(7505), pp.393–6.

Rodrigues, G.A. & Park, M., 1994. Autophosphorylation modulates the kinase activity and oncogenic potential of the Met receptor tyrosine kinase. *Oncogene*, 9(7), pp.2019–27.

Rossi, C.A. et al., 2010. Clonal characterization of rat muscle satellite cells: Proliferation, metabolism and differentiation define an intrinsic heterogeneity. *PLoS ONE*, 5(1).

Rudnicki, M.A. et al., 2008. The Molecular Regulation of Muscle Stem Cell Function. *Cold Spring Harbor Symposia on Quantitative Biology*, 73, pp.323–331.

Sabourin, L.A. et al., 1999. Reduced differentiation potential of primary MyoD-/- myogenic cells derived from adult skeletal muscle. *The Journal of Cell Biology*, 144(4), pp.631–43.

Sabourin, L.A. & Rudnicki, M.A., 2000. The molecular regulation of myogenesis. *Clinical Genetics*, 57(1), pp.16–25.

Sacco, A. et al., 2008. Self-renewal and expansion of single transplanted muscle stem cells. *Nature*, 456(7221), pp.502–6.

Saclier, M. et al., 2013. Differentially activated macrophages orchestrate myogenic precursor cell fate during human skeletal muscle regeneration. *Stem Cells*, 31(2), pp.384–96.

Sanes, J.R., 2003. The Basement Membrane/Basal Lamina of Skeletal Muscle. *Journal of Biological Chemistry*, 278(15), pp.12601–12604.

Santos, O.F. et al., 1994. Involvement of hepatocyte growth factor in kidney development. *Developmental Biology*, 163(2), pp.525–9.

Scaal, M. & Christ, B., 2004. Formation and differentiation of the avian dermomyotome. *Anatomy and Embryology*, 208(6), pp.411–24.

Scata, K.A. et al., 1999. FGF receptor availability regulates skeletal myogenesis. *Experimental Cell Research*, 250(1), pp.10–21.

Scharner, J. & Zammit, P.S., 2011. The muscle satellite cell at 50: the formative years. *Skeletal Muscle*, 1(1), p.28.

Schienda, J. et al., 2006. Somitic origin of limb muscle satellite and side population cells. *Proceedings of the National Academy of Sciences of the United States of America*, 103(4), pp.945–50.

Schlessinger, J., Lax, I. & Lemmon, M., 1995. Regulation of growth factor activation by proteoglycans: what is the role of the low affinity receptors? *Cell*, 83(3), pp.357–60.

Schmalbruch, H., 1976. The morphology of regeneration of skeletal muscles in the rat. *Tissue and Cell*, 8(4), pp.673–692.

Schmidt, C. et al., 1995. Scatter factor/hepatocyte growth factor is essential for liver development. *Nature*, 373(6516), pp.699–702.

Schubert, W. et al., 1989. Lymphocyte antigen Leu-19 as a molecular marker of regeneration in human skeletal muscle. *Proceedings of the National Academy of Sciences of the United States of America*, 86(1), pp.307–11.

Schultz, E., 1996. Satellite cell proliferative compartments in growing skeletal muscles. *Developmental Biology*, 175(1), pp.84–94.

Schultz, E., Gibson, M.C. & Champion, T., 1978. Satellite cells are mitotically quiescent in mature mouse muscle: an EM and radioautographic study. *The Journal of Experimental Zoology*, 206(3), pp.451–6.

Schultz, E., Jaryszak, D.L. & Valliere, C.R., 1985. Response of satellite cells to focal skeletal muscle injury. *Muscle & Nerve*, 8(3), pp.217–22.

Schwall, R.H. et al., 1996. Heparin induces dimerization and confers proliferative activity onto the hepatocyte growth factor antagonists NK1 and NK2. *The Journal of Cell Biology*, 133(3), pp.709–718.

Seale, P. et al., 2000. Pax7 is required for the specification of myogenic satellite cells. *Cell*, 102(6), pp.777–86.

Seale, P. & Rudnicki, M.A., 2000. A New Look at the Origin, Function, and "Stem-Cell" Status of Muscle Satellite Cells. *Developmental Biology*, 218(2), pp.115–124.

Seid, T. et al., 1991. Organization of the human hepatocyte growth factor-encoding gene. *Gene*, 102(2), pp.213–219.

Sellathurai, J. et al., 2013. A Novel In Vitro Model for Studying Quiescence and Activation of Primary Isolated Human Myoblasts. *PLoS ONE*, 8(5).

Shafiq, S.A. & Gorycki, M.A., 1965. Regeneration in skeletal muscle of mouse: Some electron-microscope observations. *The Journal of Pathology and Bacteriology*, 90(1), pp.123–127.

Shafiq, S.A., Gorycki, M.A. & Mauro, A., 1968. Mitosis during postnatal growth in skeletal and cardiac muscle of the rat. *Journal of Anatomy*, 103(Pt 1), pp.135–41.

Shafiq, S.A., Gorycki, M.A. & Milhorat, A.T., 1967. An electron microscopic study of regeneration and satellite cells in human muscle. *Neurology*, 17(6), p.567–74 passim.

Shea, K.L. et al., 2010. Sprouty1 regulates reversible quiescence of a self-renewing adult muscle stem cell pool during regeneration. *Cell Stem Cell*, 6(2), pp.117–29.

Sheehan, S.M. et al., 2000. HGF is an autocrine growth factor for skeletal muscle satellite cells in vitro. *Muscle & Nerve*, 23(2), pp.239–45.

Sheehan, S.M. & Allen, R.E., 1999. Skeletal muscle satellite cell proliferation in response to members of the fibroblast growth factor family and hepatocyte growth factor. *Journal of Cellular Physiology*, 181(3), pp.499–506.

Shen, Q. et al., 2004. Endothelial cells stimulate self-renewal and expand neurogenesis of neural stem cells. *Science*, 304(5675), pp.1338–40.

Shenoy, A. & Blelloch, R.H., 2014. Regulation of microRNA function in somatic stem cell proliferation and differentiation. *Nature Reviews Molecular Cell Biology*, 15(9), pp.565–76.

Shimomura, T. et al., 1995. Activation of hepatocyte growth factor by two homologous proteases, blood-coagulation factor XIIa and hepatocyte growth factor activator. *European Journal of Biochemistry*, 229(1), pp.257–61.

Shimomura, T. et al., 1993. Activation of the zymogen of hepatocyte growth factor activator by thrombin. *The Journal of Biological Chemistry*, 268(30), pp.22927–32.

Smith, J. & Merrick, D., 2010. Embryonic skeletal muscle microexplant culture and isolation of skeletal muscle stem cells. *Methods in Molecular Biology*, 633, pp.29–56.

Song, W.K. et al., 1992. H36-alpha 7 is a novel integrin alpha chain that is developmentally regulated during skeletal myogenesis. *The Journal of Cell Biology*, 117(3), pp.643–57.

Sonnenberg, E. et al., 1993. Scatter factor/hepatocyte growth factor and its receptor, the c-met tyrosine kinase, can mediate a signal exchange between mesenchyme and epithelia during mouse development. *The Journal of Cell Biology*, 123(1), pp.223–35.

Stamos, J. et al., 2004. Crystal structure of the HGF beta-chain in complex with the Sema domain of the Met receptor. *The EMBO Journal*, 23(12), pp.2325–35.

Steyn, P., 2015. *Il-6 and the skeletal muscle niche: A guiding hand in myoblast cell fate*. University of Stellenbosch.

Stoker, M., 1989. Effect of scatter factor on motility of epithelial cells and fibroblasts. *Journal of Cellular Physiology*, 139(3), pp.565–9.

Strain, A.J., 1993. Hepatocyte growth factor: another ubiquitous cytokine. *The Journal of Endocrinology*, 137(1), pp.1–5.

Suzuki, S. et al., 2002. Skeletal muscle injury induces hepatocyte growth factor expression in spleen. *Biochemical and Biophysical Research Communications*, 292(3), pp.709–14.

Tabll, A. & Ismail, H., 2011. The Use of Flow Cytometric DNA Ploidy Analysis of Liver Biopsies in Liver Cirrhosis and Hepatocellular Carcinoma. In *Liver Biopsy*. InTech.

Takayama, H. et al., 1996. Scatter factor/hepatocyte growth factor as a regulator of skeletal muscle and neural crest development. *Proceedings of the National Academy of Sciences of the United States of America*, 93(12), pp.5866–5871.

Tatsuguchi, M. et al., 2007. Expression of microRNAs is dynamically regulated during cardiomyocyte hypertrophy. *Journal of Molecular and Cellular Cardiology*, 42(6), pp.1137–41.

Tatsumi, R. et al., 1998. HGF/SF is present in normal adult skeletal muscle and is capable of activating satellite cells. *Developmental Biology*, 194(1), pp.114–128.

Tatsumi, R. et al., 2001. Mechanical Stretch Induces Activation of Skeletal Muscle Satellite Cells in Vitro. *Experimental Cell Research*, 267(1), pp.107–114.

Tatsumi, R. et al., 2002. Release of hepatocyte growth factor from mechanically stretched skeletal muscle satellite cells and role of pH and nitric oxide. *Molecular Biology of the Cell*, 13(8), pp.2909–18.

Tatsumi, R. et al., 2006. Satellite cell activation in stretched skeletal muscle and the role of nitric oxide and hepatocyte growth factor. *American Journal of Physiology. Cell Physiology*, 290(6), pp.C1487-94.

Tatsumi, R. & Allen, R.E., 2004. Active hepatocyte growth factor is present in skeletal muscle extracellular matrix. *Muscle & Nerve*, 30(5), pp.654–8.

Tempest, P.R., Stratton, M.R. & Cooper, C.S., 1988. Structure of the met protein and variation of met protein kinase activity among human tumour cell lines. *British Journal of Cancer*, 58(1), pp.3–7.

Thum, T. et al., 2008. MicroRNA-21 contributes to myocardial disease by stimulating MAP kinase signalling in fibroblasts. *Nature*, 456(7224), pp.980–4.

Tidball, J.G. & Villalta, S.A., 2010. Regulatory interactions between muscle and the immune system during muscle regeneration. *American Journal of Physiology. Regulatory, Integrative and Comparative Physiology*, 298(5), pp.R1173-87.

Trusolino, L., Bertotti, A. & Comoglio, P.M., 2010. MET signalling: principles and functions in development, organ regeneration and cancer. *Nature Reviews Molecular cell biology*, 11(12), pp.834–48.

Tumbar, T. et al., 2004. Defining the epithelial stem cell niche in skin. *Science*, 303(5656), pp.359–63.

Walker, N. et al., 2015. Dose-dependent modulation of myogenesis by HGF: implications for c-Met expression and downstream signalling pathways. *Growth Factors*, (September), pp.1–13.

Wang, H. et al., 2008. NF-kappaB-YY1-miR-29 regulatory circuitry in skeletal myogenesis and rhabdomyosarcoma. *Cancer Cell*, 14(5), pp.369–81.

Wang, H., Sun, H. & Guttridge, D.C., 2009. microRNAs: novel components in a muscle gene regulatory network. *Cell Cycle*, 8(12), pp.1833–1837.

Watt, D.J. et al., 1987. The movement of muscle precursor cells between adjacent regenerating muscles in the mouse. *Anatomy and Embryology*, 175(4), pp.527–36.

Wozniak, A.C. et al., 2003. C-Met expression and mechanical activation of satellite cells on cultured muscle fibers. *The Journal of Histochemistry and Cytochemistry: Official Journal of the Histochemistry Society*, 51(11), pp.1437–45.

Wu, Z. et al., 2000. Kinases Regulate the Myogenic Program at Multiple Steps p38 and Extracellular Signal-Regulated Kinases Regulate the Myogenic Program at Multiple Steps. *Molecular and*

Cellular Biology, 20(11), pp.3951–3964.

Xu, Q. & Wu, Z., 2000. The insulin-like growth factor-phosphatidylinositol 3-kinase-Akt signaling pathway regulates myogenin expression in normal myogenic cells but not in rhabdomyosarcoma-derived RD cells. *The Journal of Biological Chemistry*, 275(47), pp.36750–7.

Yablonka-Reuveni, Z. et al., 1999. The Transition from Proliferation to Differentiation Is Delayed in Satellite Cells from Mice Lacking MyoD. *Developmental Biology*, 210(2), pp.440–455.

Yamada, M. et al., 2010. High concentrations of HGF inhibit skeletal muscle satellite cell proliferation in vitro by inducing expression of myostatin: A possible mechanism for reestablishing satellite cell quiescence in vivo. *American Journal of Physiology - Cell Physiology*, 298(3), pp.C465–C476.

Yamada, M. et al., 2008. Matrix metalloproteinase-2 mediates stretch-induced activation of skeletal muscle satellite cells in a nitric oxide-dependent manner. *The International Journal of Biochemistry & Cell Biology*, 40(10), pp.2183–91.

Yamada, M. et al., 2006. Matrix metalloproteinases are involved in mechanical stretch-induced activation of skeletal muscle satellite cells. *Muscle & Nerve*, 34(3), pp.313–9.

Yamamoto, M. & Kuroiwa, A., 2003. Hoxa-11 and Hoxa-13 are involved in repression of MyoD during limb muscle development. *Development, Growth & Differentiation*, 45(5–6), pp.485–98.

Yamane, A. et al., 2004. Exogenous hepatocyte growth factor inhibits myoblast differentiation by inducing myf5 expression and suppressing myoD expression in an organ culture system of embryonic mouse tongue. *European Journal of Oral Sciences*, 112(2), pp.177–181.

Yi, R. et al., 2003. Exportin-5 mediates the nuclear export of pre-microRNAs and short hairpin RNAs. *Genes & Development*, 17(24), pp.3011–6.

Zammit, P.S. et al., 2002. Kinetics of myoblast proliferation show that resident satellite cells are competent to fully regenerate skeletal muscle fibers. *Experimental Cell Research*, 281(1), pp.39–49.

Zammit, P.S. et al., 2004. Muscle satellite cells adopt divergent fates: A mechanism for self-renewal? *Journal of Cell Biology*, 166(3), pp.347–357.

Zarnegar, R. & Michalopoulos, G.K., 1995. The many faces of hepatocyte growth factor: from hepatopoiesis to hematopoiesis. *The Journal of Cell Biology*, 129(5), pp.1177–80.

Zhang, J. et al., 2003. Identification of the haematopoietic stem cell niche and control of the niche size. *Nature*, 425(6960), pp.836–41.

Zioncheck, T.F. et al., 1995. Sulfated oligosaccharides promote hepatocyte growth factor association and govern its mitogenic activity. *Journal of Biological Chemistry*, 270(28), pp.16871–16878.

APPENDIX A - CELL CULTURE REAGENTS

PRIMARY HUMAN MYOBLAST PROLIFERATION MEDIA (PHM-PM): A solution of 361 mL of Ham F-10 Nutrient Mixture Medium (Sigma-Aldrich, Germany, N6908) was supplemented with 100 mL foetal bovine serum (Life Technologies, USA, 10499-044), 5 mL Penicillin (10,000 units/mL)/Streptomycin (10,000 µg/mL) (C_f Penicillin = 100 units/mL) (C_f Streptomycin = 100 µg/mL) (Life Technologies, USA, 15140-122), 34 mL L-glutamine (200 mM, 100x) (C_f = 13.6 mM) (Life Technologies, USA, 25030-081). 49.95 mL was filtered through a 0.22 µm PVDF membrane (Merck, Germany, SLGV033RB) and aliquoted into 50 mL centrifuge tubes (NEST Biotechnology, USA, 602072) and stored at 4 °C. Prior to use, 50 µL of 10 µg/mL of rh-FGF (Promega, USA, G5071) was added fresh to to each centrifuge tube to obtain a final concentration of 10 ng/mL rh-FGF.

PRIMARY HUMAN MYOBLAST QUIESCENCE MEDIA: A solution of 361 mL of Ham F-10 Nutrient Mixture Medium (Sigma-Aldrich, Germany, N6908) was supplemented with 100 mL KnockOut™ Serum Replacement (Life Technologies, USA, 10828-010), 5 mL Penicillin (10,000 units/mL)/ Streptomycin (10,000 µg/mL) (C_f Penicillin = 100 units/mL) (C_f Streptomycin = 100 µg/mL) (Life Technologies, USA, 15140-122), 34 mL L-glutamine (200 mM, 100x) (C_f = 13.6 mM) (Life Technologies, USA, 25030-081). The media was filtered through a 0.22 µm PVDF membrane (Merck, Germany, SLGV033RB) and aliquoted into 50 mL centrifuge tubes (NEST Biotechnology, USA, 602072) and stored at 4 °C.

PRIMARY HUMAN MYOBLAST DIFFERENTIATION MEDIA (PHM-DM): A solution of 451 mL of Dulbecco's modified Eagle's medium (Sigma-Aldrich, Grmany, D5671), 10 mL Horse Serum (Life Technologies, USA, 26-050-088), 5 mL Penicillin (10,000 units/mL)/Streptomycin (10,000 µg/mL) (C_f Penicillin = 100 units/mL) (C_f Streptomycin = 100 µg/mL) (Life Technologies, USA, 15140-122), 34 mL L-glutamine (200 mM, 100x) (C_f = 13.6 mM) (Life Technologies, USA, 25030-081). The media was filtered through a 0.22 µm PVDF membrane (Merck, Germany, SLGV033RB) and aliquoted into 50 mL centrifuge tubes (NEST Biotechnology, USA, 602072) and stored at 4 °C.

PRIMARY HUMAN MYOBLAST FREEZING MEDIA: A solution of 33.6 mL of Ham F-10 Nutrient Mixture Medium (Sigma-Aldrich, Germany, N6908) was supplemented with 10.0 mL foetal bovine serum (Life Technologies, USA, 10499-044), 0.5 mL Penicillin (10,000 units/mL)/Streptomycin (10,000 µg/mL) (C_f

Penicillin = 100 units/mL) (C_f Streptomycin = 100 µg/mL) (Life Technologies, USA, 15140-122), 34 mL L-glutamine (200 mM, 100x) (C_f = 13.6 mM) (Life Technologies, USA, 25030-081), 2.5 mL DMSO (Sigma-Aldrich, Germany, D2650). The medium was filtered through a 0.22 µm PVDF membrane (Merck, Germany, SLGV033RB) and aliquoted into 50 mL centrifuge tubes (NEST Biotechnology, USA, 602072) and stored at 4 °C.

rh-HGF TREATMENT MEDIA: High concentration of rh-HGF (10 ng/mL) was made from 30 µL of stock rh-HGF (5 µg/mL) added to 14.97 mL of quiescence media. Low concentration of rh-HGF (2 ng/mL) was made from 3 mL of High concentration (10 ng/mL) added to 12 mL of quiescence media.

rh-HGF RECONSTITUTION: 5 µg of lyophilized rh-HGF (R&D Systems, USA, 294-HG) was reconstituted at 50 µg/mL by adding 100 µL of sterile 1x PBS (Sigma-Aldrich, Germany, P4417) with 0.1% (w/v) of BSA (Roche, Germany, 10735086001). To make the 0.1% BSA, 0.05 g of Bovine serum albumin fraction V (Roche, Germany, 10735086001) was dissolved in 50 mL 1x sterile PBS (Sigma-Aldrich, Germany, P4417). This solution was then filtered through a 0.22 µm PVDF membrane (Merck, Germany, SLGV033RB). The 50 µg/mL rh-HGF was then diluted 10-fold in the PBS solution to obtain a 5 µg/mL working solution. This was aliquoted and stored at -20 °C.

rh-FGF RECONSTITUTION: 25 µg of lyophilized rh-FGF (Promega, USA, G5071) was reconstituted at 10 µg/mL by adding 2.5 mL of sterile 1x PBS (Sigma-Aldrich, Germany, P4417). This was aliquoted and stored at -20°C.

STERILE PHOSPAHTE BUFFERED SALINE: To prepare 1x PBS, 5 tablets of Sigma-Aldrich P4417 pre-made PBS tablets were dissolved in 1 L of ddH_20 to yield a 0.01 M phosphate buffer, 0.0027 M potassium chloride and 0.137 M sodium chloride, pH 7.4 solution at 25 °C. This solution was autoclaved to ensure sterility and aliquoted into 50 mL centrifuge tubes (NEST Biotechnology, USA, 602072) and stored at 4 °C.

ENTACTIN-COLLAGEN IV-LAMININ (ECL) CELL ATTACHMENT MATRIX: Stock ECL (5 mg) (1 mg/mL) (Merck, USA, 08-110) was diluted to a working stock of 20 µg/mL in 250 mL of sterile 1x PBS (Sigma-Aldrich, Germany, P4417). This solution was aliquoted into 15 mL centrifuge tubes (NEST Biotechnology, USA, 601002) and stored at -20 °C.

APPENDIX B - CELL PASSAGING, THAWING AND CRYOPRESERVATION

CELL THAWING: Cryovials (Corning, USA, 430487) were removed from LN_2 storage and placed in 37 °C water to thaw. The cell suspension was then placed in a 15 mL centrifuge tube (NEST Biotechnology, USA, 601002) containing 5 mL of pre-warmed (37 °C) primary human myoblast proliferation media (PHM-PM). Cells were placed in a centrifuge (Eppendorf, Germany, 5810R) and centrifuged for 3 min at 1500 RPM at room temperature. After centrifugation the media was aspirated to remove all traces of dimethyl sulphoxide (DMSO) (Sigma-Aldrich, Germany, D2650). The pelleted cells were resuspended in 37 °C PHM-PM and triturated. The cell suspension was then transferred to the ECL-coated (Millipore, USA, 08-110) T25 cell culture flask (NEST Biotechnology, USA, 707003), which was then placed in a temperature controlled incubator with a constant 5% CO_2 (ESCO, Singapore, CCL-170B-8-UV). Coating of cell culture flasks with ECL was performed prior to cell culturing. Flasks were incubated for at least 1 at 37 °C with ECL.

CELL PASSAGING: Once PHMs covered 70-80% of the cell culture flask growth surface cells were trypsinized and passaged. To perform cell passaging, old media was removed and cells were rinsed twice with pre-warmed 1x sterile PBS (Sigma-Aldrich, Germany, P4417). 0.25% Trypsin-EDTA (1x) (Life Technologies, USA, 25200-072) was then added to the culture flask, which was then incubated in a heated shaking incubatore set at 37 °C for 5 min, to dilodge cells from the flask surface. An equal volume of warm PHM-PM was then added to the flask and the cell suspension was transferred to a 15 mL centrifuge tube (NEST Biotechnology, USA, 601002). The culture flask was then rinsed again with PHM-PM in order to collect remaing cells and transferred to the 15 mL centrifuge tube. The centrifuge tube was then placed in a centrifuge (Eppendorf, Germany, 5810R) was spun at 1500 RPM for 3 min. After centrifugation, the media inside the 15 mL centrifuge tube was discarded and the pelleted cells were resuspended in 1 mL warm PHM-PM. Depending on the number of cells, cells were either split 1:2 or 1:3 and then transferred into a new tissue culture flask.

CRYOPRESERVATION: Once sufficient expansion of cells of each particular subject was achieved, cells were cryopreserved in liquid nitrogen LN_2 (-195 °C) for long term storage. Cells were washed with 1x PBS (Sigma-Aldrich, Germany, P4417) and trypsinized with 0.25% (1x) Trypsin-EDTA (Life Technologies, USA, 25200-072). Cells were pelleted and resuspended in ice-cold (1-4 °C) primary human myoblast freezing media. The cell suspension was then placed in cryovials (Corning, USA,

430487) in 1 mL aliquots, each containg ± 5 x 10^5 cells. Cryovials were placed in a Mr Frosty™ freezing container (Thermo Fischer, Germany, 5100-0001) and placed for 24 h in a -80 °C freezer. Cryovials were then moved to LN_2 for long term storage.

APPENDIX C - DETERMINATION OF CELL CULTURE CONTAMINATION

Contamination of PHMs, whether it be bacterial or fungal, was determined by either brightfield or confocal microscopy.

BACTERIAL OR FUNGAL CONTAMINATION: All cells grown in flasks or plates were checked on a daily basis for the presence of any possible contamination. Clear see-through media, without any change in colour visually confirmed absence of contamination. Cells were then visualized under brightfield microscopy at 4x, 10x and 20x to look for fungal spores or a motile particles in the media, generated by bacterical contamination.

MYCOPLASMA CONTAMINATION: Mycoplasma contamination was assessd *via* confocal microscopy. Briefly, cells were plated on a cover slips and incubated for 24 h at 37 °C. Media was then removed and cells were washed with 1x PBS twice. Cells were the fixed in 4% paraformaldehyde for 15 min and stained with Hoechst (1:2000) for 5 min in the dark. Cover slips were then washed with 1x PBS several times and then mounted with 4 µL of Moviol onto microscope slides. The absence of blue string-like particles around cellular nuclei, signified the absence of Mycoplasma contamination.

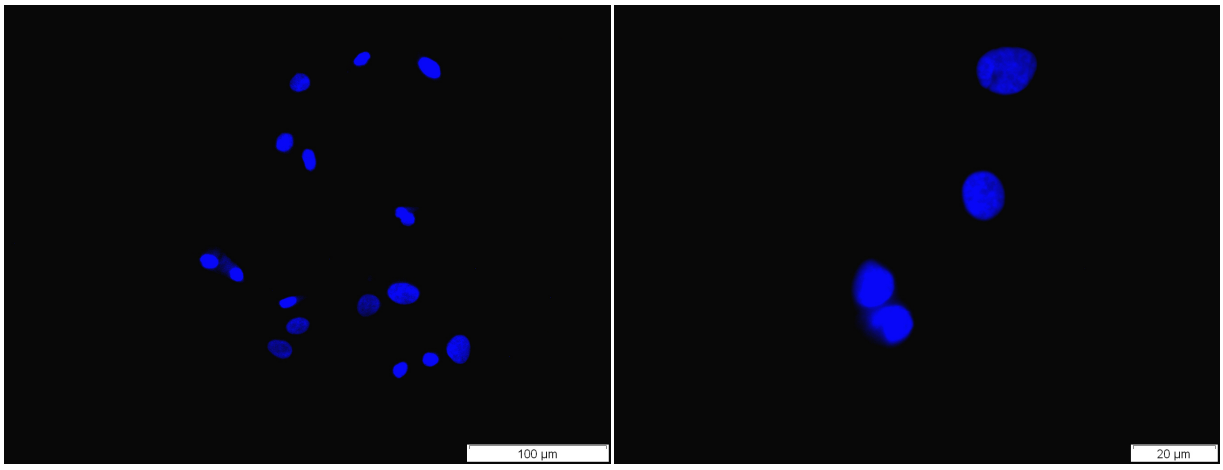

Figure C.1: Mycoplasma contamination assessement in PHM cell cultures.

Confocal microscopy image of PHMs fixed in 4% paraformaldehdye and stained with Hoescht (1:2000) to visualize micoplasma contamination in cell cultures.

APPENDIX D - FLOW CYTOMETRY SETUP AND ANTIBODY OPTIMIZATION

Table D.1: Multicolour flow cytometry antibody panel.

	1	2	3	4	5	6	7
Marker	**Ki-67**	**CD56**	**Myo-D**	**Myf-5**	**CD34**	**Pax-7**	**Zombie Aqua**
Fluorochrome	**PE/Cy7**	**PE/Dazzle**	**APC**	**Alex 488**	**APC/Cy7**	**PE**	**Aqua BV510**
Host	Mouse	Mouse	Mouse	Mouse	Mouse	Mouse	Mouse
Reactivity	Human	Human	Human	Human	Human	Human	Human
Application	Flow	Flow	Flow	Flow	Flow	Flow	Flow
Filter	780/60	610/20	660/20	530/30	780/60	585/42	530/30
Laser	Blue	Blue	Red	Blue	Red	Blue	Violet
Emmission	785nm	610nm	660nm	519nm	785nm	578nm	516nm
Concentration / 1 x 10^6 cells	5 µL	2.5 µL	5 µL	5 µL	2.5 µL	10 µL	1 µL

CYTOMETER SETTINGS:

Parameters | Spectral Overlap | Ratio

Fluorophore	A	H	W	Log	Threshold (Or)	PMT Voltage
FSC	☑	☑	☑	☐	5000	200
SSC	☑	☑	☑	☐		210
FITC	☑	☐	☐	☑		525
PE	☑	☐	☐	☑		350
PE-Texas Red	☑	☐	☐	☑		495
PerCP	☑	☐	☐	☑		100
PE-Cy7	☑	☐	☐	☑		495
APC	☑	☐	☐	☑		487
APC-Cy7	☑	☐	☐	☑		465
Alexa Fluor 430	☑	☐	☐	☑		320
DAPI	☑	☐	☐	☑		100

Footnote: Voltage settings used on the FACS Aria for the multicolour flow cytometry analyses of PHMs.

SPECTRAL OVERLAP:

Parameters | Spectral Overlap | Ratio

%	FITC	PE	PE-Texa...	PerCP	PE-Cy7	APC	APC-Cy7	Alexa Fl...	DAPI
FITC	100.00	2.22	0.81	0.00	0.32	0.02	0.05	0.00	0.00
PE	5.53	100.00	33.84	0.00	0.93	0.01	0.03	0.00	0.00
PE-Texas Red	1.90	37.57	100.00	0.00	0.42	0.01	0.01	0.00	0.00
PerCP	0.00	0.00	0.00	100.00	0.00	0.00	0.00	0.00	0.00
PE-Cy7	0.04	1.56	6.19	0.00	100.00	0.13	1.45	0.00	0.00
APC	0.00	0.08	0.83	0.00	0.04	100.00	4.73	0.00	0.00
APC-Cy7	0.00	0.01	0.13	0.00	14.07	11.54	100.00	0.00	0.00
Alexa Fluor...	0.13	0.04	0.02	0.00	0.03	0.01	0.02	100.00	0.00
DAPI	0.00	0.00	0.00	0.00	0.00	0.00	0.00	0.00	100.00

Footnote: Spectral overlap of the different fluorophores used for the multicolour flow cytometry analyses of PHMs.

ANTIBODY TITRATIONS AND TITRATION CURVES:

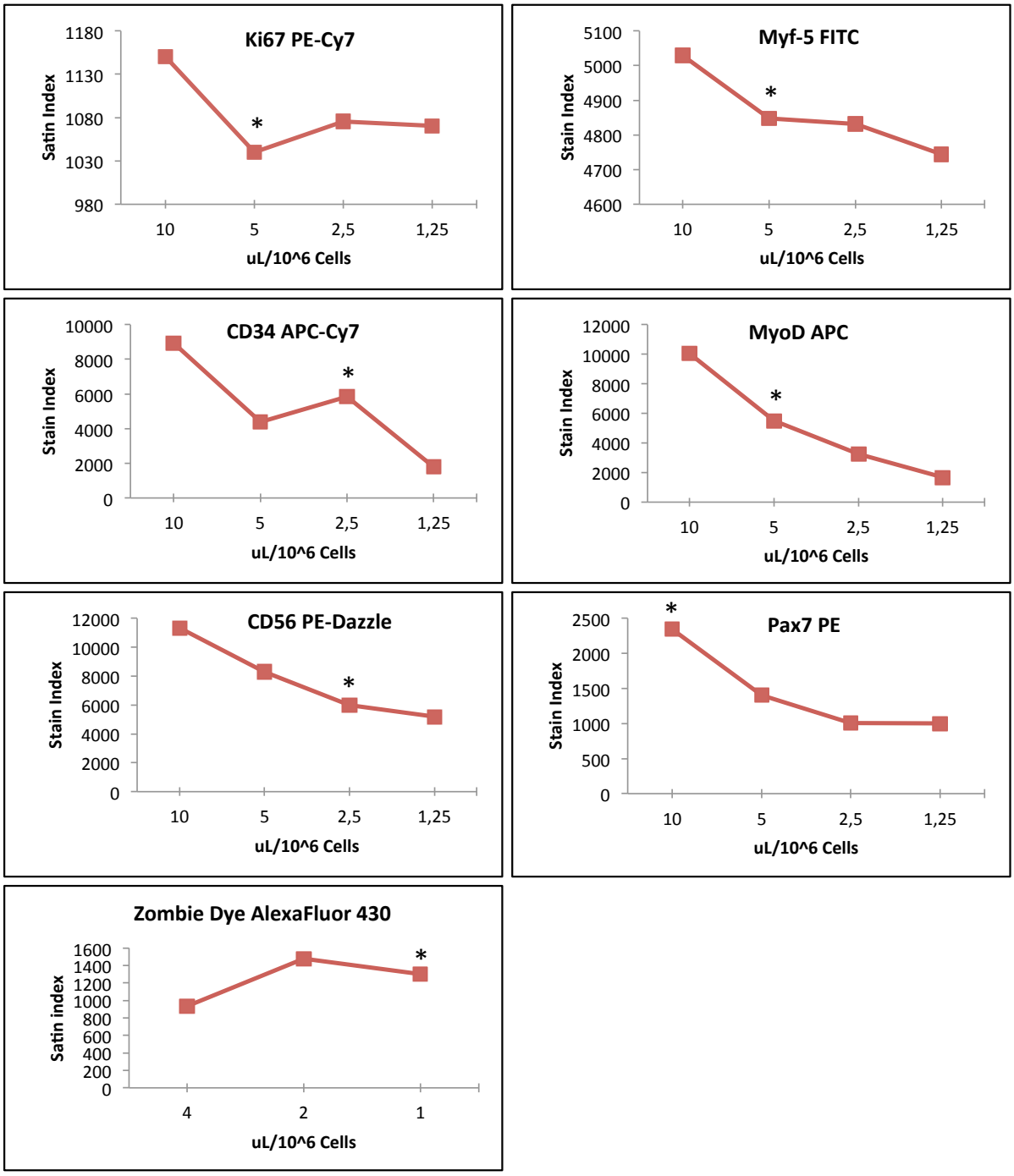

Footnote: Asterisk indicates optimal concentration of antibody.

FLUORESCENCE MINUS ONE (FMOs):

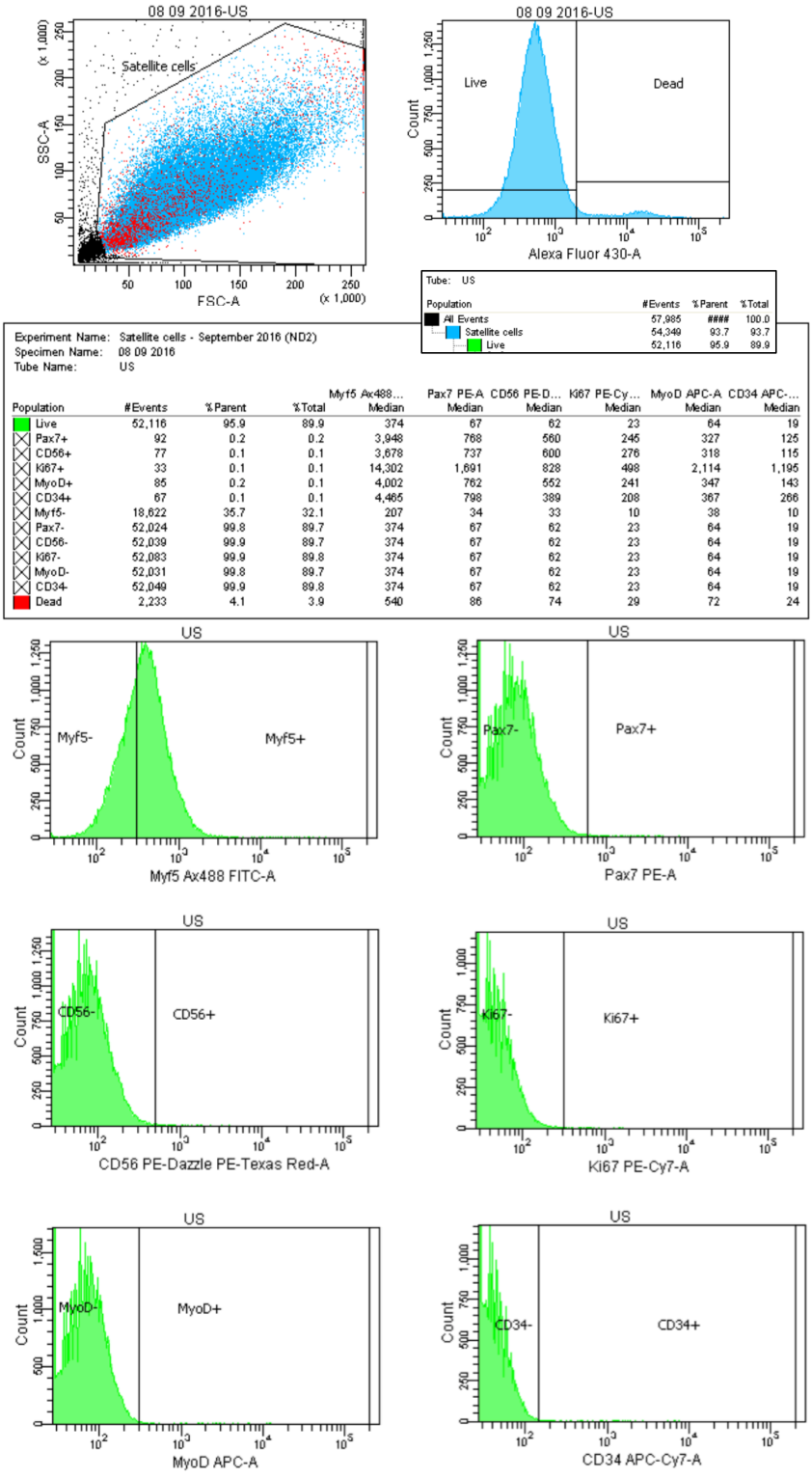

Figure D.1: Unstained FMO.

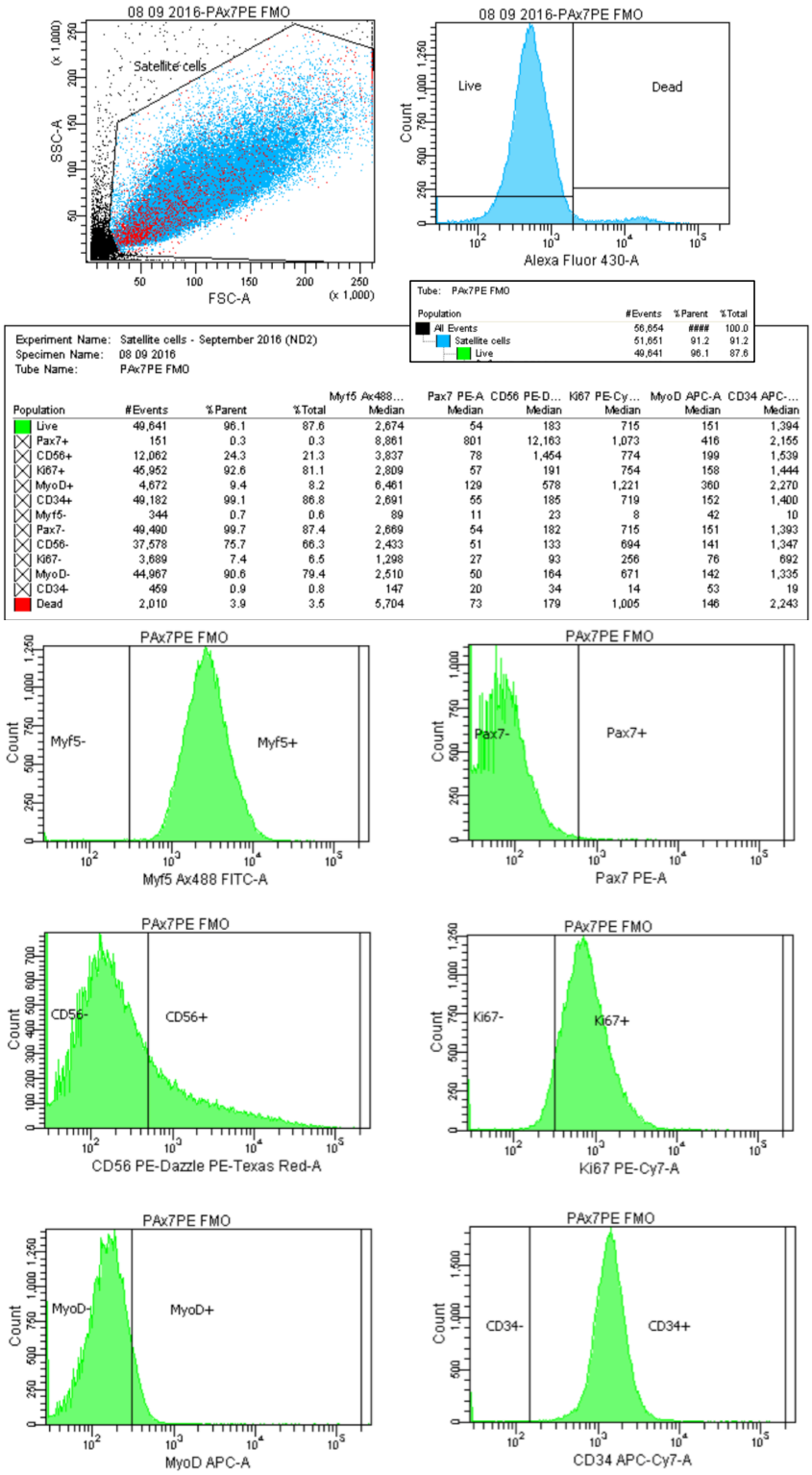

Figure D.2: Pax7 FMO.

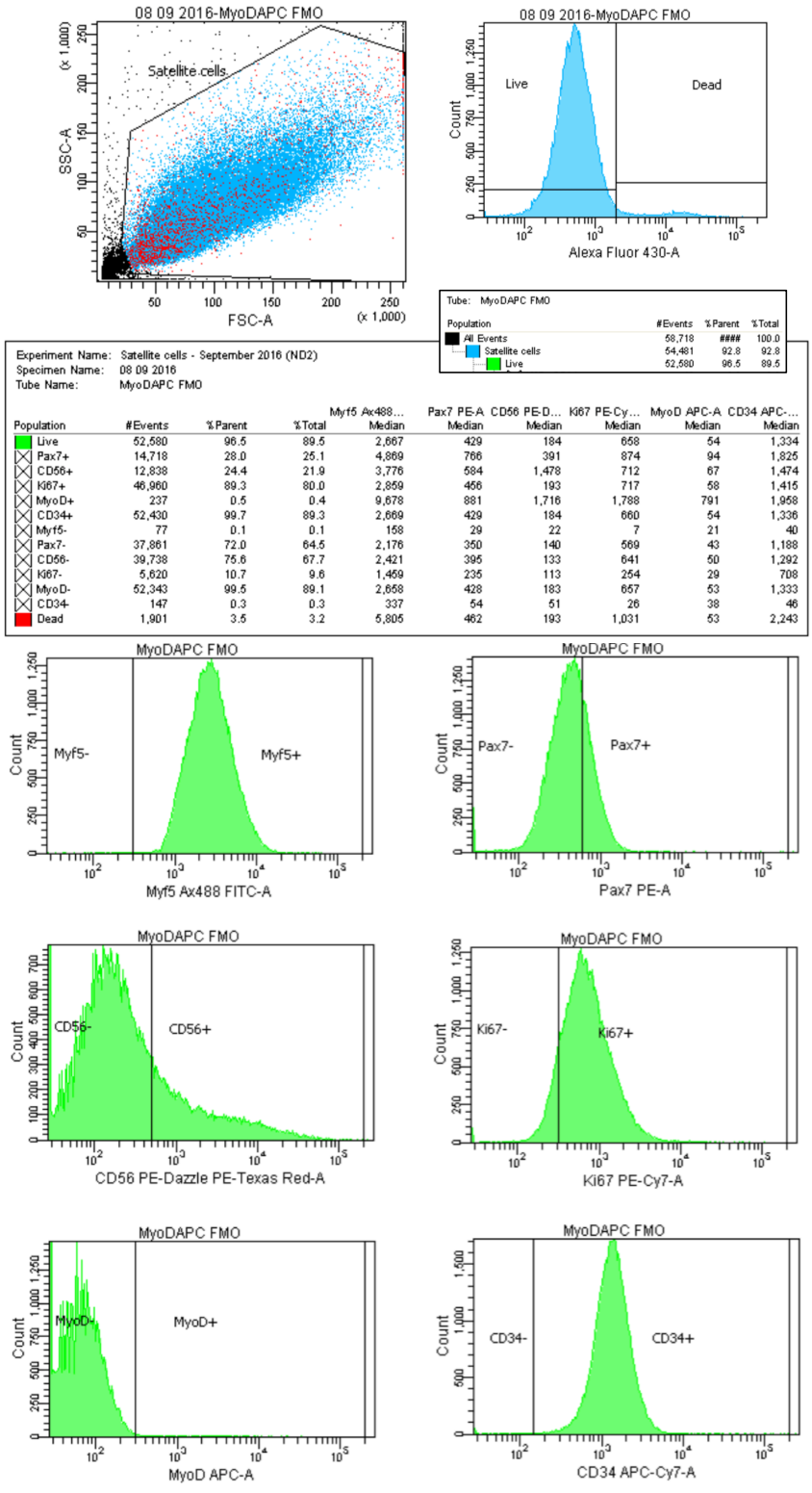

Figure D.3: MyoD FMO.

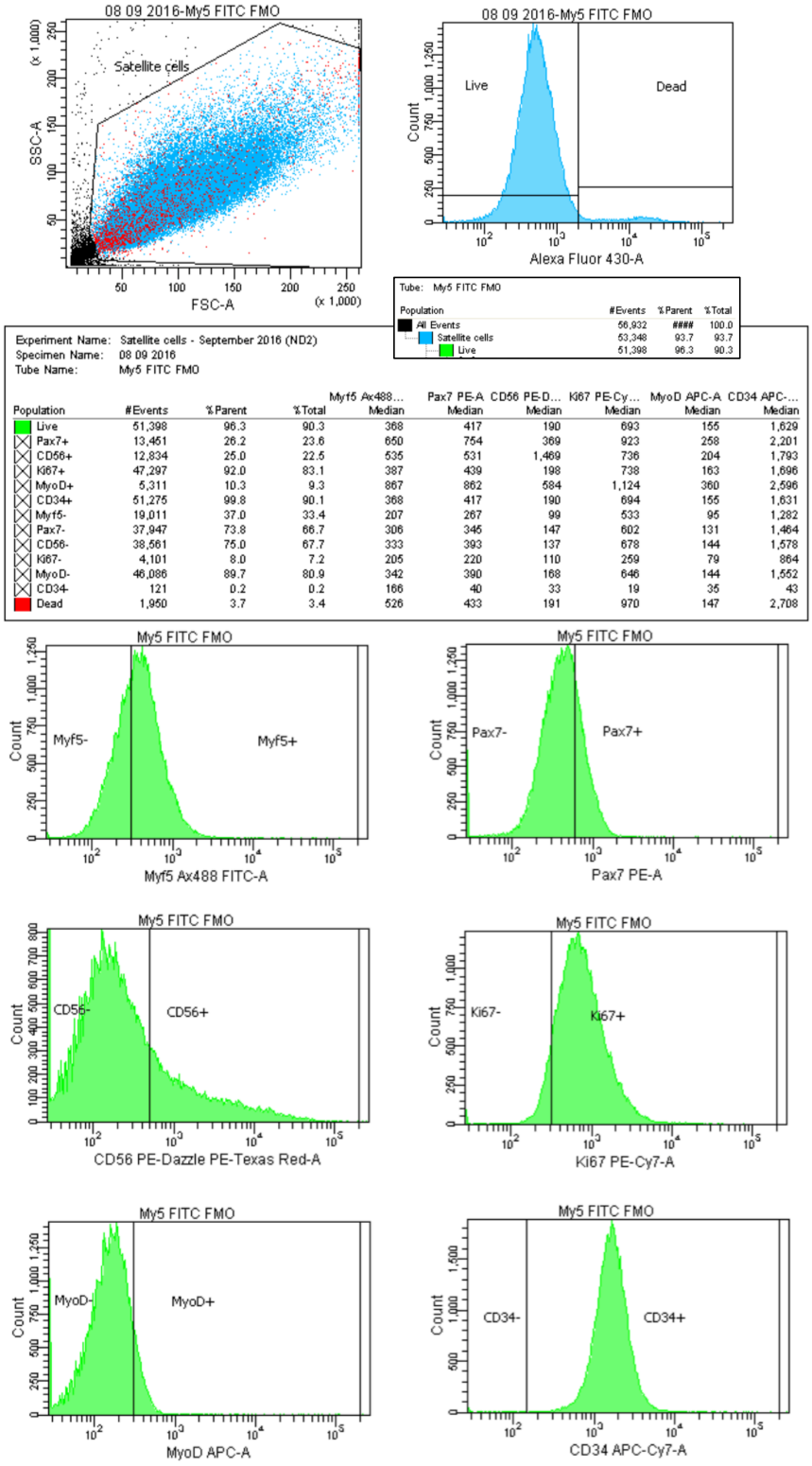

Figure D.4: Myf-5 FMO.

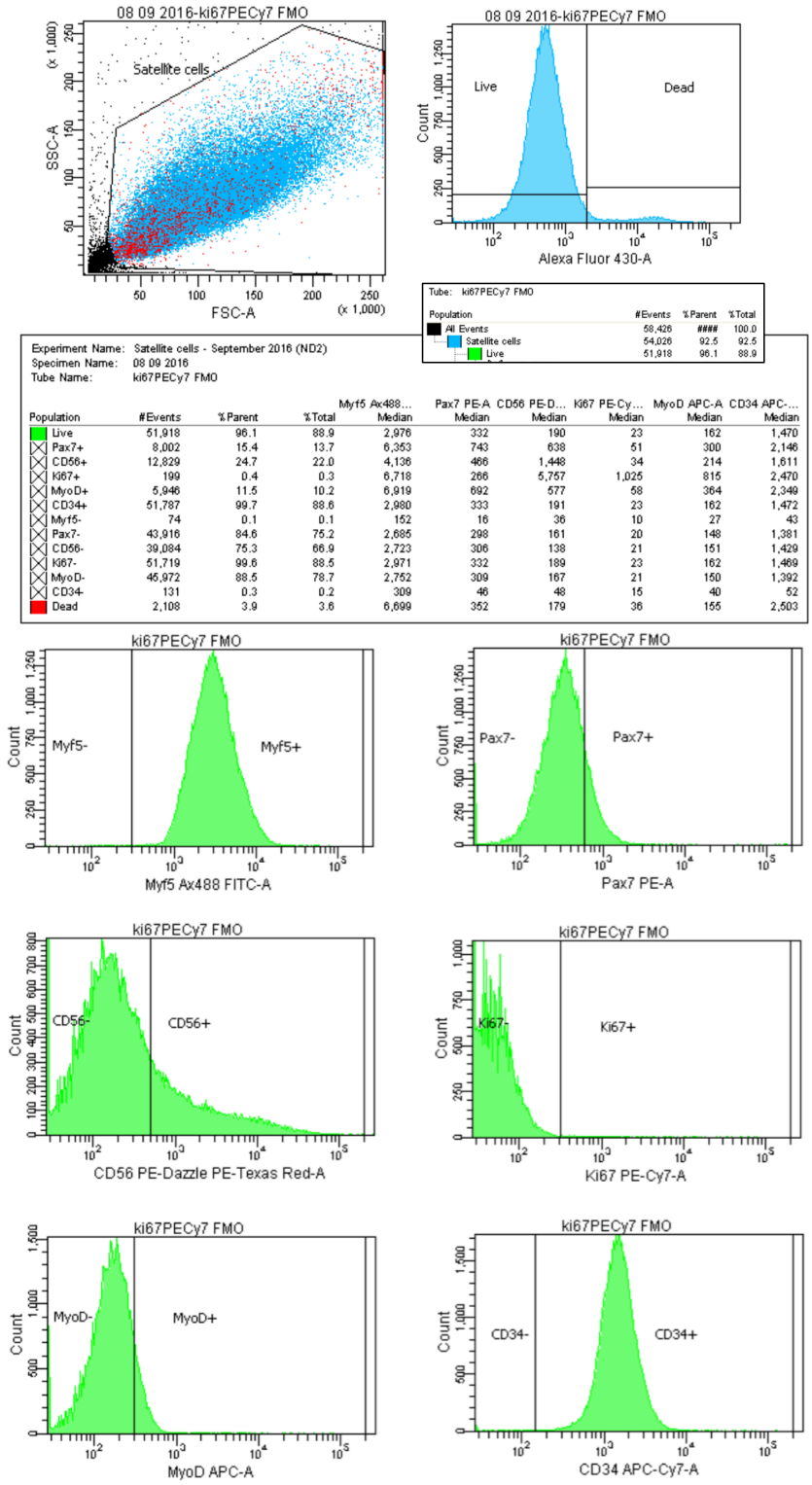

Figure D.5: Ki-67 FMO.

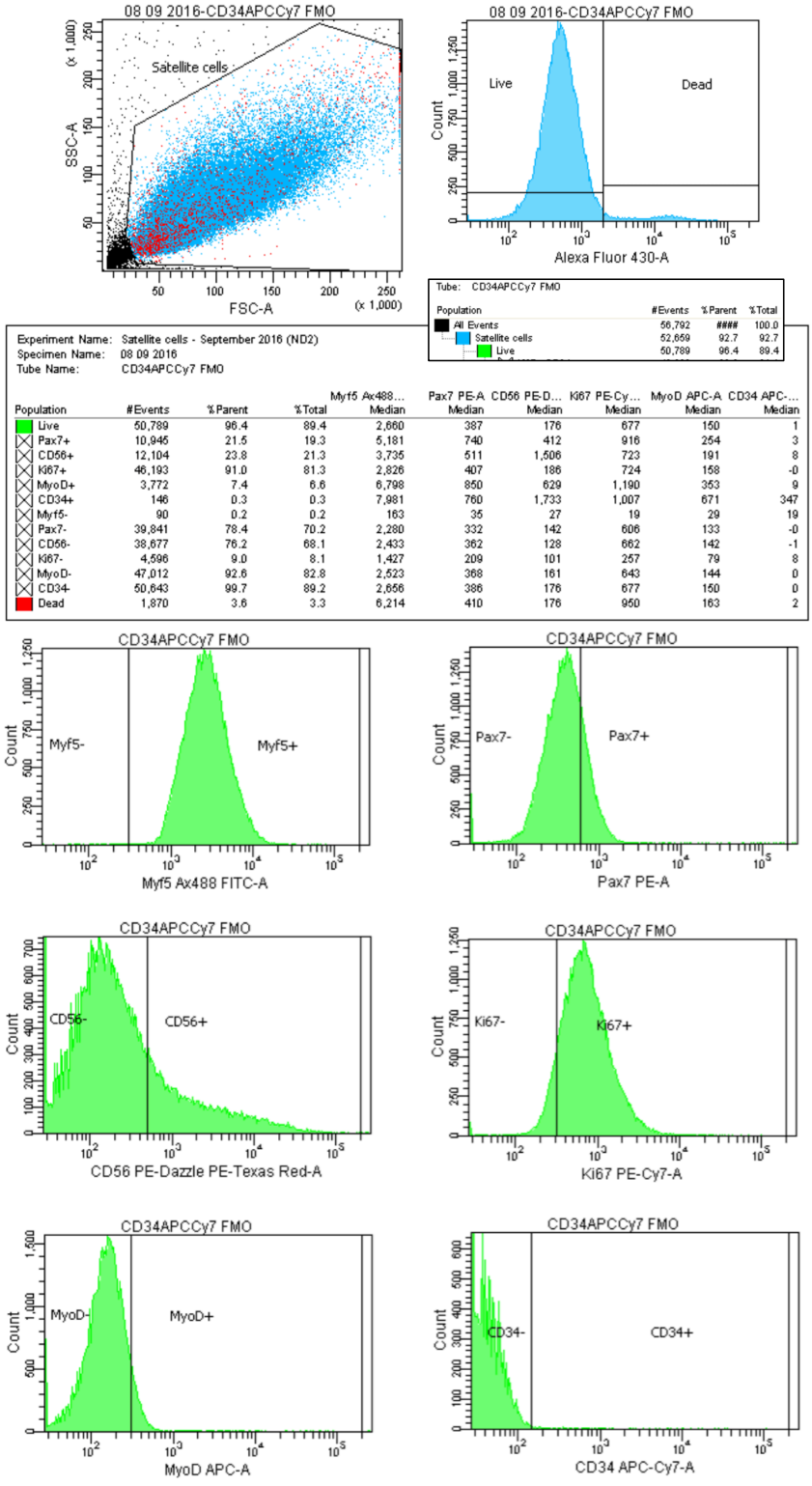

Figure D.6: CD34 FMO.

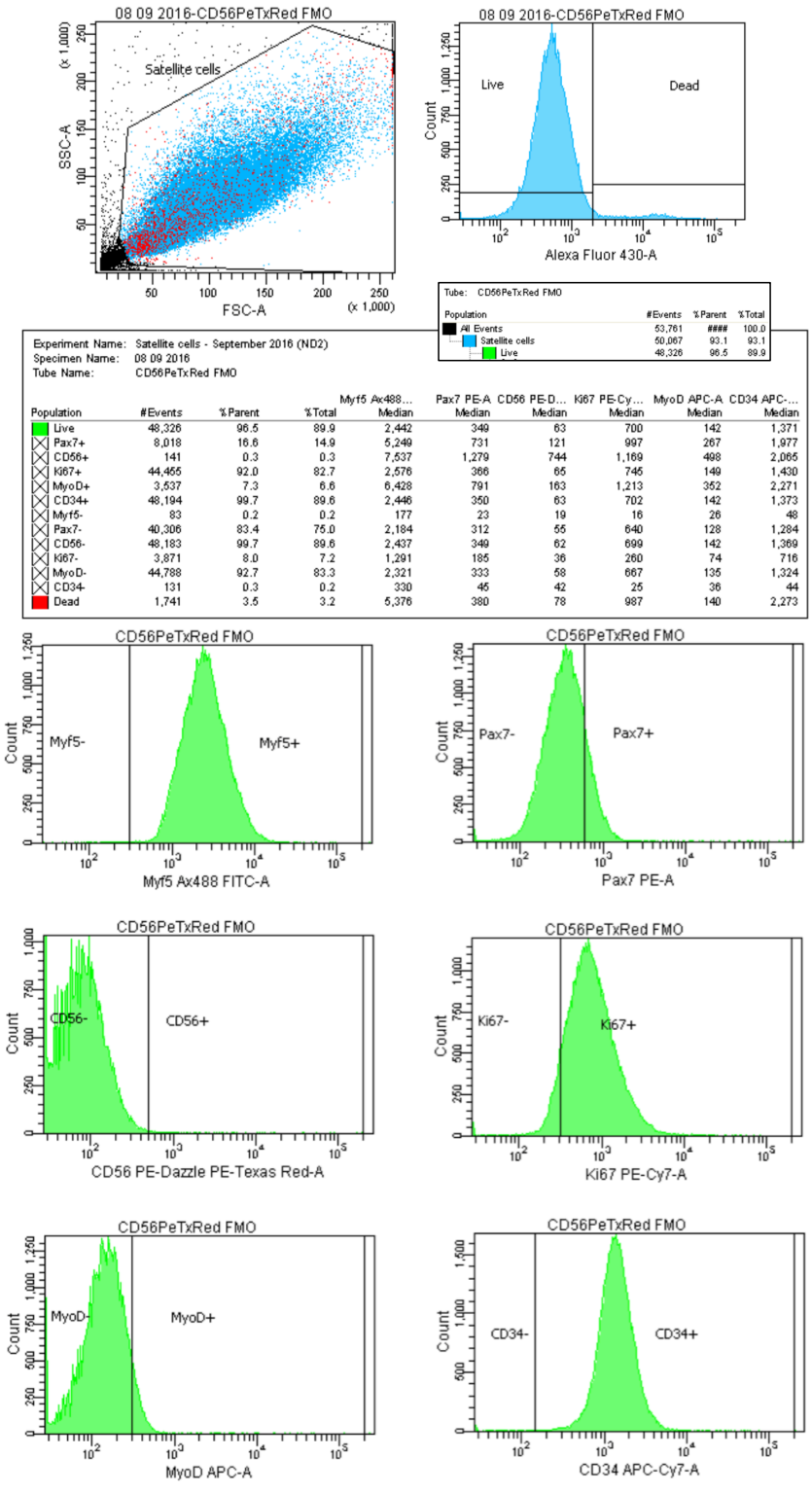

Figure D.7: CD56 FMO.

APPENDIX E - RH-HGF TREATMENT TISSUE CULTURE PLATE SETUP

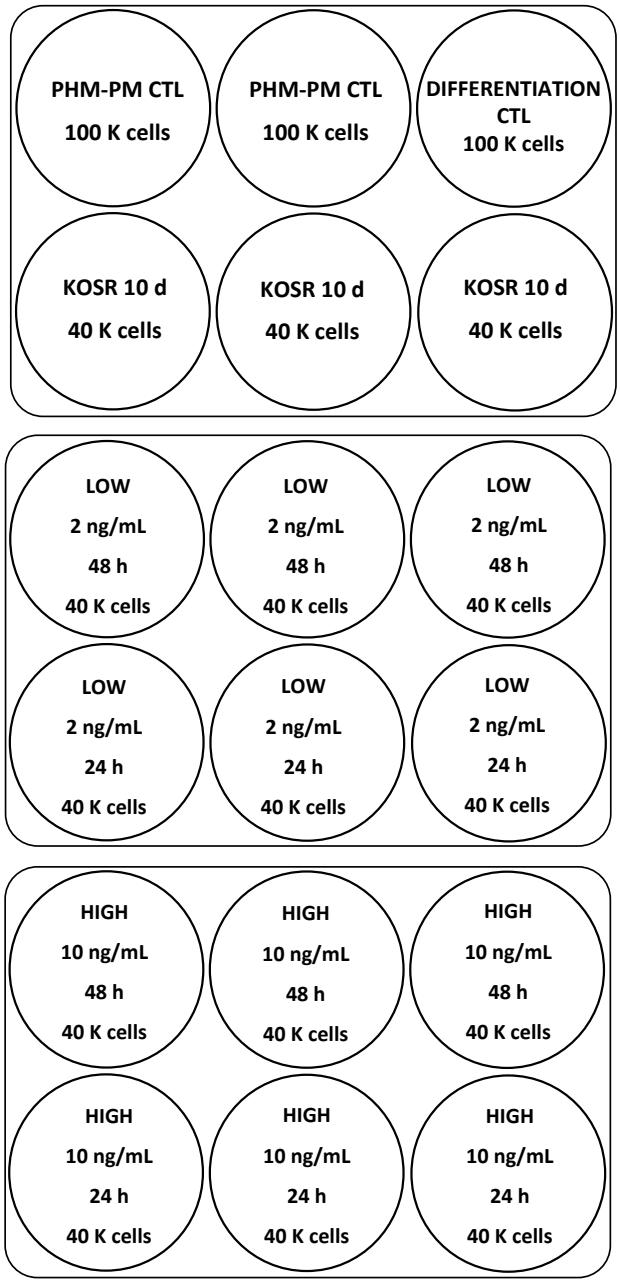

Figure E.1: 6-well (35mm) tissue culture plate set up for rh-HGF treatment.

PHMs were plated onto ECL-coated plates and cultured in quiescence media (Ham's F-10 supplemented with 20% KOSR, 1% P/S and 6.8 % L-Glu) for 10 days. The low and high treatment wells were then further cultured in quiescence media containing either 2 ng/mL (low) or 10 ng/mL (high) of rh-HGF for 24 h or 48 h. Once the experiment reached completion, cells were lysed and protein, RNA and miRNA was isolated for further analysis.

APPENDIX F - PROTEIN LYSATE PREPARATION AND QUANTIFICATION

RIPA BUFFER: 50 mM Tris (hydroxymethyl) aminomethane ($NH_2C(CH_2OH)_3$, (MW = 121.14) (Sigma-Aldrich, Germany, 201-064-4), 2.5 mM TRIS-HCl pH 7.8 1 M (Sigma-Aldrich, Germany, T2913), 1% (v/v), Triton X-100 (Sigma-Aldrich, Germany, X100), 0.5% (v/v) Sodium deoxycholate (MW = 414.55) (Sigma-Aldrich, Germany, DA5670), 0.25% (w/v) ethylenediaminetetraacetic acid disodium salt dihydrate (EDTA, M = 372.24) (Sigma-Aldrich, Germany, 205-358-3) The buffer was stored at 4 °C. Prior to protein harvesting, 80 µL of 25x protease inhibitor cocktail (Roche, Germany, 04-693-116-001) and 100 µL of 10x phosphatase inhibitor cocktail (Roche, Germany, 04-906-837-001) were added fresh to 820 µL of RIPA Buffer.

PROTEIN HARVESTING: PHMs were cultured in 6-well tissue culture plates (Corning, USA, CR3516). Media was removed and cells were washed with cold (4 °C) 1x PBS (Sigma-Aldrich, Germany, P4417) and trypsinized with 0.25% (1x) Trypsin-EDTA (Life Technologies, USA, 25200-072). Plates were placed on ice and 100 µL of RIPA Buffer was placed into each well. Cells were removed from the culture surface with a cell scraper (NEST, USA, 710001) and transferred into a 1.5 mL Eppendorf tube. The collected cell suspensions were kept on ice, sonicated for 15 seconds and then centrifuged for 10 min at 14,000 RPM at 4 °C. The supernantant was transferred into a new 1.5 mL Eppendorf tube and then protein concentrations were determined spectrophotometrically *via* the Direct Detect® infrared spectrophotometer (EDM Millipore, USA, DDHW00010-00). 2 µL of cell lysate was loaded onto Direct Detect cards and placed into the spectrophotometer. A pre-calibrated RIPA buffer standard curve was used as a reference and a sample of RIPA buffer used to harvest cells was used to blank the spectrophotometer. Samples were then stored at -80 °C.

DIRECT DETECT PROTEIN CONCENTRATION READ OUTS:

Direct Detect®

Analysis Results Report

Date / Time :	7/14/2016 4:14:25 PM	**Instrument Serial # :**	M100447
Card Name :	CARD 1	**Software Version :**	3.0.25.0
User Name :	Operator	**Company Name :**	
Protein Method :	RIPA calibration curve.q3	**Department :**	
Lipids Method :		**Location :**	
Number of Reads :	1	**Internal Humidity :**	24.508%
Modified Mass Unit :	Not Used	**21 CFR 11 :**	Disabled
Diagnostics :	Instrument Test expired All Systems Operational		
Messages :			

Sample Pos		Type	Sample Name	Protein [mg/ml]	Lipids []
4		Sample	PHM 6.3 p6 LOW	0.335	
3		Sample	PHM 6.3 p6 KOSR 10d	0.310	
2		Sample	PHM 6.3 p6 PHMPM CTL	0.613	
1		Blank	Blank	----	----

Sample Pos		Type	Sample Name	Protein [mg/ml]	Lipids []
4		Sample	PHM 6.3 p7 PHMPM CTL	0.831	
3		Sample	PHM 6.3 p6 HIGH-NONE	0.360	
2		Sample	PHM 6.3 p6 HIGH	0.486	
1		Sample	PHM 6.3 p6 LOW-NONE	0.352	

Sample Pos		Type	Sample Name	Protein [mg/ml]	Lipids []
4		Sample	PHM 6.3 p7 HIGH	0.328	
3		Sample	PHM 6.3 p7 LOW-NONE	0.317	
2		Sample	PHM 6.3 p7 LOW	0.310	
1		Sample	PHM 6.3 p7 KOSR 10d	0.423	

Sample Pos		Type	Sample Name	Protein [mg/ml]	Lipids []
4		Sample	PHM 6.3 p8 LOW	0.281	
3		Sample	PHM 6.3 p8 KOSR 10d	0.359	
2		Sample	PHM 6.3 p8 PHMPM	1.180	
1		Sample	PHM 6.3 p7 HIGH-NONE	0.339	

Sample Pos		Type	Sample Name	Protein [mg/ml]	Lipids []
4		Sample	Empty	0.000	
3		Sample	PHM 6.3 p8 HIGH-NONE	0.379	
2		Sample	PHM 6.3 p8 HIGH	0.318	
1		Sample	PHM 6.3 p8 LOW-NONE	0.407	

Direct Detect®
Analysis Results Report

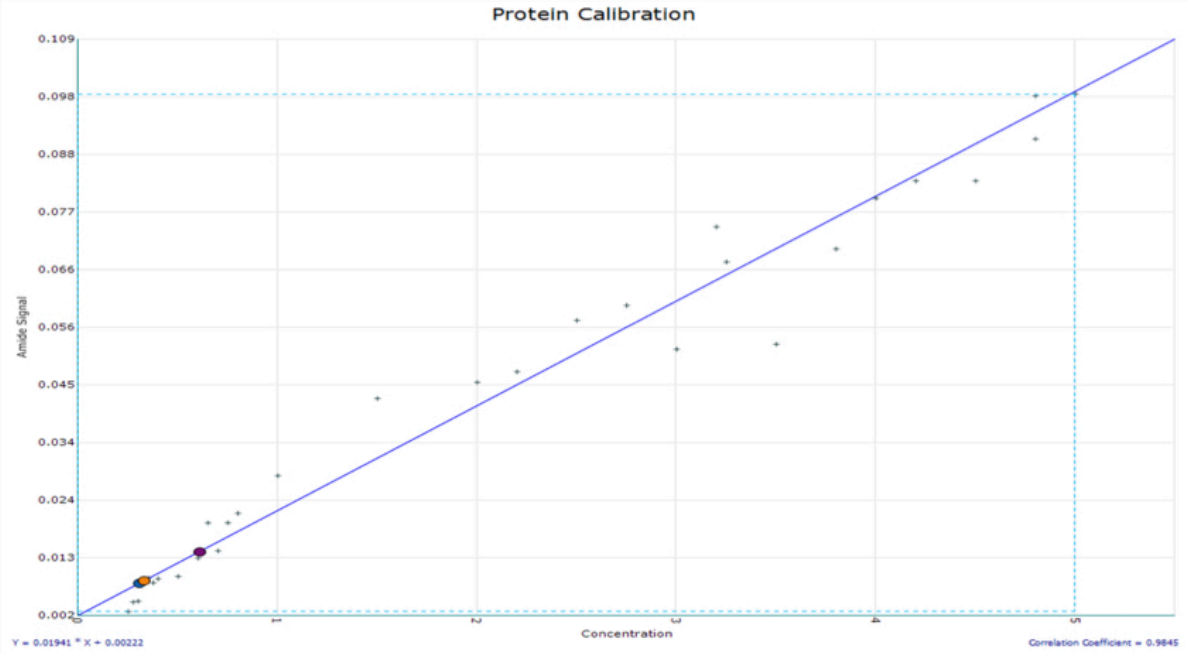

APPENDIX G - WESTERN BLOT REAGENTS

RUNNING BUFFER 10X: A solution containing 30.3 g 0.25M Tris (Merck, Germany, 648310), 144 g 1.92 M Glycine (Merck, Germany, 357002), 10 g 10% (v/v) SDS (Merck, Germany, 428023) was placed into a beaker and made up to 1 L with ddH_2O.

TRANSFER BUFFER: 200 mL of 5x Transfer buffer supplied in the Trans-Blot® Turbo™ RTA Transfer Kit, LF PVDF (Bio-Rad, USA, 170-4274) was mixed with 200 mL (95-99%) EtoH, and 600 mL ddH_2O.

TBS-T 10X: A solution containing 60 g Tris (500mM), 87 g NaCl (1.5M) and 10 mL Tween (1%) was placed into a beaker, pH to 8.3 and made up to 1 L with ddH_2O

5% MILK: 10 mL of fat free milk (Parmalat) was mixed with 190 mL of 1x TBS-Tween for blocking and secondary antibody incubation.

12% PAGE-GELS: A TGX Stain-Free™ FastCast™ Acrylamide kit, 12% (BioRad, USA, 161-0185) was used to separate proteins.
For the resolver gel 4 mL of Resolver A solution was mixed with 4 mL of Resolver B soultion. 40 µL of 10% ammonium persulfate (APS) was then added along with 15 µL of Tetramethylethylenediamine (TEMED) (Sigma-Aldrich, Germany, T7024). The solution was mixed.
For the Stacking gel 1.5 mL of Stacker A solution was mixed with 1.5 mL of Stacker B soultion. 10 µL of 10% ammonium persulfate (APS) was then added along with 5 µL of TEMED (Sigma-Aldrich, Germany, T7024). The solution was mixed.
Both stacker and resolver soultions then pipetted in between two 1.5 mm glass plates. With the resolver pipetted first followed by the stacker. The gel was then left at room temperature for 45 min to allow for polymeriziation.

10% APS: 0.1 g of ammonium persulfate (APS) (Sigma-Aldrich, Germany, A3678) was dissolved in 1 mL of ddH_2O, aliquoted and then stored at -20 °C. A fresh aliquot was thawed and used every time.

APPENDIX H - POLYACRYLAMIDE GEL ELECTROPHORESIS & WESTERN BLOTTING PROTOCOL

POLYACRYLAMIDE GEL ELECTROPHORESIS: Cast gels were placed into a Bio-Rad Mini-PROTEAN® Tetra cell gel electrophoresis system. 1x running buffer was poured into the inner and outer electrode compartments until the tank was full. 10 µL of Precision Plus Protein™ Kaleidoscope™ protein marker standard (Bio-Rad, USA, 161-0375) was added along with protein samples. The gels were run at a constant voltage of 120V for 10-15 min to allow the protein samples to pass into the resolving gel and then increased to 200V for 1 h or until satisfactory separation was observed. (Bio-Rad PowerPac 1000, Bio-Rad Laboratories, USA).

WESTERN BLOTTING: Gels were placed in a ChemiDoc™ MP Imaging System (Bio-Rads Laboratories, USA) and activated for total protein visualization and quantification. After activation, proteins samples were transferred to a 0.45 µm low-autofluorescence polyvinylidene difluoride (PVDF) membrane using a Trans-Blot® Turbo™ RTA Transfer Kit, LF PVDF (Bio-Rad, USA, 170-4274) and a Bio-Rad Trans-Blotv® Turbo™ Transfer system. Prior to transfer the membranes were first immersed in 100% Methanol for 2-3 min or until they became translucent. The PVDF membranes were then moved into 1x transfer buffer and left to equilibrate. Filter paper stacks were also placed in 1x transfer buffer and left to equilibrate. The apparatus was run according to Bio-Rad's standard protcols for 1.5 mm gels (25V and 1.3A for 10 min), to ensure maximal protein transfer onto the membrane. After proteins were successfully transferred to the LF PVDF membrane, it was washed three times in 1x TBS-Tween buffer for 5 min. The membrane was then blocked with 5% (v/v) fat free milk (Parmalat) in 1x TBS-Tween buffer for 1 h, to prevent non-specific binding. The membrane was then washed again three times in 1x TBS-Tween buffer for 5 min to remove trances of milk. Primary antibody was then added to 1x TBS-Tween with 2% (w/v) BSA (Roche, Germany, 10735086001) buffer and incubated overnight at 4 °C with constant agitation. After primary antibody incubation was complete the membrane was washed six times in 1x TBS-Tween buffer for 5 min and then incubated with secondary HRP-linked antibodies at room temperature for 1 h with constant agitation. Finally the membrane was washed again six times in 1x TBS-Tween buffer for 5 min to remove any non-specific binding. Proteins were visualized with the aid of chemiluminescence SuperSignal® West Femto Maximum Sensitivity Substrate Kit (Thermo Scientific, USA, 34096) and imaged using the ChemiDoc™ MP Imaging system (Bio-Rad Laboratories, USA). Densitometric

analysis of the protein samples was performed on the Image Lab™ Software (Bio-Rad Laboratories, USA) and normalized to total protein.

APPENDIX I - RNA QUANTIFICATION

Table I.1: mRNA nanodrop readings

PHM 6 p6	1st read		2nd read		Average	
	Concentration	A_{260}/A_{280}	Concentration	A_{260}/A_{280}	Concentration (ng/µL)	A_{260}/A_{280}
PHMPM	340.0	2.01	339.2	2.01	**339.60**	**2.01**
KOSR 10d	97.0	1.93	107.4	1.94	**102.20**	**1.935**
Low 48 h	142.4	1.98	143.8	1.95	**143.10**	**1.965**
Low 24 h	257.4	1.99	253.1	1.97	**255.25**	**1.98**
High 48 h	217.3	1.99	216.0	2.01	**216.65**	**2.00**
High 24 h	186.2	2.00	189.4	1.96	**187.8**	**1.98**

PHM 6 p7	1st read		2nd read		Average	
	Concentration	A_{260}/A_{280}	Concentration	A_{260}/A_{280}	Concentration (ng/µL)	A_{260}/A_{280}
PHMPM	243.6	2.02	244.9	2.02	**244.25**	**2.02**
KOSR 10d	60.3	1.88	62.5	1.85	**61.40**	**1.865**
Low 48 h	132.6	1.98	126.8	2.00	**129.7**	**1.99**
Low 24 h	144.9	1.92	144.8	1.97	**144.85**	**1.945**
High 48 h	125.7	1.95	125.6	1.98	**125.65**	**1.965**
High 24 h	176.8	1.98	175.0	1.99	**175.90**	**1.985**

PHM 6 p8	1st read		2nd read		Average	
	Concentration	A_{260}/A_{280}	Concentration	A_{260}/A_{280}	Concentration (ng/µL)	A_{260}/A_{280}
PHMPM	372.2	1.99	370.3	1.99	**371.15**	**1.99**
KOSR 10d	91.1	1.93	91.4	1.92	**91.25**	**1.925**
Low 48 h	127.4	1.92	112.1	1.98	**119.75**	**1.95**
Low 24 h	127.0	1.96	124.5	1.98	**125.75**	**1.97**
High 48 h	100.0	1.98	100.5	1.95	**100.25**	**1.965**
High 24 h	129.6	1.97	128.7	1.97	**129.15**	**1.97**

Table I.2: miRNA nanodrop readings

PHM 6 p6	1st read		2nd read		Average	
	Concentration	A_{260}/A_{280}	Concentration	A_{260}/A_{280}	Concentration (ng/µL)	A_{260}/A_{280}
PHMPM	270.0	1.97	270.0	1.97	**270.00**	**1.97**
KOSR 10d	124.9	1.90	125.3	1.90	**125.10**	**1.90**
Low 48 h	181.7	1.97	181.4	1.98	**181.55**	**1.975**
Low 24 h	169.9	1.94	170.3	1.93	**170.10**	**1.935**
High 48 h	180.8	1.97	181.8	1.97	**181.30**	**1.97**
High 24 h	202.9	2.00	202.9	2.00	**202.90**	**2.00**

PHM 6 p7	1st read		2nd read		Average	
	Concentration	A_{260}/A_{280}	Concentration	A_{260}/A_{280}	Concentration (ng/µL)	A_{260}/A_{280}
PHMPM	243.3	1.97	243.2	1.97	**243.25**	**1.97**
KOSR 10d	107.6	1.93	109.6	1.90	**108.6**	**1.925**
Low 48 h	142.9	1.96	143.2	1.97	**143.05**	**1.965**
Low 24 h	276.5	1.98	274.6	1.97	**275.55**	**1.975**
High 48 h	217.1	1.89	217.2	1.88	**217.15**	**1.885**
High 24 h	216.2	1.96	217.1	1.98	**216.65**	**1.97**

PHM 6 p8	1st read		2nd read		Average	
	Concentration	A_{260}/A_{280}	Concentration	A_{260}/A_{280}	Concentration (ng/µL)	A_{260}/A_{280}
PHMPM	335.8	1.94	334.8	1.94	**335.3**	**1.94**
KOSR 10d	168.0	1.83	171.0	1.82	**169.5**	**1.825**
Low 48 h	138.8	1.89	140.0	1.88	**139.45**	**1.885**
Low 24 h	110.8	1.89	109.8	1.92	**110.3**	**1.905**
High 48 h	155.2	1.98	155.0	1.98	**115.1**	**1.98**
High 24 h	127.0	1.94	125.8	1.97	**126.4**	**1.955**

APPENDIX J - qPCR RAW DATA ANALYSIS

mRNA RAW DATA ANALYSES:

Sample Name	Target Name	Cт	Cт Mean
p6 PHMPM 18S	18S	8,72720146	8,612462997
p6 PHMPM 18S	18S	8,49772549	
p6 KOSR 10d 18S	18S	8,67298889	8,661458969
p6 KOSR 10d 18S	18S	8,64992809	
p6 LOW 18S	18S	8,51294422	8,528255463
p6 LOW 18S	18S	8,54356766	
p6 LOW_NONE 18S	18S	9,0076046	9,054648399
p6 LOW_NONE 18S	18S	9,1016922	
p6 HIGH 18S	18S	8,68337727	8,644365311
p6 HIGH 18S	18S	8,6053524	
p6 HIGH_NONE 18S	18S	8,50586796	8,267632484
p6 HIGH_NONE 18S	18S	8,02939701	
p7 PHMPM 18S	18S	8,29356861	8,257759094
p7 PHMPM 18S	18S	8,22195053	
p7 KOSR 10d 18S	18S	8,73018742	8,680724144
p7 KOSR 10d 18S	18S	8,63126087	
p7 LOW 18S	18S	8,75853157	8,715736389
p7 LOW 18S	18S	8,67294025	
p7 LOW_NONE 18S	18S	8,60055065	8,518550873
p7 LOW_NONE 18S	18S	8,43655014	
p7 HIGH 18S	18S	8,78733444	8,723031044
p7 HIGH 18S	18S	8,65872765	
p7 HIGH_NONE 18S	18S	8,73664093	8,792633057
p7 HIGH_NONE 18S	18S	8,84862614	
p8 PHMPM 18S	18S	8,76671886	8,768182755
p8 PHMPM 18S	18S	8,76964569	
p8 KOSR 10d 18S	18S	8,86929131	8,891401291
p8 KOSR 10d 18S	18S	8,91351032	
p8 LOW 18S	18S	8,28086758	8,315956116
p8 LOW 18S	18S	8,3510437	
p8 LOW_NONE 18S	18S	8,64849663	8,638632774
p8 LOW_NONE 18S	18S	8,62876892	
p8 HIGH 18S	18S	9,03274727	9,03503418
p8 HIGH 18S	18S	9,03732204	
p8 HIGH_NONE 18S	18S	8,96844292	8,986784935
p8 HIGH_NONE 18S	18S	9,00512695	
REF SAMPLE 28S	18S	6,37882614	6,477839947
REF SAMPLE 28S	18S	6,57685375	

Sample Name	Target Name	Cт	Cт Mean	d-CT
p6 PHMPM PAX7	PAX7	28,6597195	28,80053329	20,1880703
p6 PHMPM PAX7	PAX7	28,941349		0
p6 KOSR 10d PAX7	PAX7	28,5954094	28,69867897	20,03722
p6 KOSR 10d PAX7	PAX7	28,8019485		0
p6 LOW PAX7	PAX7	29,5687294	29,62428284	21,09602737
p6 LOW PAX7	PAX7	29,6798382		0
p6 LOW_NONE PAX7	PAX7	30,0671711	30,05618668	21,00153828
p6 LOW_NONE PAX7	PAX7	30,0452003		0
p6 HIGH PAX7	PAX7	29,7587814	29,82271576	21,17835045
p6 HIGH PAX7	PAX7	29,8866501		0
p6 HIGH_NONE PAX7	PAX7	29,26511	29,33724976	21,06961727
p6 HIGH_NONE PAX7	PAX7	29,4093876		0
p7 PHMPM PAX7	PAX7	29,9554787	29,94314194	21,68538284
p7 PHMPM PAX7	PAX7	29,9308033		0
p7 KOSR 10d PAX7	PAX7	29,2166519	29,19285202	20,51212788
p7 KOSR 10d PAX7	PAX7	29,1690521		0
p7 LOW PAX7	PAX7	29,6203346	29,68282127	20,96708488
p7 LOW PAX7	PAX7	29,7453079		0
p7 LOW_NONE PAX7	PAX7	29,4224129	29,46364212	20,94509125
p7 LOW_NONE PAX7	PAX7	29,5048714		0
p7 HIGH PAX7	PAX7	29,6267452	29,72416878	21,00113773
p7 HIGH PAX7	PAX7	29,8215923		0
p7 HIGH_NONE PAX7	PAX7	29,9344273	29,9512558	21,15862274
p7 HIGH_NONE PAX7	PAX7	29,9680862		0
p8 PHMPM PAX7	PAX7	31,1360455	31,16293716	22,39475441
p8 PHMPM PAX7	PAX7	31,1898308		0
p8 KOSR 10d PAX7	PAX7	30,2933693	30,3055191	21,41411781
p8 KOSR 10d PAX7	PAX7	30,3176708		0
p8 LOW PAX7	PAX7	30,2746773	30,28073502	21,9647789
p8 LOW PAX7	PAX7	30,2867908		0
p8 LOW_NONE PAX7	PAX7	30,5468845	30,42866135	21,79002857
p8 LOW_NONE PAX7	PAX7	30,3104401		0
p8 HIGH PAX7	PAX7	30,7951336	30,74588776	21,71085358
p8 HIGH PAX7	PAX7	30,6966438		0
p8 HIGH_NONE PAX7	PAX7	30,7934914	30,74292755	21,75614262
p8 HIGH_NONE PAX7	PAX7	30,6923656		0
REF SAMPLE PAX7	PAX7	27,0594482	27,02383423	20,54599428
REF SAMPLE PAX7	PAX7	26,9882221		0

Sample Name	Target Name	Cт	Cт Mean	d-CT
p6 PHMPM MYOD1	MYOD1	27,4682522	27,38825607	18,77579307
p6 PHMPM MYOD1	MYOD1	27,30826		0
p6 KOSR 10d MYOD1	MYOD1	30,1453323	30,13360214	21,47214317
p6 KOSR 10d MYOD1	MYOD1	30,121872		0
p6 LOW MYOD1	MYOD1	30,8871498	30,82301712	22,29476166
p6 LOW MYOD1	MYOD1	30,7588825		0
p6 LOW_NONE MYOD1	MYOD1	32,8171578	32,82540512	23,77075672
p6 LOW_NONE MYOD1	MYOD1	32,8336525		0
p6 HIGH MYOD1	MYOD1	31,436285	31,38267517	22,73830986
p6 HIGH MYOD1	MYOD1	31,3290653		0
p6 HIGH_NONE MYOD	MYOD1	33,2808914	33,2918663	25,02423382
p6 HIGH_NONE MYOD	MYOD1	33,3028412		0
p7 PHMPM MYOD1	MYOD1	28,4715805	28,49882507	20,24106598
p7 PHMPM MYOD1	MYOD1	28,5260677		0
p7 KOSR 10d MYOD1	MYOD1	30,243248	30,12640953	21,44568539
p7 KOSR 10d MYOD1	MYOD1	30,0095711		0
p7 LOW MYOD1	MYOD1	33,4603806	33,44024658	24,72451019
p7 LOW MYOD1	MYOD1	33,4201126		0
p7 LOW_NONE MYOD1	MYOD1	33,2185211	33,21387482	24,69532395
p7 LOW_NONE MYOD1	MYOD1	33,2092285		0
p7 HIGH MYOD1	MYOD1	33,6420593	33,7011795	24,97814846
p7 HIGH MYOD1	MYOD1	33,7602959		0
p7 HIGH_NONE MYOD	MYOD1	33,8028565	33,78619385	24,99356079
p7 HIGH_NONE MYOD	MYOD1	33,7695351		0
p8 PHMPM MYOD1	MYOD1	29,8712292	29,79683685	21,0286541
p8 PHMPM MYOD1	MYOD1	29,7224464		0
p8 KOSR 10d MYOD1	MYOD1	31,8451462	31,91547394	23,02407265
p8 KOSR 10d MYOD1	MYOD1	31,9858017		0
p8 LOW MYOD1	MYOD1	34,3705254	34,30290222	25,9869461
p8 LOW MYOD1	MYOD1	34,2352829		0
p8 LOW_NONE MYOD1	MYOD1	34,3722153	34,37202454	25,73339177
p8 LOW_NONE MYOD1	MYOD1	34,3718338		0
p8 HIGH MYOD1	MYOD1	34,8150024	34,92114258	25,8861084
p8 HIGH MYOD1	MYOD1	35,0272789		0
p8 HIGH_NONE MYOD	MYOD1	34,608017	35,09883499	26,11205006
p8 HIGH_NONE MYOD	MYOD1	35,589653		0
REF SAMPLE MYOD1	MYOD1	25,4151135	25,51413727	19,03629732
REF SAMPLE MYOD1	MYOD1	25,613163		0

Sample Name	Target Name	Cт	Cт Mean	d-CT
p6 PHMPM Myf-5	Myf-5	26,0779629	26,15283203	17,54036903
p6 PHMPM Myf-5	Myf-5	26,2277031		0
p6 KOSR 10d Myf-5	Myf-5	29,3336449	29,36709785	20,70563888
p6 KOSR 10d Myf-5	Myf-5	29,4005508		0
p6 LOW Myf-5	Myf-5	29,7430286	29,5751133	21,04685784
p6 LOW Myf-5	Myf-5	29,407198		0
p6 LOW_NONE Myf-5	Myf-5	30,1672173	30,29964066	21,24499226
p6 LOW_NONE Myf-5	Myf-5	30,4320641		0
p6 HIGH Myf-5	Myf-5	30,0943527	30,0308342	21,38646889
p6 HIGH Myf-5	Myf-5	29,9673176		0
p6 HIGH_NONE Myf-5	Myf-5	29,7203999	29,66209602	21,39446354
p6 HIGH_NONE Myf-5	Myf-5	29,6037922		0
p7 PHMPM Myf-5	Myf-5	27,0123425	27,00811768	18,75035859
p7 PHMPM Myf-5	Myf-5	27,003891		0
p7 KOSR 10d Myf-5	Myf-5	29,668047	29,66497421	20,98425007
p7 KOSR 10d Myf-5	Myf-5	29,6618996		0
p7 LOW Myf-5	Myf-5	30,2847138	30,2488327	21,53309631
p7 LOW Myf-5	Myf-5	30,2129536		0
p7 LOW_NONE Myf-5	Myf-5	30,4419212	30,45293045	21,93437958
p7 LOW_NONE Myf-5	Myf-5	30,4639416		0
p7 HIGH Myf-5	Myf-5	30,3009453	30,36258698	21,63955594
p7 HIGH Myf-5	Myf-5	30,4242268		0
p7 HIGH_NONE Myf-5	Myf-5	30,4585114	30,40871048	21,61607742
p7 HIGH_NONE Myf-5	Myf-5	30,3589096		0
p8 PHMPM Myf-5	Myf-5	27,7964802	27,8704319	19,10224915
p8 PHMPM Myf-5	Myf-5	27,9443836		0
p8 KOSR 10d Myf-5	Myf-5	30,4535961	30,6472702	21,75586891
p8 KOSR 10d Myf-5	Myf-5	30,8409462		0
p8 LOW Myf-5	Myf-5	30,7584705	30,83395004	22,51799392
p8 LOW Myf-5	Myf-5	30,9094315		0
p8 LOW_NONE Myf-5	Myf-5	30,9686184	30,92282295	22,28419018
p8 LOW_NONE Myf-5	Myf-5	30,8770275		0
p8 HIGH Myf-5	Myf-5	31,2158203	31,20685959	22,17182541
p8 HIGH Myf-5	Myf-5	31,1979008		0
p8 HIGH_NONE Myf-5	Myf-5	31,0086365	31,14938164	22,16259671
p8 HIGH_NONE Myf-5	Myf-5	31,2901268		0
REF SAMPLE Myf-5	Myf-5	25,6949406	25,74334526	19,26550531
REF SAMPLE Myf-5	Myf-5	25,79175		0

Sample Name	Target Name	Cт Mean	d-CT	dd-CT	2^-(dd-CT)
p6 PHMPM PAX7	PAX7	28,8005333	20,1880703	-0,357924	1,281580
p6 KOSR 10d PAX7	PAX7	28,698679	20,03722	-0,5087743	1,422841
p6 LOW PAX7	PAX7	29,6242828	21,09602737	0,55003309	0,683004
p6 LOW_NONE PAX7	PAX7	30,0561867	21,00153828	0,45554399	0,729235
p6 HIGH PAX7	PAX7	29,8227158	21,17835045	0,63235617	0,645122
p6 HIGH_NONE PAX7	PAX7	29,3372498	21,06961727	0,52362299	0,695623
p7 PHMPM PAX7	PAX7	29,9431419	21,68538284	1,13938856	0,453952
p7 KOSR 10d PAX7	PAX7	29,192852	20,51212788	-0,0338664	1,023752
p7 LOW PAX7	PAX7	29,6828213	20,96708488	0,4210906	0,746860
p7 LOW_NONE PAX7	PAX7	29,4636421	20,94509125	0,39909697	0,758333
p7 HIGH PAX7	PAX7	29,7241688	21,00113773	0,45514345	0,729438
p7 HIGH_NONE PAX7	PAX7	29,9512558	21,15862274	0,61262846	0,654004
p8 PHMPM PAX7	PAX7	31,1629372	22,39475441	1,84876013	0,277631
p8 KOSR 10d PAX7	PAX7	30,3055191	21,41411781	0,86812353	0,547859
p8 LOW PAX7	PAX7	30,280735	21,9647789	1,41878462	0,374027
p8 LOW_NONE PAX7	PAX7	30,4286613	21,79002857	1,24403429	0,422190
p8 HIGH PAX7	PAX7	30,7458878	21,71085358	1,16485929	0,446008
p8 HIGH_NONE PAX7	PAX7	30,7429276	21,75614262	1,21014833	0,432224
REF SAMPLE PAX7	PAX7	27,0238342	20,54599428	0	1,000000
p6 PHMPM MYOD1	MYOD1	27,3882561	18,77579307	-0,2605043	1,197897
p6 KOSR 10d MYOD1	MYOD1	30,1336021	21,47214317	2,43584585	0,184815
p6 LOW MYOD1	MYOD1	30,8230171	22,29476166	3,25846433	0,104497
p6 LOW_NONE MYOD1	MYOD1	32,8254051	23,77075672	4,7344594	0,037565
p6 HIGH MYOD1	MYOD1	31,3826752	22,73830986	3,70201254	0,076839
p6 HIGH_NONE MYOD1	MYOD1	33,2918663	25,02423382	5,98793649	0,015756
p7 PHMPM MYOD1	MYOD1	28,4988251	20,24106598	1,20476865	0,433839
p7 KOSR 10d MYOD1	MYOD1	30,1264095	21,44568539	2,40938806	0,188236
p7 LOW MYOD1	MYOD1	33,4402466	24,72451019	5,68821287	0,019394
p7 LOW_NONE MYOD1	MYOD1	33,2138748	24,69532395	5,65902662	0,019791
p7 HIGH MYOD1	MYOD1	33,7011795	24,97814846	5,94185113	0,016268
p7 HIGH_NONE MYOD1	MYOD1	33,7861939	24,99356079	5,95726347	0,016095
p8 PHMPM MYOD1	MYOD1	29,7968369	21,0286541	1,99235677	0,251328
p8 KOSR 10d MYOD1	MYOD1	31,9154739	23,02407265	3,98777533	0,063032
p8 LOW MYOD1	MYOD1	34,3029022	25,9869461	6,95064878	0,008084
p8 LOW_NONE MYOD1	MYOD1	34,3720245	25,73339177	6,69709444	0,009638
p8 HIGH MYOD1	MYOD1	34,9211426	25,8861084	6,84981108	0,008670
p8 HIGH_NONE MYOD1	MYOD1	35,098835	26,11205006	7,07575273	0,007413
REF SAMPLE MYOD1	MYOD1	25,5141373	19,03629732	0	1,000000

Sample Name	Target Name	Cт Mean	d-CT	dd-CT	2^-(dd-CT)
p6 PHMPM Myf-5	Myf-5	26,152832	17,54036903	-1,7251363	3,306114
p6 KOSR 10d Myf-5	Myf-5	29,3670979	20,70563888	1,44013357	0,368533
p6 LOW Myf-5	Myf-5	29,5751133	21,04685784	1,78135252	0,290911
p6 LOW_NONE Myf-5	Myf-5	30,2996407	21,24499226	1,97948695	0,253580
p6 HIGH Myf-5	Myf-5	30,0308342	21,38646889	2,12096358	0,229893
p6 HIGH_NONE Myf-5	Myf-5	29,662096	21,39446354	2,12895822	0,228623
p7 PHMPM Myf-5	Myf-5	27,0081177	18,75035859	-0,5151467	1,429139
p7 KOSR 10d Myf-5	Myf-5	29,6649742	20,98425007	1,71874475	0,303813
p7 LOW Myf-5	Myf-5	30,2488327	21,53309631	2,267591	0,207676
p7 LOW_NONE Myf-5	Myf-5	30,4529305	21,93437958	2,66887426	0,157249
p7 HIGH Myf-5	Myf-5	30,362587	21,63955594	2,37405062	0,192903
p7 HIGH_NONE Myf-5	Myf-5	30,4087105	21,61607742	2,35057211	0,196068
p8 PHMPM Myf-5	Myf-5	27,8704319	19,10224915	-0,1632562	1,119812
p8 KOSR 10d Myf-5	Myf-5	30,6472702	21,75586891	2,4903636	0,177961
p8 LOW Myf-5	Myf-5	30,83395	22,51799392	3,25248861	0,104931
p8 LOW_NONE Myf-5	Myf-5	30,922823	22,28419018	3,01868486	0,123392
p8 HIGH Myf-5	Myf-5	31,2068596	22,17182541	2,9063201	0,133386
p8 HIGH_NONE Myf-5	Myf-5	31,1493816	22,16259671	2,89709139	0,134242
REF SAMPLE Myf-5	Myf-5	25,7433453	19,26550531	0	1,000000

PAX7	p6	p7	p8	AVERAGE	STD ERROR
PHMPM	1,2815804	0,45395193	0,277630865	0,6710544	0,309477
KOSR 10d	1,42284083	1,0237521	0,547858971	0,99815063	0,252910
LOW 48 h	0,68300446	0,74685982	0,374027274	0,60129719	0,115120
LOW 24 h	0,72923515	0,7583328	0,422190409	0,63658612	0,107526
HIGH 48 h	0,64512196	0,72943764	0,446007756	0,60685579	0,084026
HIGH 24 h	0,69562274	0,65400408	0,432224173	0,59395033	0,081751

MYOD	p6	p7	p8	AVERAGE	STD ERROR
PHMPM	1,19789732	0,43383891	0,251327985	0,62768807	0,289932
KOSR 10d	0,18481505	0,18823567	0,063031844	0,14536085	0,041176
LOW 48 h	0,10449716	0,01939444	0,008084371	0,04399199	0,030428
LOW 24 h	0,0375652	0,01979079	0,009637706	0,02233123	0,008161
HIGH 48 h	0,07683926	0,01626764	0,008669647	0,03392552	0,021569
HIGH 24 h	0,0157562	0,01609478	0,007412867	0,01308795	0,002839

MYF-5	p6	p7	p8	AVERAGE	STD ERROR
PHMPM	3,30611356	1,42913948	1,119811707	1,95168825	0,683074
KOSR 10d	0,36853318	0,30381294	0,177961418	0,28343585	0,055949
LOW 48 h	0,29091054	0,20767637	0,104930893	0,2011726	0,053786
LOW 24 h	0,25358003	0,15724933	0,123391519	0,17807363	0,038998
HIGH 48 h	0,22989332	0,19290325	0,133386069	0,18539421	0,028111
HIGH 24 h	0,22862289	0,19606826	0,134242055	0,18631107	0,027679

miRNA RAW DATA ANALYSES:

1st run				2nd run			
Sample Name	**Target Name**	**Cт**	**Cт Mean**	**Sample Name**	**Target Name**	**Cт**	**Cт Mean**
p6 PHMPM	RNU6-2	24,5921669	24,4056454	p6 PHMPM	RNU6-2	24,857214	24,698204
p6 PHMPM	RNU6-2	24,338232	24,4056454	p6 PHMPM	RNU6-2	24,6905651	24,698204
p6 PHMPM	RNU6-2	24,286541	24,4056454	p6 PHMPM	RNU6-2	24,546833	24,698204
p6 KOSR 10d	RNU6-2	26,9150105	26,8502522	p6 KOSR 10d	RNU6-2	27,0835934	27,0402756
p6 KOSR 10d	RNU6-2	26,8220139	26,8502522	p6 KOSR 10d	RNU6-2	26,9849224	27,0402756
p6 KOSR 10d	RNU6-2	26,813736	26,8502522	p6 KOSR 10d	RNU6-2	27,0523071	27,0402756
p6 LOW	RNU6-2	24,9034119	24,7814255	p6 LOW	RNU6-2	24,9423637	24,9613476
p6 LOW	RNU6-2	24,6964665	24,7814255	p6 LOW	RNU6-2	24,9784641	24,9613476
p6 LOW	RNU6-2	24,7444	24,7814255	p6 LOW	RNU6-2	24,963213	24,9613476
p6 LOW_NONE	RNU6-2	24,7470818	24,9749451	p6 LOW_NONE	RNU6-2	25,0459404	25,1852722
p6 LOW_NONE	RNU6-2	24,9873409	24,9749451	p6 LOW_NONE	RNU6-2	25,1287937	25,1852722
p6 LOW_NONE	RNU6-2	25,1904125	24,9749451	p6 LOW_NONE	RNU6-2	25,3810844	25,1852722
p6 HIGH	RNU6-2	24,2060413	24,2229481	p6 HIGH	RNU6-2	24,4602699	24,441864
p6 HIGH	RNU6-2	24,261755	24,2229481	p6 HIGH	RNU6-2	24,423542	24,441864
p6 HIGH	RNU6-2	24,2010517	24,2229481	p6 HIGH	RNU6-2	24,4417801	24,441864
p6 HIGH_NONE	RNU6-2	24,3255577	24,2578335	p6 HIGH_NONE	RNU6-2	24,5984287	24,6059647
p6 HIGH_NONE	RNU6-2	24,1766396	24,2578335	p6 HIGH_NONE	RNU6-2	24,5583706	24,6059647
p6 HIGH_NONE	RNU6-2	24,2712994	24,2578335	p6 HIGH_NONE	RNU6-2	24,6610985	24,6059647
REF SAMPLE	RNU6-2	22,4629707	22,2869816	REF SAMPLE	RNU6-2	22,8259792	22,8765545
REF SAMPLE	RNU6-2	22,2572212	22,2869816	REF SAMPLE	RNU6-2	22,8807011	22,8765545
REF SAMPLE	RNU6-2	22,1407566	22,2869816	REF SAMPLE	RNU6-2	22,9229832	22,8765545
p7 PHMPM	RNU6-2	23,8931637	24,0380878	p7 PHMPM	RNU6-2	24,5478439	24,6157074
p7 PHMPM	RNU6-2	23,9579125	24,0380878	p7 PHMPM	RNU6-2	24,7624207	24,6157074
p7 PHMPM	RNU6-2	24,2631893	24,0380878	p7 PHMPM	RNU6-2	24,5368595	24,6157074
p7 KOSR 10d	RNU6-2	28,0066567	28,1181583	p7 KOSR 10d	RNU6-2	28,4711933	28,4277477
p7 KOSR 10d	RNU6-2	28,1634884	28,1181583	p7 KOSR 10d	RNU6-2	28,3557701	28,4277477
p7 KOSR 10d	RNU6-2	28,1843319	28,1181583	p7 KOSR 10d	RNU6-2	28,4562798	28,4277477
p7 LOW	RNU6-2	24,104229	24,2130127	p7 LOW	RNU6-2	24,6528454	24,720541
p7 LOW	RNU6-2	24,3560581	24,2130127	p7 LOW	RNU6-2	24,6198292	24,720541
p7 LOW	RNU6-2	24,1787472	24,2130127	p7 LOW	RNU6-2	24,8889427	24,720541
p7 LOW_NONE	RNU6-2	23,8200283	23,8756733	p7 LOW_NONE	RNU6-2	24,4984741	24,3403835
p7 LOW_NONE	RNU6-2	23,8481941	23,8756733	p7 LOW_NONE	RNU6-2	24,2608376	24,3403835
p7 LOW_NONE	RNU6-2	23,9588013	23,8756733	p7 LOW_NONE	RNU6-2	24,2618389	24,3403835
p7 HIGH	RNU6-2	24,073822	24,0236607	p7 HIGH	RNU6-2	24,5939102	24,5433178
p7 HIGH	RNU6-2	24,1752052	24,0236607	p7 HIGH	RNU6-2	24,5406761	24,5433178
p7 HIGH	RNU6-2	23,8219528	24,0236607	p7 HIGH	RNU6-2	24,4953651	24,5433178
p7 HIGH_NONE	RNU6-2	23,7005291	23,8521137	p7 HIGH_NONE	RNU6-2	24,4463024	24,3605175
p7 HIGH_NONE	RNU6-2	23,9174347	23,8521137	p7 HIGH_NONE	RNU6-2	24,3614044	24,3605175
p7 HIGH_NONE	RNU6-2	23,9383812	23,8521137	p7 HIGH_NONE	RNU6-2	24,2738457	24,3605175
REF SAMPLE	RNU6-2	22,4629707	22,2869816	REF SAMPLE	RNU6-2	22,927824	22,9145508
REF SAMPLE	RNU6-2	22,2572212	22,2869816	REF SAMPLE	RNU6-2	22,8432674	22,9145508
REF SAMPLE	RNU6-2	22,1407566	22,2869816	REF SAMPLE	RNU6-2	22,9725609	22,9145508

1st run				2nd run			
Sample Name	**Target Name**	**Cт**	**Cт Mean**	**Sample Name**	**Target Name**	**Cт**	**Cт Mean**
p8 PHMPM	RNU6-2	23,9224606	23,89534	p8 PHMPM	RNU6-2	24,3377457	24,3361054
p8 PHMPM	RNU6-2	23,8960819	23,89534	p8 PHMPM	RNU6-2	24,3580647	24,3361054
p8 PHMPM	RNU6-2	23,8674755	23,89534	p8 PHMPM	RNU6-2	24,3125095	24,3361054
p8 KOSR 10d	RNU6-2	24,4841366	24,2980785	p8 KOSR 10d	RNU6-2	24,6734257	24,6950665
p8 KOSR 10d	RNU6-2	24,171196	24,2980785	p8 KOSR 10d	RNU6-2	24,723732	24,6950665
p8 KOSR 10d	RNU6-2	24,2389031	24,2980785	p8 KOSR 10d	RNU6-2	24,6880417	24,6950665
p8 LOW	RNU6-2	24,6020927	24,7271729	p8 LOW	RNU6-2	25,2119808	25,2115173
p8 LOW	RNU6-2	24,6568375	24,7271729	p8 LOW	RNU6-2	25,2087803	25,2115173
p8 LOW	RNU6-2	24,9225941	24,7271729	p8 LOW	RNU6-2	25,2137871	25,2115173
p8 LOW_NONE	RNU6-2	28,9267502	28,9488297	p8 LOW_NONE	RNU6-2	29,46628	29,4182968
p8 LOW_NONE	RNU6-2	28,9525509	28,9488297	p8 LOW_NONE	RNU6-2	29,2576599	29,4182968
p8 LOW_NONE	RNU6-2	28,9671879	28,9488297	p8 LOW_NONE	RNU6-2	29,5309486	29,4182968
p8 HIGH	RNU6-2	24,2893086	24,2197781	p8 HIGH	RNU6-2	24,8090477	24,8928776
p8 HIGH	RNU6-2	24,1876183	24,2197781	p8 HIGH	RNU6-2	25,0256786	24,8928776
p8 HIGH	RNU6-2	24,1824074	24,2197781	p8 HIGH	RNU6-2	24,8439064	24,8928776
p8 HIGH_NONE	RNU6-2	24,1960125	24,3511028	p8 HIGH_NONE	RNU6-2	24,8772488	25,0181427
p8 HIGH_NONE	RNU6-2	24,548851	24,3511028	p8 HIGH_NONE	RNU6-2	24,9008064	25,0181427
p8 HIGH_NONE	RNU6-2	24,3084412	24,3511028	p8 HIGH_NONE	RNU6-2	25,276371	25,0181427
REF SAMPLE	RNU6-2	22,4629707	22,2869816	REF SAMPLE	RNU6-2	22,7208328	22,8781834
REF SAMPLE	RNU6-2	22,2572212	22,2869816	REF SAMPLE	RNU6-2	22,9911614	22,8781834
REF SAMPLE	RNU6-2	22,1407566	22,2869816	REF SAMPLE	RNU6-2	22,9225617	22,8781834

1st run

Sample Name	Target Name	Cт	Cт Mean	d-Cт	dd-Cт	2^-(ddCт)
p6 PHMPM	miR-31	24,1884842	24,2938976	-0,111747742	-0,8603344	1,81545906
p6 PHMPM	miR-31	24,4141579	24,2938976	-0,111747742	-0,8603344	
p6 PHMPM	miR-31	24,279047	24,2938976	-0,111747742	-0,8603344	
p6 KOSR 10d	miR-31	26,8979416	26,7452717	-0,104980469	-0,85356712	1,8069632
p6 KOSR 10d	miR-31	26,7111378	26,7452717	-0,104980469	-0,85356712	
p6 KOSR 10d	miR-31	26,6267376	26,7452717	-0,104980469	-0,85356712	
p6 LOW	miR-31	24,8188343	24,7619114	-0,019514084	-0,76810074	1,70302633
p6 LOW	miR-31	24,6420479	24,7619114	-0,019514084	-0,76810074	
p6 LOW	miR-31	24,8248577	24,7619114	-0,019514084	-0,76810074	
p6 LOW_NONE	miR-31	24,8091888	24,9079285	-0,067016602	-0,81560326	1,76003395
p6 LOW_NONE	miR-31	24,8755455	24,9079285	-0,067016602	-0,81560326	
p6 LOW_NONE	miR-31	25,0390511	24,9079285	-0,067016602	-0,81560326	
p6 HIGH	miR-31	24,4066696	24,3904877	0,167539597	-0,58104706	1,49593455
p6 HIGH	miR-31	24,418541	24,3904877	0,167539597	-0,58104706	
p6 HIGH	miR-31	24,3462563	24,3904877	0,167539597	-0,58104706	
p6 HIGH_NONE	miR-31	24,226759	24,24543	-0,012403488	-0,76099014	1,69465329
p6 HIGH_NONE	miR-31	24,1287365	24,24543	-0,012403488	-0,76099014	
p6 HIGH_NONE	miR-31	24,3807945	24,24543	-0,012403488	-0,76099014	
REF SAMPLE	miR-31	23,1448402	23,0355682	0,748586655	0	1
REF SAMPLE	miR-31	23,0124664	23,0355682	0,748586655	0	
REF SAMPLE	miR-31	22,9494	23,0355682	0,748586655	0	
p7 PHMPM	miR-31	23,9579716	23,9745846	-0,063503265	-0,81208992	1,75575302
p7 PHMPM	miR-31	23,8890781	23,9745846	-0,063503265	-0,81208992	
p7 PHMPM	miR-31	24,076704	23,9745846	-0,063503265	-0,81208992	
p7 KOSR 10d	miR-31	25,4964752	25,4152222	-2,702936172	-3,45152283	10,9398635
p7 KOSR 10d	miR-31	25,3287087	25,4152222	-2,702936172	-3,45152283	
p7 KOSR 10d	miR-31	25,4204865	25,4152222	-2,702936172	-3,45152283	
p7 LOW	miR-31	24,1005535	24,3867626	0,173749924	-0,57483673	1,48950889
p7 LOW	miR-31	24,9171886	24,3867626	0,173749924	-0,57483673	
p7 LOW	miR-31	24,14254	24,3867626	0,173749924	-0,57483673	
p7 LOW_NONE	miR-31	23,8717899	23,9246883	0,049015045	-0,69957161	1,62402249
p7 LOW_NONE	miR-31	23,8757362	23,9246883	0,049015045	-0,69957161	
p7 LOW_NONE	miR-31	24,0265369	23,9246883	0,049015045	-0,69957161	
p7 HIGH	miR-31	24,009594	23,9957581	-0,027902603	-0,77648926	1,71295738
p7 HIGH	miR-31	24,0118237	23,9957581	-0,027902603	-0,77648926	
p7 HIGH	miR-31	23,9658546	23,9957581	-0,027902603	-0,77648926	
p7 HIGH_NONE	miR-31	24,0038815	23,9414444	0,089330673	-0,65925598	1,57926796
p7 HIGH_NONE	miR-31	23,9465218	23,9414444	0,089330673	-0,65925598	
p7 HIGH_NONE	miR-31	23,8739281	23,9414444	0,089330673	-0,65925598	
REF SAMPLE	miR-31	23,1448402	23,0355682	0,748586655	0	1
REF SAMPLE	miR-31	23,0124664	23,0355682	0,748586655	0	
REF SAMPLE	miR-31	22,9494	23,0355682	0,748586655	0	

Sample Name	Target Name	Cт	Cт Mean	d-Cт	dd-Cт	2^-(ddCт)
p8 PHMPM	miR-31	24,1070995	24,1648693	0,269529343	-0,47905731	1,39383261
p8 PHMPM	miR-31	24,3256416	24,1648693	0,269529343	-0,47905731	
p8 PHMPM	miR-31	24,0618668	24,1648693	0,269529343	-0,47905731	
p8 KOSR 10d	miR-31	24,0347767	24,1451283	-0,152950287	-0,90153694	1,86805501
p8 KOSR 10d	miR-31	24,221632	24,1451283	-0,152950287	-0,90153694	
p8 KOSR 10d	miR-31	24,1789818	24,1451283	-0,152950287	-0,90153694	
p8 LOW	miR-31	23,6792259	23,7552643	-0,971908569	-1,72049522	3,2954951
p8 LOW	miR-31	23,8420219	23,7552643	-0,971908569	-1,72049522	
p8 LOW	miR-31	23,7445488	23,7552643	-0,971908569	-1,72049522	
p8 LOW_NONE	miR-31	26,0049763	26,1584377	-2,790391922	-3,53897858	11,6235478
p8 LOW_NONE	miR-31	26,1659889	26,1584377	-2,790391922	-3,53897858	
p8 LOW_NONE	miR-31	26,3043461	26,1584377	-2,790391922	-3,53897858	
p8 HIGH	miR-31	24,2007351	24,1051941	-0,114583969	-0,86317062	1,81903162
p8 HIGH	miR-31	24,0225487	24,1051941	-0,114583969	-0,86317062	
p8 HIGH	miR-31	24,0922985	24,1051941	-0,114583969	-0,86317062	
p8 HIGH_NONE	miR-31	24,0795956	24,0637837	-0,287319183	-1,03590584	2,05040065
p8 HIGH_NONE	miR-31	24,1475315	24,0637837	-0,287319183	-1,03590584	
p8 HIGH_NONE	miR-31	23,9642239	24,0637837	-0,287319183	-1,03590584	
REF SAMPLE	miR-31	23,1448402	23,0355682	0,748586655	0	1
REF SAMPLE	miR-31	23,0124664	23,0355682	0,748586655	0	
REF SAMPLE	miR-31	22,9494	23,0355682	0,748586655	0	

2nd run

Sample Name	Target Name	Cт	Cт Mean	d-Cт	dd-Cт	2^-(ddCт)
p6 PHMPM	miR-31	24,6193543	24,6062527	-0,09195137	-0,62842178	1,54587298
p6 PHMPM	miR-31	24,6604614	24,6062527			
p6 PHMPM	miR-31	24,5389404	24,6062527			
p6 KOSR 10d	miR-31	26,9604607	26,9429226	-0,097352982	-0,6338234	1,55167175
p6 KOSR 10d	miR-31	26,9310684	26,9429226			
p6 KOSR 10d	miR-31	26,9372311	26,9429226			
p6 LOW	miR-31	25,0256081	25,068924	0,10757637	-0,42889404	1,3462012
p6 LOW	miR-31	25,1117268	25,068924			
p6 LOW	miR-31	25,0694313	25,068924			
p6 LOW_NONE	miR-31	25,1688023	25,2415142	0,056241989	-0,48022842	1,39496452
p6 LOW_NONE	miR-31	25,1470547	25,2415142			
p6 LOW_NONE	miR-31	25,4086876	25,2415142			
p6 HIGH	miR-31	24,6201935	24,6745472	0,232683182	-0,30378723	1,23438055
p6 HIGH	miR-31	24,7494221	24,6745472			
p6 HIGH	miR-31	24,6540299	24,6745472			
p6 HIGH_NONE	miR-31	24,6381035	24,6853085	0,079343796	-0,45712662	1,37280491
p6 HIGH_NONE	miR-31	24,7427559	24,6853085			
p6 HIGH_NONE	miR-31	24,6750679	24,6853085			
REF SAMPLE	miR-31	23,4882698	23,4130249	0,536470413	0	1
REF SAMPLE	miR-31	23,435318	23,4130249			
REF SAMPLE	miR-31	23,3154888	23,4130249			
p7 PHMPM	miR-31	24,634367	24,4990368	-0,116670609	-0,64296722	1,56153751
p7 PHMPM	miR-31	24,4011135	24,4990368			
p7 PHMPM	miR-31	24,4616242	24,4990368			
p7 KOSR 10d	miR-31	25,9288044	25,8265457	-2,601202011	-3,12749863	8,7391843
p7 KOSR 10d	miR-31	25,7658711	25,8265457			
p7 KOSR 10d	miR-31	25,7849636	25,8265457			
p7 LOW	miR-31	24,583519	24,5346909	-0,185850143	-0,71214676	1,63824004
p7 LOW	miR-31	24,4737034	24,5346909			
p7 LOW	miR-31	24,5468483	24,5346909			
p7 LOW_NONE	miR-31	24,4379482	24,4459133	0,105529785	-0,42076683	1,33863889
p7 LOW_NONE	miR-31	24,3915386	24,4459133			
p7 LOW_NONE	miR-31	24,5082493	24,4459133			
p7 HIGH	miR-31	24,4740677	24,4307385	-0,112579346	-0,63887596	1,5571155
p7 HIGH	miR-31	24,3962555	24,4307385			
p7 HIGH	miR-31	24,4218884	24,4307385			
p7 HIGH_NONE	miR-31	24,3626576	24,4406261	0,080108643	-0,44618797	1,36243554
p7 HIGH_NONE	miR-31	24,644392	24,4406261			
p7 HIGH_NONE	miR-31	24,3148308	24,4406261			
REF SAMPLE	miR-31	23,4418049	23,4408474	0,526296616	0	1
REF SAMPLE	miR-31	23,4593468	23,4408474			
REF SAMPLE	miR-31	23,4213867	23,4408474			

2nd run

Sample Name	Target Name	Cт	Cт Mean	d-Cт	dd-Cт	2^-(ddCт)
p8 PHMPM	miR-31	24,728447	24,7789364	0,44283104	-0,19062615	1,14125893
p8 PHMPM	miR-31	24,909935	24,7789364			
p8 PHMPM	miR-31	24,6984272	24,7789364			
p8 KOSR 10d	miR-31	24,7451553	24,6203461	-0,07472038	-0,70817757	1,63373905
p8 KOSR 10d	miR-31	24,556488	24,6203461			
p8 KOSR 10d	miR-31	24,559391	24,6203461			
p8 LOW	miR-31	24,3614712	24,243166	-0,96835136	-1,60180855	3,03523569
p8 LOW	miR-31	24,194828	24,243166			
p8 LOW	miR-31	24,1732025	24,243166			
p8 LOW_NONE	miR-31	26,6289711	26,6332188	-2,78507804	-3,41853523	10,6925588
p8 LOW_NONE	miR-31	26,5361767	26,6332188			
p8 LOW_NONE	miR-31	26,7345142	26,6332188			
p8 HIGH	miR-31	24,5286331	24,4864979	-0,4063797	-1,03983689	2,05599519
p8 HIGH	miR-31	24,4990959	24,4864979			
p8 HIGH	miR-31	24,4317646	24,4864979			
p8 HIGH_NONE	miR-31	24,3379154	24,3878765	-0,63026619	-1,26372338	2,40114642
p8 HIGH_NONE	miR-31	24,4456024	24,3878765			
p8 HIGH_NONE	miR-31	24,3801079	24,3878765			
REF SAMPLE	miR-31	23,4711781	23,5116406	0,63345719	0	1
REF SAMPLE	miR-31	23,6033688	23,5116406			
REF SAMPLE	miR-31	23,4603729	23,5116406			

1st run	PHMPM	KOSR 10 d	LOW 48 hr	LOW 24 hr	HIGH 48 hr	HIGH 24 hr
p6	1,81545906	1,8069632	1,70302633	1,760033948	1,495934552	1,69465329
p7	1,75575302	10,9398635	1,48950889	1,624022488	1,712957382	1,57926796
p8	1,39383261	1,86805501	3,2954951	11,62354779	1,819031623	2,05040065

2nd run	PHMPM	KOSR 10 d	LOW 48 hr	LOW 24 hr	HIGH 48 hr	HIGH 24 hr
p6	1,54587298	1,55167175	1,3462012	1,394964516	1,234380547	1,37280491
p7	1,56153751	8,7391843	1,63824004	1,338638888	1,5571155	1,36243554
p8	1,14125893	1,63373905	3,03523569	10,69255876	2,055995191	2,40114642

miR-31	p6	p7	p8	AVERAGE	STD ERROR
PHMPM	1,68066602	1,65864527	1,26754577	1,535619019	0,13418728
KOSR 10 d	1,67931747	9,83952388	1,75089703	4,423246129	2,708217704
LOW 48 h	1,52461376	1,56387446	3,1653654	2,084617873	0,540492601
LOW 24 h	1,57749923	1,48133069	11,1580533	4,738961065	3,209666166
HIGH 48 h	1,36515755	1,63503644	1,93751341	1,645902466	0,165314206
HIGH 24 h	1,5337291	1,47085175	2,22577353	1,743451461	0,241843149

APPENDIX K - PHM 10 DAY CULTURE IN QUIESCENCE MEDIA EXTRA DATA

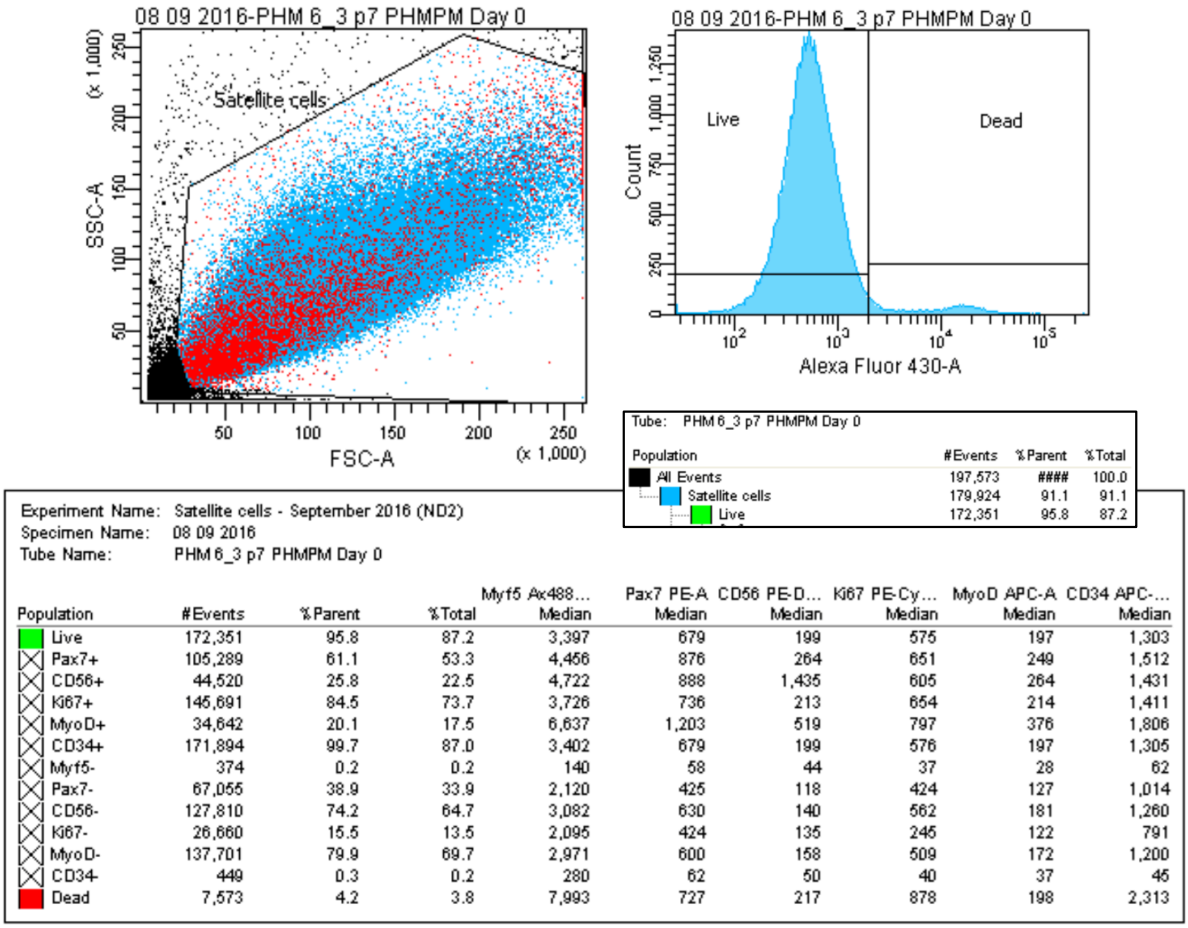

Population	#Events	%Parent	%Total	Myf5 Ax488... Median	Pax7 PE-A Median	CD56 PE-D... Median	Ki67 PE-Cy... Median	MyoD APC-A Median	CD34 APC-... Median
Live	172,351	95.8	87.2	3,397	679	199	575	197	1,303
Pax7+	105,289	61.1	53.3	4,456	876	264	651	249	1,512
CD56+	44,520	25.8	22.5	4,722	888	1,435	605	264	1,431
Ki67+	145,691	84.5	73.7	3,726	736	213	654	214	1,411
MyoD+	34,642	20.1	17.5	6,637	1,203	519	797	376	1,806
CD34+	171,894	99.7	87.0	3,402	679	199	576	197	1,305
Myf5-	374	0.2	0.2	140	58	44	37	28	62
Pax7-	67,055	38.9	33.9	2,120	425	118	424	127	1,014
CD56-	127,810	74.2	64.7	3,082	630	140	562	181	1,260
Ki67-	26,660	15.5	13.5	2,095	424	135	245	122	791
MyoD-	137,701	79.9	69.7	2,971	600	158	509	172	1,200
CD34-	449	0.3	0.2	280	62	50	40	37	45
Dead	7,573	4.2	3.8	7,993	727	217	878	198	2,313

Figure K.1: Day 0 (PHM-PM control) PHM samples.

Multicolour flow cytometry data depicting the numerical results for the entire satellite cell population analysed. Only live satellite cells were used for marker analyses.

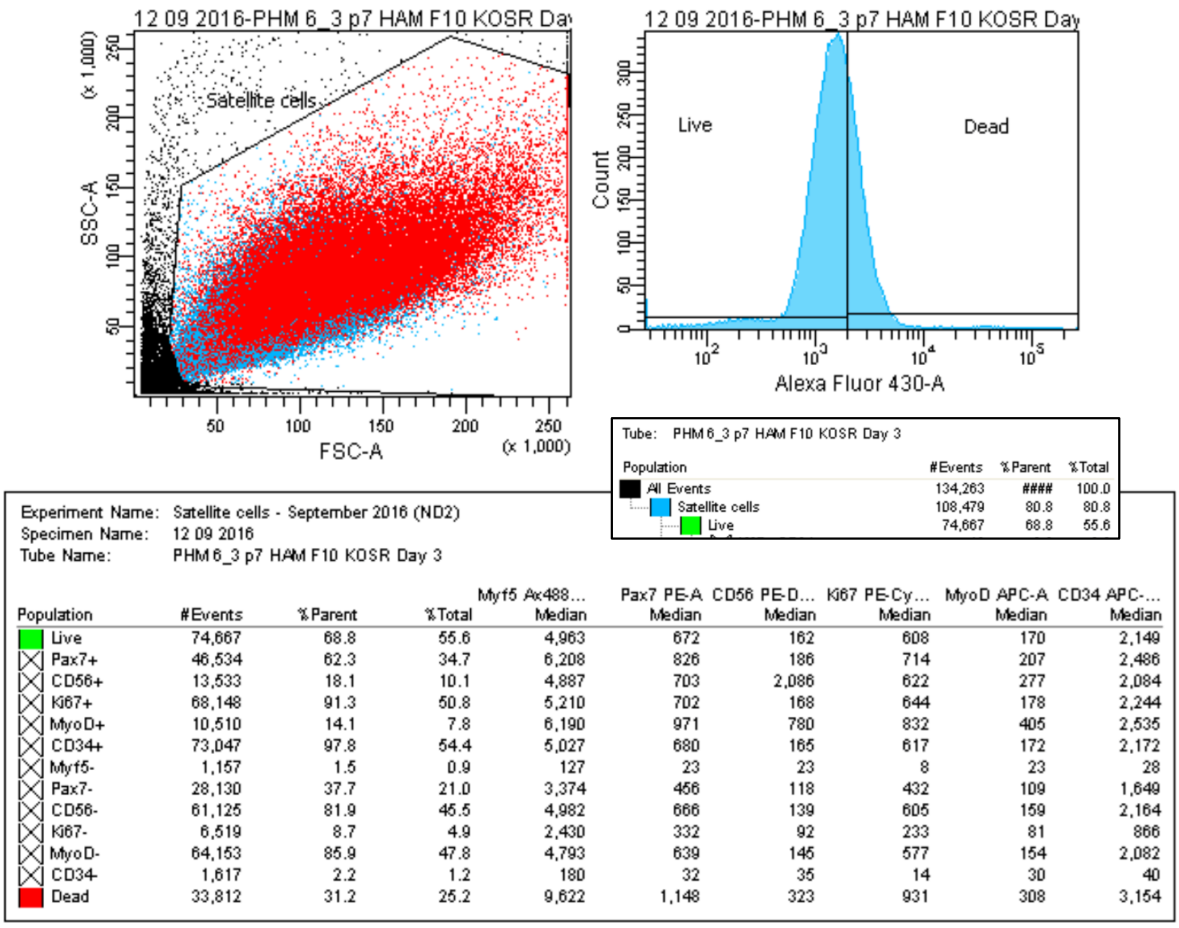

Population	#Events	%Parent	%Total	Myf5 Ax488... Median	Pax7 PE-A Median	CD56 PE-D... Median	Ki67 PE-Cy... Median	MyoD APC-A Median	CD34 APC-... Median
Live	74,667	68.8	55.6	4,963	672	162	608	170	2,149
Pax7+	46,534	62.3	34.7	6,208	826	186	714	207	2,486
CD56+	13,533	18.1	10.1	4,887	703	2,086	622	277	2,084
Ki67+	68,148	91.3	50.8	5,210	702	168	644	178	2,244
MyoD+	10,510	14.1	7.8	6,190	971	780	832	405	2,535
CD34+	73,047	97.8	54.4	5,027	680	165	617	172	2,172
Myf5-	1,157	1.5	0.9	127	23	23	8	23	28
Pax7-	28,130	37.7	21.0	3,374	456	118	432	109	1,649
CD56-	61,125	81.9	45.5	4,982	666	139	605	159	2,164
Ki67-	6,519	8.7	4.9	2,430	332	92	233	81	866
MyoD-	64,153	85.9	47.8	4,793	639	145	577	154	2,082
CD34-	1,617	2.2	1.2	180	32	35	14	30	40
Dead	33,812	31.2	25.2	9,622	1,148	323	931	308	3,154

Figure K.2: Day 3 PHM samples.

Multicolour flow cytometry data depicting the numerical results for the entire satellite cell population analysed. Only live satellite cells were used for marker analyses.

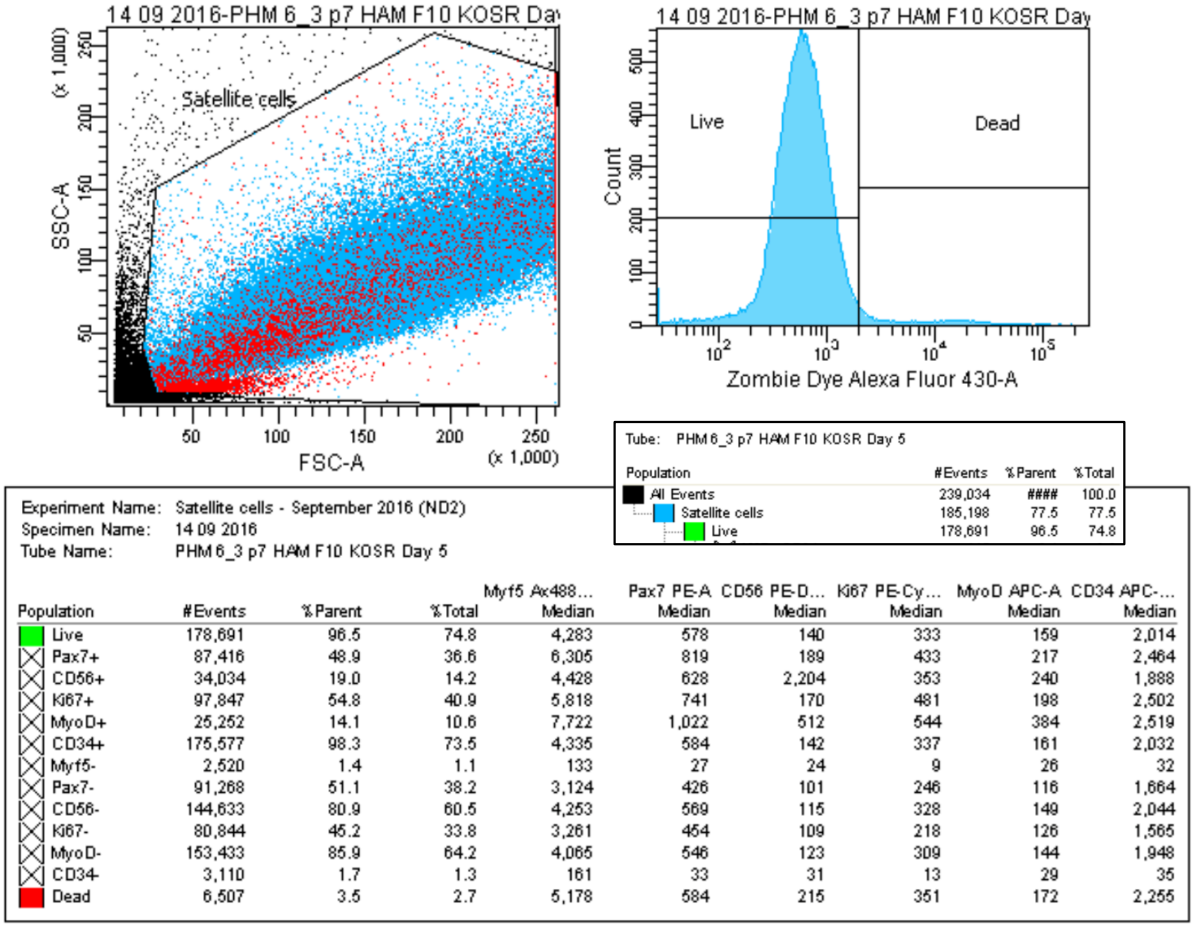

Population	#Events	%Parent	%Total	Myf5 Ax488... Median	Pax7 PE-A Median	CD56 PE-D... Median	Ki67 PE-Cy... Median	MyoD APC-A Median	CD34 APC-... Median
Live	178,691	96.5	74.8	4,283	578	140	333	159	2,014
Pax7+	87,416	48.9	36.6	6,305	819	189	433	217	2,464
CD56+	34,034	19.0	14.2	4,428	628	2,204	353	240	1,888
Ki67+	97,847	54.8	40.9	5,818	741	170	481	198	2,502
MyoD+	25,252	14.1	10.6	7,722	1,022	512	544	384	2,519
CD34+	175,577	98.3	73.5	4,335	584	142	337	161	2,032
Myf5-	2,520	1.4	1.1	133	27	24	9	26	32
Pax7-	91,268	51.1	38.2	3,124	426	101	246	116	1,664
CD56-	144,633	80.9	60.5	4,253	569	115	328	149	2,044
Ki67-	80,844	45.2	33.8	3,261	454	109	218	126	1,565
MyoD-	153,433	85.9	64.2	4,065	546	123	309	144	1,948
CD34-	3,110	1.7	1.3	161	33	31	13	29	35
Dead	6,507	3.5	2.7	5,178	584	215	351	172	2,255

Figure K.3: Day 5 PHM samples.

Multicolour flow cytometry data depicting the numerical results for the entire satellite cell population analysed. Only live satellite cells were used for marker analyses.

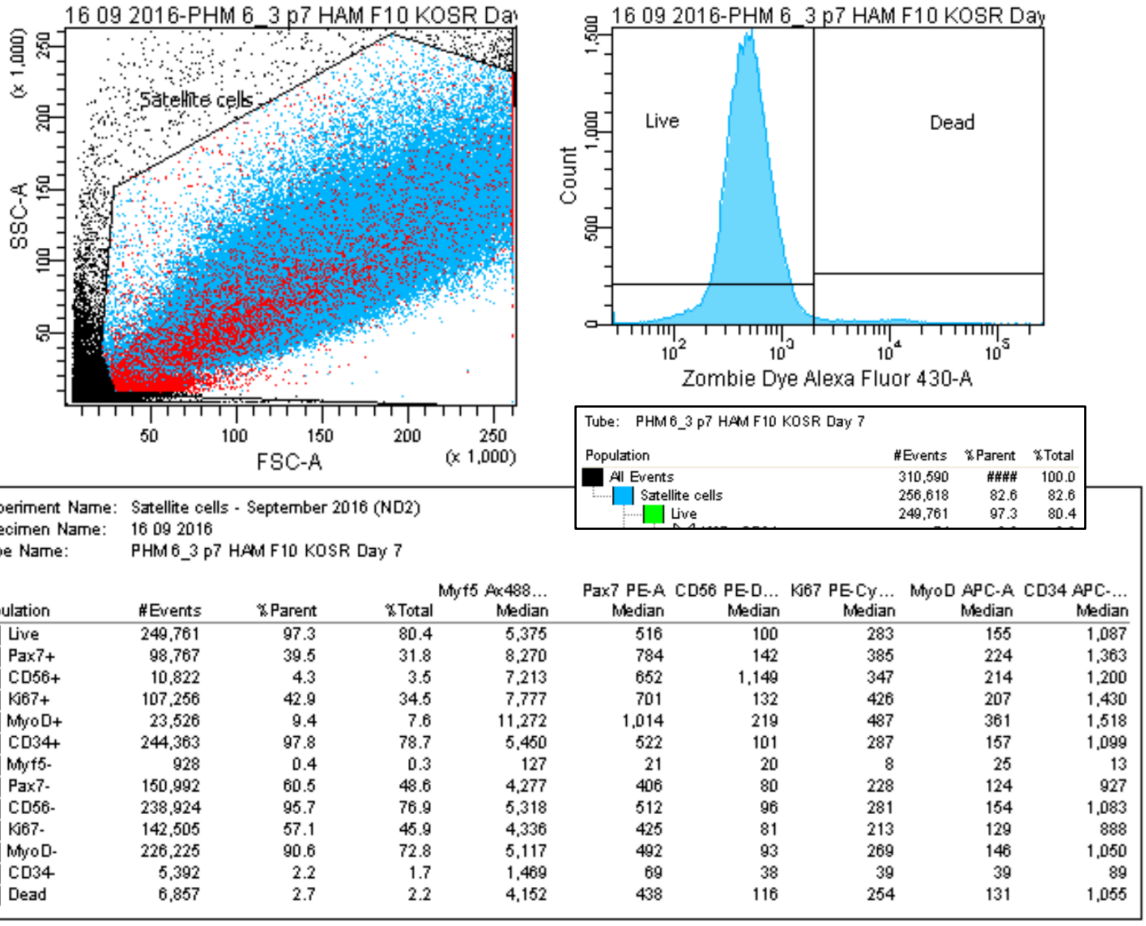

Population	#Events	%Parent	%Total	Myf5 Ax488... Median	Pax7 PE-A Median	CD56 PE-D... Median	Ki67 PE-Cy... Median	MyoD APC-A Median	CD34 APC-... Median
Live	249,761	97.3	80.4	5,375	516	100	283	155	1,087
Pax7+	98,767	39.5	31.8	8,270	784	142	385	224	1,363
CD56+	10,822	4.3	3.5	7,213	652	1,149	347	214	1,200
Ki67+	107,256	42.9	34.5	7,777	701	132	426	207	1,430
MyoD+	23,526	9.4	7.6	11,272	1,014	219	487	361	1,518
CD34+	244,363	97.8	78.7	5,450	522	101	287	157	1,099
Myf5-	928	0.4	0.3	127	21	20	8	25	13
Pax7-	150,992	60.5	48.6	4,277	406	80	228	124	927
CD56-	238,924	95.7	76.9	5,318	512	96	281	154	1,083
Ki67-	142,505	57.1	45.9	4,336	425	81	213	129	888
MyoD-	226,225	90.6	72.8	5,117	492	93	269	146	1,050
CD34-	5,392	2.2	1.7	1,469	69	38	39	39	89
Dead	6,857	2.7	2.2	4,152	438	116	254	131	1,055

Figure K.4: Day 7 PHM samples.

Multicolour flow cytometry data depicting the numerical results for the entire satellite cell population analysed. Only live satellite cells were used for marker analyses.

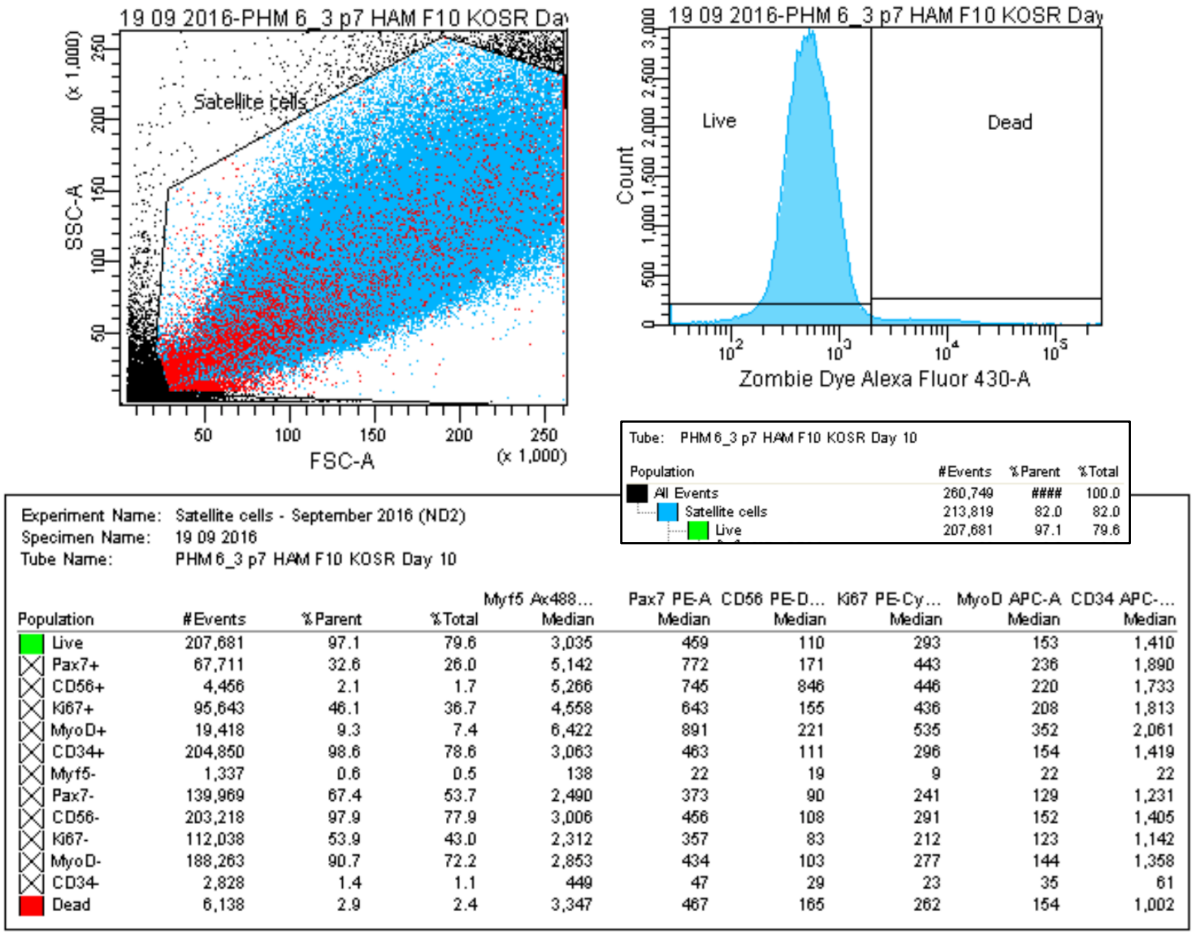

Population	#Events	%Parent	%Total	Myf5 Ax488... Median	Pax7 PE-A Median	CD56 PE-D... Median	Ki67 PE-Cy... Median	MyoD APC-A Median	CD34 APC-... Median
Live	207,681	97.1	79.6	3,035	459	110	293	153	1,410
Pax7+	67,711	32.6	26.0	5,142	772	171	443	236	1,890
CD56+	4,456	2.1	1.7	5,266	745	846	446	220	1,733
Ki67+	95,643	46.1	36.7	4,558	643	155	436	208	1,813
MyoD+	19,418	9.3	7.4	6,422	891	221	535	352	2,061
CD34+	204,850	98.6	78.6	3,063	463	111	296	154	1,419
Myf5-	1,337	0.6	0.5	138	22	19	9	22	22
Pax7-	139,969	67.4	53.7	2,490	373	90	241	129	1,231
CD56-	203,218	97.9	77.9	3,006	456	108	291	152	1,405
Ki67-	112,038	53.9	43.0	2,312	357	83	212	123	1,142
MyoD-	188,263	90.7	72.2	2,853	434	103	277	144	1,358
CD34-	2,828	1.4	1.1	449	47	29	23	35	61
Dead	6,138	2.9	2.4	3,347	467	165	262	154	1,002

Figure K.5: Day 10 PHM samples.

Multicolour flow cytometry data depicting the numerical results for the entire satellite cell population analysed. Only live satellite cells were used for marker analyses.

APPENDIX L - CELL CYCLE ANALYSES OF PHMs CULTURED IN KO-DMEM/20% KOSR FOR 10 DAYS

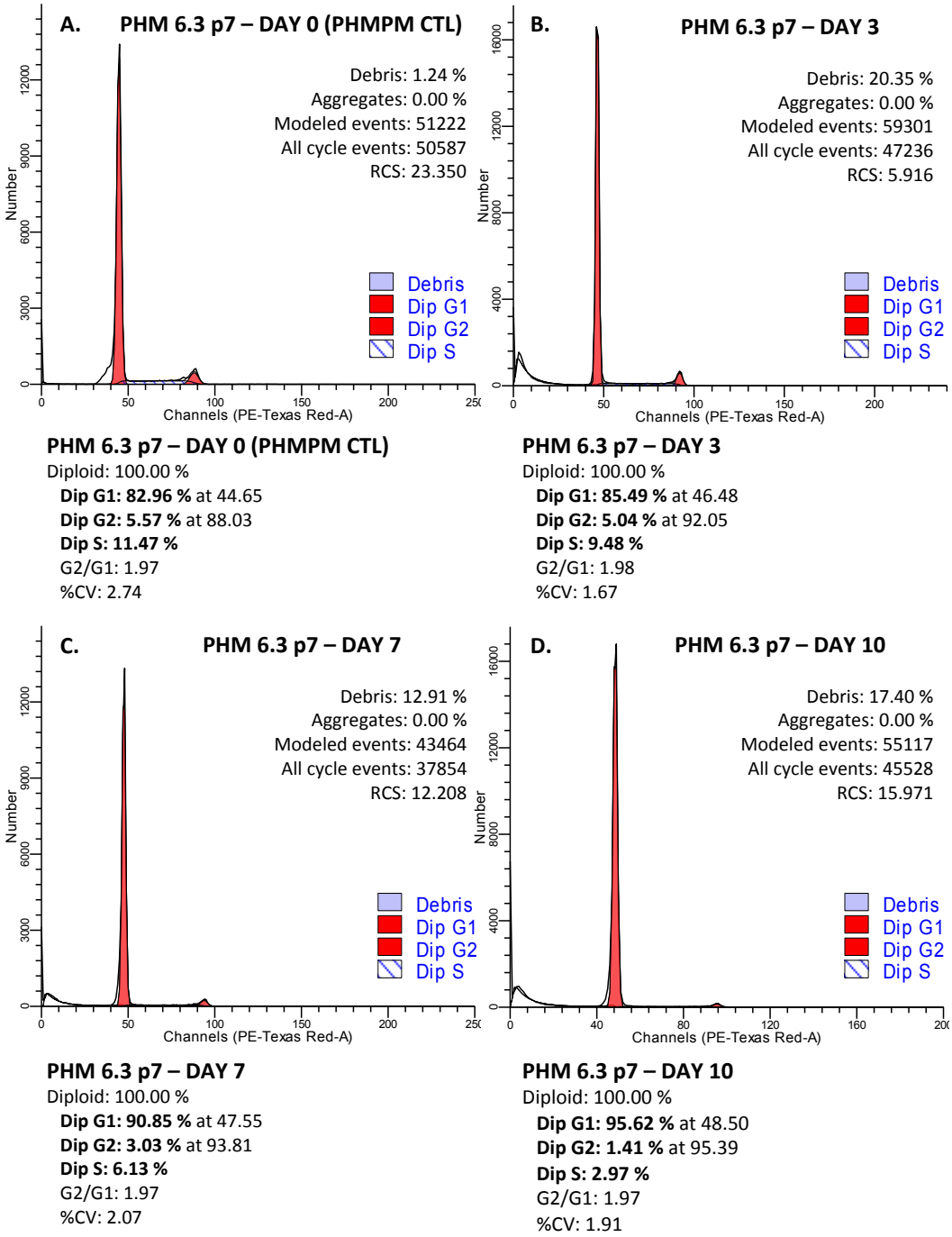

PHM 6.3 p7 – DAY 0 (PHMPM CTL)
Diploid: 100.00 %
Dip G1: 82.96 % at 44.65
Dip G2: 5.57 % at 88.03
Dip S: 11.47 %
G2/G1: 1.97
%CV: 2.74

PHM 6.3 p7 – DAY 3
Diploid: 100.00 %
Dip G1: 85.49 % at 46.48
Dip G2: 5.04 % at 92.05
Dip S: 9.48 %
G2/G1: 1.98
%CV: 1.67

PHM 6.3 p7 – DAY 7
Diploid: 100.00 %
Dip G1: 90.85 % at 47.55
Dip G2: 3.03 % at 93.81
Dip S: 6.13 %
G2/G1: 1.97
%CV: 2.07

PHM 6.3 p7 – DAY 10
Diploid: 100.00 %
Dip G1: 95.62 % at 48.50
Dip G2: 1.41 % at 95.39
Dip S: 2.97 %
G2/G1: 1.97
%CV: 1.91

Figure L.1: Cell cycle analyses of PHMs cultured in KO-DMEM/20% KOSR for 10 days.